Terms and Conditions of Use of Digitised Theses from Trinity College Library Dublin

Copyright statement

All material supplied by Trinity College Library is protected by copyright (under the Copyright and Related Rights Act, 2000 as amended) and other relevant Intellectual Property Rights. By accessing and using a Digitised Thesis from Trinity College Library you acknowledge that all Intellectual Property Rights in any Works supplied are the sole and exclusive property of the copyright and/or other IPR holder. Specific copyright holders may not be explicitly identified. Use of materials from other sources within a thesis should not be construed as a claim over them.

A non-exclusive, non-transferable licence is hereby granted to those using or reproducing, in whole or in part, the material for valid purposes, providing the copyright owners are acknowledged using the normal conventions. Where specific permission to use material is required, this is identified and such permission must be sought from the copyright holder or agency cited.

Liability statement

By using a Digitised Thesis, I accept that Trinity College Dublin bears no legal responsibility for the accuracy, legality or comprehensiveness of materials contained within the thesis, and that Trinity College Dublin accepts no liability for indirect, consequential, or incidental, damages or losses arising from use of the thesis for whatever reason. Information located in a thesis may be subject to specific use constraints, details of which may not be explicitly described. It is the responsibility of potential and actual users to be aware of such constraints and to abide by them. By making use of material from a digitised thesis, you accept these copyright and disclaimer provisions. Where it is brought to the attention of Trinity College Library that there may be a breach of copyright or other restraint, it is the policy to withdraw or take down access to a thesis while the issue is being resolved.

Access Agreement

By using a Digitised Thesis from Trinity College Library you are bound by the following Terms & Conditions. Please read them carefully.

I have read and I understand the following statement: All material supplied via a Digitised Thesis from Trinity College Library is protected by copyright and other intellectual property rights, and duplication or sale of all or part of any of a thesis is not permitted, except that material may be duplicated by you for your research use or for educational purposes in electronic or print form providing the copyright owners are acknowledged using the normal conventions. You must obtain permission for any other use. Electronic or print copies may not be offered, whether for sale or otherwise to anyone. This copy has been supplied on the understanding that it is copyright material and that no quotation from the thesis may be published without proper acknowledgement.

Investigating regulation of gene transcription by the Tup1-Ssn6 co-repressor complex in *Saccharomyces cerevisiae*.

Michael Church

Abstract

Transcriptional repression is an important part of gene regulation. In the budding yeast *Saccharomyces cerevisiae* the Tup1-Ssn6 corepressor complex is recruited to gene promoters to repress transcription in response to nutrient depletion, DNA damage and numerous other signals. One gene under transcriptional control of Tup1-Ssn6 is *FLO1*, which encodes a lectin-like cell wall protein known as a flocculin. *FLO1* is a model for gene regulation in the context of chromatin. The current model for Tup1-Ssn6-mediated repression dictates that Tup1p promotes repression, while Ssn6p acts as an adaptor between Tup1 and the target gene. The aim of this project is to (i) elucidate the contribution of the Tup1p and Ssn6p subunits of the complex to gene repression, and (ii), investigate Tup1-Ssn6 activity in the context of *FLO1* gene regulation. The results will help elucidate the precise mechanism of action of gene repression by the evolutionary conserved Tup1p-Ssn6p corepressor complex.

Investigating regulation of gene transcription by the Tup1-Ssn6 co-repressor complex in *Saccharomyces cerevisiae*

A dissertation presented for the degree of Doctor of Philosophy, in the Faculty of Science, University of Dublin, Trinity College.

May 2015 by

Michael Church

Department of Microbiology

Moyne Institute of Preventive Medicine

Trinity College Dublin

Ph.D. Genetics & Microbiology

Declaration

I, Michael Church, certify that the experimentation recorded herein represents my own work, unless otherwise stated in the text and has not been previously presented for a higher degree at this or any other University. This thesis may be lent at the discretion of the Librarian.

Summary

Eukaryotic genomes exist in the context of chromatin, a structure which not only efficiently packages the DNA, but also plays an important role in regulating transcription. The basic repeating unit of chromatin is the nucleosome, which consists of 147 base pairs of DNA wrapped around a histone core octamer. Nucleosomes are considered to have a negative role in gene transcription, though these dynamic structures can be modified or manipulated in order to regulate gene expression. Tup1-Ssn6 (Cyc8-Tup1) is an evolutionarily-conserved co-repressor complex found in the yeast *Saccharomyces cerevisiae* which is involved in repression of gene transcription. This complex mediates transcriptional repression in a chromatin-dependent manner, either by preventing recruitment of factors that activate transcription or by propagating a repressive chromatin structure over important regulatory elements at target genes. One gene under the transcriptional control of Tup1-Ssn6 is *FLO1*, whose expression confers a cell aggregation phenotype known as flocculation. *FLO1* is a model for chromatin-mediated gene regulation as the *FLO1* promoter contains an array of ordered nucleosomes which is disrupted upon loss of Tup1-Ssn6. *FLO1* is not transcribed in laboratory *S. cerevisiae* strains due to a mutation in its activator. The aim of this project was to (i) elucidate the contribution of the Tup1p and Ssn6p subunits of the complex to gene repression, and (ii), investigate the mechanism of action of the Tup1-Ssn6 complex at the *FLO1* gene.

The relative contributions of Tup1p and Ssn6p were analysed by assessing phenotypes of *tup1* and *ssn6* mutants grown under a number of conditions. It was found that there were striking phenotypic differences between these strains, especially in their response to cellular stress. Previously published and unpublished data was also analysed, and it was found that Tup1p and Ssn6p

contribute differently to repression at a number of genes, including the model gene *FLO1.* At *FLO1*, this difference could be explained by Ssn6p occupancy at the *FLO1* promoter in the absence of Tup1p where it may prevent *FLO1* promoter histone acetylation.

The histone acetyltransferases (HATs) that confer acetylation at the *FLO1* promoter were identified as Gcn5p and Sas3p; it was found that loss of these HATs dramatically reduced *FLO1* de-repression in the absence of Ssn6p. Lysine residue 14 of histone H3 was identified as the target of Gcn5p- and Sas3p-dependent acetylation which was required for *FLO1* de-repression.

A kinetic analysis of *FLO1* de-repression was carried out using the anchor away technique, which creates a conditional mutant of a nuclear protein of interest. By depleting Ssn6p using this technique, a timeline of events leading up to *FLO1* de-repression was established. This analysis demonstrated that histone acetylation played the key role in *FLO1* transcription, and not nucleosome depletion at the *FLO1* promoter, which was not sufficient in itself for activation of *FLO1.* Finally, the activator of *FLO1,* Flo8p, was restored in a laboratory strain and chromatin remodelling at the *FLO1* promoter was monitored to elucidate the role of Flo8p in de-repression of *FLO1.*

Taken together, this work provides an insight into Tup1-Ssn6 function, both on a global scale and in the context of the model *FLO1* gene and demonstrates the complexity and adaptability of this complex.

Acknowledgements

A huge thank you to my supervisor Alastair Fleming, for giving me the opportunity to study an interesting subject and for the support, advice and enthusiasm over the course of this project. Thank you to my lab-mates Suzanne and Conor for the fantastic company, constructive criticism and help in writing the thesis. Thank you to Sari Pennings and her team, for welcoming me to her lab in Edinburgh and giving me the opportunity to study in a new environment.

Thank you to members of the Moyne past and present for providing help, good conversation and occasionally materials over the last four years. Thanks also to the Moyne Technical staff and administrators Jayne and Caroline, without whom the department wouldn't function. Many thanks to my thesis committee(s) Ursula, Joan, Gus and Jay for helpful suggestions over the project.

Thanks also to my parents Michael and Mary, and brothers Aidan and Conor for their support, both psychological and financial when I needed it over the years. Special thanks to my grandad, Charlie and mother in-law Fran for their support over the years also. Thanks to my wife, Jenn, for her support over the last few years and for her boundless patience during the times when the experiment was only supposed to take another fifteen minutes.

Index of Figures

List of Tables

Table of Contents

Chapter 1

Introduction

1.1 Overview

The properties of DNA provide instructions for the synthesis of RNA and protein. The synthesis of RNA by RNA polymerase complexes allows the DNA "code" to be expressed such that specific DNA sequences give rise to unique RNAs which may have inherent roles themselves, or can be translated into proteins.

In yeast, transcription can be carried out by three RNA polymerases, RNA pol I, II and III. Although each RNA polymerase synthesises RNA in a similar manner, each has their own specificity. RNA polymerase I transcribes genes encoding the ribosomal RNA precursors (rRNAs), and RNA polymerase III transcribes the tRNAs and other small RNAs. RNA pol II on the other hand synthesises micro RNAs (miRNAs), most small nuclear RNAs (snRNAs) and transcribes the protein encoding genes into mRNAs.

Initiation of transcription by RNA polymerase II (RNAPII) first involves the binding of transcription factors (activators) upstream of target genes. This binding occurs in important regulatory regions and is required for subsequent gene transcription. The next step in transcription initiation is the assembly of the RNA polymerase complex at the gene promoter. The pre-initiation complex is formed at the core promoter, and the DNA is melted to allow access to the single stranded template by the polymerase. The carboxy-terminal domain (CTD) of Pol II is then phosphorylated and transcription is initiated. The phosphorylated CTD also recruits factors required for elongation and mRNA processing (B. Li et al., 2007).

However, DNA does not exist in isolation within cell nuclei. All transcription in eukaryotic cells takes place in the context of chromatin. Chromatin is the nucleoprotein complex that makes up chromosomes. The basic repeating unit of chromatin is the nucleosome. Nucleosomes contain the core histones, H2A, H2B,

H3 and H4. Each nucleosome consists of a single histone $(H3\text{-}H4)_2$ tetramer and two H2A-H2B dimers around which is wrapped 146 or 147 bp of DNA (Thomas and Kornberg, 1975; Richmond and Davey, 2003). This structure is generally considered repressive to gene transcription, as nucleosomes present a physical barrier to the transcription machinery and prevent initiation by RNAP II (Knezetic and Luse, 1986). However, this barrier to gene transcription can be overcome by the post-translational modification of histones and by eviction or remodelling of promoter nucleosomes by chromatin-remodelling complexes (Cote et al., 1994; Brownell and Allis, 1996; Yu et al., 2015).

The best characterised post-translational histone modification was acetylation of the amino-terminal (N-terminal) tail of histones by histone acetyltransferases (HATs). This modification is known to have a positive role in transcription. One of the first characterised HAT complexes is SAGA, which contains the Gcn5p acetyltransferase (Grant et al., 1997). SAGA is involved in activation of many stress-response genes in yeast and is highly conserved between yeast and multicellular organisms. It has been proposed that acetylation of promoter histones by SAGA and other acetyltransferase complexes causes de-repression of target genes by altering the charge of the histone thereby loosening nucleosome-DNA contacts and bringing about a more open promoter chromatin structure that is amenable to transcription (Workman and Kingston, 1998).

Another method by which transcriptional repression can be overcome is the remodelling of promoter nucleosomes by ATP-dependent remodelling complexes. The first of these complexes to be described was the Swi-Snf complex of *Saccharomyces cerevisiae* (Winston and Carlson, 1992). Swi-Snf is another example of a highly conserved complex found in yeast that is also important for gene regulation in mammals. Swi-Snf evicts nucleosomes from

gene promoters in an ATP-dependent manner, leading to an open chromatin configuration which is conducive to gene transcription. Conversely, ATP-dependent chromatin remodelling complexes can also have a repressive role, such as the ISW2 chromatin remodelling complex. ISW2 positions nucleosomes over gene promoters and creates an ordered nucleosomal landscape that prevents gene transcription (Zhang and Reese, 2004).

Both the SAGA and Swi-Snf complexes were first characterised in *Saccharomyces cerevisiae*, which is an important model organism for studying eukaryotic gene transcription. These complexes regulate a wide variety of genes involved in stress response, mating, carbon source utilisation or other processes where rapid de-repression of genes is required. Acting antagonistically to these activating complexes at many genes is the Tup1-Ssn6 (Cyc8) co-repressor complex. Tup1-Ssn6 was the first co-repressor complex characterised and is involved in repression of a wide variety of genes in *S. cerevisiae* (DeRisi et al., 1997; K. Chen et al., 2013). Tup1-Ssn6 does not bind DNA directly, but instead is recruited to target gene promoters by DNA-binding transcription factors (Treitel and Carlson, 1995). Tup1-Ssn6 is involved in repressing transcription of mating, stress response and carbon source utilisation genes in *S. cerevisiae*, and has a role in regulation of virulence factors in other fungal species (J. E. Lee et al., 2015).

One gene under the transcriptional control of Tup1-Ssn6 is *FLO1*, expression of which causes a flocculent phenotype. Flocculation is the non-sexual, calcium-dependent cell aggregation displayed by cells expressing flocculins on the cell walls. Flocculation provides defence against cellular stress, though most laboratory strains do not exhibit this phenotype (H. Liu et al., 1996). *FLO1* is the major flocculin-encoding gene in *S. cerevisiae* and has been studied as a model

for chromatin-mediated gene regulation, as the *FLO1* promoter region contains a well-ordered nucleosomal array which is disrupted upon loss of Tup1-Ssn6 (Fleming and Pennings, 2001). The interplay between important regulators of yeast gene transcription and chromatin remodelling observed at the *FLO1* gene promoter makes *FLO1* an attractive model gene for the study of chromatin-mediated gene regulation.

1.2. Chromatin

Eukaryotic cells contain large amounts of DNA that is contained within a small space. This DNA is packaged with proteins in a structure known as chromatin (B. Li et al., 2007). At the most basic level, chromatin consists of 147 base pairs (bp) of DNA wrapped around a core histone octamer. This structure is known as a nucleosome. Nucleosomes appear as "beads" along a DNA "string" when viewed on an electron microscope (Thoma et al., 1979). These nucleosomes form higher-order structures and fibres that come together to form chromosomes. There are two types of chromatin present in eukaryotic cells; heterochromatin and euchromatin. Heterochromatin is dense, prohibitive to gene transcription and is generally found near the centromere or sub-telomeres and DNA located in these regions is considered to be silent (Elgin, 1996). Euchromatin is less densely packed than heterochromatin and is located in areas of the chromosome where active transcription takes place (International Human Genome Sequencing, 2004).

Genes can broadly be divided into two categories; housekeeping genes and stress response genes (Rando and Winston, 2012). These different gene groups have distinct functions and promoter structures, in addition to different methods of regulation. Housekeeping genes are required for cell growth and are involved

in basic cellular function. These genes are constitutively expressed, though may be down-regulated during cellular stress. Housekeeping genes are generally activated by TFIID, not SAGA, and their promoters do not contain a TATA box. The structure of housekeeping gene promoters is conserved between genes; their promoters have a well-defined nucleosome-free region flanked by two well-positioned nucleosomes and, in *S. cerevisiae*, the +1 nucleosome is positioned over the transcription start site (TSS) of the gene (Figure 1.1).

In contrast to housekeeping genes, stress response genes are not constitutively expressed and instead are de-repressed in response to cellular stress, including hypoxia, starvation or heat/cold shock. Stress response genes generally contain a TATA box and are activated by the SAGA complex (Proft and Struhl, 2002). Stress response genes also contain a dense nucleosomal array upstream of the TSS which occludes important regulatory elements under repressive conditions. However, transcriptional activators may compete for DNA binding sites with promoter nucleosomes giving rise to low level or "noisy" gene transcription under repressing conditions (Rando and Winston, 2012).

Both housekeeping genes and stress-response genes display well-characterised nucleosome occupancy upstream of the TSS (Fig. 1.1). It has been shown that in addition to *trans*-acting factors such as ATP-dependent chromatin remodelling complexes, intrinsic properties of the promoter DNA can influence nucleosome positioning upstream of the TSS. The *HIS3* gene in *S. cerevisiae* has been used as an example of this phenomenon, with the divergent *HIS3-PET56* promoter region containing a large NFR whose DNA was found to be intrinsically resistant to nucleosome occupancy (Sekinger et al., 2005). It has also been shown that for a given length of DNA, there are limited nucleosome distribution patterns. This ordering of nucleosomes is known as "statistical positioning", and could account

for the ordered nucleosome arrays found at some gene promoters (Kornberg and Stryer, 1988).

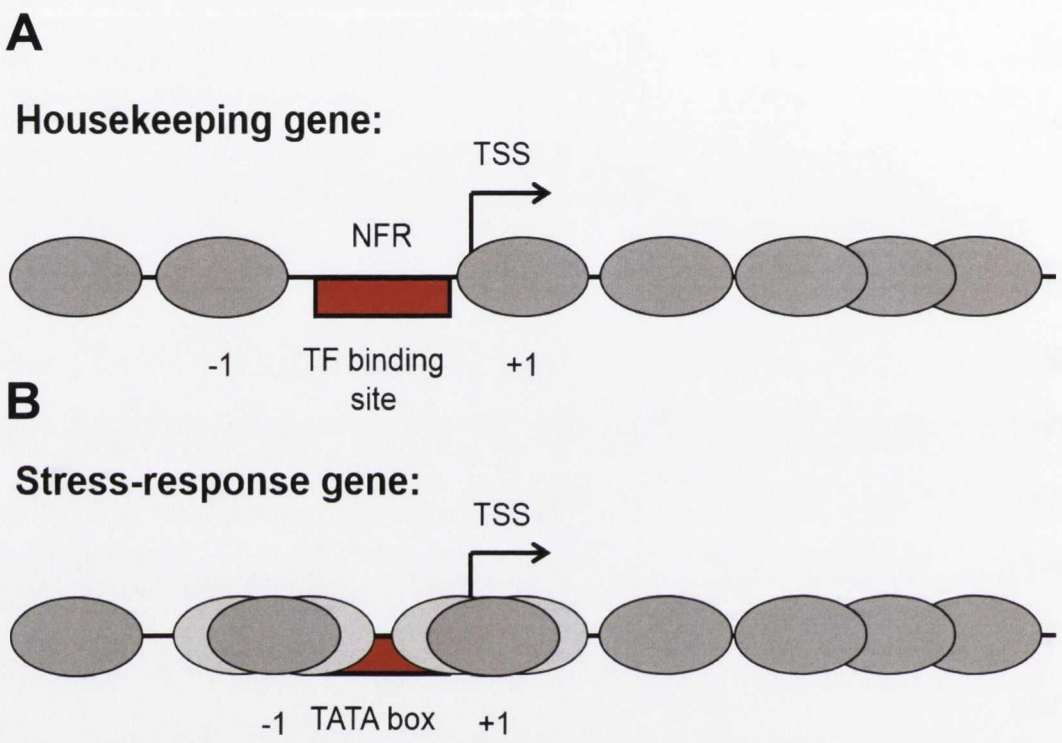

Figure 1.1. Promoter architecture of housekeeping genes vs stress genes. (A) Housekeeping gene promoters contain well-positioned -1 and +1 nucleosomes flanking a nucleosome-free region (NFR) that contains binding site(s) for transcription factors (TF) required for gene regulation. Nucleosomes downstream of the transcription start site (TSS) are less well-positioned than promoter nucleosomes. (B) Stress-response gene promoters contain a TATA box which is required for gene activation, but which may be occluded by nucleosomes depending on conditions within the cell. -1 and +1 nucleosome positions are less well defined than at housekeeping gene promoters (Rando and Winston, 2012).

1.2.1. Nucleosomes

The basic repeating unit of chromatin is the nucleosome. Nucleosomes consist of a core histone octamer which contains a single $(H3\text{-}H4)_2$ tetramer and two H2A-H2B dimers around which is wrapped 147 bp of DNA (Thomas and Kornberg, 1975; Richmond and Davey, 2003) (Figure 1.2). There is also a variant histone H2A present in *S. cerevisiae* known as H2A.Z which is generally found in the +1 nucleosome of some genes (Zlatanova and Thakar, 2008). Nucleosomes are separated by 10-90 bp of linker DNA which gives chromatin the appearance of "beads on a string". Histones contact the phosphate backbone of DNA every ~10.4 bp, which means there are 14 contact points between histones and DNA in the nucleosome, making this structure extremely stable (Luger et al., 1997). This stable histone-DNA interaction makes DNA inaccessible to the general transcription machinery, and nucleosomes have been shown to have a repressive effect on gene transcription *in vitro* (Knezetic and Luse, 1986).

Nucleosomes were also shown to have a negative effect on gene transcription *in vivo*, with cells depleted of histone H4 showing activation of the *PHO5* promoter under *PHO5*-repressing conditions (Han et al., 1988). In the case of *PHO5*, it was shown that important activator binding-sites were occluded by promoter nucleosomes which were exposed upon loss of histones from the *PHO5* promoter. Inserting these sites in a nucleosome-free region upstream of *PHO5* caused significant de-repression under *PHO5*-repressing conditions, confirming that it was by occlusion of these sites that promoter nucleosomes prevented *PHO5* activation. However, this study also found that even when occluded by nucleosomes, high-affinity regulatory regions could allow activating transcription

factors to compete with nucleosomes for DNA binding and de-repress *PHO5* under repressing conditions (Lam et al., 2008).

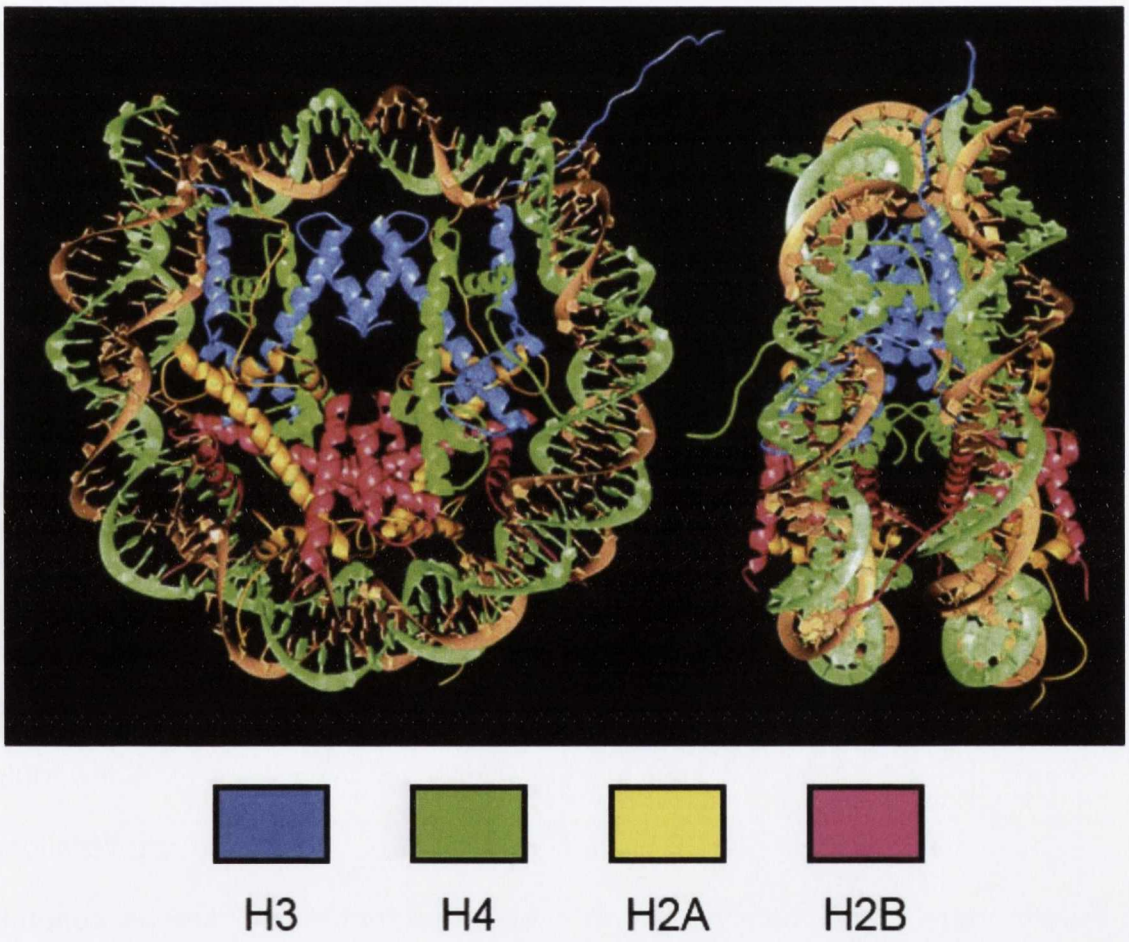

Figure 1.2. The structure of the core nucleosome. High-resolution crystal structure of the nucleosome (Luger et al., 1997). This image shows the 14 DNA-histone contacts that give rise to the stable nucleosome. Shown here is a DNA fibre wrapped around a tetramer of H3 (blue) and H4 (green) and two H2A (yellow) – H2B (pink) dimers. Histone tails can be observed protruding from the nucleosome. Figure adapted from Luger *et al* (1997).

1.2.1.1. Post-translational modification of histones

Histones are small proteins (11.3kDa-15.4kDa) that contain a globular domain and an N-terminal tail (Fig. 1.2). Both globular domains and tails are subject to post-translational modification, including methylation of arginine (R) residues, phosphorylation of serine and threonine residues and methylation, ubiquitylation, acetylation, ADP-ribosylation and sumolation of lysine (K) residues. These modifications have different effects on nucleosome structure and can affect all aspects of gene regulation, including transcriptional initiation, elongation and repression (Allfrey and Mirsky, 1964; J. S. Lee and Shilatifard, 2007; Magraner-Pardo et al., 2014).

Acetylation of N-terminal histone tails is the best characterised histone modification, and has long been associated with gene activation. Acetylation has been shown to neutralise the positive charge of the histone tails, thereby weakening histone-DNA contacts promoting a chromatin template more permissive to transcription (Hong et al., 1993). Acetylated histone tails can also be recognised by factors that remodel chromatin resulting in displacement of nucleosomes, which can lead to gene activation (Awad and Hassan, 2008). Conversely, hypoacetylated histone tails can be bound by transcriptional repressors. Thus, removal of the acetyl mark on histone tails is generally associated with transcriptional repression (Edmondson et al., 1996).

Some histone modifications recruit factors that influence gene transcription. For example, methylation of H3K36 in gene coding regions by the Set2p histone methyltransferase (HMT) during transcriptional elongation recruits the Rpd3S histone deacetylase (HDAC). (J. S. Lee and Shilatifard, 2007). Subsequent removal of the activating acetyl mark from H3 by Rpd3S then prevents spurious

transcription from occurring at internal gene sites by establishing a repressive chromatin structure.

Histone modifications can also affect other histone modifications. For example, histone H2B ubiquitylation (H2Bub) is required for the methylation of lysines 4 and 79 of histone H3 (H3K4me and H3K79me) (Nakanishi et al., 2009).

1.2.1.1.1 Histone acetylation

Histone acetylation was first implicated in gene regulation over fifty years ago (Allfrey and Mirsky, 1964). All core histones in yeast can be acetylated, and this acetyl mark is generally regarded as having a positive role in transcription. Histones H3 and H4 have been extensively studied for their acetyl marks and the impact they have on gene transcription. H3 is acetylated at residues K4, K9, K14, K18, K23 and K56, whereas H4 is acetylated at residues K5, K8, K12, K16 and K20 (Figure 1.3) (Rando and Winston, 2012). Acetylation at different residues can have different effects on gene transcription and is associated with different stages of gene activation. For example, H3K14ac is associated with transcriptional activation and has been found to have a role in DNA repair following UV damage (Duan and Smerdon, 2014). This is in contrast to another acetyl mark (H3K56ac), which is associated with transcriptional elongation as well as nucleosome dynamics during DNA replication and DNA repair (Krebs, 2007; Varv et al., 2010)Williams, 2008 #244}. The factors that confer these acetyl marks display distinct specificity which is summarised in Table 1.1. The specificity of histone-modifying enzymes in conjunction with the different acetylation sites gives histone acetylation the potential for great flexibility in gene regulation.

The factors that confer the acetyl mark on histone tails are known as histone acetyltransferases (HATs). One of the best characterised and most important

HATs in *S. cerevisiae* is Gcn5p. Gcn5p is the catalytic subunit of the ADA, SAGA and SLIK acetyltransferase complexes. It modifies N-terminal lysines on histones H2B and H3, and has also been found to post-translationally modify the ATP-dependent chromatin remodeller Swi-Snf, which has a role in regulating nucleosome remodelling at target gene promoters (J. H. Kim et al., 2010). The SAGA acetyltransferase complex in yeast is a large, multi-subunit complex composed of fifteen non-essential and six essential components. The integrity of the SAGA complex relies on Ada1p, Spt7p and Spt20p (Sterner et al., 1999). The acetyltransferase activity of SAGA resides within the Gcn5p subunit, but full HAT activity by Gcn5p also requires the Ada2p subunit (Grant et al., 1997; Syntichaki and Thireos, 1998). SAGA is required for activation of a large subset of stress-response genes in *S. cerevisiae*, and this highly-conserved complex is also important for gene regulation in *Drosophila* and mammalian cells (Wang and Dent, 2014). The subunits of these Gcn5p-containing complexes and NuA3 are shown in Figure 1.4.

Esa1p is another important acetyltransferase in *S. cerevisiae*. Esa1p functions within the NuA4 complex, where it acetylates residues on histones H2A, H2A.Z, H2B and H4 (Allard et al., 1999; Rando and Winston, 2012). *ESA1* is an essential gene due to the requirement for H4 acetylation in cell cycle progression(Clarke et al., 1999). Both Gcn5p and Esa1p can function outside of the SAGA/SLIK/ADA and NuA4 complexes. This activity has been shown to be non-targeted and essential for re-entry into the cell cycle by quiescent cells (Friis et al., 2009).

Another less well-characterised HAT in *S. cerevisiae* is Sas3p, which is part of the NuA3 acetyltransferase complex (Figure 1.5). Sas3p acetylates lysines 14, and to a lesser extent 23 of H3. This is in contrast to Gcn5p, which was shown to acetylate K9, 14, 18 and 23 of H3 in the same study (Howe et al., 2001). A *sas3*

mutant does not display as severe a phenotype as other HAT mutants, but *gcn5 sas3* double mutants are non-viable. It has been shown that similar to the role of Esa1p in regard to histone H4, this loss of viability in *gcn5 sas3* mutants is due to the requirement for these HATs in cell cycle progression, with the role of Sas3p and Gcn5p being redundant in this respect. Gcn5p and Sas3p have also been shown to be recruited to similar genes, and deletion of *SAS3* in conjunction with loss of the *ADA2* gene which disables the SAGA/ADA/SLIK complexes while retaining non-targeted Gcn5p function leads to a global loss of H3K14ac (Rosaleny et al., 2007; Maltby et al., 2012).

In addition to HATs which confer an acetyl mark on histones and are associated with gene activation, protein complexes known as histone deacetylases (HDACs) remove this mark from histone tails and are associated with gene repression. There are at least 10 HDACs in yeast grouped into three classes (X. J. Yang and Gregoire, 2005). Class I HDACs include Rpd3p, Hos1p and Hos2p, and Class II HDACs include Hda1p and Hos3p (X. J. Yang and Gregoire, 2005). Hda1p and Rpd3p have been shown to deacetylate all acetylated sites in histones H3 and H4 (Rundlett et al., 1996). These two latter HDACs have been shown to interact with transcriptional co-repressors such as the Tup1-Ssn6 complex where they function to de-acetylate gene promoter nucleosomes and repress transcription (Davie et al., 2003; Fleming et al., 2014). HDAC activity can be both targeted and un-targeted as in the case of Rpd3p, which is recruited to the *INO1* gene by the repressor Ume6p (Kurdistani et al., 2002). However, Rpd3p is also found bound to chromatin when Ume6p is absent, indicating that the HDAC also acts non-specifically (Kurdistani et al., 2002).

Sir2p is an example of a Class III HDAC which de-acetylates histones in an NAD^+-dependent manner(Blander and Guarente, 2004; X. J. Yang and Gregoire, 2005).

Sir2p is an important factor in silencing of mating type loci, telomeres, and has important roles in maintaining genome stability and ageing (Rine et al., 1979; Rine and Herskowitz, 1987; O. M. Aparicio et al., 1991). Deacetylation of telomeric chromatin by Sir2p allows additional Sir complexes to bind telomeric chromatin and spread until an entire chromatin region is silenced (Rusche et al., 2003). These important functions have made mammalian Sir proteins and HDACs targets for clinical therapies, with HDAC inhibitors being used to treat cancer, neurodegeneration, inflammation, and metabolic disorders (Micelli and Rastelli, 2015).

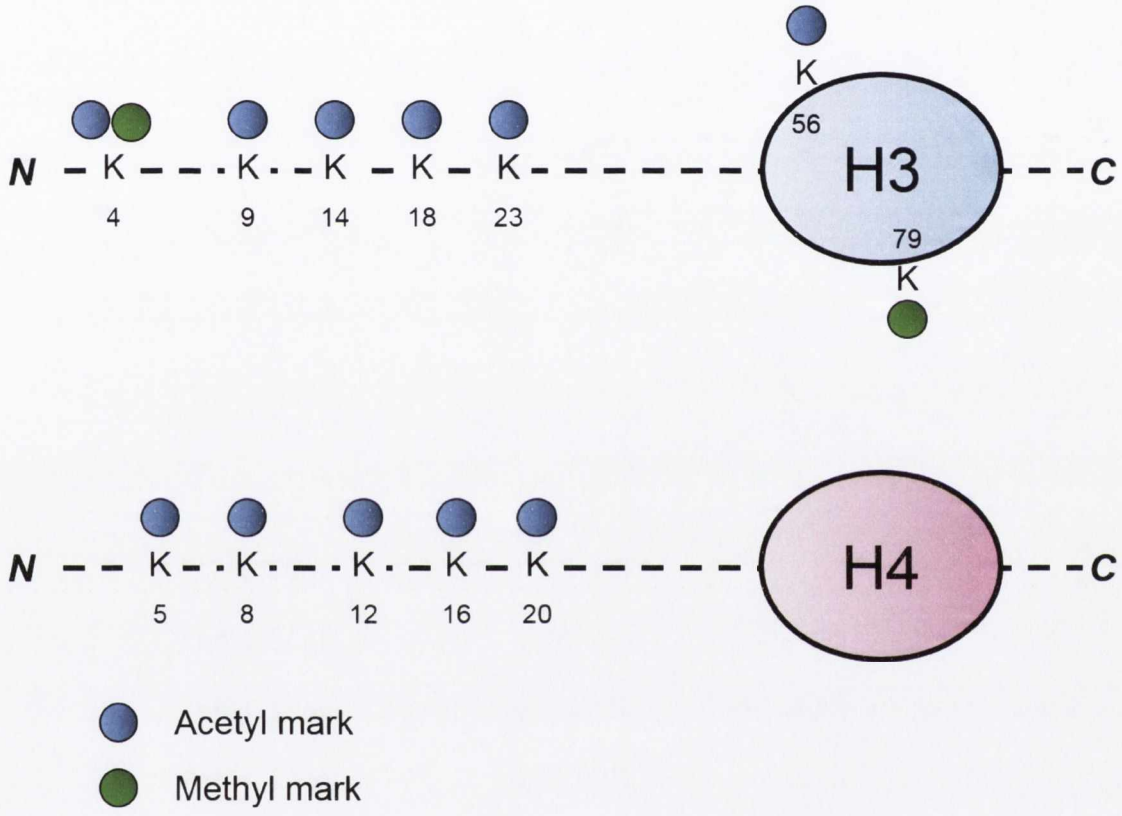

Figure 1.3. Lysine acetylation and methylation of histones H3 and H4. Residues on both N- and C-terminal tails and globular domains of histones are the target of post-translational modifications. Highlighted here are lysine residues known to be acetylated (blue) and methylated (green) on histones H3 and H4. Adapted from data in (Rando and Winston, 2012).

Histone	Acetylated Residue	HAT(s)	HDAC(s)
H2A	K5	Esa1	Rpd3
	K8	Esa1, Hat1	Rpd3
H2A.Z	K3	Esa1	
	K8	Esa1	
	K10	Esa1	
	K14	Esa1	
H2B	K11	Esa1	
	K16	Gcn5, Esa1	Rpd3
H3	K4	Rtt109, Gcn5	Rpd3, Hda1
	K9	Gcn5	Hos2, Hda1
	K14	Gcn5, Sas3	Hos2, Hda1
	K18	Gcn5	Hos2, Hda1
	K23	Gcn5	Hos2, Hda1
	K56	Rtt109	Hst3, Hst4
H4	K5	Esa1	Rpd3, Hos2
	K8	Esa1	Rpd3, Hos2
	K12	Esa1	Rpd3, Hos2
	K16	Esa1, Sas2	Sir2, Hos2, Hst1
	K20	Esa1, Sas2	Sir2, Hos2, Hst1

Table 1.1. HAT and HDAC specificity in yeast. Table adapted from data in review by Rando and Winston (2012) (Howe et al., 2001; Guillemette et al., 2011; Rando and Winston, 2012)

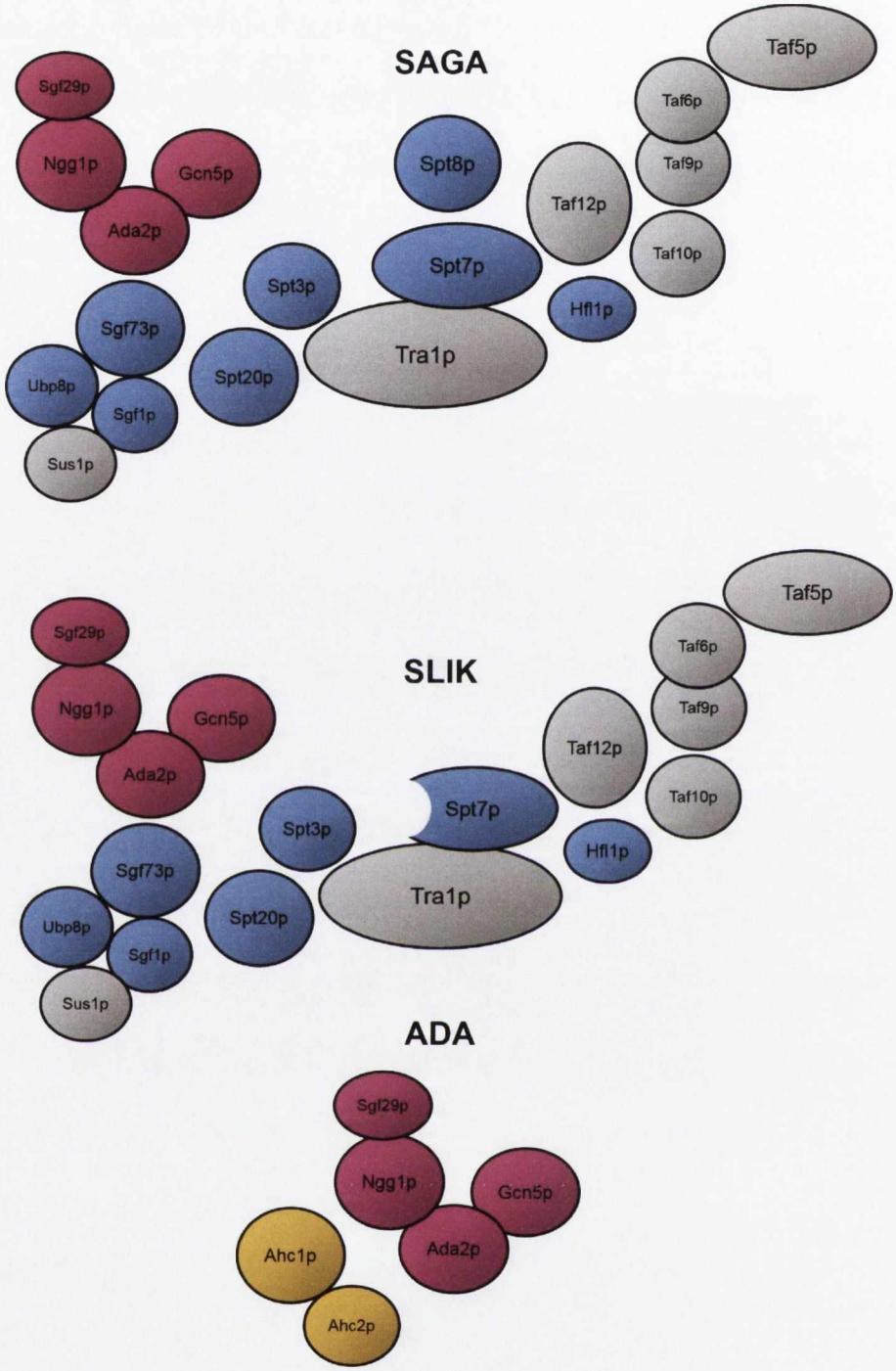

Figure 1.4. Gcn5p-containing acetyltransferase complexes. The three Gcn5p-containing complexes in *S. cerevisiae* are SAGA, SLIK and ADA. Shown here are essential proteins for cell viability (grey) and the HAT domain (pink) which is required for acetyltransferase activity. SLIK contains a truncated Spt7p and lacks Spt8p. Ahc1p and Ahc2p are unique to ADA (adapted from (Gaupel et al., 2014).

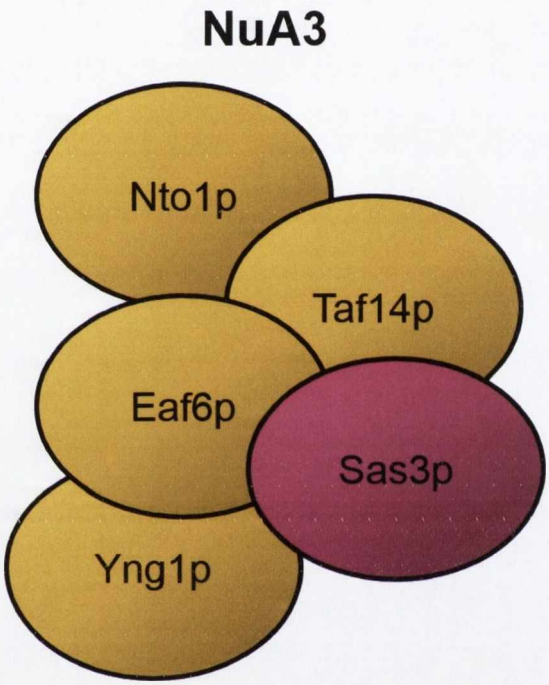

Figure 1.5. The NuA3 acetyltransferase complex. Schematic of the NuA3 acetytransferase complex containing the subunits Eaf6p, Taf14p, Yng1p, Nto1p and Sas3p, which is the catalytic HAT in the complex (adapted from (Lafon et al., 2007))

1.2.1.2 ATP-dependent chromatin remodelling

Chromatin is required for packaging the eukaryotic genome, and post-translational modification of nucleosomes provides platforms throughout the genome for factors that influence transcription, DNA damage repair, replication and a host of other processes. However, chromatin is not a static structure, and to enable all of the processes that are integral to cell viability, nucleosomes must be deposited, evicted or otherwise moved along the DNA template. This work, or remodelling, is carried out in a large part by ATP-dependent chromatin remodelling complexes. In mammals, chromatin remodelling complexes can act in a tissue-specific manner and are involved in development, with mutations affecting these complexes being implicated in oncogenesis(Rando and Winston, 2012).

There are several ATP-dependent chromatin remodellers found in yeast, and these complexes are utilised in many cellular processes (reviewed in (Clapier and Cairns, 2009). ATP-dependent remodelling complexes also function following DNA replication to establish a nucleosomal array on nascent DNA (Fyodorov et al., 2004). Chromatin remodelling is also required to expose important *cis* elements such as the TATA box at gene promoters to allow transcription initiation to occur (Venter et al., 1994; L. Wu and Winston, 1997; Kent et al., 2001). Chromatin remodellers can also eject or chaperone the nucleosomes ahead of the advancing RNA polymerase during transcription elongation. In addition, during DNA repair and recombination, specialised chromatin remodellers such as INO80 expose lengths of DNA by nucleosome eviction or sliding so that repair/recombination can take place (Tsukuda et al., 2005).

Much research has been performed into investigating how ATP-dependent chromatin remodelling complexes function, and a model of their mechanism of action has been proposed (Whitehouse et al., 1999). ATP-dependent chromatin remodelling complexes function by first binding to and anchoring the nucleosome (Figure 1.6B). The DNA-binding domain (DBD) of the complex binds to the linker DNA outside of the nucleosome and a translocation domain/remodeller ATPase (Tr) generates a small loop (or wave) that propagates along the nucleosome surface. When the DNA loop is formed, the remodeller undergoes a conformational change (ratchet), and the DNA is translocated through the Tr domain. This DNA loop propagates until the nucleosome has moved along the DNA template and the remodeller resets its conformation with original binding contacts, but further along the DNA. This model for translocation of nucleosomes by ATP-dependent nucleosome remodelling complexes is known as the wave-ratchet-wave model. Shifting the position of promoter nucleosomes has the potential to expose sites important for gene regulation, or to occlude such sites. It is in this way that ATP-dependent chromatin remodelling has a dramatic impact on gene expression in eukaryotes. It has been proposed that nucleosome eviction occurs when remodelling complexes such as Swi-Snf translocate one nucleosome into space occupied by another nucleosome, causing an H2A-H2B dimer from the downstream nucleosome to be lost first, and eventually the entire nucleosome is evicted (Dechassa et al., 2010; N. Liu and Hayes, 2010).

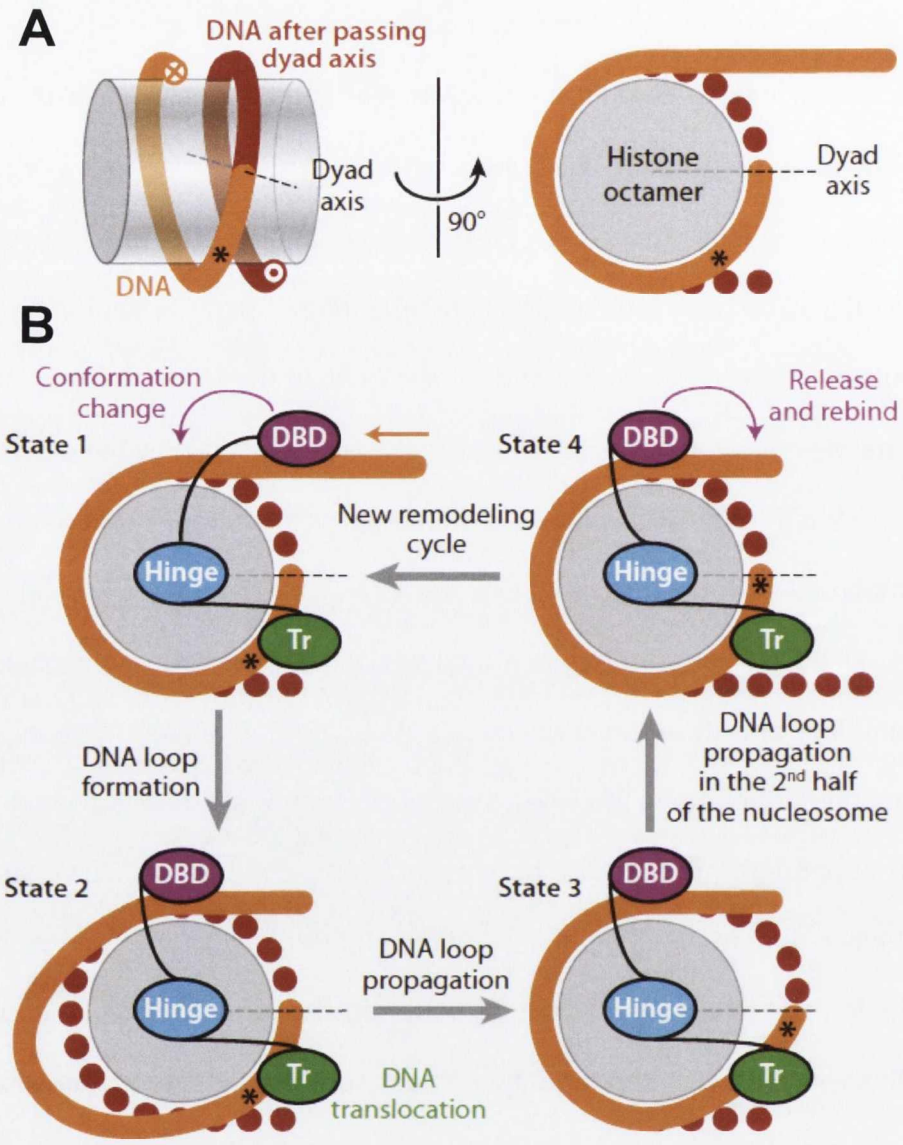

Figure 1.6. Mechanism of ATP-dependent chromatin remodelling. (A) Illustration of DNA wrapped around the histone core octamer. (B) Mechanism of action of an ATP-dependent chromatin remodelling complex using the wave-ratchet-wave model. First, the DNA-binding domain (DBD) binds linker DNA. Then, the ATPase or translocation domain (Tr) induces a conformational change in the complex which causes propagation of a DNA loop around the nucleosome. The loop continues past the Tr domain and the remodeller can than release and re-bind the nucleosome after translocation. From Clapier and Cairns (2009)(Bazett-Jones et al., 1999; Whitehouse et al., 1999).

1.2.1.2.1. Swi-Snf

The first chromatin remodelling complex discovered was found in the yeast *S. cerevisiae* (Peterson et al., 1994). This complex was named Swi-Snf after the phenotypes exhibited by mutants of the complex sub-units. Cells without Swi-Snf function are impaired for mating type switching (SWItching defective) and are unable to metabolise sucrose (Sucrose Non-Fermentable) due to an inability of these mutants to de-repress genes involved in mating and the invertase-encoding gene *SUC2*, respectively (Neigeborn and Carlson, 1984; Stern et al., 1984). Swi-Snf is a large complex (~1.2 MDa) containing multiple subunits (Table 1.2) (K. K. Lee et al., 2004). Snf2p contains the ATPase activity of Swi-Snf and is essential for complex function (Laurent et al., 1993). Early studies established a link between Swi-Snf and chromatin, as suppressors of *snf2* mutations included mutations in *HTA1-HTB1* which encode histones H2A and H2B (Hirschhorn et al., 1992). This study suggested that Swi-Snf activates gene transcription by altering chromatin structure and making important regulatory sites accessible at gene promoters.

In some of the first whole-genome transcriptional studies using micro-arrays, Swi-Snf was shown to control mRNA levels of 2-5% of all genes in *S. cerevisiae* (Holstege et al., 1998; Sudarsanam and Winston, 2000). In addition to its role in activation of *SUC2*, Swi-Snf is also required for activation of the flocculin-encoding gene *FLO1* (Fleming and Pennings, 2001). At both *FLO1* and *SUC2,* Swi-Snf was shown to be required for remodelling of the de-repressed gene promoters which occurred concomitant with gene activation (Gavin and Simpson, 1997; Fleming and Pennings, 2001). Swi-Snf contains a bromodomain in the Snf2p subunit, and this recognises and stabilises interaction between the Swi-Snf complex and acetylated histone H3 (Hassan et al., 2001). This, in addition to

the discovery that *snf2 gcn5* double mutants are either inviable or extremely sick, indicates that histone acetylation and chromatin remodelling by Swi-Snf act together to activate gene transcription (Pollard and Peterson, 1997; Roberts and Winston, 1997). In addition to recognition of acetylated gene promoters by Swi-Snf, the Snf2p subunit is also itself acetylated by Gcn5p, which inhibits Snf2p function and causes dissociation of Swi-Snf from gene promoters (J. H. Kim et al., 2010). In this study, it was found that the HDAC Rpd3p had a positive role on Swi-Snf association with gene promoters, as it deacetylated Snf2p and allowed it to recognise acetylated histones. Thus, acetylation may feed back to Swi-Snf to regulate its occupancy at target promoters

Subunit	Function	Comments
Swi2p/Snf2p	ATPase, contains bromodomain	Core subunit
Snf5p	Complex assembly	Core subunit
Snf11p	Transcriptional activator	
Swp82p	Unknown	
Rtt102p	Unknown	
Snf6p	Structural, DNA-binding	
Swi3p	Complex assembly, recruitment	Core subunit
Arp9p	Promotes Snf2p ATPase activity	Actin-related
Snf12p	Structural	
Swi1p	DNA-binding	
Taf14p	Transcription factor	
Arp7p	Promotes Snf2p ATPase activity	Actin-related

Table 1.2. List of Swi-Snf subunits. List of Swi-Snf subunits and their functions in yeast (adapted from (Sudarsanam and Winston, 2000)

1.3. Transcription

In eukaryotes, transcription is carried out by three RNA polymerases which all function to synthesise RNA in a DNA-dependent manner. RNA polymerase I is mainly concerned with transcription of ribosomal RNA (rRNA) genes (Clos et al., 1986). RNA polymerase III is responsible for transcription of tRNA genes which are involved in translation, as well as 5S rRNA genes (Weinmann and Roeder, 1974). However, most protein-encoding genes are transcribed by RNA polymerase II (RNAPII) and it is this polymerase which will form the main focus of this work.

Gene transcription by RNA Pol II occurs in three steps: initiation, elongation and termination. Transcription initiation involves the ordered assembly of the general transcription factors (GTFs) TFIID, TFIIA, TFIIB, TFIIE, TFIIF, TFIIH and RNAPII at the gene promoter which together form the pre-initiation complex (PIC). Following PIC formation transcription elongation occurs whereby RNA Pol II repeatedly traverses the gene coding region catalysing the DNA-dependent addition of nucleotides to form the full-length mRNA. Transcription termination is the final step in the process, in which the mRNA is cleaved at the 3 end and a poly A tail is added. The mature mRNA is then exported from the nucleus to the ribosome where it will be translated into amino acids, which form proteins.

1.3.1 The core promoter.

Gene promoters are DNA sequences upstream of genes that promote transcription (Butler and Kadonaga, 2002). The core promoter encompasses the transcription start site (TSS) and extends ~35 nucleotides (nt) up- or downstream of this site, meaning that most core promoters only include approximately 40 bp of DNA (Butler and Kadonaga, 2002). There are several sequences present in

the core promoter that are important for transcription (Figure 1.7). These include the TATA box, initiator (Inr), TFIIB recognition element (BRE) and down-stream core promoter element (DPE) (Fig.1.7). The orientation of the core promoter is important, as the core promoter determines the direction of transcription (Duttke et al., 2015).

The TATA box is an important element of the core promoter at many stress-response genes, but as stated previously, this is not present at all eukaryotic promoters. In fact, only 20 % of yeast genes contain TATA boxes, whose consensus sequence is TATA(a/t)A(a/t)(a/g) in *S. cerevisiae* (Basehoar et al., 2004). These sequences are recognised by the TATA binding protein (TBP), which also interacts with TFIID and SAGA (Lemon and Tjian, 2000; Agalioti et al., 2002; Hassan et al., 2002). Generally, the TATA box is located about 30 nt upstream of the metazoan TSS and between 40 and 120 bp upstream of the TSS in *S. cerevisiae* (C. Yang et al., 2007). Inr elements contain the TSS, and are found in both promoters containing and lacking a TATA box (Butler and Kadonaga, 2002). The Inr interacts with TFIID, and specifically the factors TAF2 and TAF1, giving it a similar function to the TATA box (Tora, 2002). The DPE is present downstream of the Inr most commonly at genes lacking a TATA box, and is also involved in TFIID-binding whereby TFIID binds co-operatively to the Inr and DPE (Burke and Kadonaga, 1996). Mutation of either the Inr or the DPE disrupts TFIID binding (Burke and Kadonaga, 1996). The DPE is located 28 to 32 bp downstream of the Inr, and this spacing is constant at all known genes that contain a DPE, with alteration of this spacing causing severe reduction in transcription of the genes in question (Burke and Kadonaga, 1997). The BRE is the only well-characterised core promoter element that is bound by TFIIB rather

than TFIID, and is located immediately upstream of the TATA box (Smale and Kadonaga, 2003).

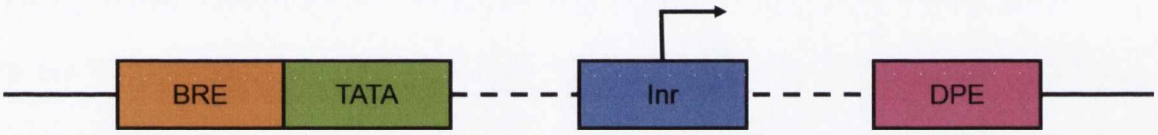

Figure 1.7. The eukaryotic core promoter. The TFIIB recognition element (BRE) is located immediately upstream of the TATA box. The BRE is recognised by the general transcription factor TFIIB. The TATA box is located between 26-31 bp upstream of the TSS in metazoans and 40-100 bp in *S. cerevisiae*. The TATA box is recognised by TBP. The initiator element (Inr) includes the TSS and is recognised by TFIID. The DPE is located 28-32 bp downstream of the TSS and is co-operatively bound by TFIID with the Inr (adapted from (Smale and Kadonaga, 2003)

1.3.1. Transcription initiation.

The control of PIC formation and transcription initiation is a key step in the regulation of gene transcription, and is stimulated by gene-specific activating proteins (activators). These activators generally contain regions that bind to specific promoter elements of target genes. One example of a well-characterised activator is the Gal4p protein. Gal4p is a DNA-binding transcription factor responsible for activation of galactose-induced genes. These genes are repressed when cells are grown in glucose, but are de-repressed during growth in galactose (Nogi and Fukasawa, 1980). *GAL1-10, GAL7* and *GAL80* are all activated by galactose in a Gal4p-dependent manner, and this activation involves disruption of nucleosomes over the TATA box and initiation sites (Lohr, 1997). In the absence of galactose, Gal4p is inactive and bound to the repressor Gal80p, and this was shown to inhibit binding of the TATA-binding protein or TFIIB (Y. Wu et al., 1996). Gal80p also blocks interaction between Gal4p and SAGA/NuA4 (Carrozza et al., 2002). This means that when the activator Gal4p is bound to the repressor Gal80p, both transcription initiation and chromatin modification are blocked. Upon growth in galactose, Gal80p and Gal4p are separated (Figure 1.8). This leaves Gal4p free to activate transcription by recruiting co-activators and the general transcription machinery. These co-activators include SAGA and Swi-Snf, demonstrating the importance of chromatin in gene regulation. It was also shown that in the case of *GAL1*, the Gcn5p acetyltransferase component of SAGA was not required for PIC formation, suggesting that SAGA acts as a scaffold to aid in PIC assembly at the promoter, and not as a HAT (Bhaumik and Green, 2001).

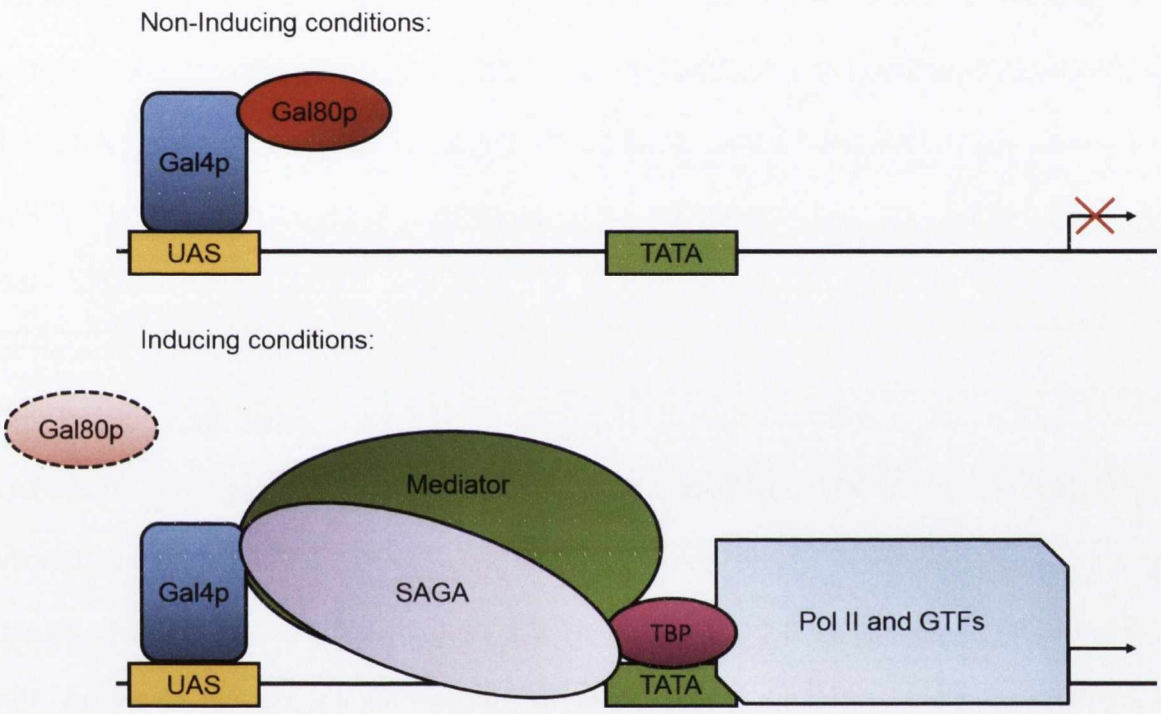

Figure 1.8. Transcriptional activation by Gal4p. Under non-inducing conditions, the Gal4p activation domain is bound by Gal80p, blocking Gal4p activity. On galactose induction (inducing conditions), Gal80p is removed from the Gal4p activation domain, which is then able to recruit the transcriptional machinery (adapted from (Carrozza et al., 2002))

The first step in PIC formation at genes that are regulated by SAGA is binding of the TATA box binding protein (TBP) to the target gene promoter at the TATA box. This leads to assembly of the PIC and recruitment of the RNAPII holoenzyme to the gene promoter. It has been shown that SAGA components Spt3p and Spt8p are required for recruitment of TBP to several SAGA-dependent gene promoters (Bhaumik and Green, 2002). However, these components are not essential for SAGA structural integrity (Sterner et al., 1999; Bhaumik and Green, 2001). Spt3p and Spt8p have been found to inhibit TBP binding at other genes, suggesting that their regulatory role depends on the target gene (Belotserkovskaya et al., 2000). In addition to its structural role in transcription, SAGA's HAT activity also promotes initiation, whereby Gcn5p, Ada2p and Ngg1p (Ada3p) form a catalytic core which acetylate histone H3K9, 14, 18 and 23. Studies have shown the requirement for Gcn5p in recruitment of TBP as well as acetylation at SAGA-regulated promoters (Shukla et al., 2006). SAGA has also been shown to directly recruit RNAPII in addition to its role in TBP recruitment (Qiu et al., 2004). These analyses show that at genes under the transcriptional control of SAGA, the complex can control transcription initiation in a number of ways at different genes. In addition to these activities, SAGA has been shown to interact with the Mediator complex, which is recruited to gene promoters following SAGA recruitment and promotes PIC formation (Bhaumik et al., 2004). Studies have shown that SAGA and Mediator are recruited to several SAGA-dependent promoters by activators such as Gcn4p (Govind et al., 2005; Jedidi et al., 2010). Together, these studies demonstrate that at SAGA-dependent genes, there are multiple paths to transcriptional initiation involving various activators.

Genes not regulated by SAGA include the housekeeping genes, whose promoters do not contain a TATA box, and are instead regulated by TFIID. TFIID

contains TBP and a set of TBP associated factors (TAFs). At promoters that contain a TATA box, TBP is sufficient to activate transcription. However, in the absence of a TATA box such as at housekeeping genes, the TAFs are required for promoter recognition. The TAFs recognise DNA-binding activators at gene promoters, and different TAFs within TFIID are required for transcription at a different subset of genes (M. R. Green, 2000). TAFs have been shown to be required for TBP recruitment to TFIID-regulated genes, while TBP is not required for TAF recruitment to these promoters (X. Y. Li et al., 2000). In contrast to SAGA-regulated genes, Mediator is not required for TBP recruitment to TFIID-regulated genes, though it is essential for transcriptional activation (X. Y. Li et al., 2000).

Once the PIC has formed at the gene promoter, it must escape the promoter in order to initiate transcription. The GTF TFIIH uses its helicase activity to unwind promoter DNA, initiating transcription (M. Lee et al., 2000). TFIIH is the factor responsible for promoter opening and formation of the first phosphodiester bond (Holstege et al., 1996). Before elongation can take place, RNAP II will produce short (2-15 nt) transcripts while bound to the promoter in a process known as abortive initiation. Once transcripts reach a threshold length of ~8-15 nt, RNAP II can break free of the promoter and begin transcriptional elongation (Goldman et al., 2009). Serine 5 of the C-terminal domain (CTD) of the Rpb1p subunit of RNAP II is also phosphorylated by TFIIH in conjunction with TFIIE, and this regulates the transition from transcriptional initiation to transcriptional elongation and is essential for promoter clearance by RNAP II (Svejstrup et al., 1996).

Once RNAP II has cleared the promoter, transcriptional elongation can occur, which involves synthesis of an mRNA transcript via addition of nucleotides to the 3' end of the growing mRNA molecule by RNAP II. During early elongation, the GTFs TFIIF and TFIIH aid RNAP II to prevent transcriptional arrest (Yan et al.,

1999). TFIIF does not travel with RNAPII throughout elongation, though it can associate with elongating RNAP II molecules that encounter a block to elongation (Sims et al., 2004). During elongation, chromatin is an impediment to RNAP II progress (Izban and Luse, 1991). In order to aid elongation and allow RNAP II to proceed along the DNA template, factors such as Swi-Snf mobilise/evict nucleosomes and prevent stalling of transcription (Davie and Kane, 2000). The FACT (facilitates chromatin transcription) complex is a highly conserved complex that allows RNAP II transcription on chromatin templates (Formosa, 2013). FACT destabilises nucleosomes, potentially by removing the H2A-H2B dimer which allows RNAP II to proceed along a nucleosome, and also deposits nucleosomes after the passage of RNAP II has occurred in order to maintain correct chromatin structure (Fleming et al., 2008; Jamai et al., 2009). Different factors associate with the phosphorylated RNAP II CTD during elongation, and this domain is alternatively modified at different stages of transcription. The first modification of the RNAP II CTD is Ser5 phosphorylation (Ser5-P) after formation of the first phosphodiester bonds by TFIIH (Akoulitchev et al., 1995). Ser5-P is prevalent at the 5' ORF, and as RNAP II proceeds along the ORF, Ser2 is also phosphorylated (Ser2-P), leading to a hyper-phosphorylated CTD (Phatnani and Greenleaf, 2006). Finally Ser5 is dephosphorylated, leading to a profile where Ser5-P levels are highest at the TSS and decline, whereas Ser2-P levels increase and reach a peak at the 3' ORF (Phatnani and Greenleaf, 2006). Differential CTD phosphorylation allows different factors to recognise and bind to the CTD at appropriate stages throughout elongation.

As elongation takes place, the nascent mRNA molecule is modified in a number of ways, which aids in the nuclear export and stability of the molecule. First, after about 20-30 nt has been transcribed, the pre-mRNA is capped at the 5' end, a

structure which is recognised by the cap binding complex (CBC) and eventually bound by a cytoplasmic translation initiation factor after nuclear export (Shatkin and Manley, 2000). Transcriptional termination involves complete dissociation of the RNA-DNA hybrid within the RNA polymerase and is dependent on a poly(A) signal (Proudfoot, 1989; Komissarova et al., 2002). This signal is present on the pre-mRNA and is recognised by factors that cleave the pre-mRNA prior to addition of a poly(A) tail to the 3' end of the molecule (Proudfoot et al., 2002). There are two models for eukaryotic transcriptional termination. The "antiterminator" model states that the transcription complex changes conformation upon recognition of the poly(A) signal, which allows termination to take place (Logan et al., 1987). The second model known as the "torpedo" model states that when the nascent mRNA is cleaved at the poly(A) site, this initiates termination by rapid degradation of the 3' portion of the RNA still attached to the polymerase (Connelly and Manley, 1988). These models are not mutually exclusive, and both may play a role in termination of transcription in eukaryotes. After termination, the mRNA is polyadenylated and transported from the nucleus, and the RNA polymerase is released from the DNA, ending that round of transcription.

1.4. The Tup1-Ssn6 co-represssor complex

Tup1-Ssn6 is a transcriptional co-repressor in *S. cerevisiae* which is highly conserved within yeast species and in higher eukaryotes. Tup1-Ssn6 was the first co-repressor discovered in yeast, and is involved in the repression of stress-response genes (Hanlon et al., 2011).The Tup1-Ssn6 complex is comprised of one Ssn6p (Cyc8p) subunit and four Tup1p subunits (Varanasi et al., 1996). As a transcriptional co-repressor, Tup1-Ssn6 does not directly bind DNA, but is

recruited to target gene promoters by DNA-binding transcription factors (Komachi et al., 1994; Treitel and Carlson, 1995). This mechanism of Tup1-Ssn6 recruitment confers great flexibility and allows the complex to regulate a wide variety of genes under various conditions.

1.4.1. Tup1p and Ssn6p.

Ssn6p is a 107 kDa protein that contains ten N-terminal tetratricopeptide repeats (TPRs), which have been shown to be important for Ssn6p function (Schultz et al., 1990). TPR domains 1-3 of Ssn6p have been shown to be essential for Tup1p-binding and Tup1-Ssn6 complex integrity (Gounalaki et al., 2000). Different TPR domains of Ssn6p have also been found to be essential for Tup1-Ssn6 recruitment to, and repression of, different genes (Tzamarias and Struhl, 1995). These TPRs interact with factors that repress gene transcription, such as HDACs, and it has further been shown that different combinations of Ssn6p TPRs interact with different factors to facilitate gene repression (Davie et al., 2002; Davie et al., 2003). Although the C-terminal portion of Ssn6p is not essential for gene repression, it was found to be phosphorylated, indicating that this region of the Ssn6p protein could have a regulatory role (Schultz et al., 1990). Ssn6p has also been found to propagate as the prion [*OCT*+] in an Hsp104p-dependent manner, introducing another possible mechanism by which this protein could be used to impact regulation of gene transcription (Patel et al., 2009; Sanada et al., 2011).

The Tup1p protein has been shown to contain three distinct domains. The Tup1p N-terminal domain is folded into a helical structure and is required for tetramerisation and interacting with Ssn6p (Jabet et al., 2000). The central or repression domain of Tup1p has been shown to interact with hypoacetylated

histone tails, linking the acetyl state of a gene promoter with the ability of Tup1-Ssn6 to repress transcription (Edmondson et al., 1996). Tup1p is generally characterised as containing the bulk of the repressive activity of the Tup1-Ssn6 complex, partly because Tup1-LexA fusions were shown to repress transcription in the absence of Ssn6p, whereas Ssn6-LexA fusions were not effective at transcriptional repression in the absence of Tup1p (Keleher et al., 1992; Tzamarias and Struhl, 1994). The C-terminal region of Tup1p contains seven WD-40 repeats, which are important protein-protein interaction domains. These repeats form a seven-bladed propeller structure, and one example of a protein that they interact with is the α2 repressor, which is a DNA-binding transcription factor involved in repression of a-specific mating type genes (S. R. Green and Johnson, 2005).

1.4.2. Recruitment of Tup1-Ssn6.

Although Tup1-Ssn6 is a transcriptional repressor, the complex contains no DNA-binding activity and is recruited to target promoters via its interaction with DNA-binding transcription factors, in common with other co-repressors (Payankaulam et al., 2010). Different subsets of genes under the regulatory control of Tup1-Ssn6 are regulated by specific transcription factor(s). Carbon source utilisation genes such as *GAL1* (which is de-repressed upon growth in galactose) and *SUC2* (which is de-repressed during growth in low glucose) contain binding sites for Mig1p, which tethers Tup1-Ssn6 to these gene promoters (Treitel and Carlson, 1995; Papamichos-Chronakis et al., 2002). A recent study identified a number of new DNA-binding proteins that recruit Tup1-Ssn6 to various gene subsets under conditions of stress (Hanlon et al., 2011). This study also found that both Tup1p and Ssn6p physically interacted with these recruiters, and concluded that Tup1p,

Ssn6p and the DNA-binding recruiting protein form a complex to repress transcription at target genes. However, in addition to a repressive role for Tup1-Ssn6-recruiting transcription factors, several studies have indicated that these proteins also have a positive role in gene regulation (Treitel and Carlson, 1995; Wong and Struhl, 2011). Overall, this gives a picture of Tup1-Ssn6 as an extremely versatile transcriptional regulator.

1.4.3. Tup1-Ssn6-mediated repression.

There are four mechanisms by which Tup1-Ssn6 has been proposed to repress gene transcription in *S. cerevisiae* which may or may not be mutually exclusive. The first is through interaction with the general transcription machinery. Previous work has shown that several subunits of the RNAPII Mediator complex are required for repression by Tup1-Ssn6 (Figure 1.9A) (Kuchin and Carlson, 1998; Papamichos-Chronakis et al., 2000). Loss of individual Mediator subunits were only found to have a modest effect on gene repression, and there was no additional impairment of gene repression when these were combined with histone tail mutations, indicating that there is redundancy between the RNAPII-mediated and chromatin-mediated gene repression pathways used by Tup1-Ssn6 (M. Lee et al., 2000). The Mediator subunit Srb7p has been shown to interact with Tup1-Ssn6, and Srb7p constructs that are unable to bind to Tup1-Ssn6 show de-repression of Tup1-Ssn6-regulated genes (Gromoller and Lehming, 2000). Interaction between Srb7p and Med6p is required for gene activation, and it is thought that binding of Tup1-Ssn6 to Srb7p prevents this association, and so leads to gene repression, though this only affects transcription of certain genes. These studies have concluded that at certain subsets of genes, Tup1-Ssn6

prevents recruitment of RNAPII to gene promoters by preventing interaction of activators and the Mediator complex (Papamichos-Chronakis et al., 2000).

The second method by which Tup1-Ssn6 has been shown to mediate gene transcription is by regulating the post-translational modification state of promoter histones (Fig. 1.9B). It has been shown that Tup1p interacts with hypoacetylated histone tails through its repression domain, and that this interaction could be essential for stabilising the Tup1-Ssn6 complex at target gene promoters to reinforce gene repression (Davie et al., 2002). Tup1-Ssn6 has also been shown to interact with multiple HDACs, and it is thought that these enzymes are recruited in order to de-acetylate promoter histones, leading to gene repression (Davie et al., 2003; Fleming et al., 2014). Ssn6p in particular may play an important role in modulation of target promoter acetylation, as the different TPR domains of Ssn6p can interact with different HDACs, and may have the ability to bind multiple HDACs simultaneously (Davie et al., 2002; Davie et al., 2003).

The third method by which Tup1-Ssn6 represses gene transcription is by exclusion of factors required for gene activation (Fig. 1.9C). Global analysis has shown that in a conditional *tup1* mutant, occupancy of the transcriptional activators Swi-Snf and Gcn4p increases at sites usually occupied by Tup1p (Wong and Struhl, 2011). This suggests that Tup1-Ssn6 prevents recruitment of factors required to modify promoter chromatin and activate gene transcription. An example of this mechanism is found with the Tup1-Ssn6 interaction with the DNA-binding protein Mig1p. Mig1p is the protein responsible for recruiting Tup1-Ssn6 to the *SUC2* gene promoter, and is required for *SUC2* repression (Treitel and Carlson, 1995). This study also found that a Mig1p-LexA fusion in an *ssn6* mutant strongly activated *SUC2* transcription, whereas a Mig1p-LexA fusion in a *tup1* mutant activated *SUC2* transcription to a lesser extent. This suggested that while

Mig1p is required for *SUC2* repression, the protein also contains an activation domain that is occluded by Ssn6p under *SUC2*-repressing conditions. However under *SUC2* activating conditions, phosphorylation of Mig1p causes a change in the interaction between Ssn6p and Mig1p, leading to exposure of the activation domain and *SUC2* activation. This model for de-repression of Tup1-Ssn6-repressed genes is supported by work on the DNA-binding protein Sko1p, which represses genes involved in osmotic and oxidative stress responses. Sko1p is phosphorylated by the Hog1p kinase and this phosphorylation converts Sko1-Tup1-Ssn6 into an activator that recruits SAGA and Swi-Snf to gene promoters (Proft and Struhl, 2002). It has also been found that the co-repressor Tup1-Ssn6 and the transcriptional activator Gcn5p co-occupy gene promoters involved in mating type switching (Desimone and Laney, 2010). This study found that at a-specific genes, Tup1-Ssn6 was required for gene repression and for Gcn5p-dependent pre-acetylation of gene promoter histones which was required for rapid mating type switching. The switch from repression to activation at Tup1-Ssn6-repressed gene promoters may therefore depend on the DNA-binding proteins that recruit Tup1-Ssn6.

The final method by which Tup1-Ssn6 can repress gene transcription is by propagating a repressive promoter chromatin structure at target promoters (Fig. 1.9D). Loss of *TUP1* or *SSN6* has been shown to result in extensive nucleosome loss at the *FLO1* and *SUC2* gene promoters in a Swi-Snf-dependent manner (Gavin and Simpson, 1997; Fleming and Pennings, 2001, 2007). This regulation of chromatin structure and transcription at these genes has been proposed to be due to the balance between Tup1-Ssn6 and Swi-Snf which evicts and remodels nucleosomes at gene promoters. In support of this antagonistic model, it has been found that Tup1-Ssn6 and Swi-Snf complex mutants show opposing

chromatin phenotypes (Gavin and Simpson, 1997). Another method by which Tup1-Ssn6 can alter promoter chromatin architecture is by co-operation with the ISW2 ATP-dependent chromatin remodelling complex. Tup1-Ssn6 and ISW2 have both been shown to be integral for correct extended nucleosome positioning at the *RNR3* gene promoter, and regulation of nucleosome positioning by ISW2 was also shown to be a feature of other Tup1-Ssn6-regulated genes (Zhang and Reese, 2004).

A genome-wide study of nucleosome occupancy in cells lacking either *TUP1* or *SSN6* found that loss of Tup1p had a greater impact on nucleosome occupancy than loss of Ssn6p (K. Chen et al., 2013). This study also identified a nucleosome within the canonical NFR in gene promoters (termed the P nucleosome) which is located adjacent to the TATA box, and found that this low-occupancy nucleosome was especially sensitive to loss of Tup1-Ssn6. This introduces the possibility that maintenance of the P nucleosome is a key role of Tup1-Ssn6 in gene repression.

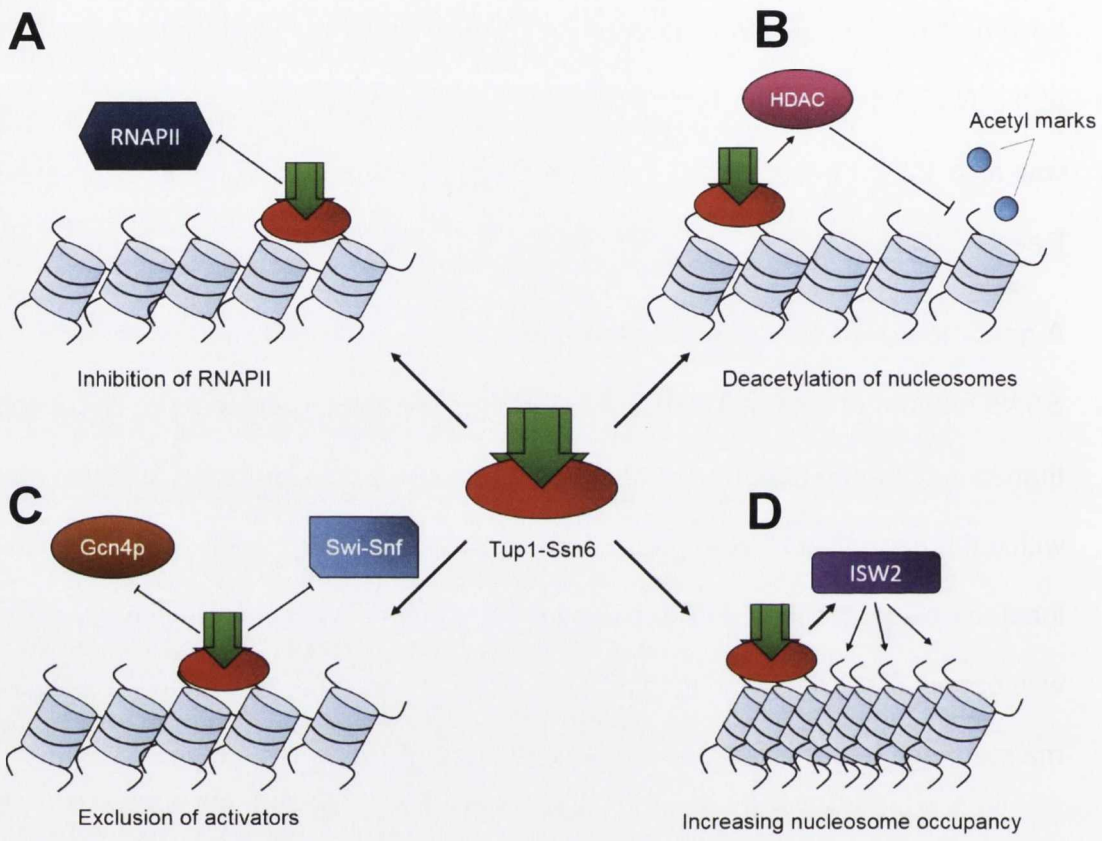

Figure 1.9. Gene repression by Tup1-Ssn6. Schematic to show the various mechanisms of Tup1-Ssn6 gene repression. (A) Tup1-Ssn6 can interfere with Mediator components to prevent transcription initiation by RNA Polymerase II (RNAPII). (B) Tup1-Ssn6 recruits histone deacetylases (HDACs) to target promoters to de-acetylate promoter nucleosomes. (C) Tup1-Ssn6 masks activation domains within transcription factors, preventing their interaction with transcriptional activators. (D) Tup1-Ssn6 interacts with ATP-dependent remodelling complexes such as ISW2 to propagate a repressive nucleosome array at target gene promoters. These models are not necessarily mutually exclusive.

1.4.4. Tup1p and Ssn6p are evolutionarily conserved proteins

Since the discovery of the Tup1-Ssn6 complex, many more co-repressor complexes have been characterised in fungi and higher eukaryotes. Tup1-Ssn6 is highly conserved in fungi and is important in the regulation of filamentation and stress responses in a number of pathogens such as *Candida albicans* and *Aspergillus spp* (Braun and Johnson, 1997; Garcia et al., 2008). Tup1-Ssn6 homologues are also found in the fission yeast *Schizosaccharomyces pombe*, where they play important roles in gene regulation. In both *S. pombe* and *A. nidulans*, *SSN6* is also an essential gene (Fagerstrom-Billai et al., 2007; Garcia et al., 2008).

In addition to the high level of conservation of Tup1-Ssn6 in other fungi, co-repressor proteins with similar domain structure and functions to Tup1p and Ssn6p can also be found in higher eukaryotes. Tup1p-like proteins include the Groucho (Gro) protein found in *Drosophila* and the transducing-like enhancer of split (TLE) and transducing beta-like related (TBL/TBLR) proteins in mammals (Courey and Jia, 2001). Similar to the C-terminal WD40 repeat of the Tup1p protein, TLE/Groucho were found to contain a seven bladed β propeller WD40 domain on their respective C-termini (Pickles et al., 2002). Gro also has a glutamine-rich N-terminal domain (also termed Q-domain) that is important for tetramerisation (Courey and Jia, 2001). Groucho is important for development in *Drosophila,* and like Tup1p it does not contain any DNA-binding activity but is recruited to target genes by DNA-binding transcription factors (Courey and Jia, 2001). Human TLE1 has the ability to interact with yeast Ssn6p and human Ssn6p-like proteins, and TLE1-bound Ssn6p has the ability to mediate repression when expressed in mammalian cells, further highlighting the conservation

between these proteins from yeast to humans (Grbavec et al., 1999). Like Tup1p, Gro and TLE also interact with histones and HDACs, illustrating that it is not just similar protein structure, but similar mechanisms which are used to repress gene transcription in yeast and higher eukaryotes.

In addition to the similarities between Tup1p and TLE/Gro, there are mammalian proteins with similar structures and functions as yeast Ssn6p. Two such protein-encoding genes were identified on the X or Y chromosomes of mice and humans, and were found to be ubiquitously transcribed tetratricopeptide repeat genes on the Y/X chromosome (UTY/X) (Greenfield et al., 1998; Mazeyrat et al., 1998). UTY/X shares the TPR domains found on the N-terminal region of yeast Ssn6p, and it was the structural similarities to Ssn6p that led to the discovery that these proteins can interact with the Tup1p-like TLE1 and TLE2 (Grbavec et al., 1999). UTX is an X-linked gene that is not X-inactivated, and it has been proposed that this gene could contribute to brain development and behaviour in humans, with females possessing two active UTX copies causing differences in brain development between the sexes (Xu and Andreassi, 2011). UTX also regulates a large subset of genes (Swigut and Wysocka, 2007), however, unlike yeast Ssn6p, UTX possesses histone demethylase activity.

Overall, Tup1-Ssn6 homologues and complexes structurally and functionally related to Tup1-Ssn6 in fungi and higher eukaryotes are important regulators of gene transcription, and elucidating the mechanisms by which these proteins regulate gene transcription is crucial for understanding human development and disease.

1.5. Flocculation

Flocculation is the non-sexual, calcium-dependent aggregation of cells that express lectin-like cell wall proteins known as flocculins (Soares, 2011). These cell aggregates are formed by binding of flocculins to mannose residues on the surface of other cells, and is an important phenotype used by wild yeast to protect cells from stress. Flocculation differs from other types of cellular aggregation in *Saccharomyces cerevisiae*, such as sexual aggregation, co-flocculation or chain formation. Sexual aggregation occurs when cells of complementary mating types express proteins on their cell walls and fuse to mate (E. H. Chen et al., 2007). Co-flocculation occurs where weakly flocculent strains and non-flocculent strains aggregate, whereas true flocculation requires a single flocculent strain (Soares, 2011). Chain formation is a failure of daughter cells to separate from mother cells during replication, and results in a chain of budded cells which will be unable to re-aggregate if mechanically separated (Soares, 2011). Flocculation is related to adhesion and biofilm formation, which is of great clinical significance as many pathogenic fungi can adhere to medical devices and cause hospital-acquired infections (Verstrepen and Klis, 2006). Flocculation is also a convenient phenotype used in brewing and other industrial processes, as aggregation of yeast cells allows for easy removal from the medium and it has been found that flocculent yeast can remove heavy metals from a synthetic effluent, highlighting the usefulness of flocculent yeast in industry (Machado et al., 2008).

1.5.1. Mechanism of Flocculation.

Flocculation is a characteristic conferred by surface proteins on the *S. cerevisiae* cell wall. It has been shown that heat-killed flocculent cells retain their ability to aggregate, indicating that flocculation is not an active process (Machado et al.,

2008). The yeast cell wall also has a net negative charge, and this prevents cell aggregation due to repulsion between non-flocculent cells which must be overcome if cells are to aggregate (Dengis et al., 1995). A positive correlation has been found between cell surface hydrophobicity and flocculation and that cell surface hydrophobicity increases when yeast express the cell wall proteins Flo1p, Flo5p, Flo9p Flo10p and Flo11p (Smit et al., 1992; Verstrepen et al., 2003; Govender et al., 2008). It was initially proposed that lectin-like proteins uniquely expressed on flocculent cell walls recognised and interacted with carbohydrate residues on neighbouring cell walls (Miki et al., 1982). This work also proposed that calcium ions are required for the lectins to achieve their active conformation to enable flocculation. The carbohydrate residue that is bound by these lectins is present on cell-surface receptors known as α-mannans. While the lectins required for flocculation are only present on flocculent cells, the α-mannans are an integral part of the *S. cerevisiae* cell wall and so are not specific to flocculent cells. In summary, flocculent cells use lectin-like proteins that recognise and bind to mannose residues on neighbouring cells in a calcium-dependent manner (Fig. 1.10).

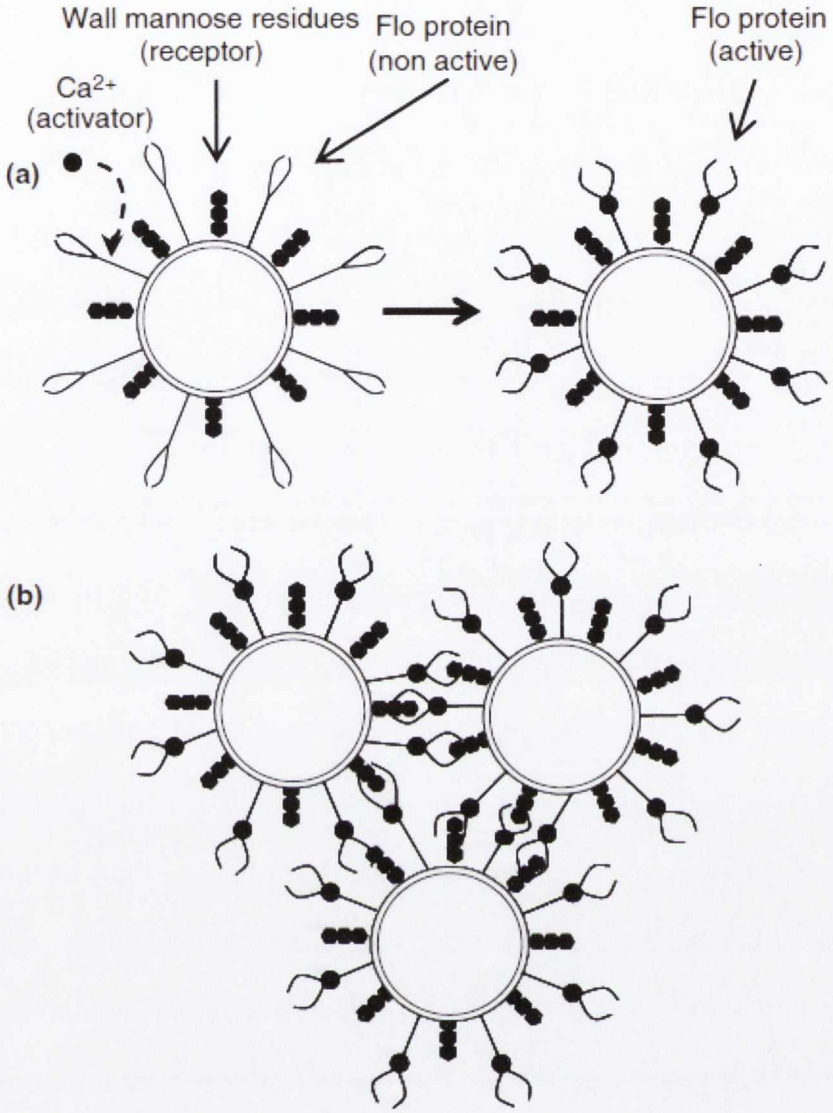

Figure 1.10. Mechanism of yeast flocculation. (A) Calcium Ions in convert inactive flocculins (Flo) to active flocculins. (B) Active flocculins have the ability to bind mannose residues on the surface of other cells. This leads to aggregate formation. Taken from Soares (2011).

1.5.2. Flocculins confer a flocculent phenotype

The lectin-like cell wall proteins responsible for flocculation are known as flocculins. The major flocculin in *S. cerevisiae* is Flo1p which was predicted to be a protein of 1537 amino acids (Watari et al., 1994). Flo1p is found on the cell wall, and confers a flocculent phenotype on cells that express it. The central portion of Flo1p contains many repeated segments, and the N- and C-termini are more hydrophobic than the rest of the protein (Soares, 2011). Flo1p is transported through the secretory pathway via the endoplasmic reticulum (Bony et al., 1997) to the cell wall. Flo1p is then anchored to the cell wall by a noncovalent stabilisation mediated via the hydrophobic C-terminal GPI-anchor, deletion of which impairs Flo1p cell wall attachment and inhibits flocculation (Watari et al., 1994; Bony et al., 1997). The central domain of Flo1p contains a high level of serine and threonine-rich repeats and the N-terminal portion of the protein is responsible for recognition of mannose residues on other cell surfaces (Verstrepen and Klis, 2006). There is a correlation between the number of repeats in the central domain in *FLO1* and the degree of flocculation, indicating that a longer Flo1p protein has a better ability to contact other cell surfaces (Bidard et al., 1995). However, longer Flo1p proteins are less stable under acid or alkaline conditions (E. Li et al., 2013). This variation in the number of internal *FLO1* repeats give rise to different flocculation phenotypes which would allow a population of cells to respond accordingly to a variety of stresses. Flo1p is just one of several flocculins found in *S. cerevisiae*, the others being Flo5p, Flo9p and Flo10p, though it is expression of Flo1p that confers the strongest flocculation phenotype (Teunissen and Steensma, 1995).

1.5.3. The major flocculin in *S. cerevisiae* is encoded by *FLO1*

FLO1 is a 4.6 kb sub-telomeric gene found on the right arm of chromosome I in *S. cerevisiae*. *FLO1* is the best known and most well-studied member of a family of *FLO* genes, all of which contain common elements. *FLO* genes are sub-telomeric, highly-similar genes characterised by a unique 5' portion followed by multiple repeat sequences and a highly conserved 3' end, with the *FLO5, FLO9* and *FLO10* genes being 96, 94 and 58% homologous to *FLO1* respectively (Teunissen and Steensma, 1995). Overexpression of these genes induces flocculation, but this phenotype varies depending on the gene involved (Govender et al., 2008).

FLO1 has long been studied as a model for chromatin-mediated gene regulation (Lipke and Hull-Pillsbury, 1984). As a gene under the antagonistic control of Tup1-Ssn6 and Swi-Snf, *FLO1* offers an insight into the interplay between repressing and activating factors at gene promoters. The flocculent phenotype exhibited by cells expressing *FLO1* is also a useful visual assay when studying gene activation. *FLO1* is especially interesting in the context of Tup1-Ssn6 and Swi-Snf-mediated gene regulation because of the long-range chromatin remodelling observed upstream of the *FLO1* ORF upon loss of Tup1-Ssn6 which occurs in a Swi-Snf-dependent manner (Fleming and Pennings, 2001). Further illustrating the role of chromatin in *FLO1* regulation, the HDACs Rpd3p and Hda1p have also been shown to co-operate with Tup1-Ssn6 to repress *FLO1* transcription (Fleming et al., 2014). However, the mechanism by which *FLO1* is de-repressed is less well-understood.

One factor known to be involved in activation of *FLO1* is Flo8p. Flo8p is a protein of 729 amino acids in size whose overexpression was found to induce flocculation

in non-flocculent yeast strains (Kobayashi et al., 1996). This study also found that the level of *FLO1* transcription was dependent on the rate of transcription of the *FLO8* gene. Flo8p activates a number of genes in *S. cerevisiae* involved in flocculation, biofilm formation and adhesion, and is highly conserved among fungi, acting as a regulator of invasive growth in pathogenic species (Cao et al., 2006; Bester et al., 2012). Flo8p is thought to activate *FLO1* through antagonism of Tup1-Ssn6 and it has also been shown that Flo8p has the ability to physically interact with Swi-Snf, a factor essential for *FLO1* de-repression (H. Y. Kim et al., 2014). However, due to a nonsense mutation in the *FLO8* ORF, Flo8p is not expressed in *S. cerevisiae* laboratory strains, and so these strains are non-flocculent (H. Liu et al., 1996).

The aim of this project was to investigate the role of Tup1-Ssn6 in gene repression in general, and gene-specifically using *FLO1* as a model. This project aimed to identify the chromatin-associated factors required for de-repression of *FLO1*, and to establish the precise mechanism of *FLO1* gene activation in the absence of Tup1-Ssn6.

Chapter 2

Materials and Methods

2.1. Strains and growth conditions

Strains used in this study are listed in Table 2.1. Yeast extract peptone with dextrose (YEPD) broth (1% yeast extract, 2% peptone & 2% glucose) (Formedium) was used for liquid culture unless otherwise indicated, and YEPD agar (1% yeast extract, 2% peptone, 2% agar & 2% glucose) was used as solid medium. Yeast cells were cultured in YEPD at 30°C in a shaking incubator at 200 rpm unless otherwise stated. Starter cultures were prepared by inoculating 10ml YEPD with a yeast colony and growing overnight. This starter culture was then sub-inoculated into a larger volume of YEPD broth and grown until log phase (Optical density was determined using a spectrophotometer, and OD_{600} 0.6-0.8 was considered to be log phase).

For growth of mutants with auxotrophic markers, synthetic complete (SC) medium was prepared using 0.19% yeast nitrogen base (Formedium), 0.059% complete supplement medium (Formedium), 0.5% $(NH_4)_2SO_4$, and for solid medium, 2% agar. This solution was autoclaved and filter-sterilised glucose was added to a final concentration of 2%. Remaining amino acids were included or omitted depending on the desired auxotrophic selection and strain genotype.

Strain	Genotype	Source
BY4741	*Mat* a *his3Δ1 leu2Δ0 met15Δ0 ura3Δ0*	(Brachmann et al., 1998)
PH499	*MAT* a *ade2-101 his3-Δ200 leu2-Δ1 ura3-52 trp1-Δ63 lys2-801*	J. Reese
HHY221	*Mat* a *tor1-1 fpr1::loxP-LEU2-loxP RPL13A-2×FKBP12::loxP*	(Haruki et al., 2008)
YMC5	*Mat* a *his3Δ1 leu2Δ0 met15Δ0 ura3Δ0 SNF5-*9Myc::*URA3 ssn6::KANMX4*	This study
YMC6	*Mat* a *his3Δ1 leu2Δ0 met15Δ0 ura3Δ0 SNF5-*9Myc::*URA3 tup1::LEU2*	This study
YMC11	*Mat* a *his3Δ1 leu2Δ0 met15Δ0 ura3Δ0 SSN6-*9Myc*::KANMX4 tup1::URA3*	This study
YMC12	*Mat* a *his3Δ1 leu2Δ0 met15Δ0 ura3Δ0 tup1::KANMX4 ssn6::URA3*	This study
YMC13	*Mat* a *his3Δ1 leu2Δ0 met15Δ0 ura3Δ0 SNF5-*9Myc::*URA3 tup1::LEU2 ssn6::KANMX4*	This study
YMC14	*Mat* a *his3Δ1 leu2Δ0 met15Δ0 ura3Δ0 GCN5-*9myc*::HPH1*	This study
YMC15	*Mat* a *his3Δ1 leu2Δ0 met15Δ0 ura3Δ0 GCN5-*9Myc*::HPH1 ssn6::URA3*	This study

YMC16	*Mat* a *his3Δ1 leu2Δ0 met15Δ0 ura3Δ0 gcn5::KANMX4 ssn6::URA3*	This study
YMC17	*Mat* a *his3Δ1 leu2Δ0 met15Δ0 ura3Δ0 gcn5::KANMX4 tup1::URA3*	This study
YMC18	*Mat* a *his3Δ1 leu2Δ0 met15Δ0 ura3Δ0 flo8::LEU2*	This study
YMC19	*Mat* a *his3Δ1 leu2Δ0 met15Δ0 ura3Δ0 YER109C::*A425G::*HPH1*	This study
YMC20	*Mat* a *his3Δ1 leu2Δ0 met15Δ0 ura3Δ0 sas3::KANMX4 ssn6::URA3*	This study
YMC22	*Mat* a *his3Δ1 leu2Δ0 met15Δ0 ura3Δ0 sas3::kanMX4 ada2::URA3*	This study
YMC23	BY4741 +pMC1(*FLO8*pGAL, TAP-tagged)	This study
YMC24	*flo8::LEU2* +pMC1(FLO8pGAL, TAP-tagged)	This study
YMC25	BY4741 +pMC1notag(*FLO8*pGAL, untagged)	This study
YMC26	*flo8::LEU2* +pMC1notag(FLO8pGAL, untagged)	This study
YMC27	*Mat* a *his3Δ1 leu2Δ0 met15Δ0 ura3Δ0 sas3::KANMX4 ada2::URA3 ssn6::LEU2*	This study
YMC28	*Mat* a *his3Δ1 leu2Δ0 met15Δ0 ura3Δ0 sas3::KANMX4 tup1::LEU2*	This study
YMC29	*Mat* a *his3Δ1 leu2Δ0 met15Δ0 ura3Δ0 ssn6::LEU2*	This study
YMC30	*Mat* a *tor1-1 fpr1::loxP-LEU2-loxP RPL13A-2×FKBP12::loxP SSN6-FRB::HIS3*	This study

YMC31	*Mat* a *tor1-1 fpr1::loxP-LEU2-loxP RPL13A-2×FKBP12::loxP SSN6-FRB::HIS3*	This study
YMC32	*Mat* a *his3Δ1 leu2Δ0 met15Δ0 ura3Δ0 SAS3-9Myc::HPH1*	This study
YMC33	*Mat* a *tor1-1 fpr1::loxP-LEU2-loxP RPL13A-2×FKBP12::loxP SSN6-FRB::HIS3 ada2::URA3 sas3::KANMX4*	This study
YMC34	*Mat* a *his3Δ1 leu2Δ0 met15Δ0 ura3Δ0 YER109C::*A425G::9Myc::*KANMX4*	This study
KLY021	*Mat* a *his3Δ1 leu2Δ0 met15Δ0 ura3Δ0 SNF5-*9Myc::*URA3*	
YPOD1	*Mat a his3Δ1 leu2Δ0 met15Δ0 ura3Δ0 SSN6-*9Myc::*KANMX4*	This study

Table 2.1. Strains used in this study.

2.2. DNA extraction

To extract yeast genomic DNA, 10 ml of an overnight cell culture was subjected to centrifugation at 376 rcf for 5 minutes. Supernatant was discarded and cells were resuspended in 1ml H_2O and transferred to a 1.5 ml microcentrifuge tube. Cells were pelleted by centrifugation at 16,363 rcf in a microcentrifuge and supernatant was discarded. Pellets were resuspended in 200 µl breaking buffer (2 % Triton X-100, 1 % SDS, 100 mM NaCl, 10 mM Tris-Cl [pH 8.0], 1 mM EDTA [pH 8.0]) and 200 µl 400 µm -600 µm glass beads were added (Sigma). 200 µl phenol/chloroform/isoamyl alcohol was added to the suspension and the samples were mixed by vortexing for 3 minutes. 200 µl TE (pH 7.5) was added, mixed and samples were subjected to centrifugation at 16,363 rcf for 5 minutes. The aqueous layer was transferred to a new 1.5 ml tube and 400 µl chloroform was added. This was mixed and subjected to centrifugation for 5 minutes at 16,363 rcf. The aqueous layer was transferred to a new 1.5 ml tube and 1ml 100 % ethanol was added. DNA was pelleted by centrifugation at 16,363 rcf for 5 minutes. Supernatant was discarded and the DNA pellet was resuspended in 500 µl 70 % ethanol. DNA was pelleted by centrifugation at 16,363 rcf for 5 minutes. The DNA pellet was dried and resuspended in 400 µl TE (pH 7.5) and 25 µg RNase A was added. This was incubated at 37°C for 1 hour. DNA was then ethanol precipitated and resuspended in 500 µl TE (pH 7.5).

2.3. RNA extraction

The RNA extraction protocol was adapted from Current Protocols (Collart and Oliviero, 2001). Cells were grown to log phase and a 5 ml volume of culture was pelleted by centrifugation. Supernatant was removed and cells were resuspended in 1 ml H_2O. The suspension was transferred to a 1.5 ml tube and

cells were pelleted by centrifugation in a microcentrifuge. Supernatant was discarded and cells were resuspended in 400 µl TES solution (10 mM Tris-Cl pH 7.5, 10 mM EDTA, 0.5% SDS) and 400 µl saturated phenol, pH 4.3 (Fisher). This suspension was incubated at 65°C for 1 hour with occasional agitation. Samples were incubated on ice for 5 minutes and centrifuged at 16,363 rcf in a microcentrifuge for 5 minutes. The aqueous layer was transferred to new 1.5 ml tubes and 400 µl saturated phenol was added. The samples were stored on ice for 5 minutes and subjected to centrifugation at 16,363 rcf for 5 minutes. The aqueous layer was transferred to a new 1.5 ml tubes and 400 µl chloroform was added, after which samples were stored on ice for 5 minutes and subjected to centrifugation at 16,363 rcf in a microcentrifuge for 5 minutes. RNA was precipitated by adding sodium acetate, pH 5.3 to a final concentration of 1 M and three sample volumes of 100 % ethanol and storing at -80°C for 1 hour. RNA was pelleted by centrifugation at 16,363 rcf and 4°C for 30 minutes. Supernatant was discarded and RNA pellets were washed in 500 µl 70 % ethanol. Samples were centrifuged again at 16,363 rcf, 4°C for 15 minutes after which supernatant was discarded and pellets were dried before being resuspended in nuclease-free water. RNA concentration was determined using a NanoDrop spectrophotometer (Thermo Scientific).

2.4. Ethanol precipitation

DNA was precipitated by adding 0.3 volumes 4 M Lithium Chloride and three volumes 100 % ethanol. This was stored at -20°C for >1 hour. Precipitated DNA was pelleted by centrifugation at 16,363 rcf for 5 minutes and resuspended in 500 µl 70 % ethanol. The centrifugation step was repeated and the DNA was dried and resuspended to the desired final volume in either water or TE buffer, pH 8.

2.5. Protein extraction

Cells were grown to log phase (OD_{600} 0.6-0.8). A cell volume equivalent to 10 OD units was taken and centrifuged at 376 rcf for 5 minutes. Supernatant was discarded and cell pellets were resuspended in 1 ml 20% trichloroacetic acid (TCA), transferred to a 1.5 ml microcentrifuge tube and centrifuged at 16,363 rcf for 1 minute. Supernatant was discarded and cell pellets were resuspended in 250 µl 20 % TCA. 600 mg 400 µm-600 µm glass beads (Sigma) were added to each tube and cells were agitated in a vortex (Genie II) mixer at maximum speed at 4°C for 15 minutes.

Cell lysate was transferred to a new 1.5 ml tube, and glass beads were further washed using 500 µl 5% TCA, and the wash added to the initial cell lysate. The suspension was stored on ice for 3 minutes before being centrifuged at 16,363 rcf for 1 minute. Supernatant was discarded and the pellet was resuspended in 300 µl Laemmli buffer (0.1 % 2-mercaptoethanol, 10 % glycerol, 2 % SDS & 63 mM Tris-Cl [pH 6.8]). This was incubated at 95°C for 5 minutes and subjected to centrifugation at 16,363 rcf for 1 minute. Supernatant was transferred to a new 1.5 ml tube.

Protein concentration was calculated by Bradford assay according to manufacturer's instructions (Sigma). Protein samples and bovine serum albumin (BSA) standards of 2, 4, 6, 8 and 10 µg/ml were prepared and diluted in H_2O and Bradford reagent (Sigma). Absorbance (A_{595}) was measured using a spectrophotometer and sample concentration was calculated by comparing absorbance to values obtained using the standard curve. Working stocks of protein samples were adjusted to a volume of 2 mg/ml prior to immediate use or storage at -80°C

2.6. SDS-Polyacrylamaide gel elctrophoresis (PAGE)

A 10 % or 15 % polyacrylamide running gel was prepared using the BioRad Mini cell apparatus, depending on the required resolution (10 %/15 % acrylamide [Protogel, National Diagnostics], 0.38 M Tris-Cl [pH8.8], 0.001 % SDS, 0.001 % ammonium persulfate [APS] & 0.001% TEMED). The gel was allowed to polymerise under isopropanol. The isopropanol was discarded and a 6 % stacking gel was poured (6 % acrylamide, 78 mM Tris-Cl [pH 6.8], 0.001% SDS, 0.001% APS & 0.001% TEMED). Unless otherwise indicated, 30 µg of protein was loaded into each well and gels were run at 100V for 120 minutes in running buffer (25 mM Tris, 190 mM glycine, 0.1 % SDS).

2.7. Microscopy

10ml of log-phase cells were centrifuged at 376 rcf for 3 minutes and supernatant was discarded. Cell pellets were resuspended in 2 ml softening buffer (0.1M Tris-Cl [pH 9.4], 10 mM DTT). This mixture was incubated at room temperature for 10 minutes and centrifuged at 376 rcf for 3 minutes. Supernatant was discarded and pellets were resuspended in 2 ml sphaeroplasting buffer (1 M sorbitol, 40 mM $KHPO_4$ in YEPD) with 75 µg/ml 20T zymolyase (AMS Biotechnology) and incubated at 30°C for 40 minutes. Formaldehyde was added to 4 % and this was incubated at 30°C for 60 minutes. Fixed cells were centrifuged at 188 rcf for 4 minutes, supernatant was discarded and 1 ml Buffer A (100 mM Tris-Cl [pH 8.0], 1 M sorbitol) was added and the mixture was transferred to a 1.5 ml tube. Tubes were centrifuged at 1377 rcf and supernatant was discarded. Pellets were resuspended in 500 µl Buffer A + 0.1 % SDS and incubated at room temperature for 10 minutes. Cells were washed twice with 1 ml Buffer A and subjected to centrifugation for 2 minutes at 1377 rcf between washes. Pellets were then

resuspended in 300 µl Buffer A. 20 µl cells were added to a prepared cover slip and incubated for 15 minutes. Cells were aspirated and cover slip was blocked for 15 minutes in 20 µl Buffer B (50 mM Tris-Cl [pH 8.0], 150 mM NaCl, 1 % dried skimmed milk, 0.5 mg/ml BSA and 0.1 % Tween-20). Buffer B was aspirated and 40 µl α-FRB (Enzo) in clarified Buffer B was added and incubated at 4°C overnight in a humidity chamber. Five 5 minute washes in clarified Buffer B were carried out, with buffer being aspirated between washes. A 1:200 dilution of fluorescently-labelled secondary antibody (AlexaFluor 488 goat anti-rabbit IgG) in clarified Buffer B and this was incubated at room temperature for 60 minutes in the dark. Slides were then washed three times for 10 minutes in Buffer B. DAPI diluted 1:10,000 in Buffer B was added to slides and incubated at room temperature for 10 minutes. Slides were washed twice more in Buffer B before being viewed on a Nikon Ti Eclipse fluorescence microscope and analysed using Volocity software at 40 X magnification.

2.8. End-point Polymerase Chain Reaction (PCR)

Unless otherwise stated, PCR was carried out using the MyTaq HS (Bioline) DNA polymerase mix. For amplification from a genomic or plasmid DNA template, 1 ng-500 ng of DNA was used and 500 nM per primer (final concentration) was included in each reaction volume.

A master mix was made using DNA polymerase, primers and water, and this mixture was distributed between PCR tubes, at which point template DNA was added. This was then mixed and incubated in a thermocycler.

Reaction conditions for PCR were as follows: initial denaturation at 95°C for 1 minute, followed by 30 cycles of denaturation, annealing and extension. This denaturation step was a 95°C incubation for 15 seconds. Annealing temperature

was determined based on the primers used and this step was for 15 seconds. Extension was at 72°C, and extension time depended on the length of the desired product, but was calculated as 30 seconds per kilobase (kb) of required product. A final extension of 72°C was carried out for 5 minutes after the cycling was complete.

PCR primers were designed using Primer3Plus (Untergasser et al., 2007), and specificity of primers was determined using NCBI's BLAST (Altschul et al., 1997).

2.9. Gene deletions and epitope tagging

Gene deletions were carried out by PCR-mediated gene disruption adapted from the Wach et al. and Longtine et al. protocols (Wach, 1996; Longtine et al., 1998). For gene deletions involving auxotrophic markers, long primers (60 bp) were designed containing 5' 40 bp overhangs that were complementary to regions up- and downstream of the target open reading frame (ORF), and 20 bp 3' regions complementary to a plasmid containing an auxotrophic or antibiotic marker (Figure 2.1A) (Brachmann et al., 1998). The pRS400 series of vectors containing auxotrophic markers were obtained from EUROSCARF and the published protocol was followed. For epitope-tagging of target genes, pFA6-Kan and hygromycin plasmids containing the Kanamycin and hygromycin resistance markers, respectively, were obtained from Janke et al (Janke et al., 2004). Purified plasmid (10-50ng) was used as template in a PCR reaction according to published protocols (Fig. 2.1B) (Longtine et al., 1998; Janke et al., 2004).

2.10. Anchor Away

The anchor away protocol was based on that used by Haruki *et al* (Haruki et al., 2008). Cells were grown in 10ml cultures overnight and a volume of this culture

was added to a larger volume of YPD (600 ml for ChIP analysis or 60 ml for RNA). This sub-inoculated culture was grown overnight and OD_{600} was measured the following day. When cultures reached OD ~0.4, the first sample was taken (time 0). For ChIP experiments, 50 ml was taken and cross-linked as described previously. For transcriptional analysis, 5 ml culture was taken, subjected to centrifugation and washed. Both cross-linked cell pellets and cell pellets for RNA extraction were stored at -80°C.

After the initial sample was taken, rapamycin (Fisher) was added to a final concentration of 1 µg/ml and cultures were incubated at 200 rpm, 30°C. Samples were taken at 10 minutes, 20 minutes, 30 minutes, 40 minutes, 60 minutes, 2 hours, 4 hours, 6 hours, 8 hours, 10 hours and 12 hours. These samples were cross-linked or prepared for RNA extraction as required and stored at 80°C.

2.11. Yeast cell Transformation

The yeast cell transformation protocol used was based on the high efficiency protocol from Gietz et al (Gietz and Schiestl, 2007). Overnight cultures were counted on a haemocytometer (Fisher) and adjusted to a cell density of 5×10^6 cells/ml in YEPD. These cells were incubated at 30°C, 200 rpm until a cell density of 2×10^7 cells was reached (~2 doublings). Cells were then centrifuged at 289 rcf for three minutes and supernatant was discarded. Cell pellets were resuspended in 1 ml of sterile 100 mM lithium acetate and transferred to a 1.5 ml microcentrifuge tube. Cells were centrifuged at 16,363 rcf for 15 seconds and supernatant was discarded.100 mM lithium acetate was added until the cell suspension volume was 500 µl, and this was divided into 50 µl aliquots. Each 50 µl aliquot was included in a transformation mix that contained 100 mM LiAC, 33 % polyethylene glycol (PEG) 4000, 0.28 mg/ml high molecular weight single-

stranded DNA from salmon testes (Sigma) and disruption fragment amplified by PCR (~1 µg total). This mixture was incubated at 42°C for 40 minutes. Cells were centrifuged at 4,600 rcf for 15 seconds and supernatant was discarded. Cells were then resuspended in 150 µl sterile H_2O. For transformations involving auxotrophic markers, cells were plated directly onto selective media. For transformations involving antibiotic markers, cells were first plated onto YEPD and incubated overnight at 30°C. Following recovery, cells were replica-plated onto selective media and incubated at 30°C. Transformants were verified by PCR.

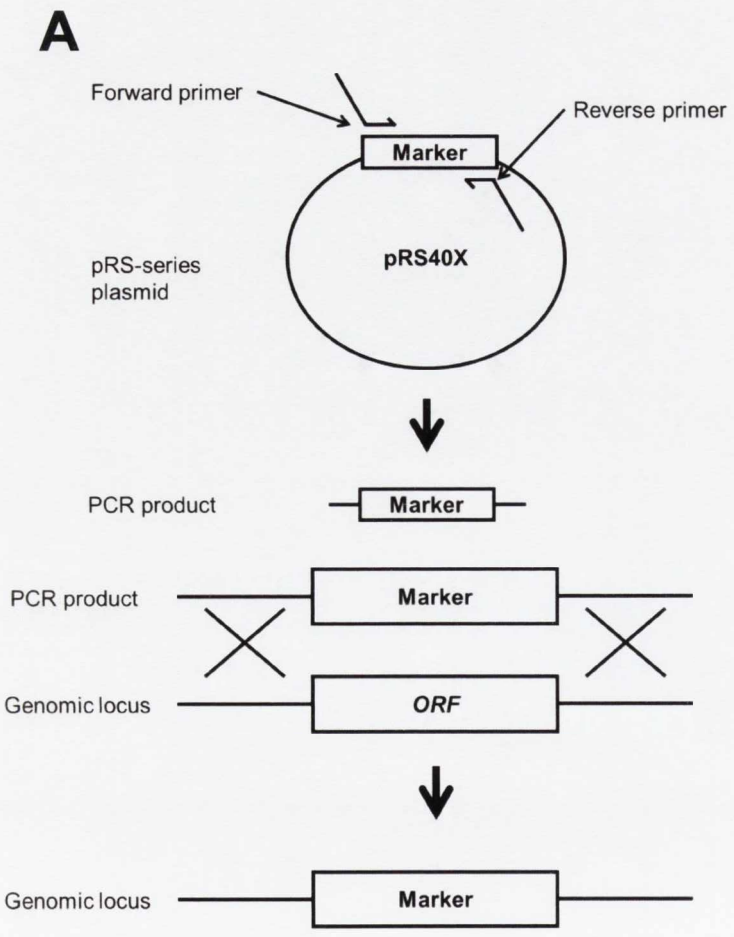
A
Forward primer
Reverse primer
Marker
pRS-series
plasmid
pRS40X
PCR product
Marker
PCR product
Marker
Genomic locus
ORF
Genomic locus
Marker

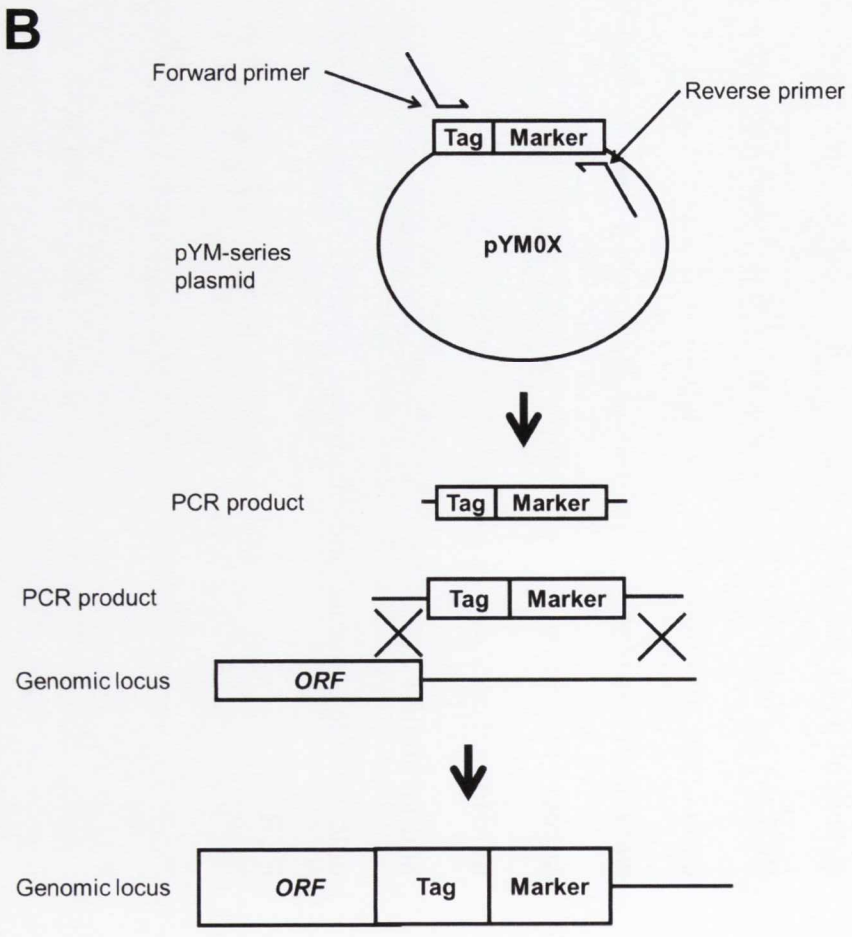
B
Forward primer
Reverse primer
Tag
Marker
pYM-series
plasmid
pYM0X
PCR product
Tag
Marker
PCR product
Tag
Marker
Genomic locus
ORF
Genomic locus
ORF
Tag
Marker

Figure 2.1. Gene deletion and epitope tagging by PCR-mediated homologous recombination. (A) Disruption fragments were generated by using primers complementary to the template plasmid. These fragments contained sequences that were homologous to DNA flanking the gene targeted for deletion (Brachmann et al., 1998). The selectable marker thus replaced the target ORF by homologous recombination. (B) Fragments amplified from the pYM vectors contain an epitope upstream of the selectable marker that is inserted on the 3' ORF via homologous recombination (Janke et al., 2004).

2.12. cDNA generation

To generate cDNA, RNA was first DNase-treated using RQ1 RNase-free DNase (Promega). 10 µg RNA was incubated with 1 unit of DNase in reaction buffer at 37°C for 1 hour. 1 µl stop solution was added and samples were incubated at 65°C for 10 minutes. cDNA was generated using a High-capacity RNA to cDNA kit (Applied Biosystems). 1 µg of DNase-treated RNA was incubated with 1 unit of reverse transcriptase in reaction buffer at 37°C for 1 hour, and this reaction was stopped by incubation at 95°C for 5 minutes.

2.13. Optimisation of Chromatin Immunoprecipitation (ChIP) protocol

2.13.1. Cell growth & formaldehyde crosslinking:

10 ml YEPD was inoculated with single colony and incubated overnight at 30°C and agitated at 200 rpm. 300 ml YEPD was inoculated the following day with starter culture and grown to an OD_{600} of ~0.8. This volume was split into 5 x 50ml cultures each in 250 ml flasks for cross-linking (10 mM EDTA was added to flocculent cells to disperse cells). Formaldehyde (Sigma, 37 %) was added to a final concentration of 1% and cells were cross-linked for 20 minutes at room temperature with shaking. To quench the cross-linking reaction, glycine was added to a final concentration of 50 mM and cultures were shaken for a further 5 minutes. Cross-linked cultures were transferred to 50 ml centrifuge tubes and centrifuged at 1000 rcf for 5 minutes at 4°C. Supernatant was discarded and cell pellets were resuspended in 25 ml ice-cold TBS. Cells were pelleted by centrifugation at 1000 rcf, 4°C and the supernatant was discarded. The TBS wash was repeated, and the resultant cross-linked cell pellets were stored at -80°C.

2.13.2. Comparing the cell breakage efficiency of glass and zirconia beads:

I wished to determine whether glass beads or the denser zirconia beads were more efficient for yeast cell lysis. I therefore vortexed cross-linked cells with both glass or zirconia beads and assayed cell breakage by measuring cell lysis and protein release over time. Cross-linked cell pellets from two 50 ml cultures were each resuspended in 400 µl FA lysis buffer (50mM HEPES, 140 mM NaCl, 1 mM EDTA,1 % Triton X-100, 0.1 % sodium deoxycholate) supplemented with a 1:100 dilution of protease inhibitor cocktail (Sigma) and 2 mM PMSF (Sigma). 250 µl of this solution was added to each tube, and cell pellets were resuspended and transferred to two 2 ml tubes. ~400 µl of acid-washed glass (Sigma) or zirconia beads (BioSpec Products, Inc.) were added to each tube.

Each tube contained half of the total cells harvested from a 50 ml culture volume. To test cell breakage, these tubes were vortexed at full speed at 4°C. Cells were counted before vortexing, and a breakage time-course was performed by taking samples at 15, 30, 45 and 60 minutes to monitor cell breakage by counting. These samples were also used to measure protein release by lysed cells.

To measure of cell lysis via protein release, , tubes were pierced with a 23G needle, placed in a 15 ml centrifuge tube and centrifuged at 1000 rcf in a table top centrifuge for 4 minutes, 4°C. Flow-through was transferred to a 1.5 ml microcentrifuge tube and spun at 16,363 rcf for 5 minutes. Supernatant was transferred to a new tube and stored at -80°C.

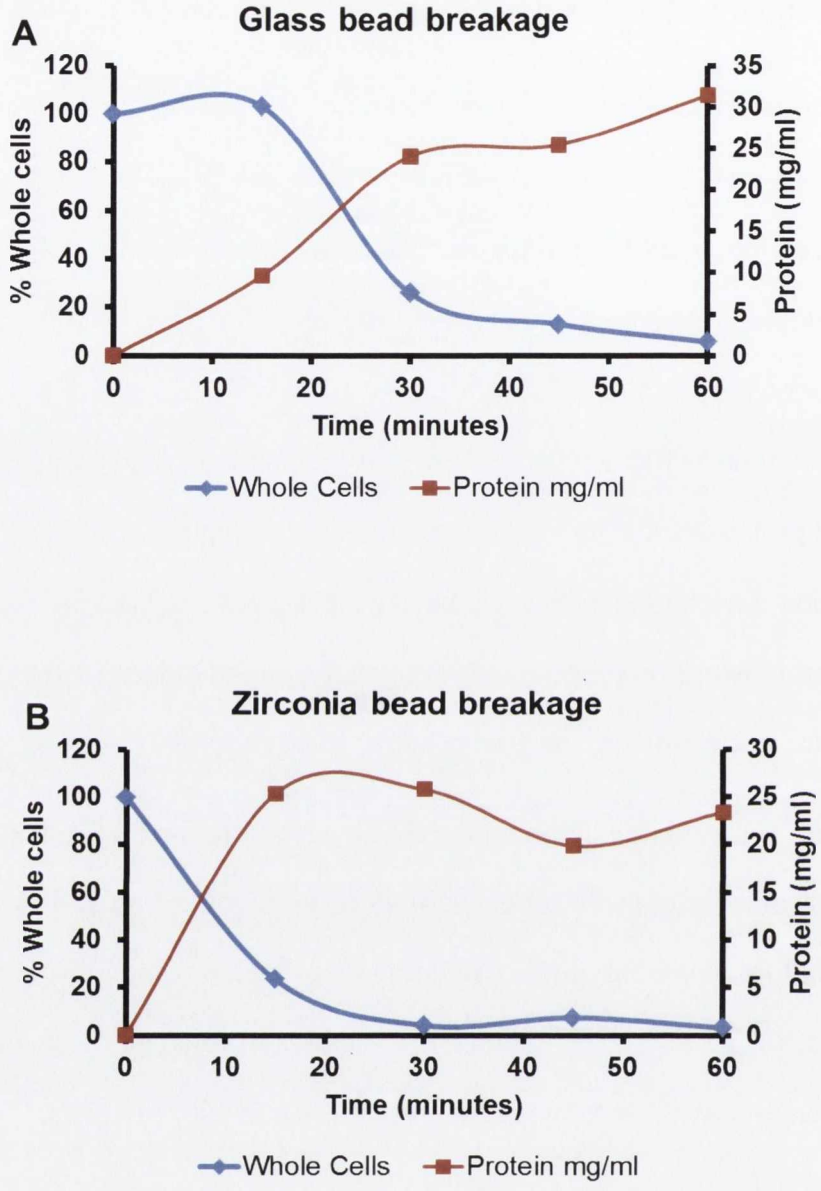

Figure 2.2. Cell lysis using Glass beads and zirconia beads. (A) Percentage whole cells and protein release in samples lysed using glass beads. (B) Percentage whole cells and protein release in samples lysed using glass beads. Percentage whole cells were calculated relative to unlysed sample set as 100 %. Protein released was calculated using Bradford assay.

Figure 2.2A and 2.2B demonstrate that a reduction in cell count corresponds with an increase in protein release, which is indicative of cell lysis. The data show that zirconia beads lyse cells more quickly than glass beads; however, 90 % of cells are lysed by 45 minutes using either bead. Despite the faster cell lysis achieved using zirconia beads, it was decided to use glass beads to lyse cells, to relieve the extra stress imposed on the vortex caused by the heavier zirconia beads.

2.13.3. Optimising chromatin sonication

The size of the fragmented DNA used in ChIP analysis determines the resolution of the technique for mapping proteins along the *in vivo* chromatin fibre. Indeed, fragments of around 500 bp are generally considered optimal for ChIP analysis (O. Aparicio et al., 2004). We therefore wanted to determine if we could achieve sufficient chromatin fragmentation by sonication using either manual or automated sonicators.

2.13.3.1. Manual sonication:

To test sonication efficiency we first used the Sanyo Soniprep 150 manual sonicator fitted with an exponential probe. Unclarified lysate was made up to 1 ml in FA lysis buffer and subjected to 10 second rounds of sonication with the instrument set to an amplitude of 9 microns per sonication pulse. The goal was to monitor a change in chromatin fragment length over a sonication time-course with a goal of achieving a 500 bp fragment size. Six samples that had been prepared under optimal cell lysis conditions were used to test sonication. Tubes 1-6, received 1, 2, 4, 6, 8 and 10 pulses respectively. Samples were kept on ice for 30 seconds between pulses. Sonicated lysate was stored at -80°C. To check DNA fragment size post-sonication, a proportion of sonicated lysate equivalent to 2 OD units of the original cell culture was protease-treated. Samples were

protease-treated by incubating with protease (Sigma) at a 1:1 sample:protease ratio with 1% $CaCl_2$ at 42°C for 2 hours. Crosslinks were reversed by incubation at 65°C overnight. Phenol-chloroform DNA extraction was performed on lysate. Half of each sample was run on a 1.5% agarose/TBE gel (Fig. 2.3).

2.13.3.2. Automated sonication

To test automated sonication we used the Diagenode Bioruptor. Unclarified lysate from bead-broken cells was made up to 1 ml with FA lysis buffer and 1 ml was transferred to each of six sonication tubes. Samples were subjected to 30 second pulses at maximum power (30 seconds sonication, 30 seconds rest). A sonication time-course was performed, with tubes receiving 2, 4, 6, 8, 10 & 12 pulses, respectively. A proportion of lysate equivalent to 4 OD units of cell culture were centrifuged for 30 minutes at 16,363 rcf, 4°C. Supernatant was transferred to a new microcentrifuge tube and 100µl protease (Sigma) added with 1% $CaCl_2$. This mixture was incubated for 2 hours at 42°C, and then 65°C overnight to reverse crosslinks. Phenol-chloroform DNA extraction was performed on lysate. Half of each sample was run on a 1.5% agarose/TBE gel (Fig. 2.4).

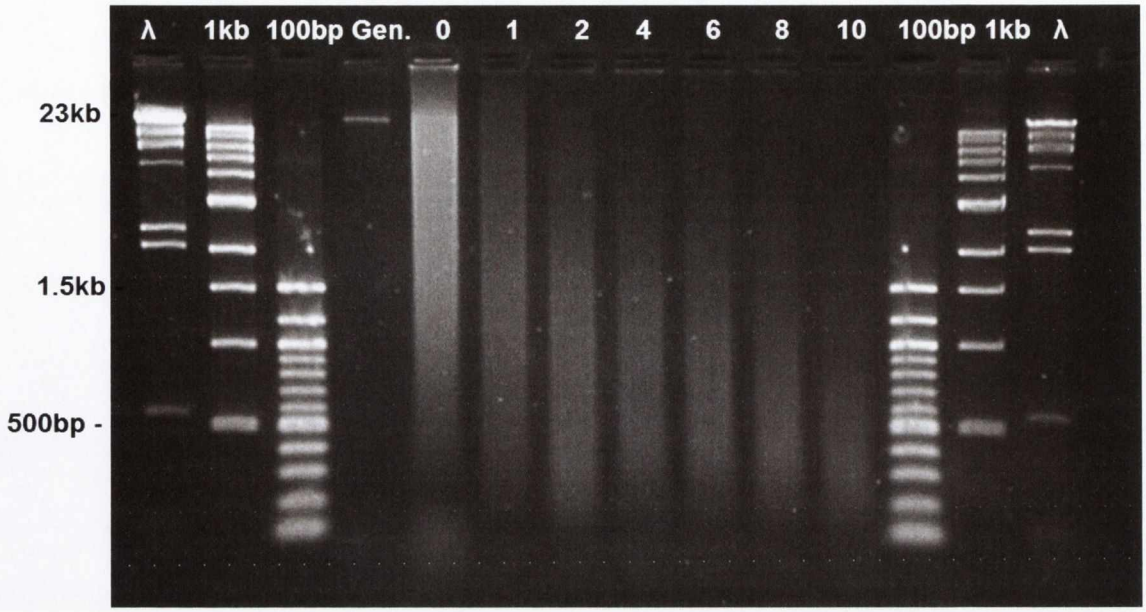

Figure 2.3. Sonication time-course using a manual sonicator. Lane 1 contains a λ phage DNA ladder (Promega; 23.1 kb, 9.4 kb, 6.6 kb, 4.4 kb, 2.3 kb, 2 kb and 524 bp), lane 2 contains a 1 kb DNA ladder (NEB; 10 kb, 8 kb, 6 kb, 5 kb, 4 kb, 3 kb, 2 kb, 1.5 kb, 1 kb and 500 bp), lane 3 contains a 100 bp DNA ladder (NEB; 1.5 kb, 1.2 kb, 1 kb, 900 bp, 800 bp, 700 bp, 600 bp, 500 bp, 400 bp, 300 bp, 200 bp and 100 bp), lane 4 contains yeast genomic DNA (Gen). Lane 5 contains DNA that was bead-broken but unsonicated (0). Lanes 6-11 contain bead-broken DNA that was subjected to 1, 2, 4, 6, 8 & 10 pulses (indicated above gel) in a manual sonicator, respectively. Lane 12 contains a 100bp DNA ladder (NEB). Lane 13 contains a 1kb DNA ladder (NEB). Lane 14 contains a λ phage DNA ladder (Promega).

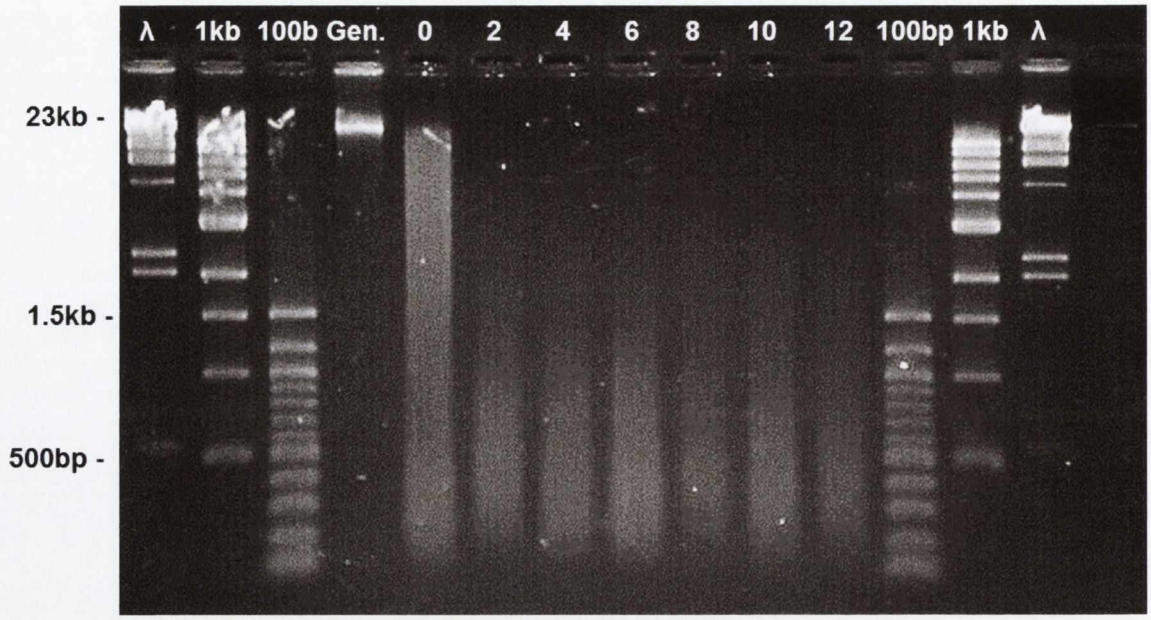

Figure 2.4. Sonication time-course using a Diagenode Bioruptor sonicator. Lane 1 contains a λ phage DNA ladder (Promega; 23.1 kb, 9.4 kb, 6.6 kb, 4.4 kb, 2.3 kb, 2 kb and 524 bp), lane 2 contains a 1 kb DNA ladder (NEB; 10 kb, 8 kb, 6 kb, 5 kb, 4 kb, 3 kb, 2 kb, 1.5 kb, 1 kb and 500 bp), lane 3 contains a 100 bp DNA ladder (NEB; 1.5 kb, 1.2 kb, 1 kb, 900 bp, 800 bp, 700 bp, 600 bp, 500 bp, 400 bp, 300 bp, 200 bp and 100 bp), lane 4 contains yeast genomic DNA (Gen). Lane 5 contains DNA that was bead-broken but unsonicated. Lanes 6-11 contain bead-broken DNA that was subjected to 2, 4, 6, 8, 10 & 12 pulses in a manual sonicator, respectively. Lane 12 contains a 100bp DNA ladder (NEB). Lane 13 contains a 1kb DNA ladder (NEB). Lane 14 contains a λ phage DNA ladder (Promega).

Figure 2.3 shows a gradual decrease in fragment length, with 10 pulses yielding an average fragment length of approximately 500 bp. Figure 2.4 shows that the DNA fragment size is also reduced using an automatic sonicator, but the near-immediate reduction in DNA fragment size may indicate DNA degradation, and for this reason it was decided to use a manual sonicator in future ChIP experiments. From this analysis, it was determined that a programme of 10 10-second pulses at 9 amplitude microns was sufficient to generate DNA fragments of 500 bp in size.

2.13.4. Chromatin immunoprecipitation (ChIP)

2.13.4.1. Cross-linking

Chromatin immunoprecipitation protocol was adapted from Current Protocols (O. Aparicio et al., 2005). Cells were grown to log phase as described previously. Formaldehyde (Sigma) was added to a final concentration of 1 % and cells were incubated for 20 minutes at room temperature with shaking. To quench the cross-linking reaction, glycine was added to a final concentration of 50 mM and cultures were incubated with shaking for a further 5 minutes. These cultures were transferred to 50 ml tubes and pelleted by centrifugation. Supernatant was discarded and cross-linked cells were washed twice in cold Tris-buffered saline (TBS). Cross-linked cells were either stored at -80°C at this stage or used immediately to prepare cell lysates.

2.13.4.2. Preparation of cell lysates

Cross-linked cell pellets were resuspended in 400 µl FA lysis buffer (50 mM HEPES, 140 mM NaCl, 1 mM EDTA,1 % Triton X-100, 0.1 % sodium deoxycholate) supplemented with a protease inhibitor (PI) mix (Sigma P2714-1BTL, resuspended according to manufacturer's instructions) and 2 mM

phenylmethylsulfonyl fluoride (PMSF) (Sigma). Resuspended cells were split between two 1.5 ml tubes and 400 µl of 400 µm-600 µm glass beads (Sigma) were added to each. All subsequent steps were performed at 4°C unless stated otherwise. Cells were lysed by vortexing for 45 minutes at maximum speed using a Genie II vortexer with 12-tube adaptor. Microcentrifuge tubes were pierced with a 23-G needle and tubes were placed in 15 ml centrifuge tubes. These 15 ml tubes were centrifuged at 1000 rcf for 5 minutes. Lysate was collected from the tubes, pooled in a 1.5 ml microcentrifuge tube and made up to 1 ml with FA lysis buffer/PI/PMSF.

Lysates were subjected to sonication in a Sanyo Soniprep 150 sonicator. Samples were sonicated in 1.5ml tubes on ice at 9 amplitude microns, and subjected to 12 pulses of 10 seconds duration. Samples were stored on ice for 1 minute between pulses to prevent over-heating.

Lysates were then clarified by centrifugation at 16,363 rcf in a microcentrifuge for 30 minutes at 4°C. Supernatant was transferred to a new 1.5ml tube and aliquots equivalent to 5 or 10 OD volumes were made. Lysate was stored at -80°C

2.13.4.3. Immunoprecipitation.

Cross-linked lysates were thawed on ice and made up to 500 µl with FA lysis buffer containing protease inhibitor. 20 µl was taken from each as input. Inputs were protease-treated by adding 100 µl ChIP elution buffer (25 mM Tris Cl [pH 7.5], 5 mM EDTA, 0.5 % SDS), 5 mM $CaCl_2$ and 2 mg/ml protease type XIV (Sigma) to each 20 µl input sample and bringing the mixture to 200 µl with 60 µl TE (pH 7.5). These samples were incubated at 42°C for 2 hours and cross-links were reversed by incubating at 65°C for 6 hours. Inputs were purified using a Qiagen QiaQuick PCR purification kit as per manufacturer's instructions.

To pre-bind antibodies to beads, 40 µl protein A sepharose beads (Sigma) or 30 µl magnetic Dynabeads (Life Technologies) were washed three times for 5 minutes in 1ml FA lysis buffer. Washed beads were resuspended in FA lysis buffer and antibody was added to the solution. Antibody-bead complexes were formed by incubation for 2 hours at 4°C followed by being washed three times for 5 minutes in 1ml FA lysis buffer. This mixture was distributed evenly between cross-linked lysates and incubated at 4°C overnight.

If antibodies and beads were not to be pre-bound, antibody was added to the remaining 480 µl lysate and incubated with rotation at 4°C overnight. The following morning, 40 µl protein A or G sepharose beads (Sigma) or 30 µl magnetic Dynabeads (Life Technologies) were washed three times for 5 minutes in 1ml FA lysis buffer. Washed beads were resuspended in FA lysis buffer and distributed evenly between lysates containing antibody. This mixture was incubated for 2 hours at 4°C.

The antibody-bead complexes were washed in 1ml FA lysis buffer for 5 minutes, followed by either one or two washes in 1 ml ChIP wash buffer #1 (50 mM HEPES [pH 7.5], 0.5 M NaCl, 1 mM EDTA, 1 % Triton X-100, 0.1 % Sodium deoxycholate), either one or two washes in 1 ml ChIP wash buffer #2 (10 mM Tris-Cl [pH 8.0], 0.25 M LiCl, 1 mM EDTA, 0.5 % NP-40, 0.5 % Sodium deoxycholate) and a single wash in 1 ml TE (pH 7.5). Beads were pelleted by centrifugation at 2152 rcf for 2 minutes (if using sepharose slurry) or bound to a magnet (if using Dynabeads) and supernatant was aspirated and discarded between washes.

After the final wash, beads were resuspended in 250 µl ChIP elution buffer (25 mM Tris Cl [pH 7.5], 5 mM EDTA, 0.5 % SDS) and mixed. The suspension was

incubated at 65°C for 20 minutes and rotated for 10 minutes at room temperature. Samples were centrifuged at 16,363 rcf for 1 minute and supernatant was transferred to a new 1.5 ml tube.

To protease-treat IP samples, 3mg/ml protease and 5mM $CaCl_2$ added and the solution was incubated at 42°C for 2 hours. Cross-links were reversed by incubation at 65°C for 6 hours. IPs were purified using a QiaQuick PCR purification kit (Qiagen) according to manufacturer's instructions. Inputs and IPs were diluted in water prior to qPCR (Table 2).

Antibody	Pre-bind?	Number of washes	Amount of antibody	Protein A or G	Source
Tup1	No	2	1.5µl	A	J. Reese
Pol II	No	2	4.5µl	A/G mix	Covance (MMS-126R)
Myc	No	2	2.5µl	G	Millipore (05-724)
H3	Yes	1	4µl	A	Active Motif (39163)
H3K9ac	No	2	2.5µl	G	Millipore (07-352)
H3K14ac	No	2	2.5µl	G	Millipore (07-353)
H4ac4	No	2	3µl	G	Millipore (06-866)
Snf2-N	No	1	2.5µl	G	J. Reese
FRB	No	2	2µl	A/G mix	Enzo (ALX-215-065-1)
H3K4me3	No	2	4µl	A	Active Motif (39159)
H3K36me3	No	1	3.5 µl	G	Abcam (ab9050)

Table 2.2. Antibodies and conditions for chromatin immunoprecipitation.

2.14. Real-time PCR (qPCR)

Template DNA for qPCR was either cDNA for transcriptional analysis or IP/Input DNA for ChIP analysis. qPCR was analysed by relative quantification using a standard curve on an Applied Biosystems StepOne Plus real-time PCR system. These standards were made using ChIP input DNA which was ten-fold serially diluted. cDNA and IP/input DNA was diluted appropriately within the standard curve. qPCR was performed using a 20µl reaction containing 1X Applied Biosystems Power SYBR Green (Thermo), 150nM of each primer, 2µl template DNA and dH_2O to 20µl. qPCR performance and analysis adhered to the Minimum Information for Publication of Quantitative Real-Time PCR Experiments (MIQE) guidelines (Bustin et al., 2009). qPCR primer specificity and efficiency was measured by melt curve analysis. Reference genes were chosen based on previously published data and in the case of novel strains or where data was unavailable, suitability was empirically tested.

cDNA generated from mRNA for transcription analysis was analysed by comparing the relative amounts of target gene cDNA to cDNA from *ACT1,* which was a control gene. *ACT1* levels are stable in all mutants tested and target gene transcripts were quantified using this as a control. Reverse-transcriptase (RT) negative samples were used to control for DNA contamination in transcription analysis.

qPCR on ChIP experiments was analysed using PCR purified IPs and inputs. Levels of enrichment were determined by comparing the levels of IP (which is indicative of protein occupancy at a given region) to input (which controls for quantities of DNA in a given sample). An example of IP/input used to determine

histone H3 levels at the *FLO1* gene promoter (FLO1) compared to an intergenic control region in chromosome V (IntV) is shown in Figure 2.5A.

When analysed using an antibody raised against histone H3, a DNA enrichment corresponding to the *FLO1* gene promoter (FLO1) is seen in wild type (wt) relative to *ssn6* mutants. This indicates that more H3 is bound to this region in wild type strains compared to *ssn6* mutants. However, at the intergenic control region used to monitor H3 occupancy (IntV), wild type and *ssn6* mutant strains have similar levels of DNA enrichment indicative of H3 occupancy at this locus. When FLO1 is normalised to IntV (Fig. 2.5B), it can be seen that wild type strains have a higher level of H3 occupancy at *FLO1* than *ssn6* mutants, but the difference in H3 occupancy in wild type and *ssn6* mutant strains is more pronounced due to the slightly higher level of enrichment at IntV in an *ssn6* mutant, which may be the result of differing IP efficiencies. Normalisation to an internal control region is not strictly required, but results in better reproducibility in analysis of ChIP qPCR data.

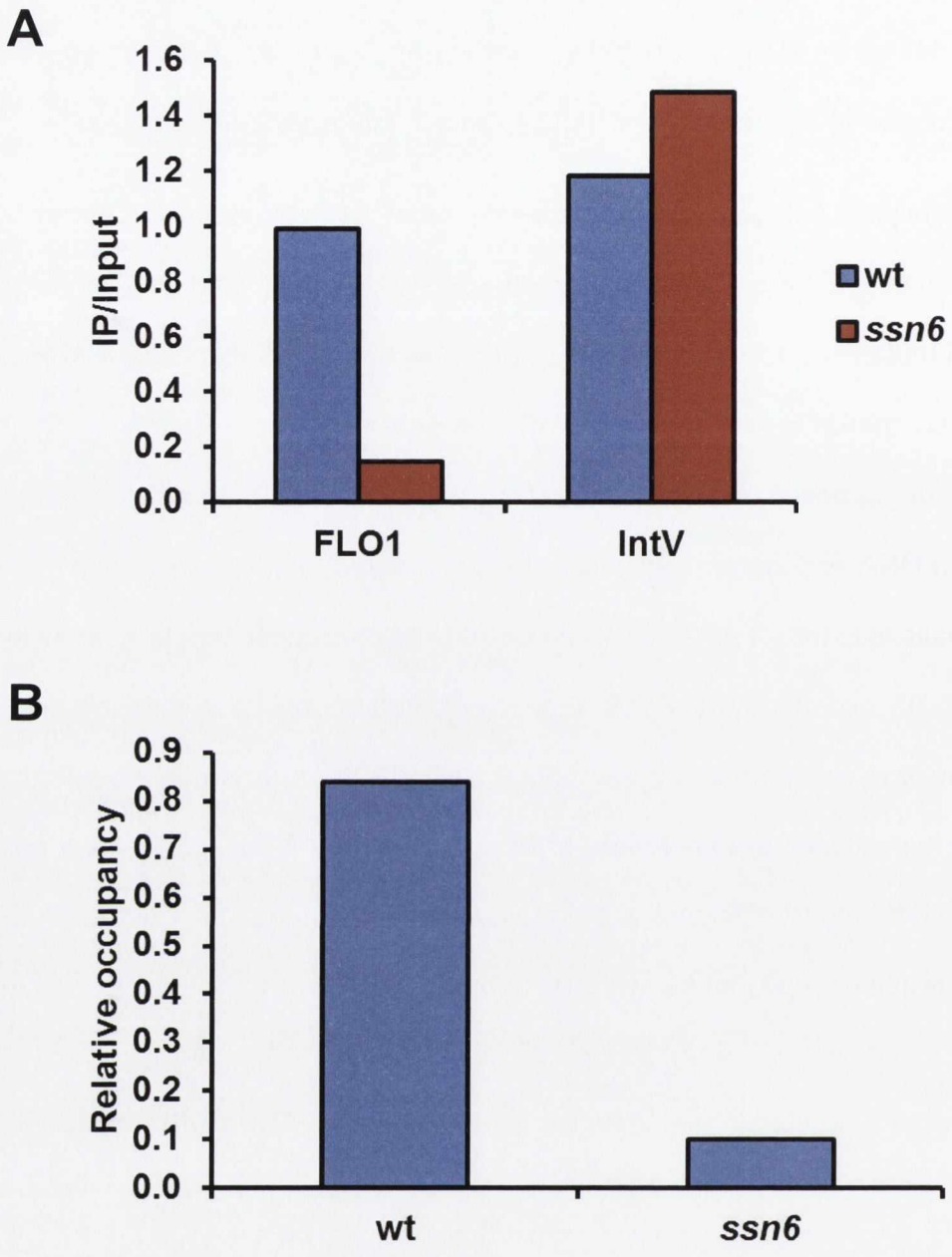

Figure 2.5. Analysis of Chromatin Immunoprecipitation (ChIP). ChIP analysis of H3 occupancy of the *FLO1* promoter in wild type (wt) and *ssn6* mutant strains. (A) IP/input of H3 occupancy 585 bp upstream of the *FLO1* transcription start site (TSS) (FLO1) and at an intergenic region of chromosome V (IntV). (B) H3 occupancy of the *FLO1* promoter 585 bp upstream of the *FLO1* TSS (FLO1) normalised to an intergenic region of chromosome V (IntV). This figure shows a single, representative example of the normalisation method (n=1).

2.15. Western Immunoblotting

SDS-PAGE gels were soaked in transfer buffer (25 mM Tris, 190 mM glycine & 20% methanol). Protein was transferred to a polyvinylidene fluoride (PVDF) membrane (Immobilon) in transfer buffer at 300 mA for 40 minutes. After transfer, membranes were blocked using blocking buffer (5% dried skimmed milk in Tris-buffered saline with 0.05% Tween 20 [TBST]) for 30 minutes. Primary antibody was diluted appropriately in blocking buffer and membranes were incubated in this solution with gentle agitation at 4°C overnight. Antibodies used in Western blot are listed in Table 2.3.

After incubation, membranes were washed 4 times for 5 minutes each in TBST. Horseradish peroxidase-conjugated secondary antibody was diluted 1:10,000 in blocking buffer, and membranes were incubated in this solution for 90 minutes at room temperature. Secondary antibody solution was poured off and membranes were washed for 10 minutes in TBST, and for three further washes of 10 minutes in TBS. Membranes were incubated in enhanced chemiluminescent (ECL) substrate (Pierce) for 5 minutes before being developed using film and/or a GE Las4000 imager.

Protein	Concentration	Species	Source
β-actin	1:3,000	Mouse	Abcam (ab8224)
Myc	1:5,000	Mouse	Millipore (05-724)
Ssn6	1:500	Goat	Santa Cruz (sc-11953)
Tup1	1:5,000	Rabbit	J. Reese
Gcn5	1:500	Rabbit	Santa Cruz (sc-9078)
H3	1:5,000	Rabbit	Active Motif (39163)
H3K9ac	1:3,000	Rabbit	Millipore (07-352)
H3K14ac	1:2,500	Rabbit	Millipore (07-353)
H4ac4	1:6,000	Rabbit	Millipore (06-866)
H3K4me3	1:3,000	Rabbit	Active Motif (39159)
H3K36me3	1:1,000	Rabbit	Abcam (ab9050)

Table 2.3. Antibodies used in Western immunoblotting. Table showing antibodies used in Western blot analysis of proteins. All antibodies were diluted in 5 % skimmed milk in tris-buffered saline with 0.05% Tween 20 (TBST)

2.15.1. Confirmation of Myc-tagged Sas3p

In some cases where ChIP was to be performed on a protein of interest, antibody with specificity to the native target protein was unavailable or not of sufficient quality for ChIP analysis. In these instances, target proteins were tagged with 9-Myc epitopes and immunoprecipitated using anti-Myc. Epitope-tagging was carried out and confirmed genomically by PCR as described previously. In order to confirm that proteins of interest were expressed with the desired tag and to the correct molecular weight, Western blots were performed, as in the case of Sas3p (Figure 2.6).

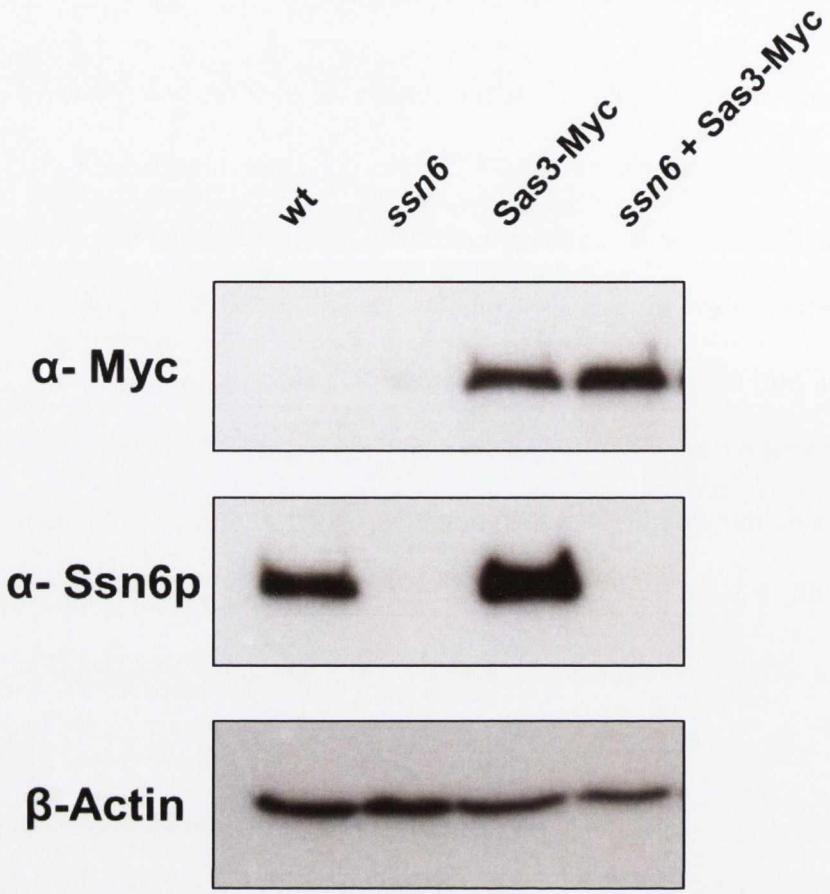

Figure 2.6. Confirmation of Myc tag in Sas3-Myc and ssn6 + Sas3-Myc. Western blot of global Myc-tagged Sas3p and Ssn6p levels in wild type (wt), *ssn6* mutant, Sas3-Myc and *ssn6* + Sas3-Myc strains. β-Actin was used as a loading control.

Ssn6p was present, though there was no Myc detected in un-tagged wild-type cells (Fig. 2.6). *ssn6* mutant strains with not Myc tag present had no detectable Myc or Ssn6p when analysed by Western blot. Strains containing a Sas3p tagged with a Myc epitope displayed a Myc-tagged Sas3p of the correct size (~107kDa) both in the presence (Sas3-Myc) and absence of Ssn6p (*ssn6* + Sas3-Myc). This analysis confirmed that a Myc-tagged Sas3p was present in these strains.

2.16 Statistical analysis of experiments.

Experiments were performed using 2-4 biological replicates (as labelled), and in the case of growth curves and qPCR, Standard Error of the Mean (SEM) was calculated. To assess the statistical significance of each result between mutant strains, an un-paired Student's T-test was performed on data using Microsoft Excel, where a result was deemed statistically significant if a p-value of <0.05 was obtained.

For comparison of microarray and cell size datasets, a Mann-Whitney test was performed using Graphpad Prism statistical analysis software. This was an unpaired, two-tailed test, where a result was deemed statistically significant if a p-value of <0.05 was obtained.

2.17 Analysis of microarray data.

tup1 mutant transcription profiles were obtained from experiments performed by DeRisi et al (DeRisi et al., 1997). *ssn6* mutant transcription data was generated by experiments performed by Fleming, A.B (personal communication). Initial bioinformatics analysis was performed by Hokamp, K and Sivasankaran, S. The two mutant datasets were then compared in Microsoft Excel and genes were

annotated using *Saccharomyces* Genome Database (SGD-www.yeastgenome.org). Gene groupings were assigned based on functions described on SGD. This data can be found on the supplementary CD (Tables S4 and S5).

Chapter 3

Investigating phenotypic differences between *tup1* and *ssn6* mutants

3.1. Introduction

Tup1-Ssn6 is a transcriptional co-repressor complex composed of a single Ssn6p subunit and 4 Tup1p subunits (Varanasi et al., 1996). The complex does not bind DNA directly, but is recruited to target genes by site-specific DNA-binding proteins (Komachi et al., 1994; Treitel and Carlson, 1995). Tup1p possesses a "repression domain" which has been shown to interact with histones (Edmondson et al., 1996). Ssn6p has been shown to bind to Tup1p and the recruiting factors thereby tethering Tup1p to target genes (Tzamarias and Struhl, 1994). This has led to the model whereby Tup1p contains the repressive activity of the complex, and Ssn6p acts as a link between Tup1p and target genes. The aim of this study was to further investigate the contributions of each subunit to gene repression and to determine if either could act independently. I therefore analysed wild type (wt) and single *tup1* and *ssn6* mutants and a *tup1 ssn6* double mutant for various phenotypes. The model would predict that if Tup1p and Ssn6p functioned solely as a complex, then single *tup1, ssn6* and double *tup1ssn6* mutants would all have the same phenotypes relative to the wild type.

3.2. Results

3.2.1. Growth differences between *tup1* and *ssn6* mutants

To investigate the effect of *tup1* and *ssn6* gene deletion mutations, I first analysed cell growth in these strains. Wild type (wt), *ssn6* and *tup1* single mutants and a *tup1 ssn6* double mutant (YMC12) were grown to log phase and each cell culture was adjusted to a starting cell density of 5×10^5 cells/ml. Cell growth was then monitored by monitoring OD_{600} values of each strain over time (Figure 3.1).

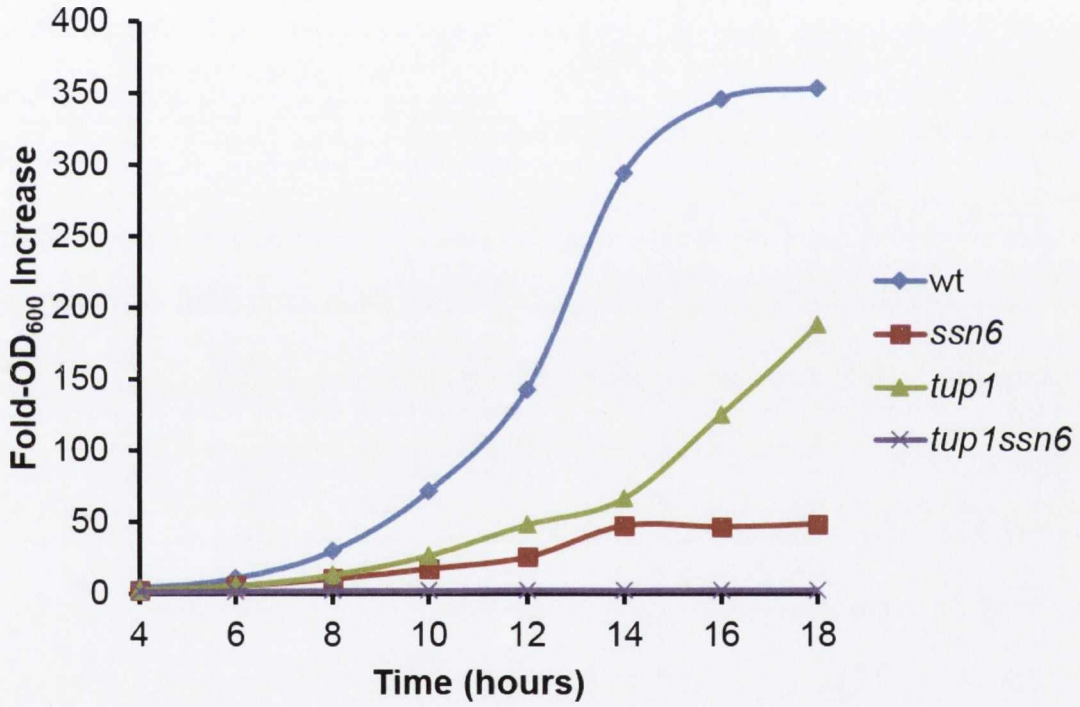

Figure 3.1: Growth differences between *tup1* and *ssn6* mutants. Wild type (wt), *tup1* and *ssn6* single mutants and a *tup1ssn6* double mutant were diluted to $2x10^5$ cells/ml and grown at 30°C for 18 hours. OD_{600} readings were taken every 2 hours. The fold-increase in OD_{600} reading relative to the first reading over the time course is shown. Data shown is from a single experiment, representative of the relative growth rates between mutants.

The *tup1* mutant had a slower growth rate than the wild type (Fig. 3.1). However, the *ssn6* single and the *tup1 ssn6* double mutant have progressively slower growth rates than either the wild type or the *tup1* single mutant. This suggests that deletion of *SSN6* has a more severe impact on cell growth than loss of *TUP1* and loss of both *TUP1* and *SSN6* has the most severe impact on growth.

3.2.2 *tup1* and *ssn6* mutants have distinct stress-response phenotypes

Having established that *tup1* and *ssn6* mutants exhibit different growth rate phenotypes, it was decided to investigate whether there were other differences in phenotypes between the mutant strains. Wild type, *tup1* and *ssn6* single mutants and a *tup1 ssn6* double mutant were therefore assayed for their response to various stresses using plate assays (Figure 3.2). The phenotypes of the strains were examined in response to heat shock (Fig. 3.2B and 3.2C), cell wall stress (Fig. 3.2D), and DNA replication stress (Fig. 3.2E)

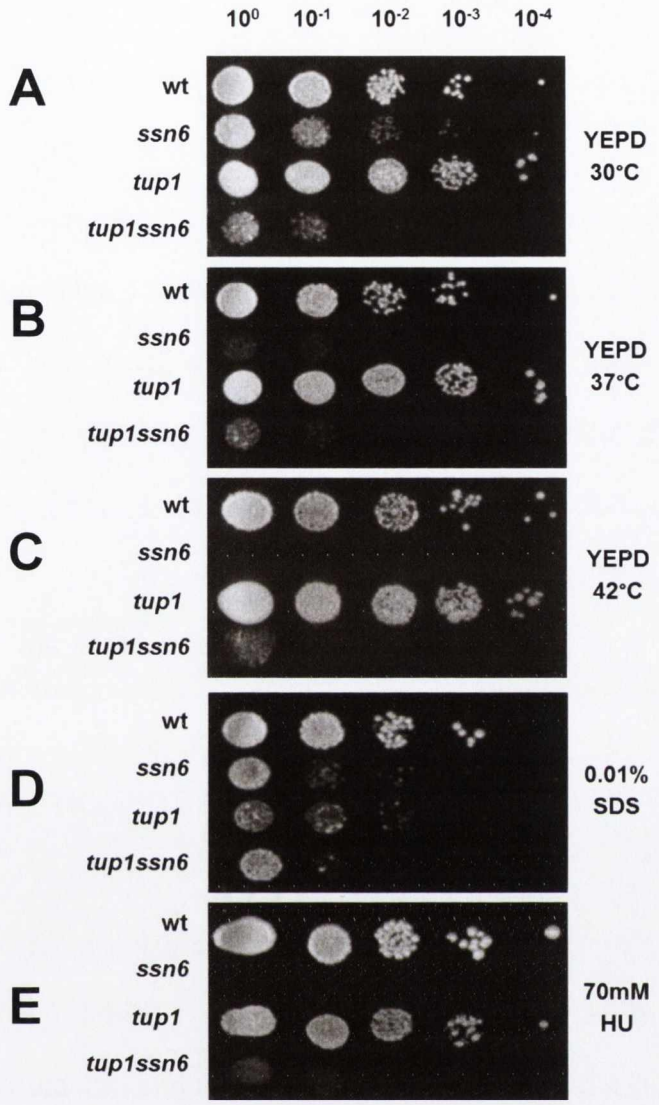

Figure 3.2. Phenotypic differences between tup1 and ssn6 mutants. (A) Wild type, *ssn6* and *tup1* single mutants and a *tup1ssn6* double mutant were grown on YEPD at 30°C as a control for cell growth on solid medium. (B) Cells were grown on YEPD at 37°C to test temperature stress phenotypes. (C) Cells were grown on YEPD at 42°C to test temperature stress phenotypes. (D) Cell wall stress. Cells were grown at 30°C on YEPD containing 0.01% SDS (E) Replication stress. Cells were grown on YEPD and YEPD containing 70mM hydroxyurea (HU) at 30°C. All cells were serially diluted from an initial cell density of 2 x10^7 cells/ml prior to growth on solid media.

Figure 3.2 shows cell growth of each strain on plates under the conditions indicated following serial dilution of strains normalised to the same starting cell density. All mutant growth phenotypes were compared to the growth of each strain on the 30°C YEPD control plate (Fig. 3.2A). It is important to note that the difference in the growth rate of the mutants compared to wild type, as shown in figure 3.1 is evident on the 30°C YEPD control plate. Taking the different growth rates into account, the data show that compared to wild type cells, *tup1* mutants showed no sensitivity to heat shock at both 37°C and 42°C (Fig. 3.2B and 3.2C). However, both *ssn6* single and *tup1 ssn6* double mutants displayed severe growth impairment under these conditions, with the *ssn6* mutant being the most heat-sensitive.

When cells were exposed to cell wall stress caused by the addition of SDS to the growth medium, all mutants exhibited impaired growth compared to wild type cells (Fig. 3.2D). However, the *tup1* mutant was inhibited the most by SDS. I next examined the sensitivity of the mutants to hydroxyurea (HU). HU causes replication stress by inhibiting the enzyme ribonucleotide reductase and therefore reducing the pool of available deoxyribonucleotides (Elford, 1968). The data show that the *tup1* mutant showed no growth defect on YEPD agar containing HU compared to wild type cells (Fig. 3.2E). However, an *ssn6* single mutant and a *tup1 ssn6* double mutant were more sensitive to HU and growth on the HU plates was drastically impaired. Again, the *ssn6* mutant showed the most severe phenotype, being the most sensitive to HU. This suggests that Tup1p and Ssn6p contribute differently to various cell stresses.

3.2.3. *tup1* and *ssn6* mutants exhibit different cell size phenotypes

Having established that *tup1* and *ssn6* mutants display distinct growth and stress response phenotypes, I next investigated cell morphology. Cells were grown to log phase and equal numbers of cells were viewed on a light microscope (Fig. 3.3A). Cells were also analysed using a Tali image-based cytometer, and histograms were constructed representing the distribution of cell sizes in wild type, *ssn6* and *tup1* single mutant and *tup1 ssn6* double mutant cell populations (Fig. 3.3B).

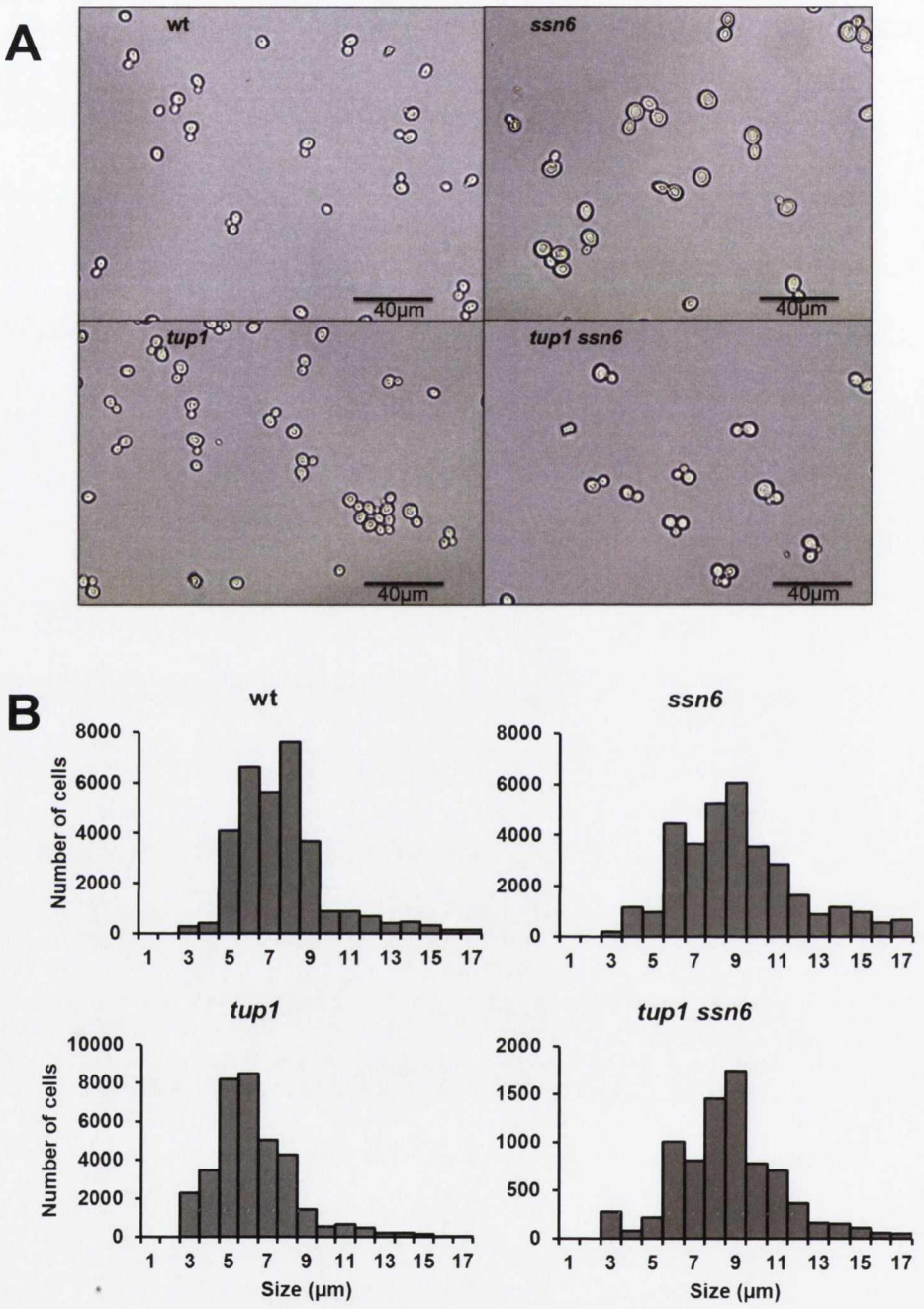

Figure 3.3. Cell phenotype in wild-type, *ssn6* and *tup1* mutant strains. Cultures were adjusted to $2x10^7$ cells/ml and cells were (A) observed at 400x magnification and (B) analysed using a Tali Image Cytometer to assess cell size in wild type, *ssn6, tup1* and *tup1 ssn6* mutants. Data was analysed using a Mann-Whitney test to compare cell size distribution between mutants.

The data show differences in cell size between *tup1* and *ssn6* mutants (Fig. 3.3). Fig. 3.3A shows a large cell phenotype in *ssn6* single and *tup1 ssn6* double mutants. *tup1* single mutants did not appear enlarged relative to the wild type. Figure 3.3B shows histograms indicating cell size distributions within the cell populations. Wild type cells had an average size of 7.6μm, *ssn6* mutants were an average size of 8.5μm, *tup1* mutants displayed an average size of 6.3μm and *tup1 ssn6* double mutants had an average cell size of 8.6 μm. While the average size of the *ssn6* single and *tup1 ssn6* double mutants were greater than that of both the wild type and *tup1* mutant, the histograms showed that this may be due to a greater variety in cell size seen in these mutants compared to the other strains rather than a uniform increase in cell size. Statistical analyisis of cell size distribution using Mann-Whitney tests to compare strains revealed that *ssn6* mutants were significantly larger than *tup1* mutants ($p=0.035$) and *tup1 ssn6* mutants ($p=0.001$). The impact of the loss of Ssn6p on cell size in the *tup1 ssn6* double mutant compared to the *tup1* single mutant suggests that it is the loss of Ssn6p that causes an increase in cell size.

3.2.4. *tup1* and *ssn6* mutants exhibit different flocculation phenotypes

One striking phenotype exhibited by *tup1* and *ssn6* mutants is flocculation. Flocculation is the non-sexual, calcium-dependent aggregation of cells due to expression of lectin-like cell wall proteins known as flocculins (Smukalla et al., 2008). This phenotype is a stress response, and the major flocculin-encoding gene in *S. cerevisiae* is *FLO1*. In order to establish whether there were differences in the flocculation phenotypes of *tup1* and *ssn6* mutants, two flocculation assays were performed. In one, which was designed to determine the size and morphology of flocs, cultures were adjusted to the same cell density in

tissue culture plates and cells were dispersed by agitation. Five minutes after the cessation of agitation, the cells were photographed. Flocculating cells form clumps whereas non-flocculent cells do not and remain dispersed. The experiment was repeated in the presence of EDTA as a control which inhibits flocculation by chelating Ca^{2+} ions (Figure 3.4A).

In the second assay, which was designed to address the rate of cell sedimentation between *tup1* and *ssn6* mutants, cultures were adjusted to the same cell density, agitated to disperse flocs and then the optical density of the cultures was analysed by spectrophotometry over time. The flocculent cultures displayed a drop in optical density over time (Figure 3.4B).

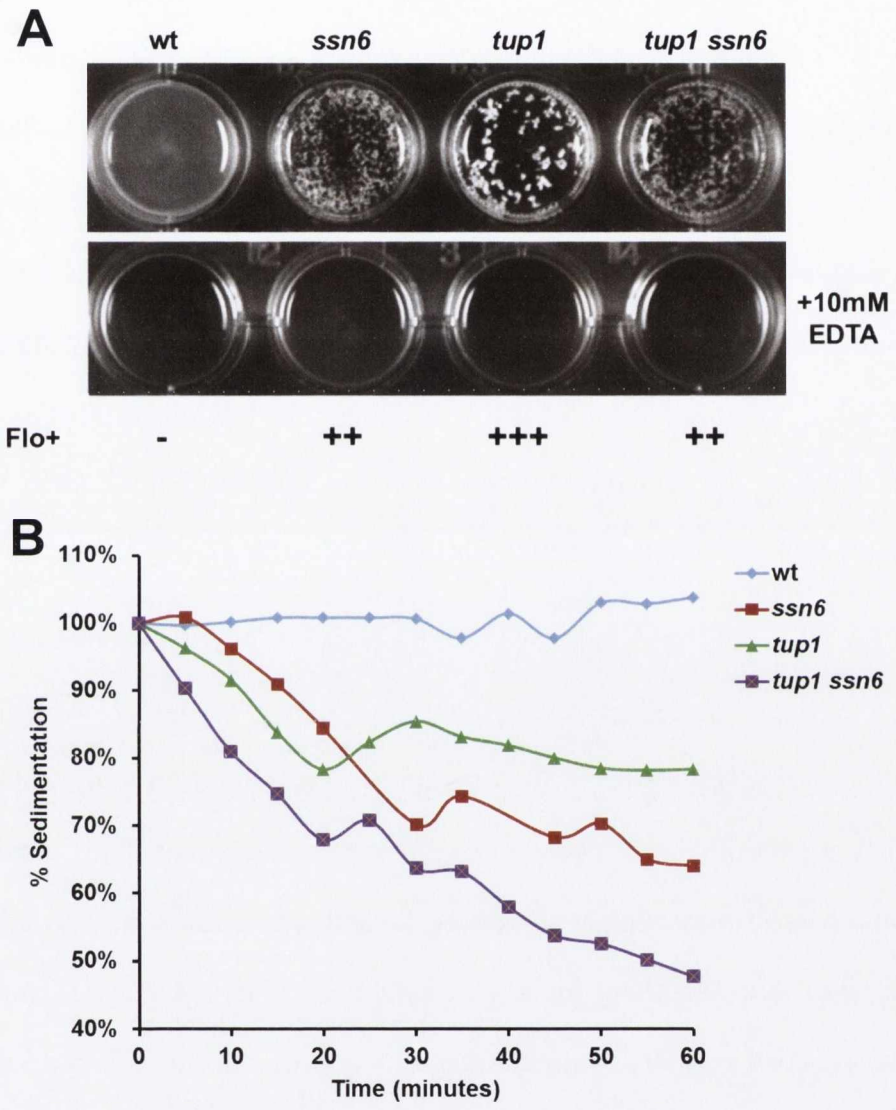

Figure 3.4. Flocculation in wild-type, *ssn6*, *tup1* and *tup1 ssn6* mutant strains. Cultures were adjusted to $2x10^7$ cells/ml and observed in tissue culture plates, both without (A) and with the addition of 10mM EDTA. Level of flocculation (Flo+) is scored underneath. (B) Sedimentation of wild type (wt), *ssn6* and *tup1* single mutants and a *tup1 ssn6* double mutant measured by spectrophotometry. Values shown are optical density (OD_{600}) readings normalised to the original OD_{600} value of the culture.

In the first assay, wild type cultures did not have a flocculent phenotype in the presence or absence of 10mM EDTA (Fig. 3.4A, wt). *ssn6* mutants were highly flocculent, but this phenotype was lost upon the addition of EDTA (Fig. 3.4A, *ssn6*). *tup1* mutants also exhibited a flocculent phenotype which was dispersed by EDTA, but these mutants appeared to form larger, tighter flocs than *ssn6* mutants (Fig. 3.4A, *tup1*). *tup1 ssn6* double mutants displayed a similar flocculation phenotype to *ssn6* single mutants where flocs were less dense than *tup1* single mutants. *tup1 ssn6* mutant flocs were also dispersed by the addition of 10mM EDTA (Fig. 3.4A, *tup1 ssn6*). This suggests that *tup1* and *ssn6* mutants display different flocculation phenotypes, with *ssn6* and *tup1 ssn6* mutants forming smaller flocs than *tup1* mutants.

In a separate assay measuring cell sedimentation, wild type cultures did not exhibit a decrease in optical density over time, due to the lack of flocculation in this strain (Fig. 3.4B, wt). *ssn6* mutants showed a rapid drop in optical density, indicating sedimentation of flocculent cells in this strain (Fig. 3.4B, *ssn6*). *tup1* mutants also sediment rapidly compared to wild type strains, though this strain "settled" less than the *ssn6* mutant by one hour (Fig. 3.4B, *tup1*). *tup1 ssn6* mutants exhibit the most dramatic sedimentation by one hour and do so more quickly than both *ssn6* and *tup1* single mutants (Fig. 3.4B, *tup1 ssn6*). This suggests that there are different rates of sedimentation between *tup1* and *ssn6* mutants, and that a *tup1 ssn6* double mutant exhibits the most dramatic sedimentation due to its flocculent phenotype.

3.2.5. *FLO1, FLO5* and *FLO9* transcription is de-repressed in *tup1* and *ssn6* mutants

FLO1 is the dominant member of a family of flocculin-encoding genes in *S. cerevisiae* (Teunissen and Steensma, 1995). *FLO5* and *FLO9* are also genes responsible for flocculation. *FLO5* and *FLO9* are 96% and 94% identical to *FLO1,* respectively, and confer distinct flocculation phenotypes of their own (Teunissen and Steensma, 1995; Van Mulders et al., 2009). However, while *FLO1* regulation by Tup1-Ssn6 is well-characterised, it is unknown if *FLO5* and *FLO9* are regulated by the complex.

Having established differences in flocculation phenotype between *tup1* and *ssn6* mutants (Fig. 3.4), it was decided to monitor transcription of the *FLO1, FLO5* and *FLO9* genes in these strains to determine if differences are solely due to *FLO1* transcription, or arise from transcription of the other flocculin-encoding genes in *tup1* and *ssn6* mutants (Figure 3.5).

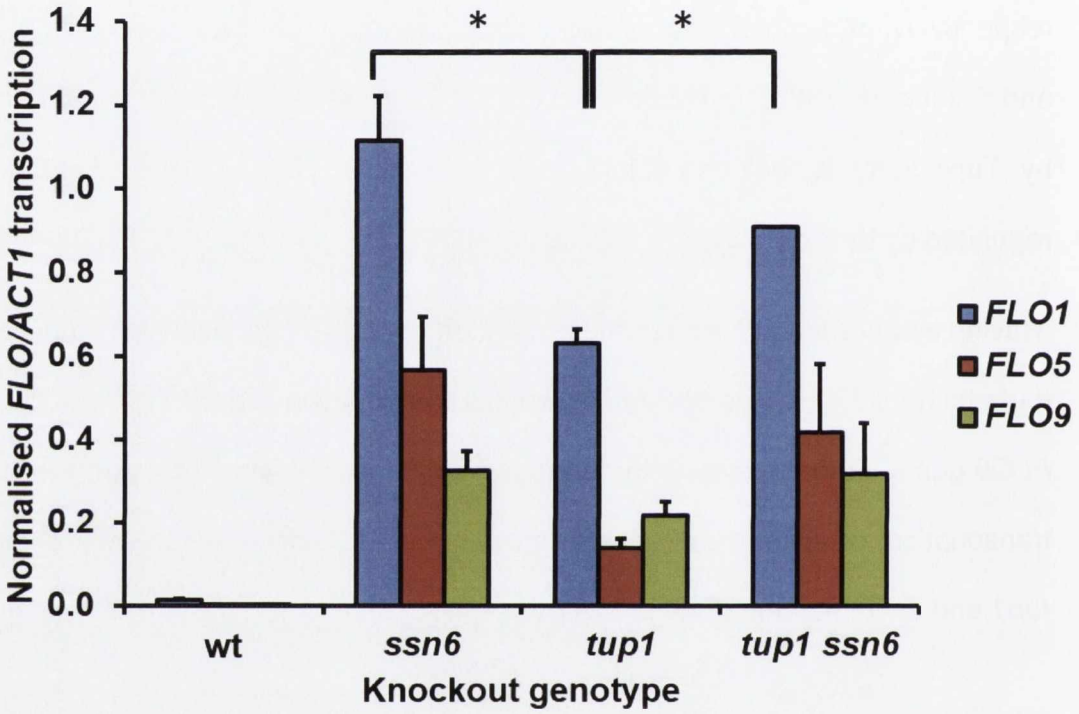

Figure 3.5. *FLO1*, *FLO5*, and *FLO9* transcription. *FLO1*, *FLO5*, and *FLO9* transcription in wild type cells, *ssn6* and *tup1* single mutants and a *tup1ssn6* double mutant was measured by qRT-PCR. *FLO* transcripts were normalised to transcription of the *ACT1* gene. Asterisks represent a p-value of p=<0.05 obtained from a Student's t-test. Values represent data from 2-4 independent experiments.

In the non-flocculent wild type (wt) strain, there was no detectable *FLO1* transcription (Fig. 3.5). In an *ssn6* single mutant, *FLO1* was highly de-repressed. The *tup1* mutant exhibited *FLO1* de-repression, but displayed a significantly lower level of *FLO1* transcription compared to an *ssn6* mutant. This suggests a greater role for Ssn6p in repression of *FLO1* transcription. However, when both *SSN6* and *TUP1* were deleted (*tup1 ssn6*), a similar level of *FLO1* transcription to an *ssn6* single mutant was evident. This suggests that Ssn6p may retain a repressive role in the *tup1* single mutant.

I next investigated *FLO5* and *FLO9* transcription in the *tup1* and *ssn6* mutants to determine if these genes contributed to the flocculation phenotypes observed in figure 3.4. In the non-flocculent wild type (wt) strain, there was no detectable *FLO5* or *FLO9* transcription (Fig. 3.5). In an *ssn6* single mutant, *FLO5* and *FLO9* were highly de-repressed, though to a lower level than *FLO1*. The *tup1* mutant exhibited *FLO5* and *FLO9* de-repression, but displayed a reproducibly lower level of *FLO5* and *FLO9* transcription compared to an *ssn6* mutant, though this difference was more apparent at *FLO5*. This suggests a greater role for Ssn6p in repression of *FLO5* and *FLO9* transcription. However, when both *SSN6* and *TUP1* were deleted (*tup1 ssn6*), a similar level of *FLO5* and *FLO9* transcription to an *ssn6* single mutant was evident. This suggests that Ssn6p may retain a repressive role in the *tup1* single mutant at *FLO5* and *FLO9* as well as at *FLO1*.

Taken together, the data show that in the absence of Tup1p or Ssn6p *FLO1* is de-repressed to the greatest extent, followed by *FLO5* and then *FLO9*. The data show that Ssn6p has the greatest role in *FLO* gene repression, since in its absence *FLO* gene transcription is de-repressed the most. Furthermore, the data suggests Ssn6p may exert a repressive effect in the absence of Tup1p.

3.2.6. *tup1* and *ssn6* mutants display different levels of *SUC2* transcription

Another gene under the transcriptional control of Tup1-Ssn6 is *SUC2*. *SUC2* encodes invertase; an enzyme required for the metabolism of sucrose, and has been studied extensively in the context of Tup1-Ssn6 gene regulation (Fleming and Pennings, 2007), (Treitel and Carlson, 1995). *SUC2* is repressed by Tup1-Ssn6 in the presence of high glucose concentrations and is transcribed in response to low glucose (Ozcan et al., 1997).

I therefore monitored transcription of *SUC2* in *ssn6* and *tup1* mutants during growth in media containing either high or low glucose concentrations. (Figure 3.6)

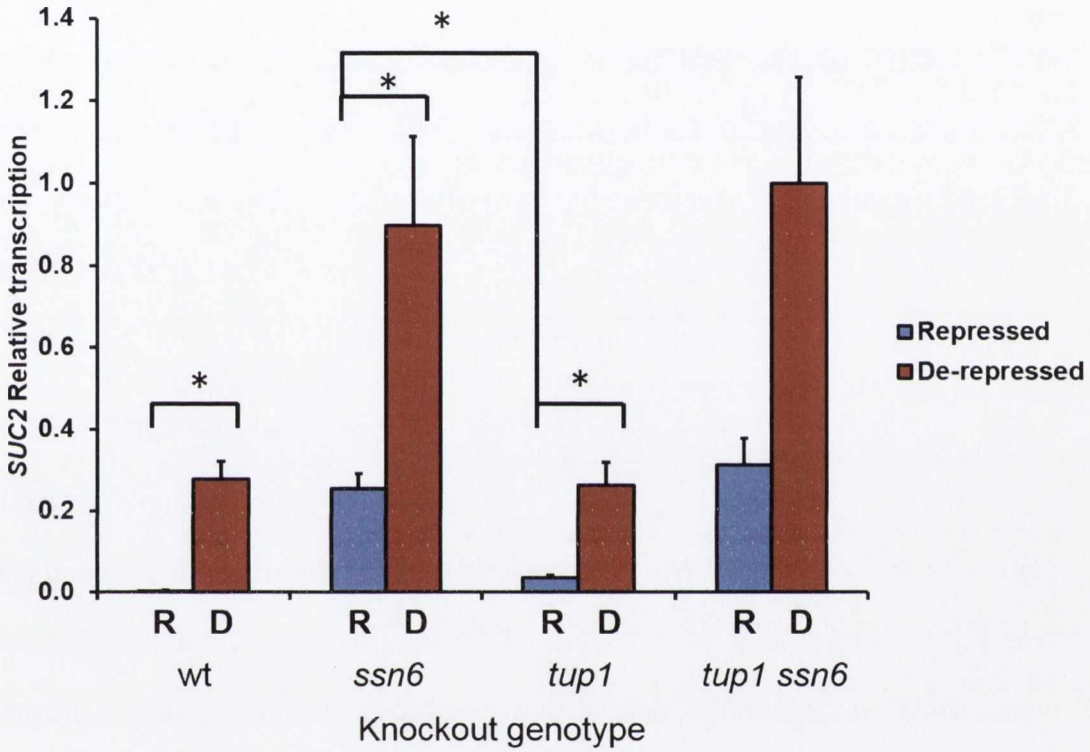

Figure 3.6. *SUC2* transcription in *tup1* and *ssn6* mutants. *SUC2* transcription was monitored in wild type, *ssn6*, *tup1* single mutants and a *tup1ssn6* double mutant grown in 2% glucose (repressed) and 0.05% glucose (de-repressed), by qRT-PCR. Transcription is shown relative to *ACT1* gene transcription with all strains relative to de-repressed *tup1ssn6* transcript levels. Asterisks represent a p-value of p=<0.05 obtained from a Student's t-test. Error bars represent standard error of the mean (SEM) from 3 independent experiments.

When wild type cells were grown in high glucose (2%), *SUC2* transcription was repressed (Fig. 3.6) (Ozcan et al., 1997). However, *ssn6* mutants showed a high level of *SUC2* de-repression compared to wild type under these conditions (Fig. 3.6, compare *ssn6* R to wt R). When grown in high glucose, *tup1* mutants showed significant *SUC2* de-repression relative to wild type cells, but transcription was significantly lower compared to *ssn6* mutants (Fig. 3.6; compare *ssn6* R to *tup1* R). This suggests a greater role for Ssn6p in repression of *SUC2* transcription. Interestingly, *tup1 ssn6* mutants showed similar levels of *SUC2* de-repression to the *ssn6* single mutant under conditions of high glucose (Fig. 3.6, compare *tup1 ssn6* R to *ssn6* R). This suggests that under *SUC2*-repressing conditions, Ssn6p may retain a repressive role in the *tup1* single mutant.

When wild type cells were grown in low glucose (0.05%), *SUC2* was de-repressed (Fig. 3.6, wt) (Ozcan et al., 1997). However, *ssn6* mutants showed a high level of *SUC2* de-repression compared to wild type under these conditions (Fig. 3.6, compare wt D and *ssn6* D). Furthermore, the transcription was significantly higher than the level of *SUC2* de-repression in this mutant grown in high glucose (Fig. 3.6, compare *ssn6* D and *ssn6* R). Under growth in low glucose, *tup1* mutants also showed significant *SUC2* de-repression relative to *tup1* mutants grown in high glucose (Fig. 3.6, compare *tup1* D and *tup1* R), but *SUC2* transcription was significantly lower compared transcription in to *ssn6* mutants grown in low glucose (Fig. 3.6, compare *tup1* D and *ssn6* D). This again suggests a greater role for Ssn6p in repression of *SUC2* transcription. In the *tup1 ssn6* mutant grown in low glucose, the levels of *SUC2* de-repression were similar to the levels in the *ssn6* single mutant (Fig. 3.6, compare *tup1 ssn6* D and *ssn6* D). This suggests that under *SUC2* de-repressing conditions, Ssn6p may retain a repressive role in the *tup1* single mutant.

Under both *SUC2* repressing and de-repressing growth conditions, *SUC2* transcription in *ssn6* single and *tup1 ssn6* double mutants was more highly de-repressed than in *tup1* mutants. Furthermore, when grown under *SUC2* de-repressing conditions (D), *ssn6* and *tup1 ssn6* showed further *SUC2* de-repression compared to transcription in *SUC2*-repressing conditions (R). This suggests that Ssn6p may be carrying out a repressive role at *SUC2* even under conditions of wild type and *tup1* mutant *SUC2* de-repression.

3.2.7. *tup1* and *ssn6* mutants show different patterns of global gene de-repression

The *FLO1* and *SUC2* data suggested a greater role for Ssn6p in repression of gene transcription (Fig. 3.5 and 3.6). It was therefore decided to investigate transcription of Tup1-Ssn6-regulated genes on a global scale in *tup1* and *ssn6* mutants. To do this, I analysed transcription microarray data showing gene de-repression in a *tup1* mutant from DeRisi et al, by obtaining the gene list from the Yeast Microarray Global Viewer (http://www.transcriptome.ens.fr/ymgv/), and identifying genes that were >2-fold up-regulated in a *tup1* mutant compared to wild type. This was compared to transcription microarray data obtained from an *ssn6* mutant from Fleming, AB (See Supplemental data) (DeRisi et al., 1997). The fold-de-repression compared to a wild type control in each case was used to determine the effect of each mutant on transcription (Figure 3.7).

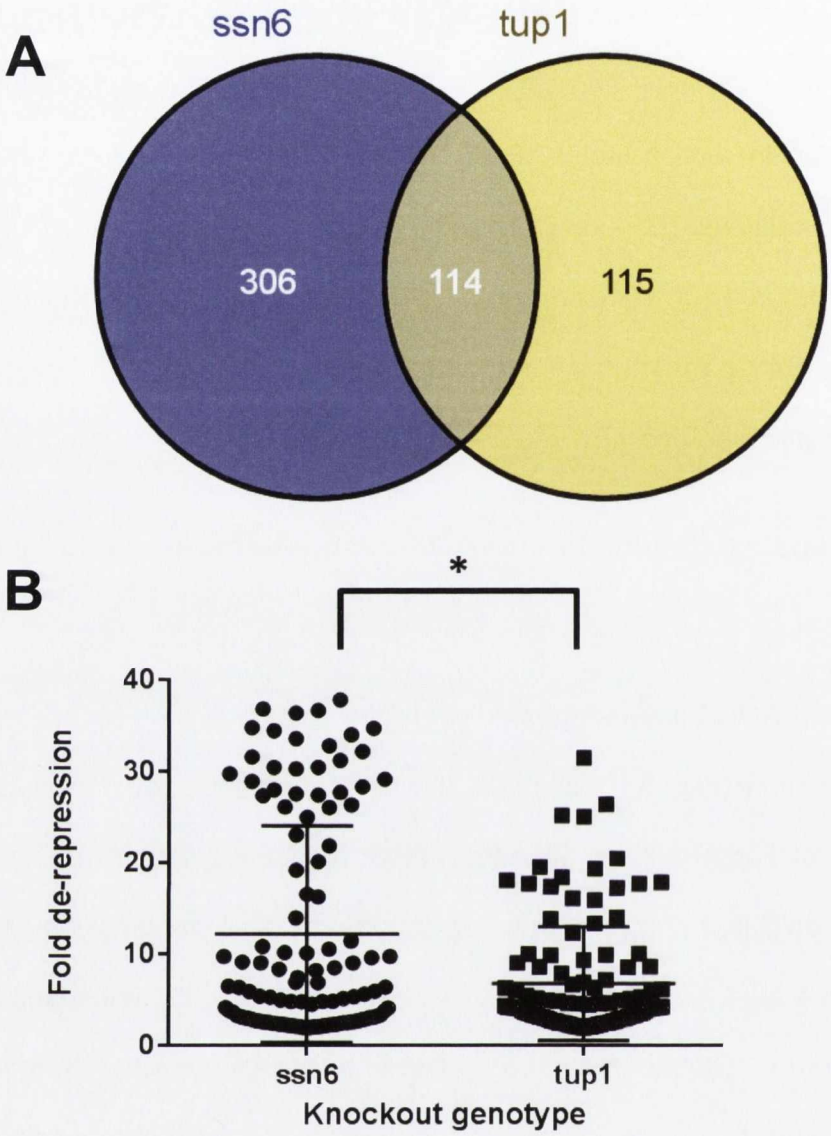

Figure 3.7. Global gene transcription in *tup1* and *ssn6* mutants. (A) Venn Diagram of genes de-repressed at least two-fold in *tup1* and *ssn6* mutants relative to wild type. (B) Fold-de-repression of genes de-repressed in both *tup1* and *ssn6* mutants relative to wild type strains (114). Venn diagram was generated using Venny (http://bioinfogp.cnb.csic.es/tools/venny/index.html). Asterisks represent a p-value of <0.05 as determined using a Mann-Whitney U test.

According to this analysis, 420 genes were found to be de-repressed over two-fold relative to the wild type control in an *ssn6* single mutant, whereas 229 genes were de-repressed relative to the wild type in a *tup1* mutant (Fig. 3.7A). This included 114 genes that were de-repressed in both *tup1* and *ssn6* mutants. Thus, Ssn6p repressed a greater number of genes than Tup1p.

In the subset of 114 genes that were de-repressed in both *tup1* and *ssn6* mutants, gene de-repression in an *ssn6* mutant showed transcription 12.2-fold greater than in the wild type. However, *tup1* mutants showed gene de-repression that was only 6.8 times that seen in the wild type control. This suggests that when loss of either Tup1p or Ssn6p causes de-repression of a gene, *ssn6* mutants cause genes to be more highly de-repressed than *tup1* mutants. Thus, on average, Ssn6p plays a greater role in gene repression than Tup1p.

3.2.8. Different classes of genes are de-repressed in *tup1* and *ssn6* mutants.

The previous analysis established that different numbers of genes were de-repressed in *tup1* and *ssn6* mutants, and that the commonly de-repressed subset of genes were repressed to different levels in the strains (Fig. 3.7). The aim of this analysis was to determine if Tup1p and Ssn6p regulated distinct classes of genes. To investigate this, genes de-repressed only in the *tup1* (115) or *ssn6* (306) mutants and the genes commonly de-repressed in both strains (114) were analysed for gene ontology using the same data used to construct figure 1.7. (Fig. 3.8).

tup1

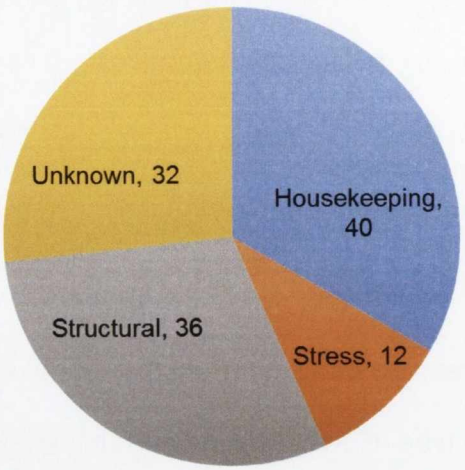

ssn6

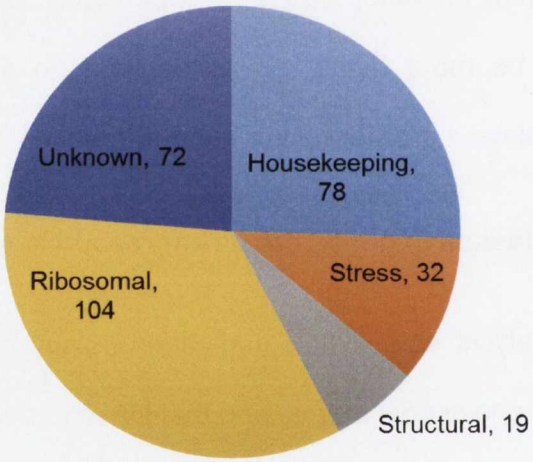

Common

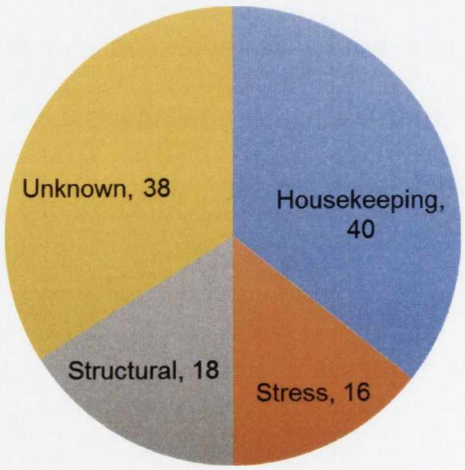

Figure 3.8. Analysis of genes transcribed in *tup1* and *ssn6* mutants. Breakdown of gene functions found to be de-repressed at least two-fold in *tup1* and *ssn6* mutants relative to wild type. (A) Genes de-repressed in *tup1* mutants only (115). (B) Genes de-repressed in *ssn6* mutants only (306). (C) Genes de-repressed in both *tup1* and *ssn6* mutants relative to wild type (114).

The cellular functions of genes de-repressed by Tup1p and Ssn6p were different depending on the mutant studied (Fig. 3.8). 36 structural genes were uniquely de-repressed in a *tup1* mutant (Fig. 3.8, *tup1*). This includes proteins involved in cell wall synthesis. 12 genes involved in stress responses and 40 housekeeping genes were also found to be de-repressed only in this strain. *ssn6* mutants had 19 structural genes, 32 stress response genes and 78 housekeeping genes de-repressed unique to this strain (Fig. 3.8, *ssn6*). 104 genes encoding ribosomal proteins were also found to be de-repressed only in an *ssn6* mutant. Genes de-repressed in both *tup1* and *ssn6* mutants included 40 housekeeping genes, 18 genes involved in cell structure and 16 stress response genes (Fig. 3.8, common).

These data suggest that Tup1p and Ssn6p repress different classes of genes. Tup1p repressed more structural genes than Ssn6p whereas Ssn6p repressed ribosomal protein-encoding genes uniquely. This indicates that Tup1p and Ssn6p may be regulating unique groups of genes separately from each other and that these genes have different functions. These data are in agreement with van Bakel et al who mapped nucleosome and transcription changes in *tup1* and *ssn6* mutants and found differences in gene expression between mutant strains (van Bakel et al., 2013). , though in their own study, Hughes et al described the de-repression observed in *tup1* and *ssn6* mutants as very large and very similar (Hughes et al., 2000).

3.2.9. Tup1p and Ssn6p display differences in global occupancy

The previous data indicated that *tup1* and *ssn6* mutants regulate distinct subsets of genes (Fig. 3.7 and 3.8). This suggests that Tup1p and Ssn6p may be directly recruited to different subsets of genes. If Ssn6p was regulating a greater number

of genes than Tup1p directly, it would be expected that Ssn6p would be detected at a greater number of genes than Tup1p. To test whether this was the case, I analysed TAP-tagged Tup1p and Ssn6p global binding data from experiments carried out by Venters et al (Venters et al., 2011). As part of this analysis, Tup1p and Ssn6p binding to gene upstream activation sequence (UAS) regions was compared (Figure 3.9).

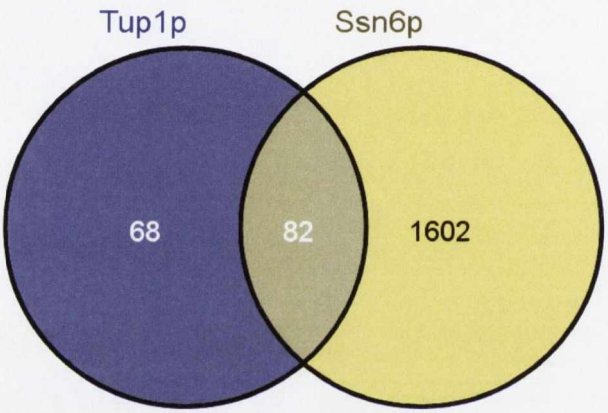

Figure 3.9. Occupancy of gene promoters by Ssn6p and Tup1p. ChIP-chip data from Venters et al (Venters et al., 2011). Tup1-TAP and Ssn6-TAP presence over the −320 to −260 upstream activation sequence (UAS) regions scoring above the false discovery rate (FDR) was included in this analysis. Venn diagram was generated using Venny (http://bioinfogp.cnb.csic.es/tools/venny/index.html).

Strikingly, the data showed that TAP-tagged Ssn6p (Ssn6-TAP) was detected at 1684 gene promoters in total (Fig. 3.9). However, Tup1-TAP was only detected at 150 sites in the same analysis. Both Ssn6-TAP and Tup1-TAP were detected together at 82 gene promoters in this analysis. This suggests that Ssn6p bound a much greater number of gene promoters globally than Tup1p, and this difference in promoter occupancy may explain the greater number of genes de-repressed in an *ssn6* mutant compared to a *tup1* mutant (Fig. 3.7).

3.2.10. *ssn6* mutants display an increase of small RNA under glucose starvation

During the analysis of *SUC2* transcription, RNA was visualised on formaldehyde-agarose gels (Figure 3.10).

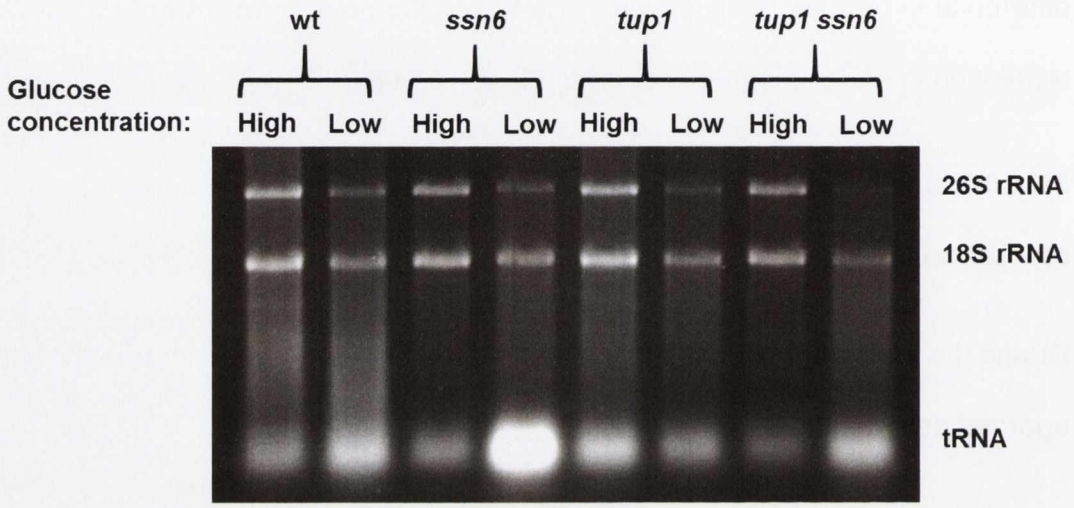

Figure 3.10. Small RNA vs ribosomal RNA (rRNA) in glucose-starved cells. Cells were grown to log phase and washed. Half were incubated with 2% glucose (high) and half with 0.05% glucose (low); Formaldehyde-agarose gel (1 %) showing RNA in wild type (wt), *ssn6* and *tup1* single mutants and a *tup1ssn6* double mutant under high and low glucose.

In wild type cells, strong bands representing 26S rRNA, 18S rRNA and tRNA were visible on the formaldehyde-agarose gels under conditions of both high and low glucose (Fig. 3.10), although there was a slight increase in small RNAs relative to 18S rRNA in glucose-starved cells. However, there was a dramatic increase in apparent tRNAs in the *ssn6* mutant under low-glucose conditions (Fig. 3.10, see *ssn6*, low glucose). *tup1* mutants did not display an increase in this small RNA to the same level as seen in an *ssn6* mutant when cells were grown in low glucose. However, *tup1 ssn6* double mutants did exhibit a similar increase in small RNAs relative to 18S and 26S rRNA under glucose starvation to *ssn6* single mutants, indicating that it is the lack of Ssn6p that causes this phenotype. This intriguing data may suggest a repressive role for Ssn6p in RNA Polymerase III transcription of tRNA genes.

3.3. Discussion

Taken together, this analysis of phenotypes in mutants deleted for either *TUP1* or *SSN6* shows clear differences between *tup1* and *ssn6* mutants. Figure 3.1 shows that there is a growth defect in both *tup1* and *ssn6* mutants compared to wild type cells, although the defect is greatest in the *ssn6* mutants. Importantly, the *tup1 ssn6* double mutant's growth rate was slower than either single mutant. This suggests that *tup1* mutants and *ssn6* mutants could have distinct defects in metabolism and growth, and combining these mutations leads to a more severe phenotype than either individual mutation.

The data show that *tup1* and *ssn6* mutants displayed sensitivity to a number of stresses relative to the wild type strain (Fig. 3.2). An *ssn6* single mutant was severely impaired by growth at 37°C and 42°C, whereas *tup1* mutants were not affected by heat shock at 37°C or 42°C (Fig. 3.2B and 3.2C). However, *tup1 ssn6*

double mutants were also dramatically inhibited by growth at both 37°C and 42°C, but there was less inhibition than in an *ssn6* single mutant, suggesting that additional loss of Tup1p in an *ssn6* mutant improves cell survival following heat shock.

tup1 mutants were more severely impaired by growth in the presence of SDS than *ssn6* mutants relative to growth on YEPD (Fig. 3.2D). This suggests that loss of Tup1p affected cell wall integrity more severely than loss of Ssn6p. Finally, while *tup1* mutants were not impaired while growing in the presence of hydroxyurea (HU), *ssn6* mutant growth was completely inhibited (Fig. 3.2E). Furthermore, *tup1 ssn6* mutants appeared to be less inhibited by HU than *ssn6* single mutants, indicating that *ssn6* mutants have a DNA replication defect, but additional loss of Tup1p lessens the severity of this phenotype.

When viewed under the microscope, both *ssn6* single mutants and *tup1 ssn6* double mutants had a large cell phenotype (Fig.3.3A). When further analysed using a cytometer, *ssn6* mutants actually displayed a wider variety in cell size. While there were some *ssn6* mutant cells of a similar size to wild type, there was a much higher proportion of *ssn6* mutants that were >9μm in size when compared to wild type cells and *tup1* mutants. This indicates that loss of Ssn6p, but not Tup1p, leads to a fault in cell size regulation, which could involve defective budding, cell wall maintenance or protein synthesis.

The most striking phenotype displayed by *tup1*, *ssn6* and *tup1 ssn6* mutants is flocculation. Flocculation is the calcium-dependent, non-sexual aggregation exhibited by cells expressing cell wall proteins known as flocculins. This phenotype can be abolished by the addition of EDTA to the growth medium, which sequesters calcium ions and disperses flocs (Smukalla et al., 2008). When

viewed in tissue culture plates, wild type cells did not have a flocculent phenotype (Fig. 3.4). However, *ssn6* single mutants were highly flocculent, with these flocs dispersing with the addition of EDTA. *tup1* mutants appeared to form "tighter" flocs than *ssn6* single mutants, which were also dispersed with EDTA. *tup1 ssn6* double mutants had a similar phenotype to *ssn6* single mutants, being highly flocculent, though not forming flocs as tightly as *tup1* single mutants.

Following further analysis of this phenotype, *tup1* and *ssn6* mutants both showed faster cell sedimentation compared to wild type cells (Fig. 3.4C). This indicated that all mutants studied were flocculent, with *ssn6* single and *tup1 ssn6* double mutants sedimenting more quickly than *tup1* single mutants. The differences in sedimentation and flocculation phenotypes between *tup1* and *ssn6* mutants may be partly due to differences in cell size between the mutants, with the larger *ssn6* and *tup1 ssn6* mutants unable to pack as tightly as the *tup1* mutants (Fig. 3.3).

Flocculation is dependent on the expression of a family of flocculin-encoding genes. These genes are not transcribed in wild type cells, but the major flocculin-encoding gene in *S. cerevisiae, FLO1* has been shown to be de-repressed in *tup1* and *ssn6* mutants (Teunissen and Steensma, 1995; Fleming and Pennings, 2001). *FLO1* transcription was therefore monitored alongside *FLO5* and *FLO9* transcription in *tup1* and *ssn6* mutants to determine whether Tup1p and Ssn6p also regulate *FLO5* and *FLO9* repression, and to investigate the relative contribution of *FLO1, FLO5* and *FLO9* in the flocculent phenotypes previously observed (Fig. 3.4).

In non-flocculent wild type cells, there was no *FLO1, FLO5* or *FLO9* transcription detected (Fig. 3.5). However, *ssn6* mutants displayed de-repression of all three genes, with *FLO1* transcription being the highest, followed by *FLO5* and then

FLO9 transcription. *tup1* mutants showed *FLO1, FLO5* and *FLO9* de-repression, but to a lesser extent than *ssn6* mutants. *tup1 ssn6* double mutants also exhibited de-repression of *FLO1, FLO5* and *FLO9* transcription to a similar level to that seen in *ssn6* single mutants. This suggests that Tup1-Ssn6 does contribute to repression of *FLO5* and *FLO9*, and loss of Ssn6p has a greater impact on transcription of *FLO1, FLO5* and *FLO9.* The data also suggest that Ssn6p may be carrying out repression of *FLO1* transcription in the absence of Tup1p. Finally, this analysis indicates that *FLO1* is the most highly-transcribed flocculin gene regulated by Tup1-Ssn6 and likely shows the greatest contribution to flocculation in *tup1* and *ssn6* mutants.

SUC2 is another gene under the transcriptional control of Tup1-Ssn6. *SUC2* transcription is repressed in the presence of high glucose and is de-repressed in response to low glucose (Ozcan et al., 1997). The data confirmed that *SUC2* was not transcribed under repressing (R) conditions in wild type strains (Fig. 3.6). However, under these same conditions of high glucose, *SUC2* was most highly de-repressed in *ssn6* single mutants as compared to the lower level of *SUC2* de-repression evident in *tup1* mutants. Finally, *tup1 ssn6* double mutants showed *SUC2* de-repression at levels similar to those measured in the *ssn6* single mutants when grown in high glucose.

When grown in *SUC2* de-repressing (D) conditions, wild type cells displayed *SUC2* de-repression, as previously published (Fig. 3.6). However, *ssn6* mutants exhibited higher levels of *SUC2* de-repression than wild type cells when grown in low glucose. *tup1* mutants on the other hand, showed a similar level of *SUC2* de-repression to wild type cells when grown in low glucose. When both Tup1p and Ssn6p were absent, the *tup1 ssn6* double mutants showed high *SUC2* de-repression similar to that of the *ssn6* single mutant. Importantly, the level of *SUC2*

transcription in the *ssn6* mutant grown under low glucose (D) conditions was higher than transcription of *SUC2* in the wild type strain grown under these *SUC2* de-repressing conditions. This therefore suggests that Ssn6p may still be having a repressive role at *SUC2* during normal *SUC2* induction.

Together, these data indicate that (i) Ssn6p has a greater role in *SUC2* repression than Tup1p (ii) Ssn6p may be carrying out repression in the absence of Tup1p at *SUC2* and (iii) that even under *SUC2* de-repressing conditions, Tup1-Ssn6 may be acting to partially repress *SUC2* in wild type strains.

Tup1-Ssn6 regulates a large number of genes in *S. cerevisiae*, and data generated by DeRisi et al and Fleming, AB (unpublished) was analysed in order to compare the contributions of each subunit to repression of transcription on a global scale (Fig. 3.7)(DeRisi et al., 1997). In *ssn6* mutants, 420 genes were de-repressed >2-fold relative to wild type strains (Fig. 3.7A), whereas *tup1* mutants exhibited de-repression of 229 genes. 114 genes were found to be de-repressed in both *tup1* and *ssn6* mutants. Within the set of 114 commonly de-repressed genes, *ssn6* mutants showed levels of de-repression almost two-fold higher than those of *tup1* mutants (Fig. 3.7B). These data indicate that Ssn6p regulates more genes than Tup1p and that loss of Ssn6p had a greater impact on gene repression than loss of Tup1p.

In the groups of genes that were uniquely de-repressed in *tup1* or *ssn6* mutants, there were some interesting patterns. *tup1* mutants had many structural genes de-repressed, especially related to cell wall structure (Fig. 3.8). This may help to explain the fact that *tup1* mutants were more vulnerable to cell wall stress than *ssn6* mutants (Fig. 3.2D). However, *ssn6* mutants de-repressed many genes that express ribosomal proteins, none of which were de-repressed in *tup1* mutants.

This suggests that *tup1* and *ssn6* mutants may regulate different subsets of genes, and in the gene subsets that are regulated in common, loss of Ssn6p appears to have a more severe impact on gene transcription than loss of Tup1p.

This gene transcription data is supported by the fact that Ssn6-TAP was found to bind a higher number of gene promoters than Tup1-TAP in a published study (Fig. 3.9). This suggests that the greater number of genes de-repressed in an *ssn6* mutant when compared to a *tup1* mutant was due to the fact that Ssn6p bound a greater number of genes than Tup1p. However, the large number of genes bound by Ssn6-TAP compared to the lower number de-repressed in an *ssn6* mutant suggest that the majority of genes bound by Ssn6p were not de-repressed in the absence of Ssn6p, whereas the majority of genes bound by Tup1-TAP were de-repressed upon loss of Tup1p.

When total RNA was visualised on a formaldehyde-agarose gel, *ssn6* mutants showed an increase in small RNAs relative to 18S rRNA in RNA extracted from cells grown in low glucose (Fig. 3.10). This increase in small RNA was not seen in wild type cells or *tup1* single mutants, but was observed in *tup1 ssn6* double mutants, albeit to a lesser extent. It is intriguing to suggest that this small RNA may in fact be tRNA, as it runs at the same position as tRNA on a formaldehyde-agarose gel. If this is the case, this may indicate a role for Ssn6p in repression of tRNA-encoding genes and therefore Pol III transcription. This would be a significant result, as a role for Tup1-Ssn6 in Pol III transcription has not been established previously. In support of a potential role for Tup1-Ssn6 in regulation of tRNA synthesis is the fact that Tup1p and Ssn6p have both been found to bind 13 tRNA genes in a genome-wide study of Tup1-Ssn6 occupancy (Hanlon et al., 2011).

From this analysis, it is evident that *tup1* and *ssn6* mutants have different phenotypes, suggesting distinct roles for Tup1p and Ssn6p. Not only do Tup1p and Ssn6p appear to act separately, but different global binding profiles indicate that Ssn6p binds many regions in the absence of Tup1p. The *FLO1* and *SUC2* transcription data indicate that Ssn6p is capable of exerting repression in the absence of Tup1p, even at genes that are known to be de-repressed upon loss of Tup1p. Numerous previous studies have used *tup1* mutants as representative of strains that have no Tup1-Ssn6 activity (Wong and Struhl, 2011), (DeRisi et al., 1997). However, the data presented here would suggest that to study Tup1-Ssn6 complex function, strains should be selected on a gene-specific basis as it is apparent that different gene subsets may be affected separately by *tup1* or *ssn6* mutants.

Chapter 4

Tup1p and Ssn6p have different contributions to *FLO1* regulation

4.1. Introduction

The different phenotypes identified in *tup1* and *ssn6* mutants suggest that Tup1p and Ssn6p play distinct roles in various cellular processes, including transcription. Considering the flocculation phenotype was one of the most striking phenotypes displayed by *tup1* and *ssn6* mutants, I decided to focus on the differences in *FLO1* transcription that were shown in *tup1* and *ssn6* mutants in order to determine the contribution of each subunit to regulation of *FLO1* transcription. The *FLO1* gene was chosen for analysis as it encodes the major yeast cell wall protein responsible for the cell-to-cell aggregation, or flocculation, phenotype.

The mechanism of *FLO1* repression by Tup1-Ssn6 is not currently well-understood. There are a number of mechanisms by which Tup1-Ssn6 has been proposed to repress gene transcription. Firstly, Tup1-Ssn6 can directly interact with RNA Polymerase II (Pol II) to prevent gene transcription (M. Lee et al., 2000). Secondly, Tup1-Ssn6 can interact with multiple histone deacetylases (HDACs) in order to remove the gene-activating histone acetyl marks from target promoters (Watson et al., 2000; Davie et al., 2003). Tup1-Ssn6 can also propagate a repressive nucleosomal array at gene promoters, which is thought to prevent access by Pol II and prevent transcription (B. Li and Reese, 2001). Finally, Tup1-Ssn6 can mask activation domains on DNA-binding proteins and prevent promoter access to factors that activate gene transcription (Wong and Struhl, 2011).

FLO1 is repressed by Tup1-Ssn6 which has been shown to promote strongly positioned nucleosomes across the gene promoter. This ordered promoter chromatin structure is lost, and histones are depleted, upon deletion of *TUP1* or *SSN6* (Fleming and Pennings, 2001). *FLO1* de-repression in the absence of

Tup1-Ssn6 has been shown to be dependent on the ATP-dependent nucleosome-remodelling Swi-Snf complex, since *FLO1* is not transcribed in a strain null for both Swi-Snf and Tup1-Ssn6 (Fleming and Pennings, 2001). One model for regulation of *FLO1* transcription might be that Swi-Snf acts in conjunction with histone acetyltransferases (HATs) to disrupt promoter chromatin structure and de-repress *FLO1* when Tup1-Ssn6 is absent (Wong and Struhl, 2011). To gain insight into the regulation of *FLO1* transcription, I examined the occupancy of Swi-Snf, nucleosomes and selected histone post-translational modifications in *tup1* and *ssn6* mutants.

In the previous chapter, I had shown that there were differences in *FLO1* gene transcription in *tup1* and *ssn6* mutants. Indeed, an *ssn6* mutant had a significantly greater level of *FLO1* de-repression than that measured in a *tup1* mutant (Figure 3.5). In this section I aimed to determine if there were any differences in histone occupancy and levels of histone post-translational modifications (PTMs) that might correlate with transcription at the *FLO1* promoter in *tup1* and *ssn6* mutants. Based on the current models for Tup1-Ssn6 activity, the *FLO1* transcription data might predict that histone levels may be lower in the more highly de-repressed *ssn6* mutant compared to the less highly de-repressed *tup1* mutant and , that histone PTMs associated with active transcription may be more pronounced in the *ssn6* mutant compared to the *tup1* mutant.

4,2, Results

4.2.1. Swi-Snf is present at the *FLO1* promoter in both *tup1* and *ssn6* mutants.

Having observed differences in *FLO1* transcription between *tup1* and *ssn6* mutants (Fig. 3.5), it was decided to investigate the factors involved in *FLO1* repression and de-repression in these mutants. The aim was to identify what was responsible for the difference in transcription in these strains. I therefore investigated the promoter occupancy of the Swi-Snf co-activator complex. Swi-Snf had previously been shown to be required for *FLO1* de-repression via a genetic analysis, but its presence at the *FLO1* promoter had not been demonstrated (Fleming and Pennings, 2001). I therefore decided to investigate if Swi-Snf could be detected at the de-repressed *FLO1* promoter and if so, to determine if its occupancy would be different in the absence of Tup1p, Ssn6p or both. If Swi-Snf was directly regulating *FLO1* de-repression, I hypothesised that there would be increased occupancy at the *FLO1* promoter by Swi-Snf in *ssn6* single and *tup1 ssn6* double mutants, where *FLO1* transcription is highest, compared to a *tup1* mutant. To test this hypothesis, ChIP analysis was performed using a Myc epitope-tagged Snf5p sub unit of Swi-Snf (Figure 4.1). Snf5p is essential for Swi-Snf function and its presence at *FLO1* would be indicative of the presence of the Swi-Snf complex (Geng et al., 2001).

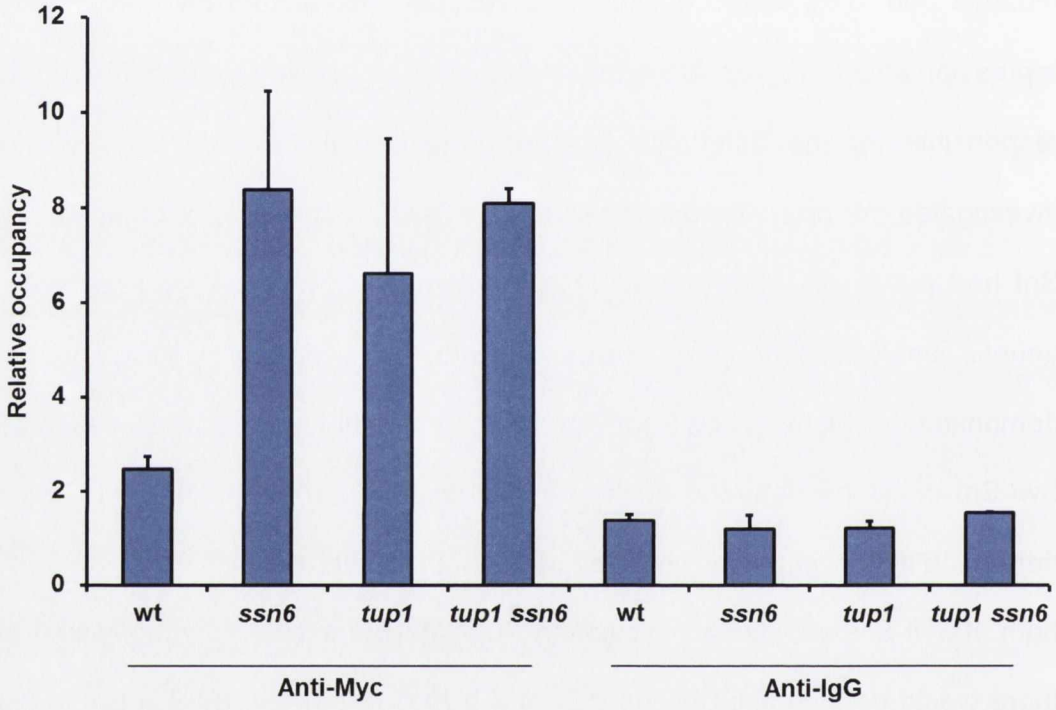

Figure 4.1. Snf5-Myc occupancy at the *FLO1* promoter. Chromatin immunoprecipitation (ChIP) analysis of Snf5-Myc occupancy in wild type (wt), *tup1. ssn6* and *tup1 ssn6* mutant strains. Strains containing Myc-tagged Snf5p were analysed by ChIP using antibodies directed against Myc (Anti-Myc) and a nonspecific IgG antibody (Anti-IgG). Snf5-Myc occupancy at the *FLO1* promoter was normalised to an intergenic region of chromosome V. Error bars represent standard error of the mean (SEM) from two independent experiments.

Snf5-Myc occupancy was investigated at a position 585 bp upstream of the *FLO1* transcription start site (TSS). This site was chosen because it is the DNase I hypersensitive site at which Tup1-Ssn6 has been shown to bind and which expands in the absence of Tup1-Ssn6, indicating that extensive nucleosome remodelling activity occurs in this region (Fleming and Pennings, 2001). In addition, previous global analysis of Swi-Snf occupancy in a Tup1p anchor away strain, in which Tup1p is conditionally removed, has shown Swi-Snf preferentially binds the same sites in promoters previously occupied by Tup1-Ssn6 (Wong and Struhl, 2011).

The data revealed Snf5-Myc enrichment was detectable in *tup1*, *ssn6* and *tup1 ssn6* mutants compared to wild type and controls using a non-specific IgG antibody (Fig. 4.1). Although enrichment was observed in *tup1*, *ssn6* and *tup1 ssn6* mutants, no significant difference in the levels of Snf5-Myc between these three strains was detected. This suggests that different levels of Swi-Snf occupancy at *FLO1* cannot account for the differences in *FLO1* transcription in these mutant strains.

4.2.2. *tup1* and *ssn6* mutants display significant histone loss at the *FLO1* promoter.

It has been shown that when *FLO1* transcription is repressed, an array of strongly positioned nucleosomes occupies the *FLO1* gene promoter. However, in an *ssn6* mutant this ordered array is lost and the data suggests nucleosomes are extensively evicted across the *FLO1* gene promoter and upstream region (Fleming and Pennings, 2001). However, in a *snf2 ssn6* double mutant, this nucleosome eviction and *FLO1* transcription are absent suggesting *FLO1* promoter nucleosome eviction and transcription are Swi-Snf dependent.

I next investigated whether any differences in nucleosome loss at the *FLO1* promoter could be detected in the *tup1* and *ssn6* mutants, which would correlate with the difference in *FLO1* transcription in these strains. Although the previous data indicated that there was no difference in the levels of the Swi-Snf co-activator at the *FLO1* promoter in the *tup1* and *ssn6* mutants, this does not address whether Swi-Snf activity was altered in these strains. I therefore examined if there was evidence that Swi-Snf was more active in the *ssn6* mutant compared to the *tup1* mutant by analysing histone density at the *FLO1* promoter in these strains (Figure 4.1). I used chromatin immunoprecipitation (ChIP) to detect histone H3 occupancy at the *FLO1* promoter in the wild type, *tup1* and *ssn6* single mutants and a *tup1 ssn6* double mutant (-585bp upstream of the *FLO1* ORF) (Figure 4.2). If Swi-Snf activity was greatest in the *ssn6* mutant, the prediction would be that H3 levels would be lower in this strain than in the *tup1* mutant strain.

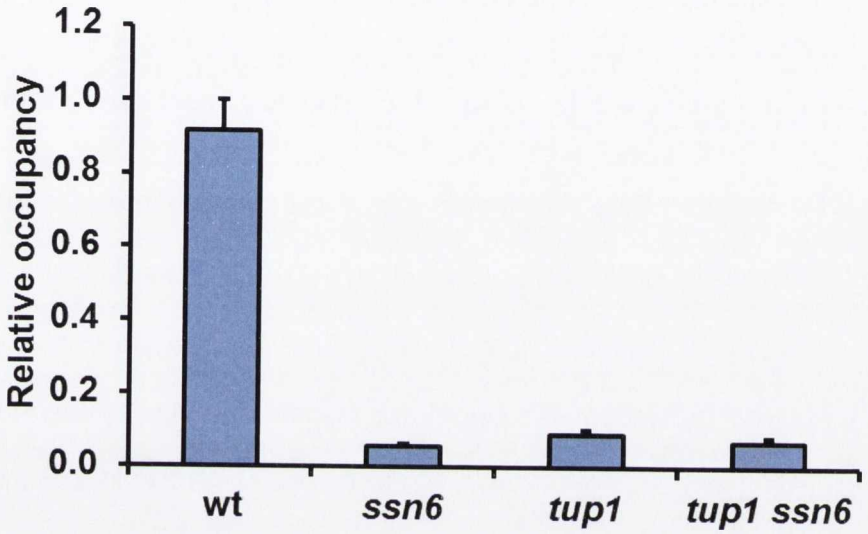

Figure 4.2. H3 occupancy at the *FLO1* promoter. Histone H3 occupancy at the *FLO1* gene promoter was measured by ChIP in wild type (wt), *tup1* and *ssn6* single mutants and a *tup1ssn6* double mutant. H3 enrichment at the *FLO1* promoter was compared to H3 enrichment at an intergenic region of chromosome V. Error bars represent standard error of the mean (SEM) from 3-5 independent experiments.

The data revealed significant histone loss occurred at the de-repressed *FLO1* promoter in the *tup1* and *ssn6* single mutants and the *tup1 ssn6* double mutant compared to wild type strains (Fig. 4.2). However, no significant differences in H3 occupancy could be detected between these mutants. This suggests that differences in *FLO1* transcription cannot be accounted for by differences in nucleosome eviction at the gene promoter.

4.2.3. Cellular histone levels are unaffected in *tup1* and *ssn6* mutants

Nucleosome density at the *FLO1* promoter is dramatically reduced in *tup1* and *ssn6* mutants relative to wild type strains (Fig. 4.2). It has been shown that Tup1-Ssn6 aids in the deposition of nucleosomes leading to a repressive chromatin structure at target genes, and the complex is also antagonistic to the nucleosome-remodelling Swi-Snf complex (Fleming and Pennings, 2001; Zhang and Reese, 2004). However, the possibility that *tup1* and *ssn6* mutants caused a decrease in global histone levels was not addressed. Levels of histones H3, H2A and H2B were therefore monitored by Western blot in wild type strains, *ssn6* and *tup1* single mutants and a *tup1 ssn6* double mutant (Figure 4.3).

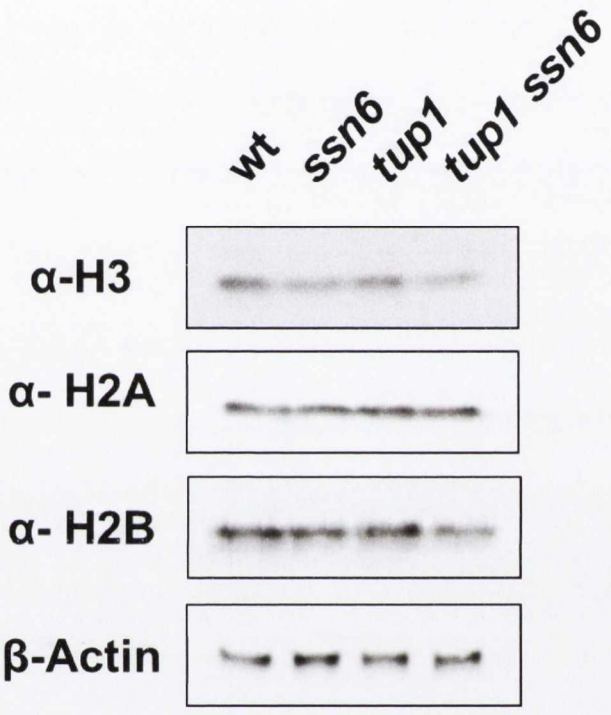

Figure 4.3. Histone levels in *tup1* and *ssn6* mutants. Western blot analysis of H3, H2A and H2B in wild type (wt), *ssn6* and *tup1* single mutants and a *tup1 ssn6* double mutant. β-Actin was used as a loading control.

Despite the dramatic histone loss observed at the *FLO1* promoter in *ssn6* mutants (Fig. 4.2), similar levels of H3, H2A and H2B were observed in cell lysates from wild type cells and *ssn6* mutants. *tup1* single mutants also displayed wild type levels of H3, H2A and H2B, despite the nucleosome depletion observed at *FLO1* in this strain. Finally, the combined loss of Tup1p and Ssn6p (*tup1 ssn6*) does not affect histone H3, H2A or H2B levels relative to wild type strains. This suggests that any histone loss observed at *FLO1* in *tup1* and *ssn6* mutants is due to eviction at the gene promoter by Swi-Snf and is not a consequence of a global lack of histones in these strains.

4.2.4. *ssn6* mutants display elevated histone H3 lysine 4 trimethylation (H3K4me3) of compared to *tup1* mutants.

Figures 4.1 and 4.2 indicated that neither differences in Swi-Snf occupancy nor nucleosome eviction correlated with the differences in *FLO1* transcription observed in *tup1* and *ssn6* mutants. Another method by which Tup1-Ssn6 regulates gene transcription is by negatively regulating histone post-translational modifications (PTMs) that are associated with active transcription. This can be achieved either by exclusion of factors catalysing the addition of the PTMs (Wong and Struhl, 2011), or by recruitment of factors that remove these marks, thus preventing gene transcription (Watson et al., 2000).

The first histone PTM studied in relation to Tup1-Ssn6 function was trimethylation of lysine 4 of histone H3 (H3K4me3) which is a mark associated with active gene transcription (Maltby et al., 2012) (Figure 4.4). If differences in H3K4me3 between *tup1* and *ssn6* mutants mirrored the transcriptional differences in these strains, it might implicate this PTM in the regulation of *FLO1* gene transcription by Tup1-Ssn6 and offer new insight into the contribution of each subunit to repression.

H3K4me3 levels at the *FLO1* promoter were analysed by ChIP and compared to levels at the transcriptionally-active and Tup1-Ssn6 independent *PMA1* gene.

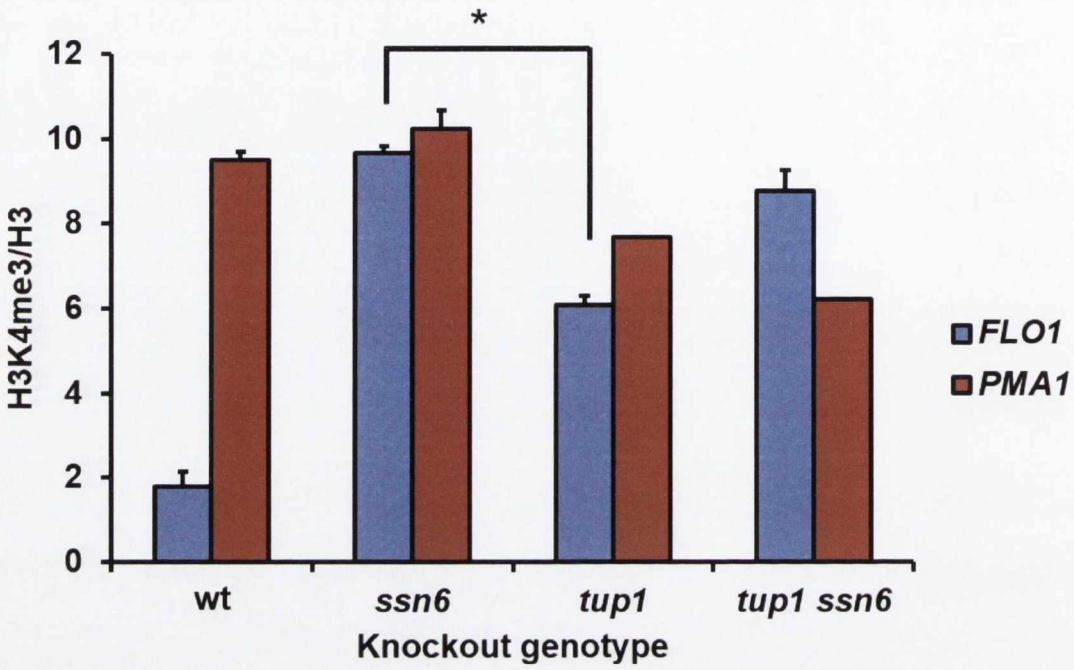

Figure 4.4. H3K4me3 occupancy at *FLO1* and *PMA1* in *tup1* and *ssn6* mutants. ChIP analysis of H3K4me3 occupancy in wild type (wt), *tup1* and *ssn6* single mutants and *tup1ssn6* double mutants. H3K4me3 occupancy of the *FLO1* promoter (-585bp) and the 5' ORF of *PMA1*. In both cases, enrichment of the target gene was normalised to enrichment at a telomeric region on chromosome I. This normalised value was further normalised to H3 occupancy at the target region. Error bars represent standard error of the mean (SEM). Asterisks represent a p-value of p=<0.05 obtained from a Student's t-test. Values represent data from 1-2 independent experiments.

Figure 4.4 shows levels of H3K4me3 relative to H3 occupancy at both *FLO1* and *PMA1*. In wild type cells, H3K4me3 levels were low at the inactive *FLO1* promoter but were high at the active *PMA1* gene. However, in an *ssn6* mutant, where *FLO1* is transcribed, H3K4me3 levels were increased at *FLO1* and were at similar levels to those measured at *PMA1* in both wild type and the *ssn6* strain. In a *tup1* mutant, there was a lower level of H3K4me3 at *FLO1* than in the *ssn6* mutant. However, in a *tup1 ssn6* double mutant there was a level of H3K4me3 at *FLO1* which was comparible to an *ssn6* single mutant and significantly higher than a *tup1* single mutant. At the constitutively-transcribed *PMA1* gene, an equally high level of H3K4me3 was observed in all strains. This data shows that differences in H3K4me3 levels at the *FLO1* promoter in *tup1* and *ssn6* mutants mirrored the differences in *FLO1* transcription observed in these strains. Furthermore, the data sugests that Ssn6p plays the greatest role in preventing H3K4me3 at the repressed *FLO1* promoter, and can partially impose this negative effect in the absence of Tup1p.

4.2.5. H4ac4 levels are elevated in tup1 and ssn6 mutants.

Having established that there were differences in H3K4me3 at the *FLO1* promoter in *tup1* and *ssn6* mutants (Fig. 4.4), it was decided to investigate other histone PTMs associated with active transcription in these strains. Histone acetylation is a well-characterised mark that has been shown to have a positive role in gene transcription (Allfrey and Mirsky, 1964). One method by which Tup1-Ssn6 can regulate gene transcription is by preventing acetylation or promoting removal of this mark from histones at gene promoters (Watson et al., 2000; Wong and Struhl, 2011). To investigate potential differences in the levels of histone acetylation at the *FLO1* promoter between *tup1* and *ssn6* mutants, it was first decided to

monitor acetylation at lysines 5, 8, 12 and 16 of histone H4 (H4ac4) using ChIP (Figure 4.5).

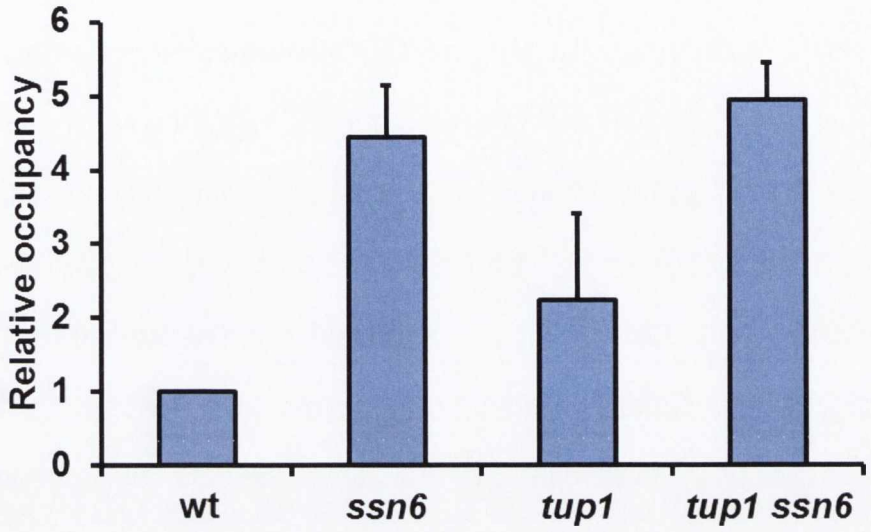

Figure 4.5. Histone H4 tetra-acetylation (H4ac4) at the *FLO1* promoter in *tup1* and *ssn6* mutants. ChIP analysis of H4ac4 in wild type (wt), *ssn6* and *tup1* single mutants and a *tup1ssn6* double mutant. Enrichment at the *FLO1* promoter was normalised to enrichment at a telomeric region on chromosome I. This normalised value was further normalised to H3 occupancy at the target region. All values are relative to wild type strains. Error bars represent standard error of the mean (SEM) from two independent experiments.

In the wild type, where *FLO1* is not transcribed, there were low levels of H4ac4 at the *FLO1* promoter (Fig. 4.5). When Ssn6p was absent (*ssn6*), and *FLO1* is de-repressed, there was an enrichment of H4 acetylation relative to the wild type strain. There was also enrichment of H4ac4 in the *tup1* mutant. However, levels were lower in the tup1 mutant than those in the *ssn6* mutant. Interestingly, when both *SSN6* and *TUP1* were deleted, H4ac4 levels were similar to the levels in the *ssn6* single mutant. These data are consistent with the role of Tup1-Ssn6 in facilitating the propagation of hypo-acetylated promoter histones at the repressed *FLO1* promoter (Watson et al., 2000). In addition, the data suggest Ssn6p plays the major role in maintaining or establishing hypoacetylated *FLO1* promoter chromatin and that this activity by Ssn6p persists in the absence of Tup1p, albeit not as efficiently. The pattern of H4ac4 observed in Figure 4.5 also correlated with the levels of *FLO1* de-repression in *tup1* and *ssn6* mutants. This suggests that H4ac4 at *FLO1* is negatively regulated by Tup1-Ssn6, and that the presence of this mark in the absence of Tup1-Ssn6 may contribute to *FLO1* transcription.

4.2.6. Levels of H3K9ac at *FLO1* are significantly different in *tup1* and *ssn6* mutants.

Having observed elevated levels of H4 acetylation at *FLO1* in *tup1* and *ssn6* mutants (Fig. 4.5), it was decided to investigate acetylation of other histones. Acetylation of lysine 9 on histone H3 (H3K9ac) is another mark associated with actively-transcribed genes (C. L. Liu et al., 2005). It was decided to monitor H3K9ac in *tup1* and *ssn6* mutants in order to establish whether H3K9ac patterns in *tup1* and *ssn6* mutants also matched patterns of *FLO1* transcription in these strains. H3K9ac at the *FLO1* promoter in wild type, *ssn6* and *tup1* single mutants

and a *tup1ssn6* double mutant was monitored by ChIP using an antibody specific to H3K9ac (Figure 4.6).

In the wild type strain, where *FLO1* is not transcribed, a low level of H3K9ac was detected at *FLO1* promoter (Fig. 4.6). In the *ssn6* single mutant, there was a significant increase in H3K9ac at *FLO1* which corresponds to the high level of *FLO1* de-repression in this strain. A *tup1* mutant also had elevated levels of H3K9ac at *FLO1*, but this was not to the same extent as an *ssn6* mutant. This result mirrors transcriptional differences at *FLO1* between *tup1* and *ssn6* mutants (Fig. 3.5). Once again, the *tup1 ssn6* double mutant was similar to an *ssn6* single mutant, having higher levels of H3K9ac than a *tup1* single mutant. These results suggest that Ssn6p plays the major role in ensuring the *FLO1* promoter has low H3K9ac levels, and that this activity, albeit less strongly, can be exerted by Ssn6p in the absence of Tup1p.

4.2.7. Cellular levels of H3K4me3 and H3K9ac/H4ac4 in *tup1* and *ssn6* mutants.

Previous data has shown that in strains lacking Ssn6p, levels of H3K4me3, H3K9ac and H4ac4 were elevated at *FLO1* to a greater extent than in strains lacking Tup1p (Fig. 4.4-4.6). To investigate whether this was a gene-specific effect, or the result of a general alteration of histone PTMs in *tup1* and *ssn6* mutants, global levels of H3K4me3, H3K9ac and H4ac4 were monitored in cell extracts from wild type strains, *tup1* and *ssn6* single mutants and a *tup1 ssn6* double mutant by Western blot (Figure 4.7).

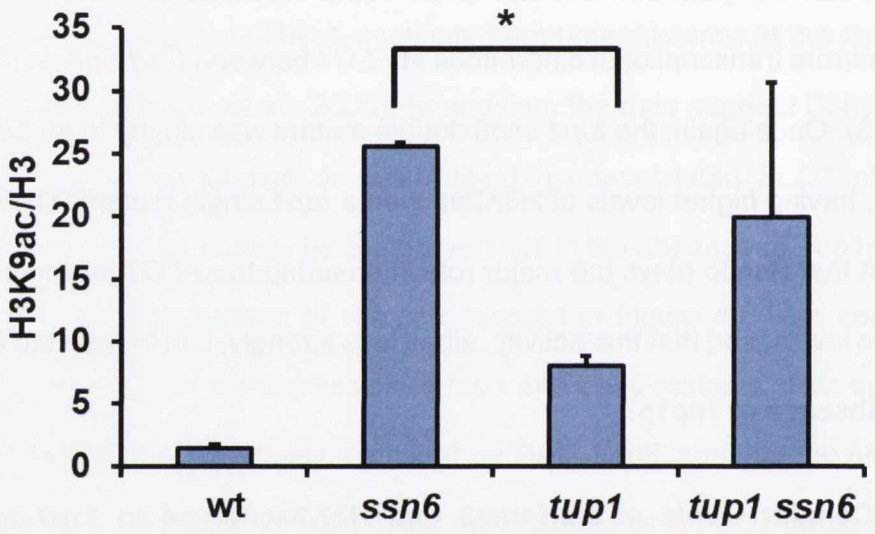

Figure 4.6. Histone H3 lysine 9 acetylation (H3K9ac) at the *FLO1* promoter in *tup1* and *ssn6* mutants. ChIP analysis of H3K9ac in wild-type, *ssn6* and *tup1* single mutants and a *tup1ssn6* double mutant. Enrichment of the *FLO1* promoter was normalised to enrichment at a telomeric region on chromosome I. This normalised value was further normalised to H3 occupancy at the target region. Error bars represent standard error of the mean (SEM) from 2-4 independent experiments. Asterisks represent a p-value of p=<0.05 obtained from a Student's t-test.

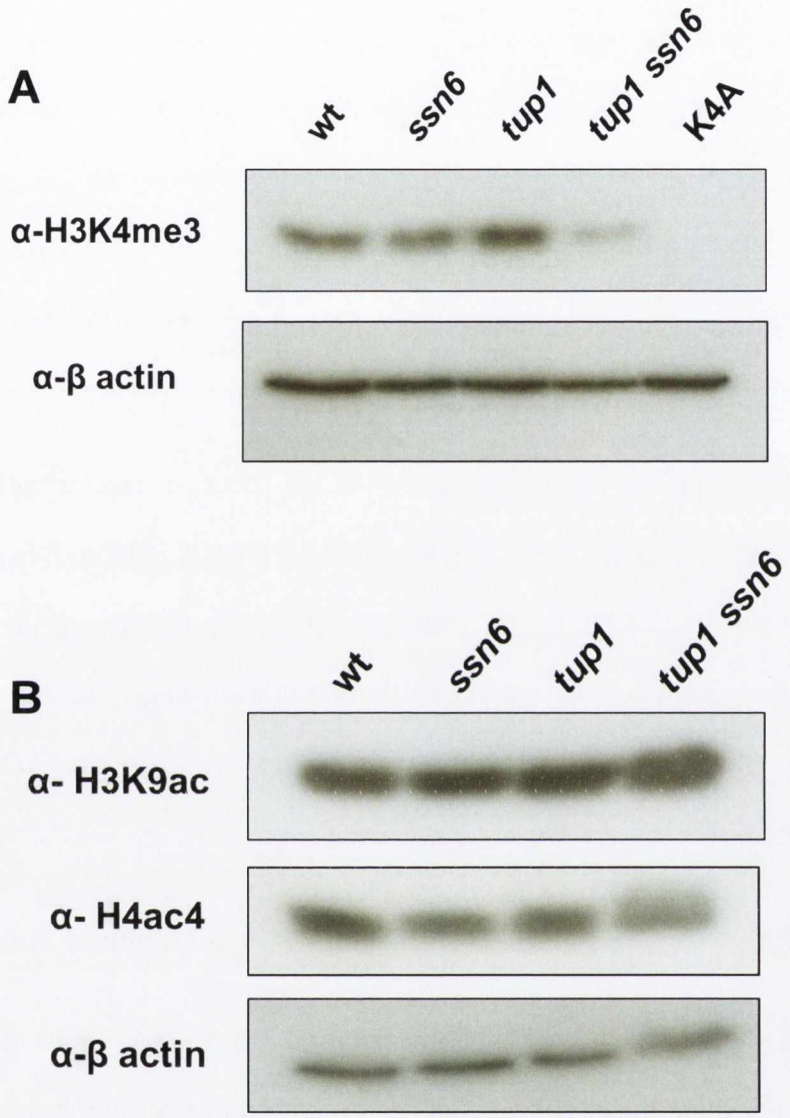

Figure 4.7. Cellular levels of H3K4me3, H3K9ac and H4ac4 in *tup1* and *ssn6* mutants. (A) Western blot analysis of H3K4me3 in wild type cells, *ssn6* and *tup1* single mutants and a *tup1 ssn6* double mutant. A histone H3 mutant which cannot be methylated at H3K4 due to a K to A substitution at this site (*hht1*-K4A) was used as a negative control(B) Western blot monitoring H3K9ac and H4ac4 in wild type cells, *ssn6* and *tup1* single mutants and a *tup1 ssn6* double mutant. β-Actin was used as a loading control in (A) and (B).

In contrast to the increased levels of H3K4me3 seen at *FLO1* (Fig. 4.4) in *ssn6* and *tup1* mutants compared to wild type, all these cells displayed similar H3K4me3 levels as detected by Western blot analysis. However, the *tup1 ssn6* double mutant showed a lower level of H3K4me3 globally. There was no H3K4me3 detected in the negative K4A control strain confirming the specificity of the antibody. These data indicate that the low level of H3K4me3 observed at *FLO1* in a *tup1* mutant relative to the *ssn6* single and *tup1 ssn6* double mutants is not due to a global alteration of H3K4me3 in this strain.

There was also no difference in H3K9ac or H4Aac4 levels in cell extracts from wild type strains, *ssn6 and tup1* single mutants and the *tup1 ssn6* double mutant (Fig. 4.7B). Together, this suggests that differences in H3K9ac and H4ac4 occupancy at *FLO1* between *tup1* and *ssn6* mutants are not due to differences in global acetylation levels, but reflect the action of Tup1-Ssn6 on the *FLO1* gene promoter specifically.

4.2.8. Myc-Ssn6p occupies the *FLO1* promoter in the absence of Tup1p

Chapter one examined various cellular phenotypes in *tup1* and *ssn6* mutants. The data revealed *FLO1* transcription was de-repressed to a greater extent in an *ssn6* mutant compared to de-repression in a *tup1* mutant (Fig. 3.5). Furthermore, *FLO1* transcription in the absence of both Tup1p and Ssn6p was at the same high level as that found in the *ssn6* single mutant. This suggests that Ssn6p has a greater role in *FLO1* repression than Tup1p, and that Ssn6p can exert partial repression of *FLO1* transcription independent of Tup1p. One explanation for this could be that in the absence of Tup1p, Ssn6p was directly carrying out repression of *FLO1* transcription. To test this hypothesis, Tup1p and Ssn6p occupancy were

analysed at the *FLO1* promoter by ChIP in the presence and absence of each other.

To analyse Ssn6p occupancy a 9Myc-tagged Ssn6p (Ssn6-Myc) strain was used since an Ssn6p-specific antibody for ChIP was not commercially available. Tup1p protein levels were detected using an antibody specific to this protein which was generously provided by J. Reese (Zhang and Reese, 2004). The Ssn6-Myc strain had previously been constructed in our laboratory but had not been fully validated. Before ChIP could be attempted, the Ssn6-Myc strain was analysed by Western blot to detect Ssn6-Myc protein levels and to confirm that the Myc tag did not affect Tup1-Ssn6 co-repressor activity. Transcription of genes repressed by Tup1-Ssn6, were also monitored in the tagged strain relative to an un-tagged wild type to confirm that the presence of the Myc tag on Ssn6 did not affect the ability of Tup1-Ssn6 to repress transcription.).

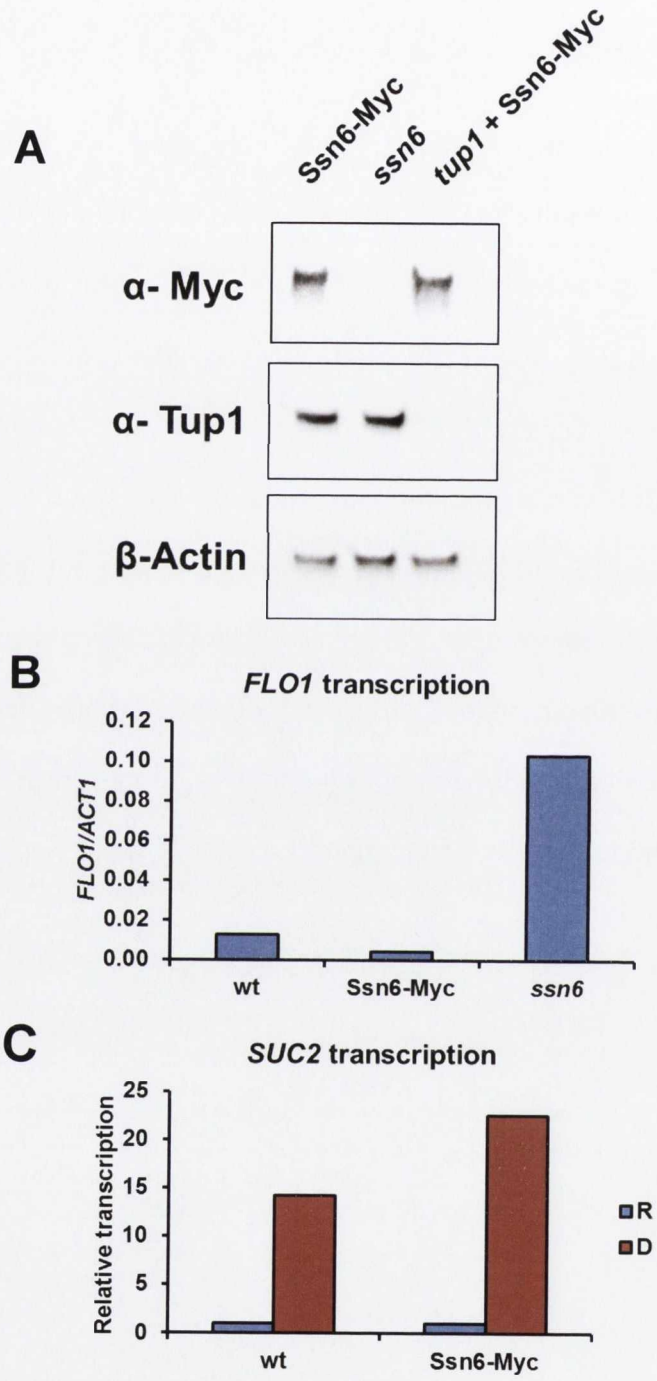
A
Ssn6-Myc
ssn6
tup1 + Ssn6-Myc
α- Myc
α- Tup1
β-Actin
B
FLO1 transcription
FLO1/ACT1
0.12
0.10
0.08
0.06
0.04
0.02
0.00
wt
Ssn6-Myc
ssn6
C
SUC2 transcription
Relative transcription
25
20
15
10
5
0
R
D
wt
Ssn6-Myc

Figure 4.8. Verification of Ssn6-Myc expression and function. (A) Western blot of Myc and Tup1p in Ssn6-Myc, an *ssn6* mutant and a *tup1* mutant in an Ssn6-Myc background. β-Actin was used as a loading control. (B) *SUC2* transcription was analysed by qPCR in un-tagged (wt) and Ssn6-Myc strains under *SUC2* repressing (R) and de-repressing (D) conditions. *SUC2* transcription was normalised to levels of repressed *SUC2* for each strain. (C) *FLO1* transcription in un-tagged (wt), Ssn6-Myc and *ssn6* mutant strains. Both *FLO1* and *SUC2* transcription was normalised to *ACT1* transcription.

I first measured Ssn6-Myc protein levels and showed the epitope-tagged protein was expressed and was of the expected size of 117 kDa (Fig 4.8A, lane 1); Tup1p levels in the Myc-tagged Ssn6p strain were also measured to ensure the tag had not affected the stoichiometry of the co-repressor complex subunits. I found that the presence of Myc-tagged Ssn6p did not affect levels of Tup1p compared to Tup1p levels in an untagged strain (Fig 4.8A, lane 1). These data suggest (i) Ssn6p was successfully tagged and (ii) that Tup1p levels in the tagged strain were unaffected.

I next examined transcription of *FLO1* in the tagged strains compared to untagged strains to test if the tag impacted repression by the Tup1-Ssn6 complex. The data showed repression of *FLO1* was the same in the tagged strain as in the untagged strain (wt) (Fig. 4.8B). The *ssn6* data was included to demonstrate the high level of *FLO1* de-repression in the absence of Ssn6p.

Transcription of the *SUC2* gene in the tagged strain was also analysed. *SUC2* encodes invertase and its transcription is repressed by Tup1-Ssn6 in response to glucose (Ozcan et al., 1997). Under conditions of low glucose, *SUC2* transcription is induced. I therefore measured *SUC2* transcription in the Myc-tagged strain under conditions of repression and de-repression to ensure the tag did not affect repression and de-repression of this gene. The data showed that under *SUC2*-repressing conditions (R), *SUC2* transcription was not detected in either untagged or Ssn6-Myc strains, indicating that Ssn6-Myc retains its ability to repress transcription of this gene (Fig. 4.8C). In addition, under *SUC2*-de-repressing conditions (D), *SUC2* de-repression was detected at similar levels in both tagged and untagged strains (Fig. 4.8C). Together these data suggest that

Ssn6p function is not altered in the Ssn6-Myc strain compared to the untagged strain for regulation of transcription of both *FLO1* and *SUC2*.

I next examined the protein levels of each subunit in the absence of the other to determine if each protein was stable in the absence of the other. Thus I measured Ssn6-Myc expression in the *tup1* mutant and Tup1p levels in the *ssn6* mutant (Fig. 4.8A, lanes 2 and 3). The data showed that cellular protein levels of Ssn6-Myc were the same as levels in wild type in a *tup1* mutant and that Tup1p levels were similarly unaffected in the *ssn6* mutant (Fig. 4.8A lanes 2 and 3 respectively). Overall the data suggest that the presence of the Myc tag does not affect cellular Tup1p or Ssn6p levels in the Ssn6-Myc background compared to the untagged strains and that the Tup1-Ssn6 complex is active (Fig. 3.5). The data also showed the Tup1p and Ssn6p subunits of the complex remain stable in the absence of each other.

4.2.8.1. Ssn6p occupies the *FLO1* promoter in the absence of Tup1p

FLO1 was shown to be de-repressed to a greater extent in an *ssn6* mutant compared to a *tup1* mutant (Fig. 3.5). Greater levels of H3K4me3, H3K9ac and H4ac were also detected at the *FLO1* promoter in an *ssn6* mutant compared to a *tup1* mutant (Fig. 4.4 – 4.6). Importantly, additional deletion of *ssn6* in a *tup1* mutant resulted in the levels of transcription and the histone PTMs in this strain being the same as in the *ssn6* single mutant. Considering these data, and the fact that these PTMs are associated with transcriptionally-active genes, I hypothesised that Ssn6p could carry out partial repression of *FLO1* transcription in the absence of Tup1p. To test this hypothesis, Ssn6-Myc occupancy at *FLO1* was investigated in wild type cells and *tup1* mutants by ChIP (Figure 4.9). Tup1p occupancy at *FLO1* was also investigated in wild type cells and *ssn6* mutants. If

Ssn6p was directly repressing *FLO1* in the absence of Tup1p, it was expected that Ssn6-Myc would be detected at the *FLO1* promoter in a *tup1* mutant.

In wild type cells, Tup1p occupancy was detected at the repressed *FLO1* promoter (Fig.4.9A). In a *tup1* mutant control which lacks Tup1p, no Tup1p was detected confirming the specificity of the antibody. In *ssn6* mutants, Tup1p was also undetectable at the *FLO1* promoter. This suggests that Ssn6p is required for Tup1p occupancy at the *FLO1* promoter, presumably in the context of the Tup1-Ssn6 complex.

I next investigated Ssn6-Myc occupancy and found Ssn6-Myc can be detected at the repressed *FLO1* promoter in wild type cells (Fig. 4.9B). In an *ssn6* mutant control which lacks Ssn6p, Ssn6-Myc cannot be detected at *FLO1.* However, in a *tup1* mutant, Ssn6-Myc was detected at *FLO1* at levels similar to those in wild type where the complex is intact. This suggests that Ssn6p is present at the *FLO1* promoter in the absence of Tup1p.

FLO1 transcription data in *tup1* and *ssn6* mutants shows that in a *tup1* mutant background, *FLO1* was de-repressed to a lesser extent than in an *ssn6* mutant (Fig. 3.5). A *tup1 ssn6* double mutant exhibited similar levels of *FLO1* de-repression to an *ssn6* single mutant. This suggests that Ssn6p is partially repressing *FLO1* in the absence of Tup1p. H3K9ac, H4ac4 and H3K4me3 occupancy data also follow this pattern with absence of Ssn6p leading to increased PTM occupancy in both *ssn6* single and *tup1 ssn6* double mutants but with *tup1* single mutants leading to lower levels of PTM occupancy, suggesting that Ssn6p prevents H3K9ac, H4ac4 and H3K4me3 occupancy at *FLO1* in the *tup1* mutant strain as well as in the wild type. Together these data suggest that in wild type cells Tup1p and Ssn6p are present at the *FLO1* promoter, where they

establish or maintain a *FLO1* promoter devoid of H3K4me3 and histone acetylation and repress *FLO1* transcription. In an *ssn6* mutant neither Tup1p nor Ssn6p are present at the *FLO1* promoter resulting in high levels of acetylation and H3K4 methylation across the promoter and *FLO1* is fully de-repressed. Interestingly however, in a *tup1* mutant, Ssn6p remains present at the *FLO1* promoter which is now only partially acetylated and methylated and *FLO1* is partially de-repressed.

This suggests that Tup1-Ssn6 acts at the *FLO1* promoter to block acetylation and H3K4me3 and repress *FLO1* transcription. In addition, the data suggests that Ssn6p can directly function independently of the Tup1-Ssn6 complex to bind the *FLO1* promoter where it partially decreases these histone PTMs and partially inhibits *FLO1* transcription in the absence of Tup1p. This partial reduction of acetylation, methylation and transcription in *tup1* single mutants is in contrast to strains lacking Ssn6p which show higher levels of acetylation, methylation and transcription.

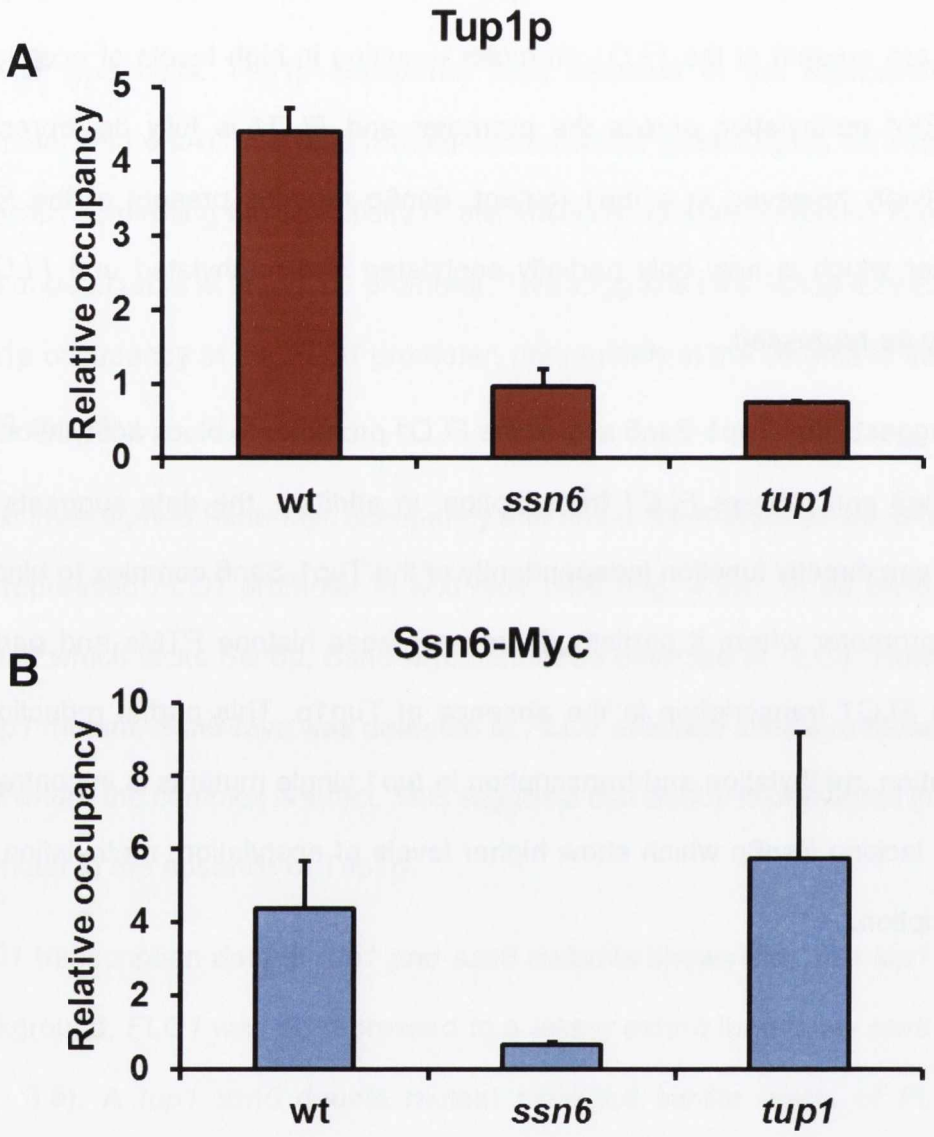

Figure 4.9. Ssn6-Myc and Tup1p occupancy of *FLO1*. (A) Ssn6-Myc occupancy of the *FLO1* gene promoter in a Ssn6-Myc strain (wt), an *ssn6* mutant and a *tup1* mutant in the Ssn6-Myc background (*tup1*). (B) Tup1p occupancy in the wild type strain (wt), an *ssn6* mutant and a *tup1* mutant. Enrichment of Ssn6-Myc and Tup1p the target gene was normalised to enrichment at the *STE6* gene promoter. Error bars represent standard error of the mean (SEM) from two independent experiments.

4.3. Discussion

The individual contribution of Tup1p and Ssn6p to regulation of *FLO1* transcription was investigated by examining *ssn6* and *tup1* mutants. Tup1-Ssn6 can repress transcription by propagating a repressive chromatin structure, by excluding factors that promote nucleosome eviction or by recruiting factors that promote nucleosome occupancy at gene promoters (B. Li and Reese, 2001; Wong and Struhl, 2011). One factor that is responsible for nucleosome eviction at Tup1-Ssn6-regulated genes and also required for *FLO1* de-repression is the ATP-dependent chromatin remodelling Swi-Snf complex (Fleming and Pennings, 2001).

Previous data had shown that an *ssn6* mutant had a significantly greater level of *FLO1* de-repression than that measured in a *tup1* mutant (Figure 3.5). If Swi-Snf was directly required for *FLO1* transcription, I hypothesised that more Swi-Snf would occupy the *FLO1* promoter in an *ssn6* mutant than in a *tup1* mutant. However, analysis of Snf5-Myc occupancy at the *FLO1* promoter by ChIP in *tup1*, *ssn6* and *tup1 ssn6* mutants revealed that there was no difference in the levels of Snf5-Myc bound to the *FLO1* promoter in these strains (Fig. 4.1).

Swi-Snf activates transcription by evicting nucleosomes from gene promoters, which are considered barriers to gene transcription (Schwabish and Struhl, 2007). As Swi-Snf occupancy at *FLO1* was identical in *tup1* and *ssn6* mutants, despite the differences in *FLO1* transcription in these strains, I next investigated the possibility that Swi-Snf activity was different in these strains. I therefore determined histone density at the *FLO1* promoter in *tup1* and *ssn6* mutants as a measure of Swi-Snf activity. Working with the model that a high level of nucleosome occupancy at the *FLO1* promoter would impair *FLO1* transcription, I

hypothesised that in an *ssn6* mutant where *FLO1* de-repression was greatest, H3 occupancy at the *FLO1* promoter would be lower than in a *tup1* mutant.

Histone H3 occupancy at *FLO1* was analysed in wild type cells, *tup1* and *ssn6* single mutants and a *tup1 ssn6* double mutant by ChIP and it was found that there was no significant difference in H3 occupancy at *FLO1* in the *tup1* and *ssn6* single or double mutants (Fig. 4.2). The low histone occupancy at *FLO1* was not due to a global reduction in histone levels in *tup1* or *ssn6* mutants (Fig. 4.3). Thus, the difference in *FLO1* transcription between *tup1* and *ssn6* mutants was not due to differences in Swi-Snf occupancy or activity at the *FLO1* promoter in these strains.

Since the differences in *FLO1* transcription in *tup1* and *ssn6* mutants could not be explained by differences in nucleosome occupancy at the *FLO1* promoter, it was evident that other factors were responsible. Some histone post-translational modifications (PTMs) at promoters correlate with gene activation, including methylation and acetylation of histone tails (Allfrey and Mirsky, 1964). Indeed, Tup1-Ssn6 is known to repress transcription by recruiting factors that deacetylate histones, leading to gene repression (Davie et al., 2003). However, the first PTM to be investigated was H3K4me3. This PTM was chosen because of its association with actively transcribed genes and the correlation between this mark and histone acetylation at gene promoters (Maltby et al., 2012). In wild type cells where *FLO1* is not transcribed, a low level of H3K4me3 was detected compared to the high level found at the actively transcribed *PMA1* gene which was used as a positive control for H3K4me3 occupancy (Fig. 4.4). However an *ssn6* mutant displayed a high level of H3K4me3 at the *FLO1* promoter which correlated with the high level of *FLO1* de-repression in this strain. Indeed the H3K4me3 level at

the de-repressed *FLO1* promoter was as high as that found at the active control gene, *PMA1*. On the other hand, a significantly lower level of H3K4me3 was detected at *FLO1* in a *tup1* mutant compared to an *ssn6* mutant. Importantly though, a similar level of H3K4me3 occupancy at *FLO1* was detected in the *tup1 ssn6* double and *ssn6* single mutant.

These data suggest that Ssn6p plays the greatest role in inhibiting H3K4me3 at the repressed *FLO1* promoter, and that Ssn6p can partially achieve this role independent of Tup1p. In addition, the patterns of H3K4me3 detected at the *FLO1* promoter in the mutant strains correlated with *FLO1* transcription in these strains (Fig. 3.5). The data also suggest the impact of Tup1p and Ssn6p on H3K4me3 is specific to *FLO1* since levels of H3K4me3 at *PMA1* remained at similar levels in all the mutants tested.

Histone acetylation has been shown to be involved in activation of Tup1-Ssn6-repressed genes, and this modification is targeted for removal by histone deacetylases which can be recruited by Tup1-Ssn6 to some gene promoters (Watson et al., 2000). To investigate whether histone acetylation patterns at the *FLO1* promoter correlated with *FLO1* transcription in *tup1* and *ssn6* mutants, histone H4 tetra-acetylation (H4ac4) and histone H3K9 acetylation (H3K9ac) were monitored by ChIP in these strains (Fig. 4.5).

It was found that levels of histone H4 and H3K9 acetylation matched the pattern of *FLO1* transcription in *tup1* and *ssn6* mutants. The data also showed that in wild type, where there is no *FLO1* transcription; there was a very low level of histone H4 and H3K9 acetylation at the *FLO1* promoter. In *ssn6* mutants, where *FLO1* transcription was de-repressed, there was a high level of histone H3K9 and H4 acetylation at the *FLO1* promoter. In *tup1* mutants where *FLO1* was de-

repressed to a lower level than in *ssn6* mutants, there was also a correspondingly lower level of histone acetylation at the *FLO1* promoter than was detected in an *ssn6* mutant. However, in *tup1 ssn6* double mutants where *FLO1* was de-repressed to a high level similar to that in *ssn6* single mutants, there was also a high H3K9ac and H4ac4 occupancy at *FLO1* which was again similar to levels seen in the *ssn6* single mutant. This suggests that Ssn6p has a dominant role in preventing H3K9ac and H4ac4 at *FLO1,* and also indicates that Ssn6p partially inhibits histone H4 and H3K9 acetylation levels at *FLO1* in the absence of Tup1p.

Overall the data show that Ssn6p and Tup1p both inhibit Swi-Snf occupancy and histone eviction at the *FLO1* promoter to the same extent. However, Ssn6p contributes the most to preventing H3K4me3, H4ac4 and H3K9ac levels at the repressed *FLO1* promoter in line with its similarly greater role for blocking *FLO1* transcription. In addition the data suggest that Ssn6p can partially impose inhibition of transcription, H3K4me3 and histone acetylation independent of Tup1p. Together the data suggest that Tup1-Ssn6 mediated repression of *FLO1* transcription could involve the exclusion or removal of histones mods associated with gene transcription.

These data also led to the hypothesis that Ssn6p could be present at the *FLO1* promoter in the absence of Tup1p and could function independently to directly repress *FLO1* transcription by removal of H3K4me3 and histone H3K9 and H4 acetylation. To test this hypothesis, the occupancy of a fully functional Myc-epitope tagged Ssn6p was examined at the *FLO1* promoter in the presence and absence of Tup1p using ChIP (Fig. 4.9). It was found that in both wild type strains and *tup1* mutants, a similar level of Ssn6-Myc was detected at the *FLO1* promoter. However, in the reciprocal experiment, Tup1p was not detected at

FLO1 in an *ssn6* mutant. Thus, Tup1p binds the promoter in an Ssn6-dependent manner, consistent with its recruitment in the context of the Tup1-Ssn6 complex. Conversely, Ssn6p can bind the de-repressed *FLO1* promoter in the absence of Tup1p where it may directly impart partial inhibition of *FLO1* promoter acetylation, methylation and transcription.

These data indicate that in the wild type, where *FLO1* is repressed (Fig. 3.5), both Tup1p and Ssn6p occupy the *FLO1* promoter, as would be expected with an intact Tup1-Ssn6 complex present. I have also shown there is an absence of Swi-Snf occupancy at the *FLO1* promoter (Fig. 4.1) and consequently there is a high level of H3 occupancy at *FLO1* (Fig. 4.2). Wild type strains also have low levels of histone post-translational modifications associated with gene activation at the *FLO1* promoter (Fig. 4.10, wt)

However, in *ssn6* single mutants, where *FLO1* is highly de-repressed (Fig. 3.5), there is a high level of Swi-Snf occupancy at the *FLO1* promoter (Fig. 4.1) which correlates with low H3 occupancy at *FLO1* (Fig. 4.2). In addition, H3K4me3, H4ac4 and H3K9ac occupancy at the *FLO1* promoter are all elevated in *ssn6* mutants, corresponding to the high level of *FLO1* transcription (Fig. 4.4-4.6). Finally, in *ssn6* mutants, Tup1p cannot be detected at the *FLO1* promoter, suggesting that Ssn6p is required for Tup1-Ssn6 complex occupancy at *FLO1.* (Fig 4.10, *ssn6*)

In a *tup1* single mutant, *FLO1* is de-repressed to a lesser extent than in an *ssn6* mutant (Fig. 3.5). There is high Swi-Snf occupancy at the *FLO1* promoter in this strain, which is comparable to that seen in an *ssn6* mutant (Fig. 4.1) and H3 occupancy at the *FLO1* promoter is also low, and not significantly different to H3 occupancy at *FLO1* observed in an *ssn6* mutant (Fig. 4.2). H3K4me3, H4ac4 and

H3K9ac occupancy at the *FLO1* promoter in a *tup1* mutant is higher than in the wild type, but lower than in an *ssn6* mutant (Fig. 4.4-4.6). Importantly, Ssn6p can also be detected at the *FLO1* promoter in a *tup1* mutant, indicating that Ssn6p may be carrying out a repressive role in the absence of Tup1p (Fig. 4.9). This repression may involve removal or prevention of histone post-translational modifications associated with gene activation at the *FLO1* promoter (Fig. 4.10, *tup1*).

Finally, *tup1 ssn6* double mutants show a similar level of *FLO1* de-repression to *ssn6* single mutants (Fig. 3.5). *ssn6* single mutants and *tup1 ssn6* double mutants also have similarly high levels of H3K4me3, H4ac4 and H3K9ac occupancy at the *FLO1* promoter (Fig. 4.4-4.6). This indicates that the loss of Ssn6p completely abolishes Tup1-Ssn6 occupancy and function at *FLO1*, unlike a *tup1* single mutant where Ssn6p persists at the *FLO1* promoter (Fig 4.10, *tup1 ssn6*). Another interesting result that has arisen from this analysis is that *FLO1* de-repression is not entirely dependent on the level of histone eviction at the *FLO1* promoter. Histone H3 is evicted to the same extent in *tup1* and *ssn6* single mutants, yet transcription is greater in the *ssn6* mutant. The data therefore suggests that it is not the level of promoter histone depletion that is the critical factor for *FLO1* de-repression, but rather it is the levels of PTMs associated with the depleted chromatin template at the promoter that are key.

Overall, these data suggest that Tup1-Ssn6 may repress *FLO1* transcription by regulating histone post-translational modifications at the *FLO1* promoter. These data also suggest that Ssn6p may be able to play a partially repressive role at *FLO1* in the absence of Tup1p.

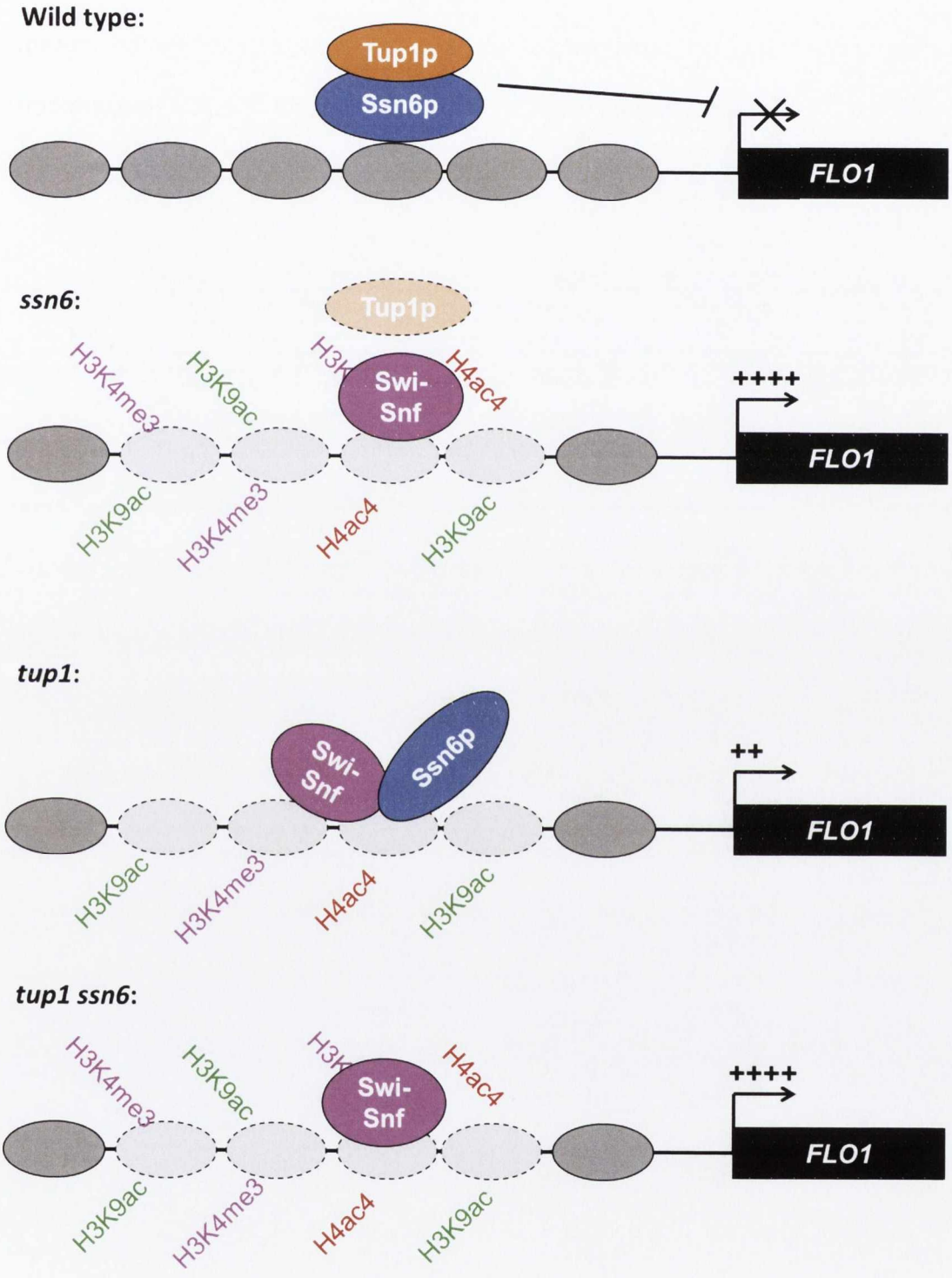
Wild type:
Tup1p
Ssn6p
FLO1
ssn6:
Tup1p
H3K4me3
H3K9ac
H3K
Swi-
Snf
H4ac4
++++
FLO1
H3K9ac
H3K4me3
H4ac4
H3K9ac
tup1:
Swi-
Snf
Ssn6p
++
FLO1
H3K9ac
H3K4me3
H4ac4
H3K9ac
tup1 ssn6:
H3K4me3
H3K9ac
H3K
Swi-
Snf
H4ac4
++++
FLO1
H3K9ac
H3K4me3
H4ac4
H3K9ac

Figure 4.10. Model for Tup1-Ssn6 action at the *FLO1* promoter. Summary of protein occupancy at the *FLO1* promoter and *FLO1* transcription in wild type strains, *ssn6* single mutants, *tup1* single mutants and *tup1 ssn6* double mutants. Dashed lines indicate protein loss. "++++" indicates level of *FLO1* transcription.

Chapter 5

Identification of factors responsible for *FLO1* activation

5.1. Introduction

The previous work had shown that *FLO1* transcription was de-repressed to different extents in *tup1* and *ssn6* mutants (Fig.3.5). We showed that *FLO1* transcription in the absence of Ssn6p was greater than transcription in the absence of Tup1p. In addition, we showed histone acetylation correlated with the levels of *FLO1* de-repression in these mutants. Thus, histone acetylation at the *FLO1* promoter was greater in the *ssn6* mutant than in the *tup1* mutant. These data led to the hypothesis that acetylation of histone H3 in the *FLO1* promoter was a key determinant of *FLO1* gene transcription. To test this hypothesis, we aimed to delete the key yeast histone acetyltransferases (HATs) in an *ssn6* mutant and determine the impact of acetylation on *FLO1* transcription. The prediction was that if we deleted the HAT responsible for histone acetylation at the *FLO1* promoter in the *ssn6* mutant, and that acetylation was required for *FLO1* transcription, we should see decreased *FLO1* promoter histone acetylation and reduced *FLO1* transcription in the *ssn6*-HAT double mutant. We chose to examine events in the *ssn6* mutant, and not in the *tup1* mutant, since we had shown the Tup1-Ssn6 complex occupancy at *FLO1* is abolished in strains lacking Ssn6p (Fig. 4.7).

The histone acetyltransferases chosen for analysis were Gcn5p and Sas3p. Gcn5p is the best characterised HAT in *S. cerevisiae* and is the catalytic subunit of the SAGA, SLIK and ADA acetyltransferase complexes responsible for acetylating lysine (K) residues 4, 9, 14, 18 and 23 of histone H3, along with lysine residues on H4 and H2B (Rando and Winston, 2012). Sas3p is the catalytic subunit of the NuA3 HAT complex which specifically acetylates histone H3 K14 and to a lesser extent, K23 of histone H3 (Howe et al., 2001). Gcn5p was chosen

because it had previously been shown to regulate Tup1-Ssn6-repressed genes, and Sas3p was investigated because of its occupancy at many Gcn5p-regulated genes (Rosaleny et al., 2007; Desimone and Laney, 2010).

To determine whether H3 acetylation is required for *FLO1* transcription, *GCN5* and *SAS3* were deleted in the presence and absence of Ssn6p and *FLO1* transcription was analysed. Histone acetylation across the *FLO1* promoter region was also monitored in these strains. To establish whether these HATs acted directly on *FLO1,* Gcn5p and Sas3p occupancy at the *FLO1* promoter was analysed by ChIP.

5.2. Results.

5.2.1. Gcn5-containing complexes and Sas3p are redundantly required for *FLO1* de-repression in the absence of Ssn6p.

In order to determine which HAT was required for *FLO1* transcription, a mutational analysis was first carried out whereby candidate HATs thought to be responsible for acetylation of *FLO1* promoter histones were deleted. Null mutations of *GCN5* and *SAS3* were made in *ssn6* mutant strains where *FLO1* is de-repressed, and in wild type cells where *FLO1* is repressed. If either HAT mutant showed reduced *FLO1* de-repression in the *ssn6* mutant background, this would indicate a role for that HAT in activation of *FLO1* (Grant et al., 1997; Pray-Grant et al., 2002).

To investigate the role of Gcn5p and Sas3p on *FLO1* transcription, *gcn5 ssn6* and *sas3 ssn6* mutants were constructed and *FLO1* transcription was analysed by RT-qPCR (Figure 5.1).

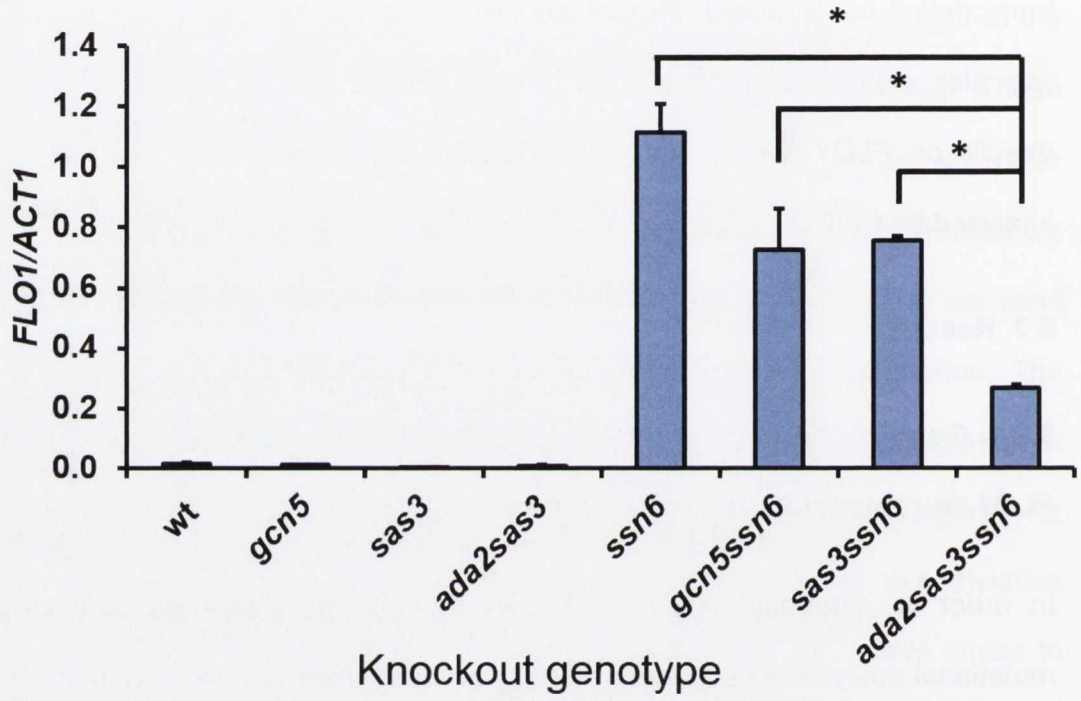

Figure 5.1 *FLO1* transcription in HAT mutants. *FLO1* gene transcription in the wild type (wt), *ssn6, gcn5* and *sas3* single mutants, *ada2 sas3, gcn5 ssn6* and *sas3 ssn6* double mutants and an *ada2 sas3 ssn6* triple mutant. Transcript levels at the *FLO1* 5' ORF were normalised to transcript levels at the *ACT1* 5' ORF. Error bars represent standard error of the mean (SEM) from 2-4 independent experiments. Asterisks represent a p-value of p=<0.05 obtained from a Student's t-test.

The data in Figure 5.1 confirms that in wild type cells, *gcn5* and *sas3* single mutants and *ada2 sas3* double mutants, *FLO1* was not transcribed. A deletion of Ada2p was included since Gcn5p activity in the SAGA, ADA and SLIK complexes requires Ada2p. Thus, the *ada2* and *gcn5* mutants are both representative of strains deficient for SAGA, ADA and SLIK HAT activities (Maltby et al., 2012). An *ssn6* single mutant, on the other hand, displayed a high level of *FLO1* de-repression. Upon additional deletion of *gcn5* or *sas3* in the *ssn6* mutant background, the *gcn5 ssn6* and *sas3 ssn6* double mutants displayed only a minor reduction in *FLO1* gene transcription compared to the *ssn6* single mutant. To investigate whether Gcn5p and Sas3p were acting redundantly to regulate *FLO1* transcription in the absence of Ssn6p, a mutant deficient for Gcn5p activity and Sas3p was constructed. Since a *gcn5 sas3* double mutant is inviable, an *ada2 sas3 ssn6* mutant was constructed in order to disable both NuA3 and Gcn5p HAT activity in an *ssn6* mutant background (Howe et al., 2001). This triple mutant is null for NuA3 and SAGA, ADA and SLIK activity, since Gcn5p requires Ada2p for its catalytic function *in vivo* (Howe et al., 2001). Whereas the *ada2sas3* mutant showed no *FLO1* de-repression, an *ada2sas3ssn6* triple mutant displayed significant reduction in *FLO1* transcription compared to an *ssn6* single mutant and *gcn5 ssn6* and *sas3 ssn6* double mutants. This suggests that Gcn5p-containing complexes and Sas3p are redundantly required for full de-repression of *FLO1* in an *ssn6* mutant background, and loss of these complexes severely impairs *FLO1* transcription in the absence of Ssn6p.

5.2.2. Nucleosome occupancy across the *FLO1 promoter* is reduced in all ssn6-HAT mutants independent of transcription

The previous data showed that both Sas3p and Ada2p, which is required for Gcn5p activity, are required for *FLO1* transcription in the absence of Ssn6p (Fig. 5.1). This suggests Gcn5p-containing and NuA3 HAT complexes are required for *FLO1* transcription. In order to determine if it is the HAT activity of these complexes which is required for *FLO1* transcription, we next wanted to analyse histone acetylation at the *FLO1* promoter region in the *ssn6* mutant additionally deleted for the various HAT genes either on their own or in combination. However, before we could embark on an analysis of histone acetylation at the *FLO1* promoter in these mutant backgrounds, we first needed to establish the histone levels at the *FLO1* promoter in these strains. This is important, since to understand *FLO1* promoter acetylation levels we need to account for any differences in histone occupancy which may be apparent in the various mutant strains. Indeed, it is known there is a dramatic loss of histones across the *FLO1* promoter region in *ssn6* mutant strains (Chatterjee et al., 2011; K. Chen et al., 2013). Therefore, levels of histone H3 across the *FLO1* promoter were monitored by ChIP in wild type, *ssn6*, *gcn5 ssn6, sas3 ssn6, ada2 sas3* and the *ada2 sas3 ssn6* triple mutant strains (Figure 5.2).

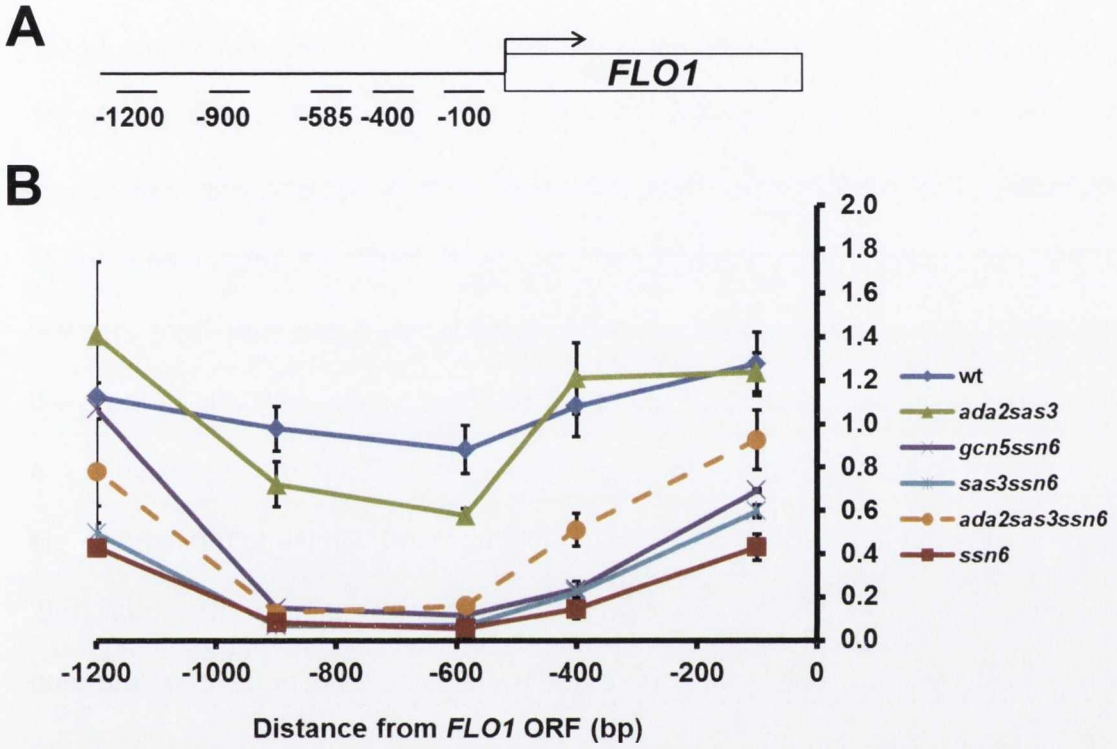

Figure 5.2. H3 occupancy of the *FLO1* promoter in HAT mutants. (A) Schematic of regions analysed upstream of the *FLO1* ORF. Positions shown indicate the midpoint of amplicons generated by qPCR shown in bp realative to the ATG (B) ChIP analysis of H3 occupancy in wild-type, *ssn6* single mutants, *ada2 sas3, gcn5 ssn6* and *sas3 ssn6* double mutants and an *ada2 sas3 ssn6* triple mutant. Ada2p is functionally redundant with Gcn5p, and an *ada2 sas3* mutant is used to substitute for a *gcn5 sas3* mutant which is inviable. Enrichment of the target gene was normalised to H3 occupancy at an intergenic region of chromosome V. Error bars represent standard error of the mean (SEM) from 2-4 independent experiments.

In wild type cells, where *FLO1* transcription is repressed, high H3 occupancy was confirmed across the entire *FLO1* promoter region tested (Fig. 5.2). Conversely, *ssn6* single mutants in which *FLO1* is highly de-repressed exhibit extensive histone loss across the entire *FLO1* promoter region, as has been reported previously (Fleming and Pennings, 2001). In the *ada2 sas3* mutant, where *FLO1* transcription remains repressed, high levels of H3 occupancy at the *FLO1* promoter were also detected; H3 levels were similar to H3 occupancy observed in the wild type. In the *gcn5 ssn6* and *sas3 ssn6* double mutants, where *FLO1* transcription was de-repressed to an extent slightly lower than that in *ssn6* mutants, H3 occupancy at the *FLO1* promoter was similar to levels in the *ssn6* mutant. Interestingly though, the *ada2 sas3 ssn6* triple mutant exhibited a dramatic histone loss across the entire *FLO1* promoter, similar to the *ssn6* single mutant H3 data, despite the low level of *FLO1* de-repression in this strain (Fig. 5.1). This was surprising in that we expected histone eviction to correlate with *FLO1* de-repression and thus expected to see higher histone occupancy in the *ada2 sas3 ssn6* mutant in accordance with the reduced *FLO1* transcription in this strain. Thus, these data highlight that in a strain deficient for Ssn6p, Gcn5p-containing complexes and Sas3p, de-repression of *FLO1* transcription is impaired despite the *FLO1* promoter region being extensively depleted of histones.

5.2.3. H3K9ac levels at the de-repressed *FLO1* promoter are dependent on Gcn5p-containing complexes

Having determined *FLO1* promoter histone occupancy levels in wild type, *ssn6* *and* the *ssn6* mutant strains additionally mutated for the HATs under investigation, we next wanted to determine the impact on histone acetylation at

the *FLO1* promoter in these strains. The previous data suggested Gcn5p-containing complexes and the Sas3p HAT were both required for *FLO1* de-repression in the absence of Ssn6p. To determine if the role of these HATs in regulating *FLO1* transcription was at the level of their HAT activities as opposed to an indirect role, we analysed histone acetylation at the *FLO1* promoter in the *ssn6* mutant additionally deleted for the various HATs. The prediction would be that if the HAT activities were playing a role in de-repressing *FLO1*, acetylation levels in the *ssn6* mutant additionally deleted for the HATs should be reduced. We would also predict that this would be particularly apparent in the *ada2 sas3 ssn6* triple mutant in which *FLO1* transcription is most severely impaired. Additionally, if H3K9ac was required for *FLO1* activation, H3K9ac occupancy at the *FLO1* promoter should reflect *FLO1* transcription previously observed in HAT mutants (Fig. 5.1). We first investigated the levels of H3K9ac which we had previously shown were elevated at the *FLO1* promoter in *tup1* and *ssn6* mutants (Fig. 4.6). H3K9ac was therefore monitored across the entire *FLO1* gene promoter by ChIP and levels were normalised to the histone occupancy levels previously determined to account for any changes in histone occupancy (Figure 5.3).

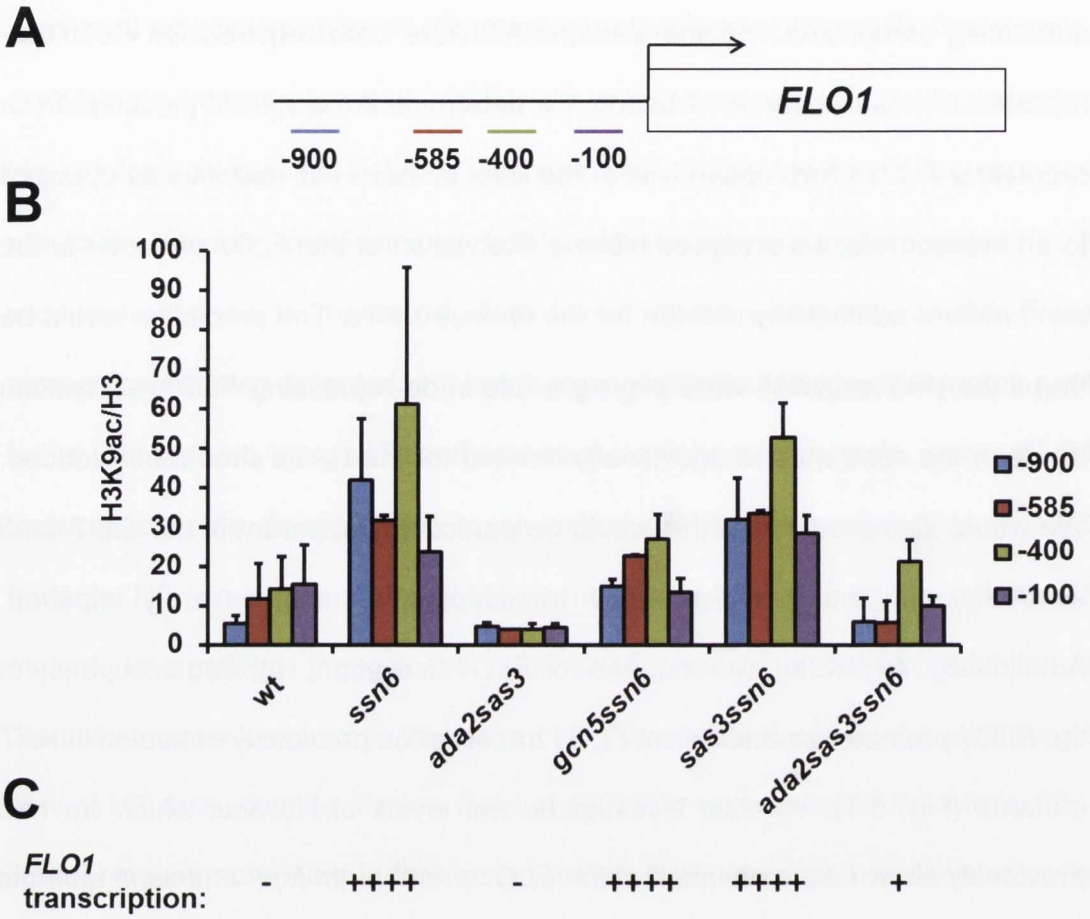

Figure 5.3. Acetylation of lysine 9 of histone H3 in HAT mutants. (A) Schematic of regions analysed upstream of the *FLO1* ORF. (B) ChIP analysis of H3K9ac in wild-type, *ssn6* single mutants, *ada2sas3, gcn5ssn6* and *sas3ssn6* double mutants and an *ada2 sas3 ssn6* triple mutant. Ada2p is functionally redundant with Gcn5p, and an *ada2 sas3* mutant is used to substitute for a *gcn5 sas3* mutant which is inviable. Enrichment of the target gene was normalised to H3 occupancy at the target region. Error bars represent standard error of the mean (SEM) from 2-4 independent experiments. (C) *FLO1* transcription profiles taken from Figure 5.1, with "++++" indicating a high level of de-repression and "-" indicating a repressed *FLO1* gene.

In wild type strains where *FLO1* is inactive, there was a low level of H3K9ac (Fig. 5.3). However, in *ssn6* single mutants where *FLO1* is highly de-repressed, a high level of H3K9ac across the entire *FLO1* promoter was detected. The *ada2 sas3* HAT double mutant has a very low level of H3K9ac, corresponding to the lack of *FLO1* transcription in this strain. When *GCN5* is additionally deleted in the *ssn6* mutant background, (Fig. 5.3B, *gcn5 ssn6)* this double mutant has a reproducibly lower level of H3K9ac at *FLO1* than the *ssn6* single mutant. This suggests that Gcn5p is required for H3K9ac at the *FLO1* promoter in the absence of Ssn6p. Conversely, when *SAS3* is deleted in the *ssn6* mutant background (Fig. 5.3B, *sas3 ssn6*); this double mutant was unaffected for H3K9ac and displays levels of H3K9ac similar to those of an *ssn6* single mutant. Finally, when *ADA2* and *SAS3* were both deleted in the *ssn6* mutant (Fig. 5.3B, *ada2 sas3 ssn6* triple mutant) there were lower levels of H3K9ac present at the *FLO1* promoter compared to the *ssn6* single and *ssn6 sas3* double mutant, though there was not a significant reduction compared to a *gcn5 ssn6* double mutant. These data suggest that Gcn5p-containing complexes are required for H3K9ac levels at *FLO1* in the absence of Ssn6p

5.2.4. H3K14ac levels at the de-repressed *FLO1* promoter are dependent on Gcn5p-containing complexes and Sas3p.

We next investigated H3K14ac at the de-repressed *FLO1* promoter to determine if the HATs under investigation were responsible for adding this post-translational modification to the *FLO1* promoter when active. H3K14ac occupancy across the *FLO1* promoter region was therefore was monitored by ChIP and levels were normalised to the histone levels previously determined in each case (Figure 5.4).

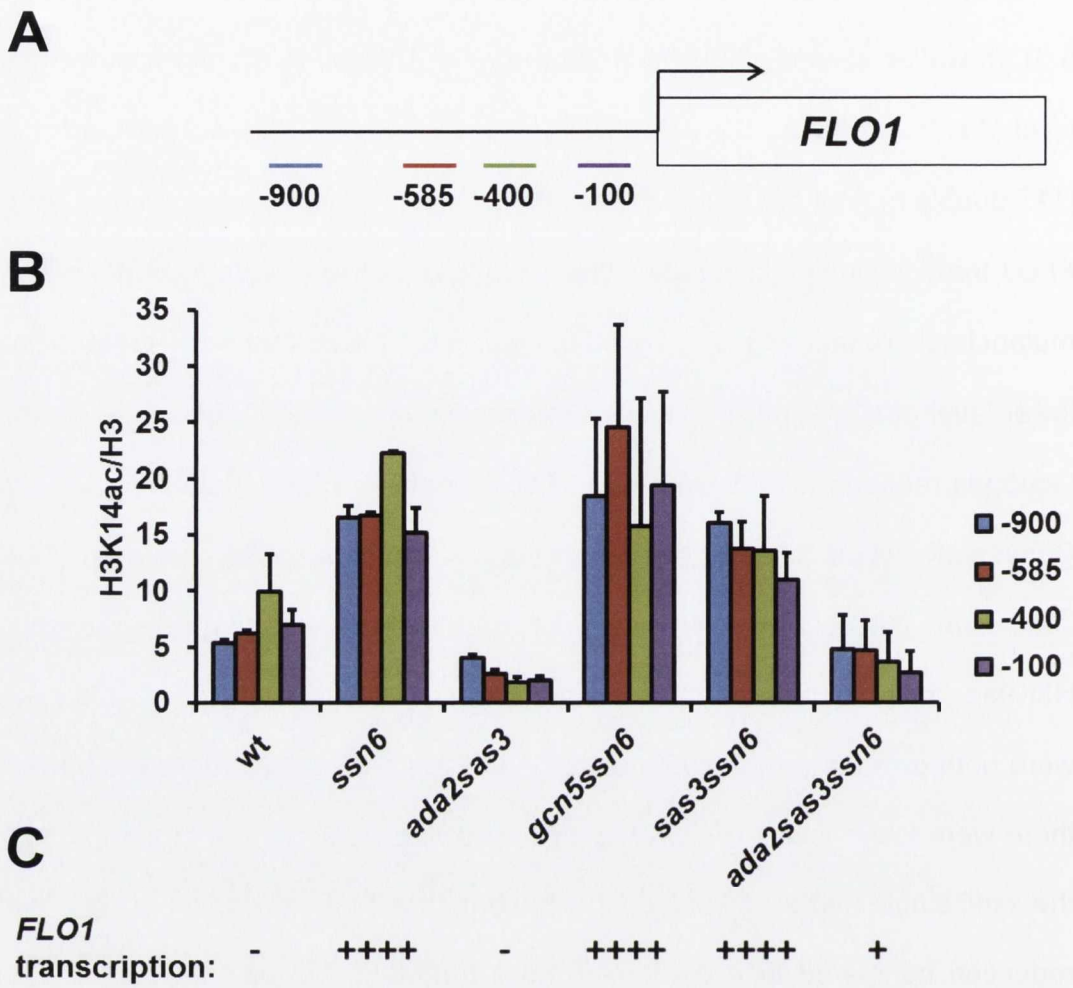

Figure 5.4. Acetylation of lysine 14 of histone H3 in HAT mutants. (A) Schematic of regions analysed upstream of the *FLO1* ORF. (B) ChIP analysis of H3K14ac in wild-type, *ssn6* single mutants, *ada2 sas3, gcn5 ssn6* and *sas3 ssn6* double mutants and an *ada2 sas3 ssn6* triple mutant. Ada2p is functionally redundant with Gcn5p, and an *ada2 sas3* mutant is used to substitute for a *gcn5 sas3* mutant which is inviable. Enrichment of the target gene was normalised to H3 occupancy at the target region. Error bars represent standard error of the mean (SEM) from 2-4 independent experiments. (C) *FLO1* transcription profiles taken from Figure 5.1, with "++++" indicating a high level of de-repression and "-" indicating a repressed *FLO1* gene.

In the transcriptionally-inactive wild type strain, there was a low level of H3K14ac across the *FLO1* promoter region tested (Figure 5.4). In the *ada2 sas3* double mutant where *FLO1* is also not transcribed, there was an even lower level of H3K14ac detected at the *FLO1* promoter. However, in *ssn6* single mutants and in *ssn6* mutants additionally deleted for either Gcn5p (*gcn5 ssn6)* or Sas3p (*sas3 ssn6)* similarly high levels of H3K14ac at the *FLO1* promoter were detected. Conversely, in an *ada2 sas3 ssn6* triple mutant, where both Gcn5p-containing complexes and Sas3p were deleted in the absence of Ssn6p, H3K14ac levels were dramatically lower than those detected in *ssn6* and *gcn5 ssn6* and *sas3 ssn6* double mutants. These data suggest that the H3K14ac mark is conferred redundantly by Gcn5p and Sas3p at *FLO1* in the absence of Ssn6p and may be required for *FLO1* transcription.

5.2.5. H4ac4 levels at the de-repressed *FLO1* promoter are independent of Gcn5p-containing complexes and Sas3p

Having implicated Gcn5p and Sas3p HAT activities as being required for H3K9ac and H3K14ac at the de-repressed *FLO1* promoter, we next examined histone H4 acetylation (H4ac). Acetylation of lysine residues (K) 5, 8, 12 and 16 of histone H4 was monitored at the *FLO1* promoter using ChIP to determine if Gcn5p-containing complexes and Sas3p influenced H4ac at de-repressed *FLO1* also (Figure 5.5).

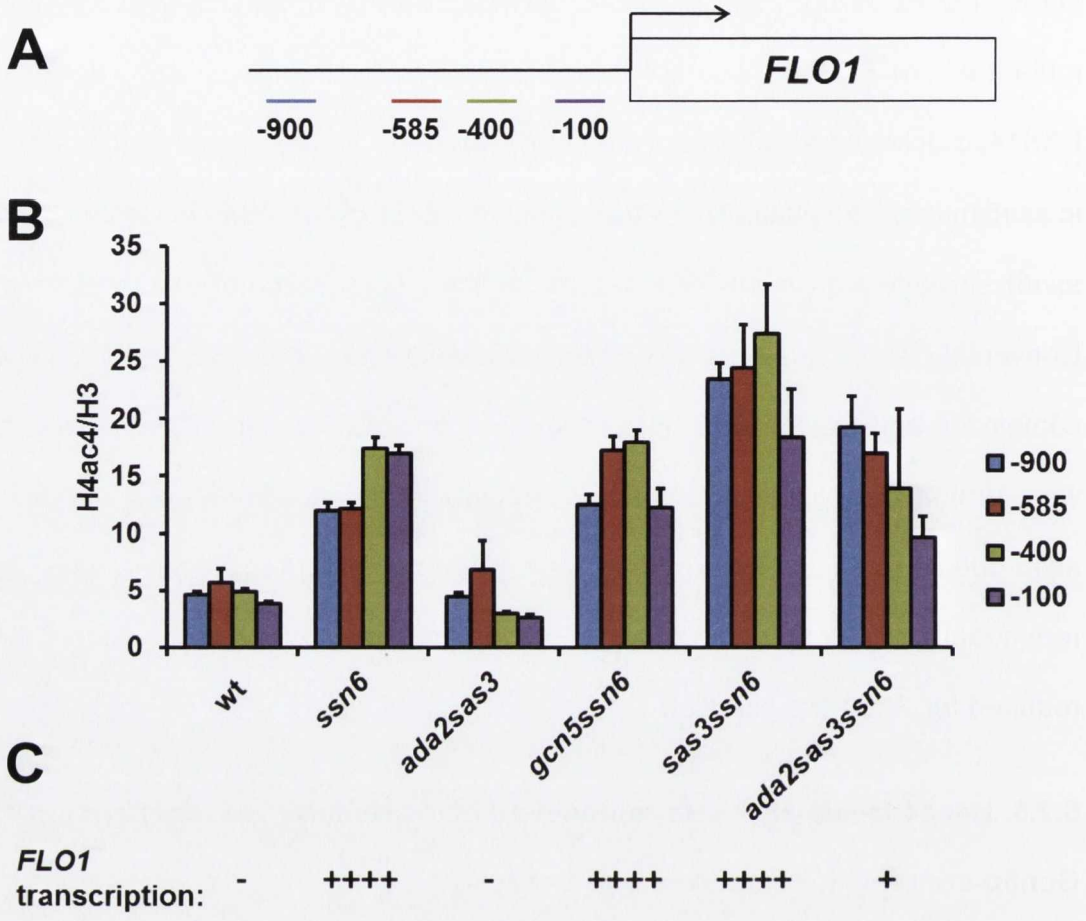

Figure 5.5. Tetra-acetylation of histone H4 in HAT mutants. (A) Schematic of regions analysed upstream of the *FLO1* ORF. (B) ChIP analysis of H4ac4 in wild-type, *ssn6* single mutants, *ada2 sas3, gcn5 ssn6* and *sas3 ssn6* double mutants and an *ada2 sas3 ssn6* triple mutant. Ada2p is functionally redundant with Gcn5p, and an *ada2 sas3* mutant is used to substitute for a *gcn5 sas3* mutant which is inviable. Enrichment of the target gene was normalised to H3 occupancy at the target region. Error bars represent standard error of the mean (SEM) from 2-4 independent experiments. (C) *FLO1* transcription profiles taken from Figure 5.1, with "++++" indicating a high level of de-repression and "-" indicating a repressed *FLO1* gene.

In wild type and *ada2 sas3* mutant strains that lack *FLO1* transcription, there was an equally low level of H4ac4 occupancy detected at the *FLO1* promoter (Figure 5.5). In the *ssn6* single mutant where *FLO1* is highly de-repressed, there was a high level of H4ac4 occupancy at the *FLO1* promoter. In *ssn6* mutant strains additionally lacking either Gcn5p or Sas3p (*gcn5 ssn6* and *sas3 ssn6*) which also show significant de-repression of *FLO1*, there was also a high level of H4ac4 detected at the *FLO1* promoter. Interestingly, the levels of H4ac4 at the *FLO1* promoter in the *sas3 ssn6* double mutant were reproducibly higher than those in the *ssn6* single and *gcn5 ssn6* double mutants. However, in strains lacking both Ada2p and Sas3p in an *ssn6* mutant background (*ada2 sas3 ssn6*); there was a level of H4ac4 occupancy across the *FLO1* promoter which was comparable to that seen in the *ssn6* single mutant, despite the impaired *FLO1* transcription in this strain. Thus, in the absence of Ssn6p, the additional loss of Gcn5p and Sas3p does not impair H4ac4 at the *FLO1* promoter region, suggesting Gcn5p-containing complexes and Sas3p play no role in establishing H4ac4 at the *FLO1* promoter. Furthermore, the data shows H4ac4 occurs independent of transcription since it is present at the *FLO1* promoter in the *ada2 sas3 ssn6* triple mutant which in which *FLO1* is not fully de-repressed. Together, the data suggest H4ac4 is not required for *FLO1* transcription.

In summary, the data has shown Gcn5p and Sas3p are required for *FLO1* de-repression in the absence of Ssn6p. We have also shown Gcn5p preferentially targets H3K9 and Gcn5p-containing complexes and Sas3p redundantly target H3K14 for acetylation at the de-repressed *FLO1* promoter, and in their absence these sites are not acetylated and *FLO1* transcription is severely impaired. However, although H4ac4 levels are high at the de-repressed *FLO1* promoter in *ssn6* mutants, H4ac4 deposition is not dependent on Gcn5p or Sas3p either

individually or acting together. Furthermore, H4ac4 levels also remain high in the absence of high *FLO1* transcription, suggesting *FLO1* transcription is independent of H4ac4. Taken together, this suggests the redundant activities of Gcn5p-containing complexes and Sas3p especially in the establishment of H3K14ac at the *FLO1* promoter are required for *FLO1* transcription.

5.2.6. Gcn5p-containing complexes and Sas3p are required for global H3K14ac

De-repressed *FLO1* transcription was significantly reduced in *ssn6* mutants deficient for both Gcn5p-containing complexes and Sas3p (Fig. 5.1, compare *ssn6* single and *ada2 sas3 ssn6* triple mutants). This reduction of *FLO1* transcription correlated with reduced levels of H3K9ac and H3K14ac, at the *FLO1* promoter in the *ada2 sas3 ssn6* mutant (Fig. 5.3, compare ssn6 single and *ada2 sas3 ssn6* triple mutants). We next wanted to determine if the reduction of acetylation in the HAT mutants was specific to the *FLO1* promoter, or loss of histone acetylation was occurring globally in mutant strains defective for the two HAT activities. We therefore analysed H3K9ac, H3K14ac and H4ac4 levels by Western blot in whole cell extracts derived from wild type, *gcn5*, *ada2*, *sas3* and *ada2 sas3* mutants and also *ssn6* and *ada2 sas3 ssn6* mutants (Figure 5.6).

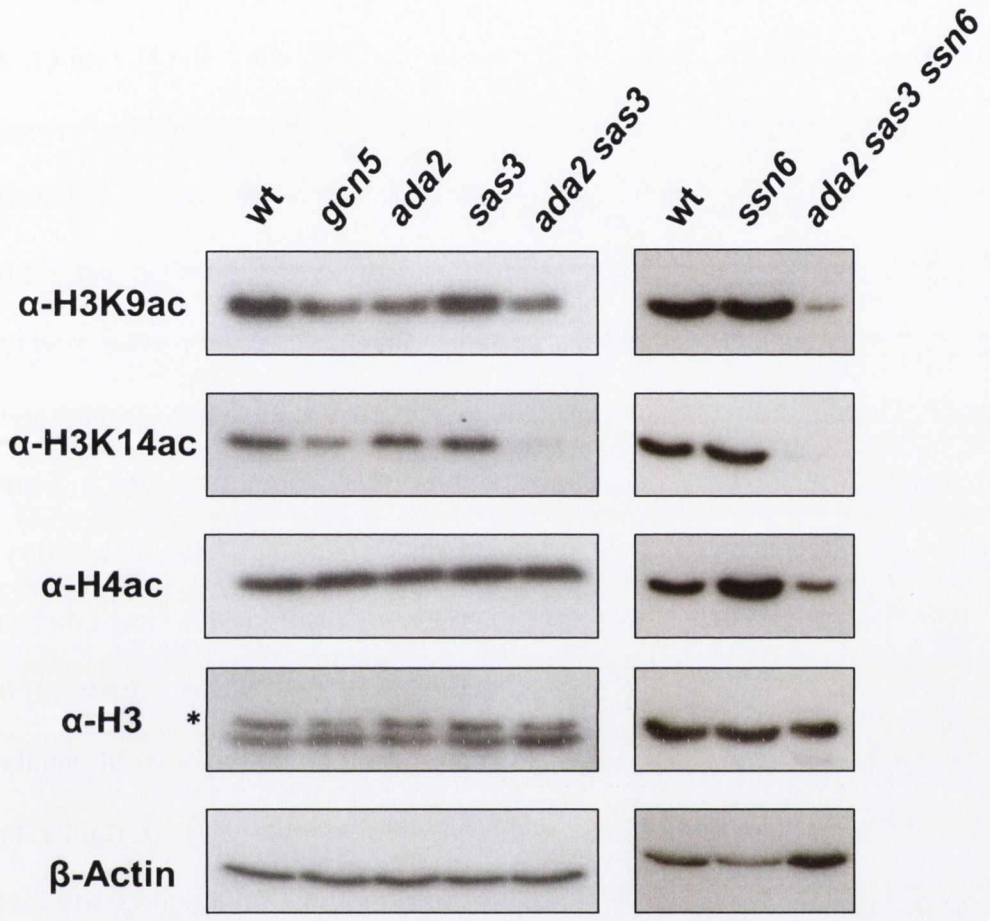

Figure 5.6 Global histone acetylation in HAT mutants. Western blot of H3, H3K9ac, H3K14ac and H4ac4 occupancy in wild type (wt), *gcn5, ada2, sas3* and *ssn6* single mutants, an *ada2sas3* double mutant and an *ada2 sas3 ssn6* triple mutant. Wild type, *ssn6* single mutants and *ada2 sas3 ssn6* triple mutants are separated as they were run on a separate gel. β-Actin was used as a loading control. Asterisks represent nonspecific antibody binding.

In whole cell extracts derived from wild type cells, H3K9ac, H3K14ac and H4ac were all detected at significant levels (Figure 5.6, wt). In *gcn5* single mutants levels of H3K9ac and H3K14ac were lower than in wild type cells, although H4ac4 levels were unaffected. Similar to *gcn5* mutants, the *ada2* single mutant also displayed low H3K9ac levels; however H3K14ac and H4ac levels were the same as wild type. Conversely, *sas3* single mutants showed no differences in H3K9ac, H3K14ac and H4ac levels which were all similar to wild type. In *ssn6* single mutants, H3K9ac and H3K14ac levels were similar to those seen in the wild type. In the *ada2 sas3* double mutant levels of H3K9ac were similar to those found in the *gcn5* and *ada2* single mutants and levels of H4ac were unaffected and similar to wild type. Strikingly however, H3K14ac levels were completely abolished in the *ada2 sas3* double mutant. Upon the additional loss of Ssn6p in the *ada2 sas3* mutant background (*ada2 sas3 ssn6*), H3K9ac and H4ac4 levels were lower than those seen in wild type strains, and H3K14ac was completely absent, similar to the loss of this modification seen in *ada2 sas3* double mutants. Importantly, there was no global loss of histone H3 in any of the mutants suggesting any loss in acetylation was due to loss of the specific modification as opposed to loss of the H3 protein itself. (Maltby et al., 2012).

Together these data suggest Gcn5p-containing complexes contribute most to H3K9 and H3K14 acetylation in contrast to Sas3p which, on its own, has no impact on the cellular levels of these PTMs. Our data also showed H4ac was not dependent on Gcn5p-containing complexes or Sas3p since none of the mutations studied have an effect on H4ac4 levels relative to wild type strains.

5.2.6.1. Loss of H3K14ac does not reduce transcription of *SUC2* or *PMA1*

In summary, the data has shown Gcn5p and Sas3p are required for *FLO1* de-repression in the absence of Ssn6p. We have also shown Gcn5p preferentially targets H3K9 and Gcn5p-containing complexes and Sas3p redundantly target H3K14 for acetylation at the de-repressed *FLO1* promoter, and in their absence these sites are not acetylated and *FLO1* transcription is severely impaired. However, although H4ac4 levels are high at the de-repressed *FLO1* promoter in *ssn6* mutants, H4ac4 deposition is not dependent on Gcn5p or Sas3p either individually or acting together. Furthermore, H4ac4 levels also remain high in the absence of high *FLO1* transcription, suggesting *FLO1* transcription is independent of H4ac4. Taken together, this suggests the redundant activities of Gcn5p-containing complexes and Sas3p especially in the establishment of H3K14ac at the *FLO1* promoter are required for *FLO1* transcription.

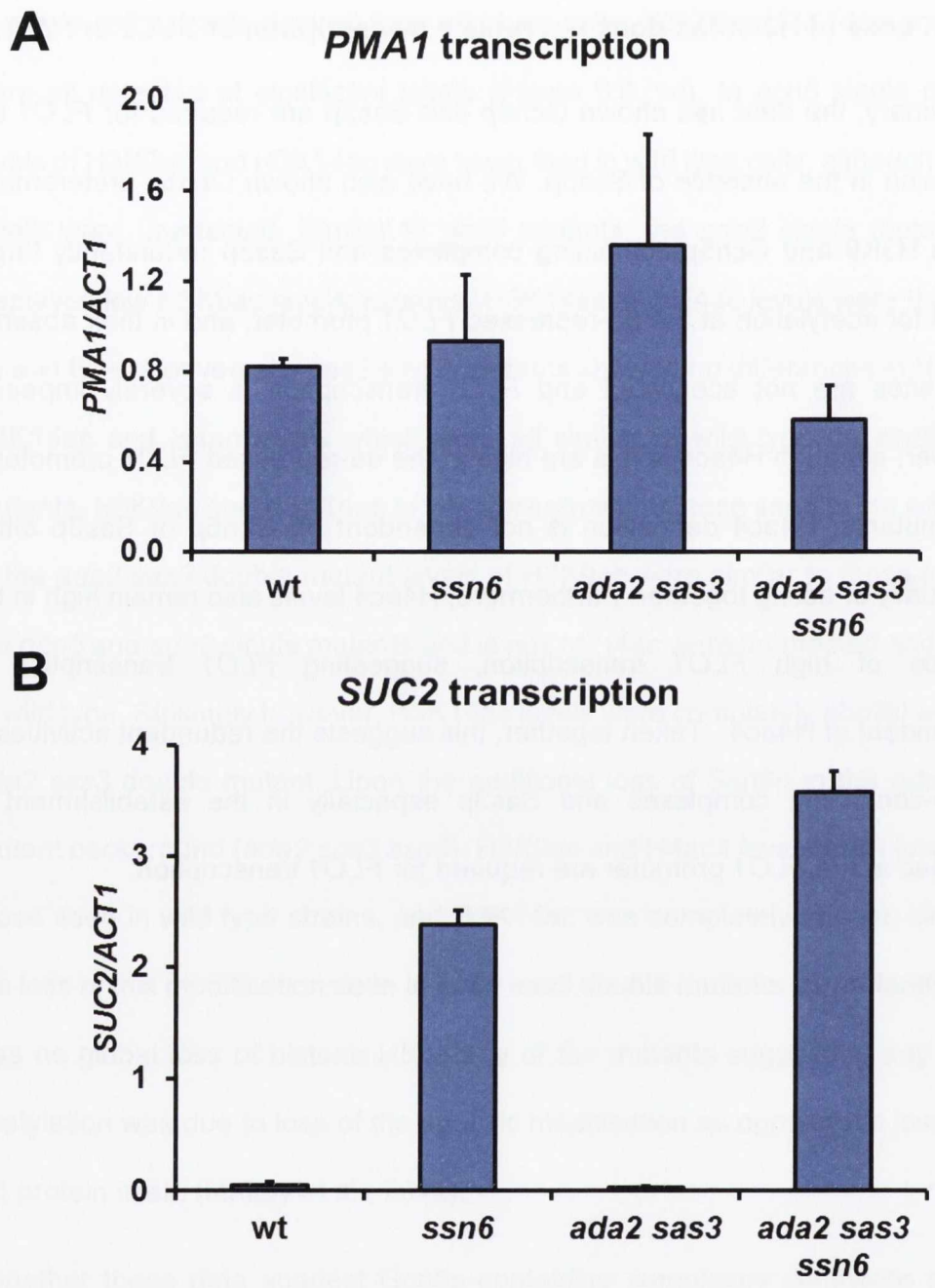

Figure 5.7. Transcription in the absence of H3K14ac. (A) *PMA1* and (B) *SUC2* gene transcription in the wild type (wt), *ssn6* single mutant, *ada2 sas3* double mutant and an *ada2 sas3 ssn6* triple mutant. Transcript levels at the *PMA1* and *SUC2* 5' ORF were normalised to transcript levels at the *ACT1* 5' ORF. Error bars represent standard error of the mean (SEM) from two independent experiments

In the absence of both Ada2p and Sas3p, where global H3K14ac levels are abolished, transcription of *PMA1* was unaffected compared to the wild type (Fig. 5.7A, compare wt to *ada2 sas3*). Indeed, *ssn6* single mutants, *ada2 sas3* double mutants and *ada2 sas3 ssn6* triple mutants all showed no significant differences in *PMA1* transcription compared to wild type. This suggests deletion of both HATs and the resultant global loss of H3K14ac, either in the absence or presence of Ssn6p, has no negative effect on *PMA1* transcription.

We next analysed *SUC2* transcription, which is a Tup1-Ssn6-repressed gene under glucose control (Fleming and Pennings, 2007). Wild type cells do not display *SUC2* transcription when grown on glucose-rich media (YPD) due to Tup1-Ssn6 mediated glucose repression. No *SUC2* transcription was detected in an *ada2 sas3* double mutant, suggesting the Tup1-Ssn6 complex and glucose repression remains functional in this strain. However, *ssn6* mutants show a high level of *SUC2* de-repression in the presence of glucose due to the absence of Tup1-Ssn6 (Fig. 5.7B). Importantly, in the *ssn6* mutant additionally deleted for both *ada2* and *sas3* (*ada2 sas3 ssn6*) *SUC2* transcription was de-repressed to a similar level to that seen in the *ssn6* mutant. This suggests that despite the global loss of H3K14ac due to the absence of Ada2p and Sas3p, there is no impact of the loss of H3K14ac on transcription in general in the *ada2 sas3 ssn6* mutant. Furthermore, the data suggests that not all Tup1-Ssn6-regulated genes require H3K14ac for de-repression since, unlike transcription of *FLO1*, *SUC2* transcription is unaffected in this mutant.

5.2.7. Gcn5-Myc strains contain a functional Gcn5p

The data have shown a requirement for the redundant activities of Ada2p/Gcn5p and Sas3p for *FLO1* de-repression, potentially through their role in histone

acetylation (Fig. 5.1 and Fig. 5.3-5.5). However, the presence of Gcn5p had not previously been observed at *FLO1,* and it was not clear whether the histone acetylation and H3K14ac in particular was due to direct action by the HATs studied on the *FLO1* promoter. In order to investigate whether Gcn5p acted directly on the *FLO1* promoter epitope-tagged Gcn5p strains were constructed in wild type and *ssn6* mutant backgrounds by the addition of a 9-Myc epitope to the C-terminal end of the protein using standard methods (see Materials and Methods). *ssn6* mutants were included in the analysis because *FLO1* is de-repressed in these strains and it was predicted Gcn5p would bind to the *FLO1* promoter in the absence of Ssn6p. Prior to analysis, the presence of the epitope tag and confirmation of the tagged Gcn5p function was first monitored by Western blot (Figure 5.8).

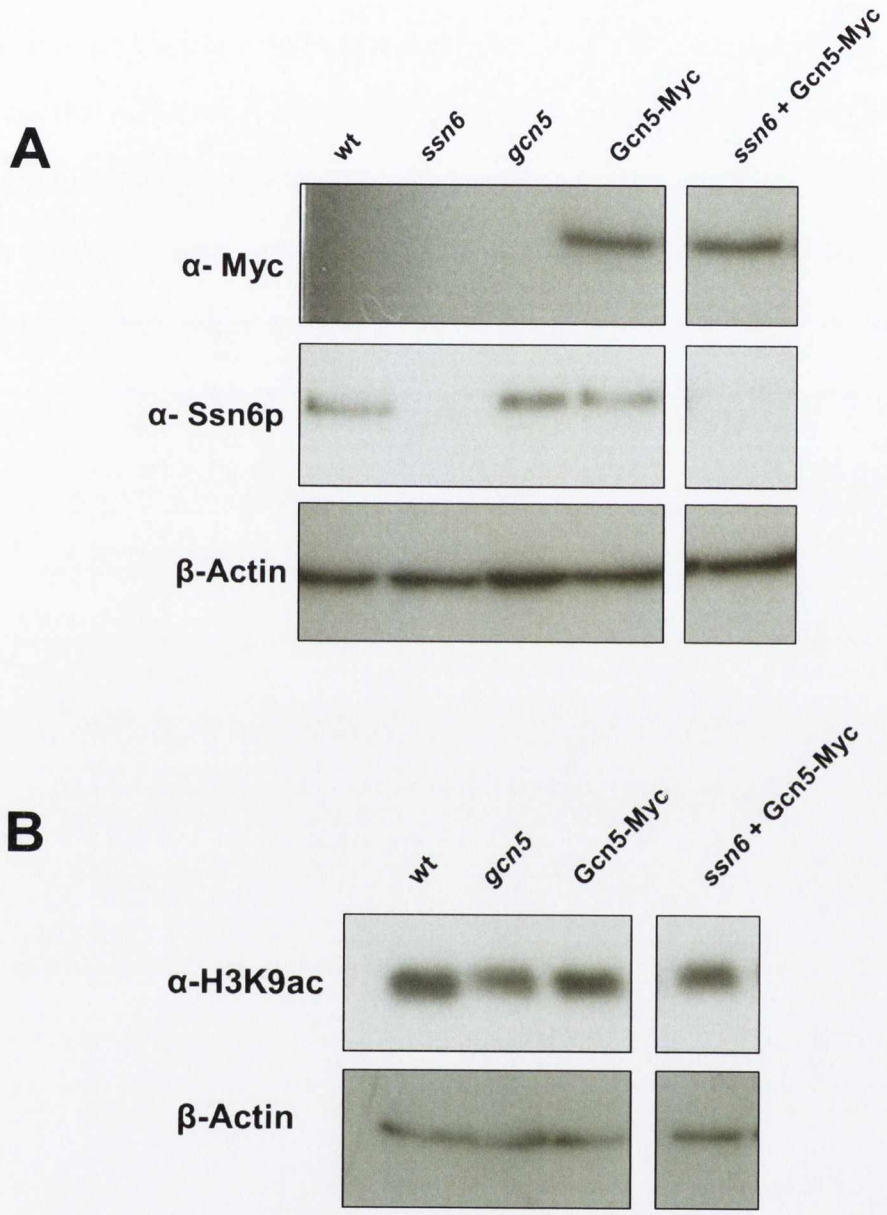
A
wt
ssn6
gcn5
Gcn5-Myc
ssn6 + Gcn5-Myc
α- Myc
α- Ssn6p
β-Actin
B
wt
gcn5
Gcn5-Myc
ssn6 + Gcn5-Myc
α-H3K9ac
β-Actin

Figure 5.8. Presence and function of the Myc-tagged Gcn5p. Western blot of (A) Myc and Ssn6p global levels in wild type (wt), *ssn6* and *gcn5* mutants and Myc-tagged Gcn5p strains both with (Gcn5-Myc) and without (*ssn6* + Gcn5-Myc) Ssn6p. (B) H3K9ac levels in Myc and Ssn6p global levels in wild type (wt), *gcn5* mutants and Myc-tagged Gcn5p strains both with (Gcn5-Myc) and without (*ssn6* + Gcn5-Myc) Ssn6p. β-Actin was used as a loading control. All strains were run on the same gel, with the *ssn6* + Gcn5-Myc strain being separated due to the presence of multiple Gcn5-Myc strains between the last two lanes.

In the Gcn5-Myc tagged wild type and *ssn6* strains, the epitope-tagged protein was expressed and was of the correct size of 61 kDa (Fig 5.8A, lanes 4 and 5). However, no Myc tag could be detected in the untagged wild type (wt), *ssn6* and *gcn5* mutant strains, which were used as negative controls (Fig. 5.8.A, lanes 1-3). Ssn6p levels in the Myc-tagged Gcn5p strains were also measured to ensure the tag had not affected the stoichiometry of the co-repressor complex subunit and to confirm that the *ssn6* + Gcn5-Myc strain lacked Ssn6p. Indeed, the data showed that the presence of a Myc-tagged Gcn5p did not affect levels of Ssn6p compared to Ssn6p levels in an untagged wild type or *gcn5* mutant strain (Fig 5.8A, compare lane 4 with lanes 1 and 3). Ssn6p was not detected in the untagged *ssn6* mutant or the *ssn6* + Gcn5-Myc strain (Fig. 5.8A, lanes 2 and 5). Together, these data confirm (i) Gcn5p was successfully tagged, (ii) that Ssn6p levels in this tagged strain were unaffected and (iii) Ssn6p was absent in the *ssn6* + Gcn5-Myc strain.

We next investigated whether the presence of a Myc-tag on Gcn5p affected Gcn5p activity by measuring global levels of H3K9ac in the tagged strain relative to wild type strains and a *gcn5* mutant. Gcn5p-containing complexes catalyse the addition of an acetyl mark to H3K9, and in order to confirm that Gcn5p was functioning properly when tagged, H3K9ac levels were measured (Howe et al., 2001). The addition of the Myc tag to Gcn5p did not affect global levels of H3K9ac either in the presence (Gcn5-Myc) or absence of Ssn6p (*ssn6* + Gcn5-Myc) compared to untagged wild type cells (Fig. 5.8, compare lanes 1, 3 and 4). A *gcn5* mutant was included as a control and shows the lower levels of H3K9ac in cell extracts when *GCN5* is deleted. Together, these data show that Gcn5p has been successfully tagged and its activity is unaffected relative to wild type strains.

5.2.7.1. Gcn5p acts directly on the *FLO1* promoter in an *ssn6* mutant.

Having established the importance of Gcn5p-containing complexes and Sas3p on acetylation at the *FLO1* promoter and *FLO1* de-repression in the absence of Tup1-Ssn6, the occupancy of Gcn5p and Sas3p was investigated at *FLO1*. The reduction in H3 acetylation at the *FLO1* promoter region observed in *ssn6* mutants lacking Gcn5p-containing complexes and Sas3p suggests the HATs may act directly at the de-repressed *FLO1* promoter. However, no evidence for Gcn5p or Sas3p occupancy on the *FLO1* promoter has been shown previously. Therefore to directly determine if Gcn5p and Sas3p were present at the de-repressed *FLO1* promoter, wild type and *ssn6* strains were constructed in which Gcn5p and Sas3p were Myc-tagged and their occupancy at the *FLO1* promoter was monitored by ChIP (Figure 5.9).

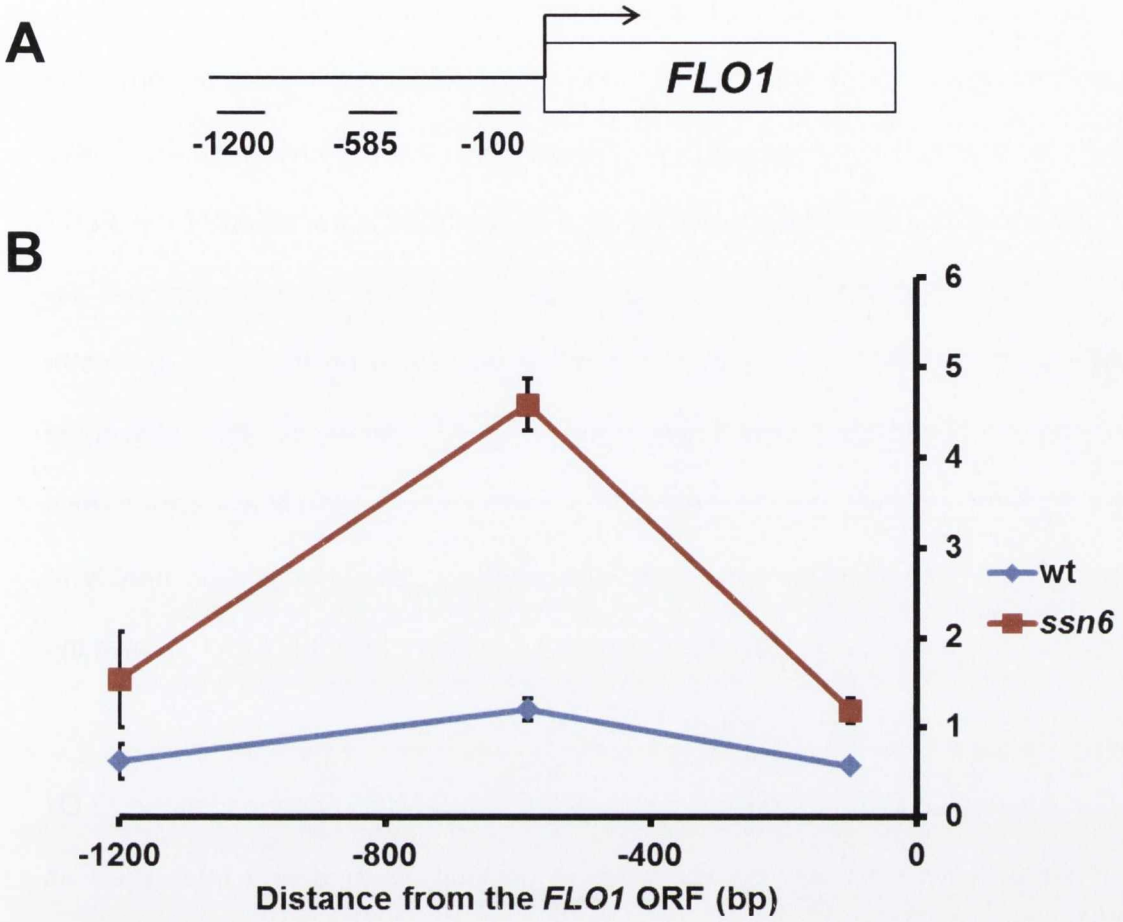

Figure 5.9 Gcn5-Myc occupancy of *FLO1* in the wild type and *ssn6* mutant. (A) Schematic of regions analysed upstream of the *FLO1* ORF. (B) ChIP analysis of Gcn5-Myc occupancy in wild type (wt) cells and *ssn6* single mutants at the *FLO1* promoter (-100bp, -500bp and -1200bp). Values at *FLO1* were normalised to an intergenic region of chromosome V. Error bars represent standard error of the mean (SEM) from two independent experiments.

Following confirmation of the tagging and functionality of Gcn5-Myc (Fig. 5.8), ChIP analysis of Gcn5-Myc across the *FLO1* promoter region was performed in the presence (wt) and absence of Ssn6p (*ssn6*). The results revealed Gcn5-Myc enrichment was detected specifically at a region 585 bp upstream of the *FLO1* transcription start site (TSS) in an *ssn6* mutant, where *FLO1* transcription is de-repressed (Fig. 5.9). Importantly, this is the same site on the *FLO1* promoter occupied by Tup1-Ssn6 in wild type strains (Fig. 4.9). However Gcn5-Myc could not be detected anywhere on the *FLO1* gene promoter region in wild type strains when the *FLO1* gene is repressed. This suggests that Gcn5p acts directly at *FLO1* in the absence of Tup1-Ssn6 where it occupies the *FLO1* promoter at the same site previously occupied by Tup1-Ssn6.

Sas3p was also Myc-tagged in order to detect Sas3-Myc occupancy at the *FLO1* promoter. The Sas3-Myc protein was successfully tagged and expressed as evidenced by Western blot analysis revealing the presence in whole cell lysates of a protein of the expected size (see Materials and Methods). However, initial attempts to determine its occupancy by ChIP were unsuccessful since it could not be detected at any published loci purported to be Sas3p binding sites (Rosaleny et al., 2007). Attempts to detect Sas3-Myc at the *FLO1* promoter either in the presence (wt) or absence of Ssn6p (*ssn6*) were also unsuccessful.

Considering our previous data showed that Gcn5p-containing complexes and Sas3p were redundantly required for *FLO1* de-repression (Fig. 5.1), it was reasoned that Sas3p may not be detectable by ChIP in the presence of Gcn5p which might either exclude Sas3p from binding, or obscure its presence. With this in mind, *gcn5* mutants were made in Sas3-Myc strains both containing and lacking Ssn6p and ChIP analysis of Sas3-Myc across the *FLO1* promoter was

performed. However Sas3-Myc was still not detected at the *FLO1* promoter or at any other site studied in any of the strains tested. Thus, although we confirmed the presence of Gcn5-Myc at the de-repressed *FLO1* promoter, under our conditions, we were unable to detect Sas3p occupancy by ChIP at *FLO1*, or indeed any other region.

5.2.8. Swi-Snf localises to the *FLO1* promoter in *ada2 sas3 ssn6* mutant strains in the absence of H3K14 acetylation.

Our data showed that in an *ssn6* mutant we detected high histone acetylation and significant histone eviction at the *FLO1* promoter which was accompanied by *FLO1* de-repression (compare Fig. 4.6 and Fig. 3.5). When Gcn5p-containing complexes and the Sas3p HAT were additionally deleted in the *ssn6* mutant, acetylation of the *FLO1* promoter and *FLO1* transcription were greatly diminished. This suggests Gcn5p-containing complexes and Sas3p cooperate to promote *FLO1* promoter acetylation and transcription in the absence of Ssn6p.

The current model for chromatin-mediated gene regulation by Tup1-Ssn6 states that promoter histones are acetylated by HATs upon loss of Tup1-Ssn6. This acetylated histone template is recognised by and/or stabilises binding of Swi-Snf, which can remodel gene promoters via histone eviction, allowing access by RNA Polymerase II and de-repression of target genes (Hassan et al., 2001). However, in the *ssn6* mutant additionally deleted for the HATs Ada2p and Sas3p (*ada2 sas3 ssn6*), we still observed significant histone depletion at the *FLO1* promoter despite the dramatically reduced *FLO1* promoter acetylation and transcription in this strain (Fig. 5.2).

We therefore wanted to determine the occupancy of Swi-Snf at the de-repressed *FLO1* promoter in *ssn6* mutants (*ssn6*), and in the *ssn6* mutant additionally deleted for the two HAT activities (*ada2 sas3 ssn6*) where *FLO1* promoter acetylation and transcription are impaired. Considering our data suggests the extent of histone depletion in the *ada2 sas3 ssn6* mutant was similar to that seen in the *ssn6* single mutant, if Swi-Snf occupancy at *FLO1* was similar in the two strains it would suggest that Swi-Snf could carry out nucleosome eviction in the absence of acetylation, contrary to the current model for Swi-Snf activity.

To investigate this, Snf2p occupancy was analysed by ChIP across the *FLO1* promoter in wild type (wt), *ssn6* and *ada2 sas3 ssn6* mutant strains (Figure 5.10). Snf2p is the catalytic subunit of Swi-Snf and its presence is indicative of Swi-Snf complex occupancy (Carlson and Laurent, 1994).

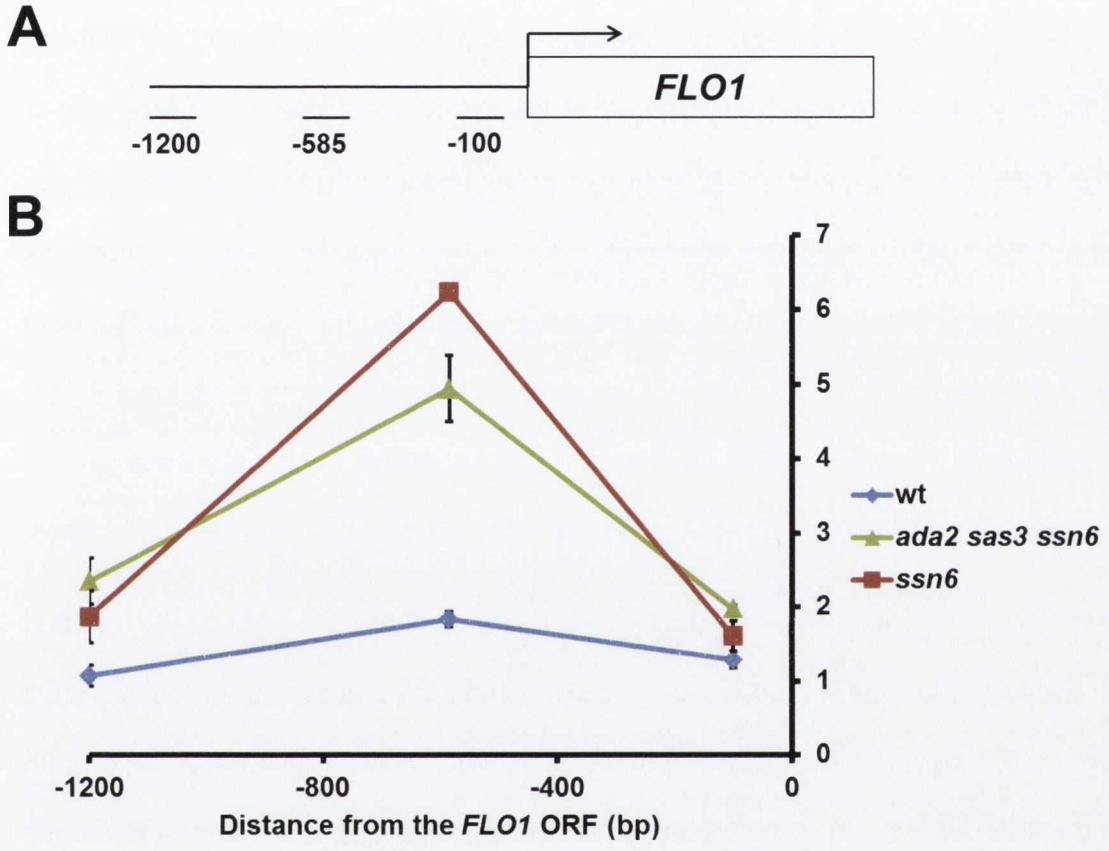

Figure 5.10 Snf2p occupancy at *FLO1* in wt, *ssn6* and *ada2 sas3 ssn6* mutants. (A) Schematic of regions analysed upstream of the *FLO1* ORF. (B) ChIP analysis of Snf2p occupancy in wild type (wt) cells, *ssn6* single mutants and *ada2 sas3 ssn6* triple mutants at the *FLO1* promoter (-100 bp, -500 bp and -1200 bp). Values at *FLO1* were normalised to an intergenic region of chromosome V. Error bars represent standard error of the mean (SEM) from two independent experiments.

The data revealed Snf2p occupancy was specifically enriched at the *FLO1* promoter region 585 bp upstream of the transcription start site (TSS) in the *ssn6* single mutant where *FLO1* is highly de-repressed (Fig. 5.10). In wild type cells where *FLO1* is not transcribed no Snf2p was detected at any region across the *FLO1* promoter. These data are consistent with the current models for Swi-Snf activity such that Swi-Snf was present at the highly acetylated *FLO1* promoter in the *ssn6* mutant, concomitant with extensive histone depletion and *FLO1* de-repression. Additionally, we showed Swi-Snf was recruited to the *FLO1* promoter in the absence of Ssn6p to the site previously occupied by Tup1-Ssn6. The data also shows that Swi-Snf was absent from the inactive, hypoacetylated *FLO1* promoter in wild type strains where there was no histone eviction and the gene is repressed.

However, analysis of Swi-Snf occupancy in the *ssn6* mutant additionally mutated for *ada2* and *sas3* (*ada2 sas3 ssn6*), which has severely reduced *FLO1* transcription, revealed that Snf2p occupancy was also detected at a region 585 bp upstream of the *FLO1* TSS, at levels similar to that in the *ssn6* mutant. These data suggest that Swi-Snf is recruited to the site at the *FLO1* promoter previously occupied by Tup1-Ssn6 in both the *ada2 sas3 ssn6* triple and *ssn6* single mutants at similar levels. Surprisingly, the recruitment of Swi-Snf to the *FLO1* promoter in the *ada2 sas3 ssn6* mutant occurs in the absence of highly acetylated histones. Furthermore, the data suggests that high histone eviction of *FLO1* promoter nucleosomes does not promote high transcription at *FLO1.* Thus, one interpretation of the data might be that it is not promoter histone eviction that is the key event in allowing *FLO1* de-repression, rather it may be the subsequent H3K14 acetylation levels at the depleted promoter chromatin template which is key to allowing full transcription.

5.3. Discussion

The data in chapter 4 showed that levels of H4ac4 and H3K9ac correlated with *FLO1* transcription in *tup1* and *ssn6* mutants (compare Fig. 4.4 and 4.7 and Fig. 3.5). We therefore further investigated the requirement for histone acetylation at *FLO1* and aimed to identify the factors responsible for catalysing the addition of this modification. A genetic analysis was carried out whereby *GCN5, ADA2* and *SAS3* were deleted in the presence and absence of Ssn6p and *FLO1* transcription was monitored in these mutants (Fig. 5.1). A deletion of *ADA2* was included since Gcn5p activity in the SAGA, ADA and SLIK complexes requires Ada2p. Thus, the *ada2* and *gcn5* mutants are both representative of strains deficient for SAGA, ADA and SLIK HAT activities (Maltby et al., 2012). In addition, to cripple both Gcn5p-containing complexes and Sas3p, an *ada2 sas3* mutant had to be used since a *gcn5 sas3* mutant is inviable (Howe et al., 2001). An *ssn6* mutant was used to cripple Tup1-Ssn6 function because we had previously shown that in a *tup1* mutant, Ssn6-Myc was still present at the *FLO1* promoter where our data suggested it might be exerting an independent repressive role. However, an *ssn6* single mutant was null for the Tup1-Ssn6 complex at *FLO1* (Fig. 4.9).

The data showed mutation of either *GCN5* or *SAS3* in an *ssn6* mutant background had only a small effect on *FLO1* transcription (Fig. 5.1; compare *ssn6* with *gcn5 ssn6* and *sas3 ssn6*). However, deletion of Gcn5p-containing complexes and Sas3p in an *ssn6* mutant (*ada2 sas3 ssn6*) reduced *FLO1* transcription dramatically, suggesting a redundant role for these HATs in *FLO1* de-repression. This result is supported by the fact that Gcn5p and Sas3p have been shown to be recruited to similar genes (Rosaleny et al., 2007).

In order to examine the histone acetylation activity of Gcn5p and Sas3p HATs at *FLO1,* we first examined histone density at the *FLO1* promoter in strains deleted for these HATs in the presence and absence of Ssn6p. This is because in *ssn6* mutants, the de-repressed *FLO1* promoter exhibited extensive histone loss which must be taken into account when interpreting histone acetylation data (Fig. 4.2). Histone levels were therefore determined by H3 ChIP across the *FLO1* promoter in the various HAT mutant strains (Fig. 5.2). This analysis confirmed previous data for *ssn6* mutants whereby transcription correlated with histone loss and revealed that *gcn5 ssn6*, *sas3 ssn6* and *ada2 sas3* mutants all showed similar levels of H3 depletion at the *FLO1* promoter compared to *ssn6*. Surprisingly however, an *ada2 sas3 ssn6* triple mutant also displayed extensive histone loss at the *FLO1* Tup1-Ssn6 binding site despite the low level of *FLO1* transcription observed in this mutant.

Having analysed histone occupancy at the *FLO1* promoter in the HAT mutants, we next examined acetylation levels at the *FLO1* promoter in these strains. The aim of this analysis was to determine if the impact of loss of Gcn5p/Ada2p and Sas3p on *FLO1* transcription in an *ssn6* mutant was due to a loss of acetylation at the *FLO1* promoter in these strains. As before, *ada2* mutants were used in combination with *sas3* mutants because *gcn5 sas3* mutants are inviable and *ada2* mutant strains lack active Gcn5p-containing complexes (Maltby et al., 2012).

In the *ssn6* single mutant which has a high level of *FLO1* de-repression, there was an increase in the level of H3K9ac detected across the *FLO1* gene promoter compared to wild type (Fig. 5.3). In the *ssn6* mutant additionally deleted for Gcn5p (*gcn5 ssn6*) where *FLO1* is also highly de-repressed H3K9ac occupancy across

the *FLO1* promoter was reduced compared to the levels in the *ssn6* single mutant (Fig. 5.3 compare *ssn6* to *gcn5 ssn6*). However, *ssn6* strains additionally mutated for *sas3* showed no decrease in acetylation levels compared to *ssn6*. The *ada2 sas3 ssn6* triple mutant, which lacks both HATs and Ssn6p, displayed H3K9ac occupancy levels that were not significantly different to those found in the *gcn5 ssn6* double mutant. These data suggest only Gcn5p-containing complexes play a role in acetylation of the *FLO1* promoter in absence of Ssn6p. Thus, Gcn5p is required for H3K9ac at the de-repressed *FLO1* promoter in the absence of Ssn6p. However, since H3K9ac levels between *gcn5 ssn6* and *sas3 ssn6* mutants are different (Fig. 5.3) yet *FLO1* transcription levels in these strains are identical (Fig. 5.1), it is unlikely that H3K9ac is the determining factor in *FLO1* transcription.

Our data also suggested Gcn5p-containing complexes and Sas3p played redundant roles in acetylation of H3K14 in the absence of Ssn6p. In this case, the high H3K14ac levels detected in the *ssn6* single mutant were unaffected when either *SAS3* or *GCN5* were individually mutated in this background. However, in a strain lacking both Gcn5p-containing complexes and Sas3p in an *ssn6* mutant (*ada2 sas3 ssn6*), this mark was abolished. This suggests that there is an equal reliance at *FLO1* on Gcn5p-containing complexes and Sas3p for H3K14ac at the de-repressed *FLO1* promoter. Importantly, H3K14ac levels at *FLO1* do correlate with *FLO1* transcription in all strains studied (Compare Fig. 5.1 and Fig. 5.4), indicating that this mark may be important for de-repression of *FLO1* in the absence of Ssn6p.

In summary, Gcn5p/Ada2p and Sas3p are redundantly required for *FLO1* transcription and H3K14ac at the de-repressed *FLO1* promoter in the absence of Ssn6p.

The classic model for chromatin remodelling is that acetylated histones promote eviction of promoter nucleosomes by chromatin remodelling complexes such as Swi-Snf, leading to gene transcription. However, the *ada2 sas3 ssn6* mutant does not appear to fit this model, as this strain exhibits dramatic nucleosome loss at the *FLO1* promoter yet has very low *FLO1* transcription (Fig. 5.2). Our data suggests H3K14ac and possibly H3K9ac are required for *FLO1* de-repression in the absence of Ssn6p (Fig. 5.1 and Fig. 5.4). This suggests that acetyl marks related to *FLO1* transcription may not be the same marks required for nucleosome eviction. . Interestingly, *ssn6* single mutants and strains lacking Ada2p/Gcn5p and Sas3p in an *ssn6* mutant background (*gcn5 ssn6*, *sas3 ssn6* and *ada2 sas3 ssn6*) all display similar elevated levels of H4ac4 at the *FLO1* promoter, suggesting this acetylation mark is not affected by loss of any of the HATs studied (Fig. 5.5). Thus the possible separation of function of acetylation might be that H4ac4 may be required for the dramatic histone eviction at the de-repressed *FLO1* promoter, whereas H3K14ac may be required for transcription. Also, the data highlights repression can occur even at a promoter that shows severe nucleosome depletion, meaning that loss of nucleosomes at *FLO1* is not sufficient for gene activation. The Snf2p data may support this; Snf2p still arrives at mutants in the absence of H3K14ac, but where H4ac4 is present at the *FLO1* promoter.

In line with previous studies, H3K14ac was abolished globally in *ada2 sas3* mutants and in *ada2 sas3 ssn6* mutant strains (Fig. 5.6) (Maltby et al., 2012). These data also suggested that H3K9ac was reduced globally in *gcn5* and *ada2* mutants relative to wild type cells. This latter result is supported by the reduction of H3K9ac at the *FLO1* promoter in these strains (Fig. 5.3). In light of the lack of H3K14ac in *ada2 sas3 ssn6* mutants and the impact on *FLO1* transcription in this

strain, it was hypothesised that the dramatic loss of H3K14ac may have a general effect on transcription in these mutants. However, it was found that no reduction in transcription of the constitutively-transcribed *PMA1* gene or the inducible *SUC2* gene could be detected in in the *ada2 sas3 ssn6* mutant compared to wild type (Fig. 5.7). This suggests that the critical role of H3K14ac in *FLO1* transcription is not common to all genes in *S. cerevisiae* or even those under Tup1-Ssn6 control. This dependence on H3K14ac may be specific to *FLO1* or specific subsets of genes.

Although the dependence on Gcn5p and Sas3p of *FLO1* transcription was indicated genetically through analysis of mutants, it was unknown whether these factors acted directly on the *FLO1* promoter or indirectly. However, Gcn5-Myc was indeed detected at the *FLO1* promoter in an *ssn6* mutant (Fig. 5.9), indicating that Gcn5p binds to the Tup1-Ssn6 binding site, which it potentially co-occupies with Swi-Snf in the absence of Tup1-Ssn6 (Fig. 5.10).

Sas3-Myc occupancy was also investigated at several locations based on data from Rosaleny et al (Rosaleny et al., 2007), but this protein could not be detected in wild type strains or *ssn6* mutants. In light of the fact that Gcn5p and Sas3p appear to act redundantly at *FLO1*, it was reasoned that Gcn5p may be responsible for H3K14ac levels at *FLO1* in the absence of Ssn6p and that Sas3p may only act on *FLO1* in a *gcn5* mutant. To test this, a *gcn5* deletion was made in a Sas3-Myc strain lacking Ssn6p, but this also failed to uncover Sas3-Myc at any locus. The failure to detect Sas3p could be a technical issue rather than the absence of the protein at the *FLO1* promoter, as it was not detected at any site studied.

Having already detected Swi-Snf at *FLO1* (Fig. 4.1), it was decided to compare Swi-Snf occupancy in the highly de-repressed *ssn6* single mutant and the much less de-repressed *ada2 sas3 ssn6* triple mutant. Although H3 occupancy was at a similar level between these two mutant strains at the *FLO1* Tup1-Ssn6 binding site, Snf2p occupancy at *FLO1* was monitored in order to confirm that Swi-Snf recruitment to *FLO1* was occurring in the absence of the transcriptionally-important H3K14ac mark (Fig. 5.10). The results showed that Snf2p was detected at the Tup1-Ssn6 binding site in both strains, and was found to be present at similar levels. This, in conjunction with the H3K14ac occupancy data observed in Figure 5.4 suggests that Swi-Snf recruitment to *FLO1* is not dependent on H3K14ac, though this mark is important for *FLO1* activation (Fig. 5.1).

In summary, these data indicate that in the wild type strains in which *FLO1* was not transcribed, there was high nucleosome occupancy of the *FLO1* promoter (Fig. 5.11, Wild type). Wild type strains had Tup1-Ssn6 present at the *FLO1* promoter, which repressed *FLO1* transcription. There were low levels of histone H3K9, H3K14 and H4 acetylation upstream of *FLO1* in this strain which correlated with the lack of *FLO1* transcription and high nucleosome occupancy. Swi-Snf and Gcn5p were not detected at the repressed *FLO1* promoter in the wild type.

However, in *ssn6* single mutants, where *FLO1* is highly de-repressed, there is an extensive nucleosome eviction across the *FLO1* promoter (Fig. 5.11, *ssn6*). *ssn6* mutants also displayed elevated levels of H3K9ac, H3K14ac and H4ac4 across the *FLO1* promoter. Swi-Snf and Gcn5p occupied the *FLO1* promoter at the Tup1-Ssn6 binding site in the absence of Ssn6p, indicating that loss of Ssn6p in this strain allowed binding by these transcriptional activators.Sas3p may also

occupy this site with Gcn5p or in a *gcn5* mutant, though it could not be detected by ChIP analysis.

ada2 sas3 ssn6 triple mutants had very low levels of *FLO1* de-repression, though these mutants unexpectedly showed a high level of nucleosome eviction across the *FLO1* promoter (Fig. 5.11, *ada2 sas3 ssn6*). In the absence of Gcn5p HAT activity and Sas3p in an *ssn6* mutant background, the H3K14ac mark was abolished and H3K9ac was reduced across the *FLO1* promoter compared to an *ssn6* single mutant. However, there was a high level of H4ac4 across the *FLO1* promoter which was not affected by the loss of Gcn5p-containing complexes and Sas3p. Snf2p was detected in this mutant to a level comparable with that of an *ssn6* single mutant. The *ada2 sas3 ssn6* triple mutant therefore show extensive nucleosome loss without the corresponding extensive *FLO1* de-repression.

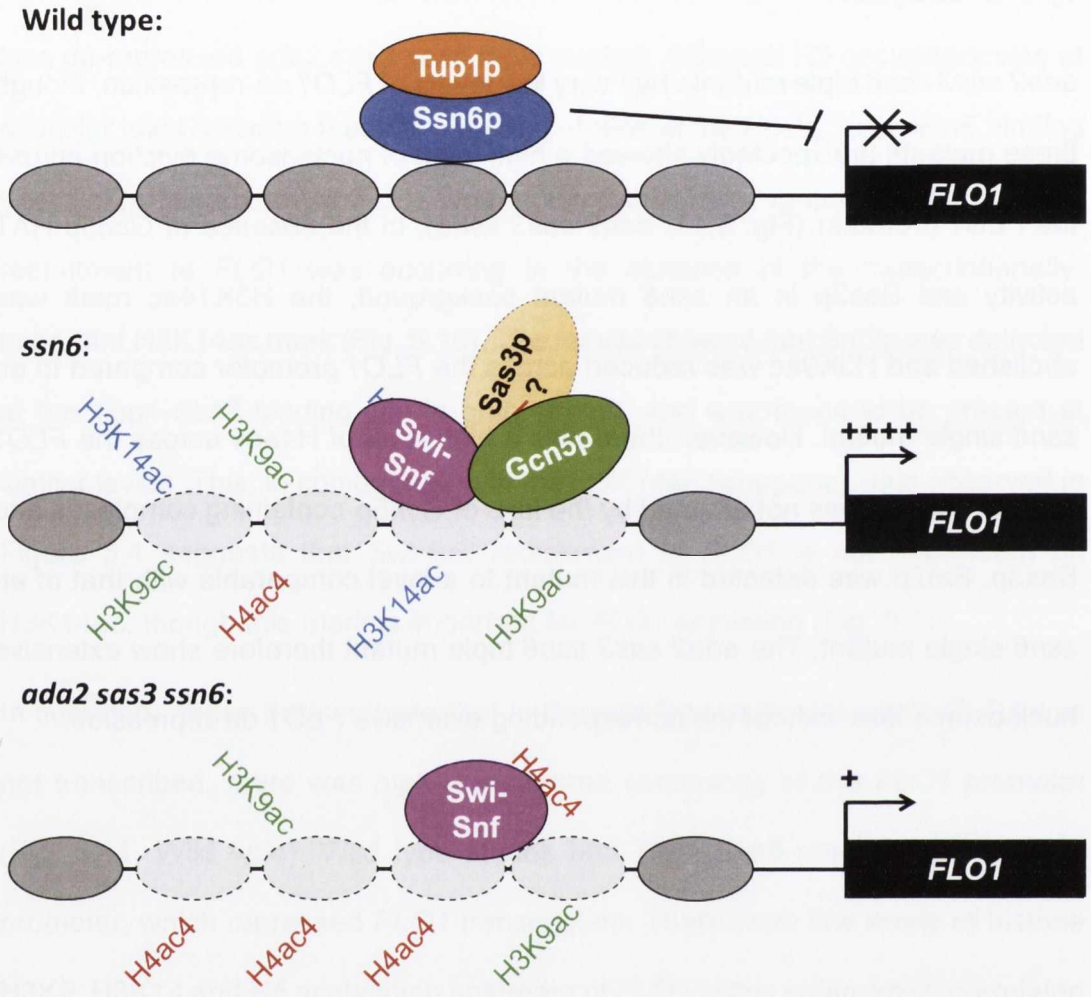

Figure 5.11. Model for Tup1-Ssn6 and HAT action at the *FLO1* promoter. Summary of protein occupancy at the *FLO1* promoter and *FLO1* transcription in Wild type strains, *ssn6* single mutants and *ada2 sas3 ssn6* triple mutants. Dashed lines indicate protein loss. "++++" indicates level of *FLO1* transcription.

Chapter 6

Kinetic analysis of *FLO1* de-repression

6.1. Introduction

The data presented in chapter 5 indicated that Gcn5p and Sas3p were redundantly required for *FLO1* gene activation, possibly due to their conferral of the H3K14ac mark at the *FLO1* gene promoter. Indeed, it was found that cells lacking a combination of these HATs in an *ssn6* mutant background did not display *FLO1* de-repression to any great extent (Fig. 5.1) and were deficient in the H3K14ac mark at the *FLO1* gene promoter (Fig. 5.6). These data highlighted the importance of histone acetylation in regulation of *FLO1,* and also identified the factors responsible for this PTM at the gene promoter in *tup1* and *ssn6* mutants. However, this analysis was carried out in steady-state mutants which offer limited insight when analysing an inducible gene such as *FLO1*, and when studying a complex with such a wide variety of target genes as Tup1-Ssn6.

There are several issues to be considered when using classic null gene mutations to study gene transcription. Firstly, gene transcription is a highly dynamic process, with many factors occupying gene promoters, in some cases transiently, and steady-state genetic analysis only allows a snapshot of events within a population of cells at any particular moment (Magraner-Pardo et al., 2014). Secondly, null mutants of genes such as *SSN6* display pleiotropic phenotypes that could indirectly influence transcription of a target gene in ways that would be difficult to discern due to the volume of genes under transcriptional control of Tup1-Ssn6 (DeRisi et al., 1997). Finally, in order to establish the mechanism of *FLO1* de-repression in the absence of Tup1-Ssn6, it is necessary to identify factors required for the recruitment of RNA Polymerase II and its stability at the gene promoter, and any possible link between transcription and nucleosome remodelling at the *FLO1* promoter. Since steady-state mutants only offer a

glimpse of events at a gene that is either repressed or actively transcribed, it is desirable to perform a kinetic analysis to observe the steps that lead to gene activation.

The Anchor Away (AA) technique is a relatively recent development, which allows the creation of a conditional mutant of any nuclear protein (Haruki et al., 2008). The protein of interest (in this case Ssn6p) is C-terminally tagged with an 11 kDa epitope which is the FKBP12-rapamycin-binding (FRB) domain of human mTOR to form the "target". The "anchor" is the ribosomal protein RPL13A, C-terminally fused to the human 12 kDa FK506 binding protein (FKBP12), which will bind to FRB in the presence of rapamycin. Ribosomal proteins naturally transit the nucleus during assembly of the 40S and 60S ribosome subunits(Kohler and Hurt, 2007). These abundant proteins, when tagged with FKBP12, will bind FRB in the presence of rapamycin. The target protein is then shuttled from the nucleus bound to the anchor, creating a rapamycin-induced conditional mutant (Figure 6.1). Because rapamycin is toxic to wild type yeast, Haruki et al. constructed host a strain containing a mutated *TOR1* and deleted *FPR1* gene which confers resistance to rapamycin, and allows for successful anchor-target interaction upon addition of rapamycin.

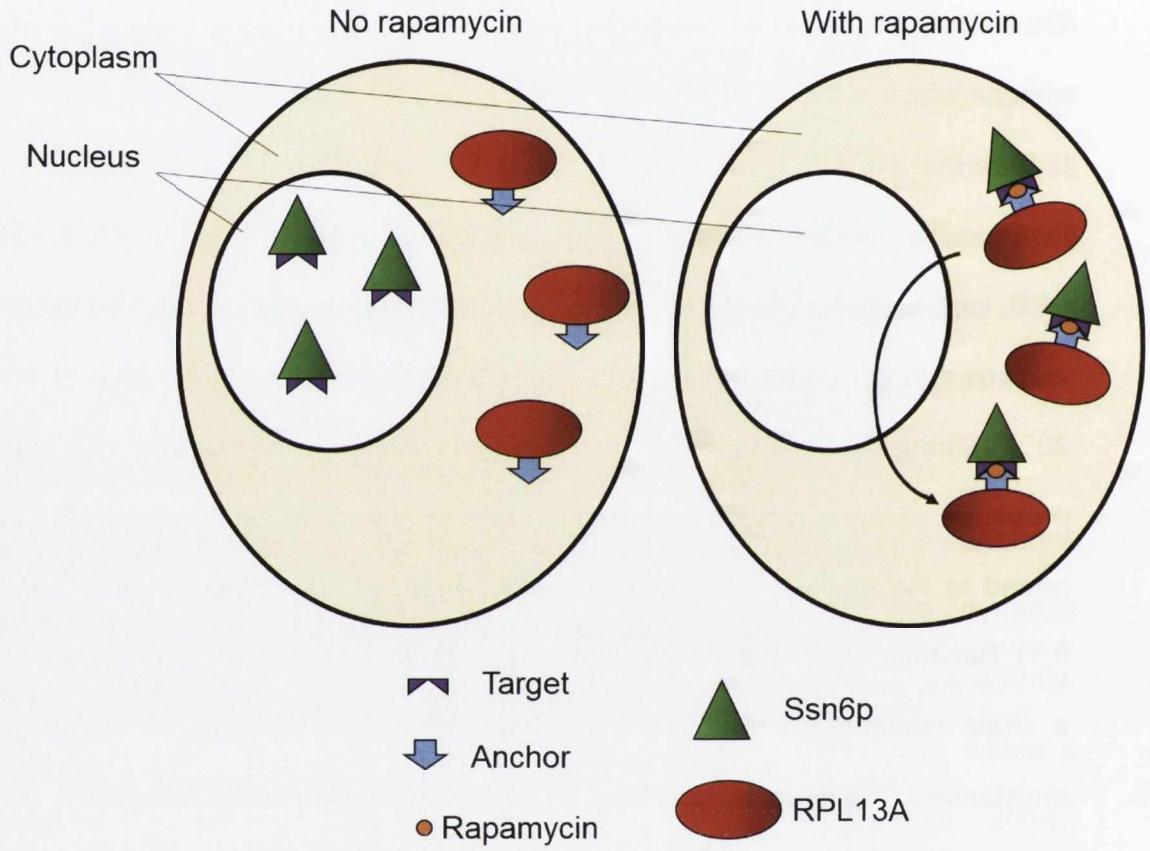

Figure 6.1. The anchor away technique. Schematic depiction of the anchor away technique. The protein of interest (Ssn6p) is tagged with an FRB epitope (target) and the ribosomal protein RPL13A is tagged with an FKBP12 epitope (anchor). Upon addition of rapamycin, the anchor binds to the target, and the FRB-tagged Ssn6p is shuttled out of the cell nucleus, bound to the FKBP12-tagged RPL13A.

The purpose of the anchor away analysis was to generate a timeline of events that lead to de-repression of *FLO1* upon loss of Ssn6p. Since acetylation of H3K14 by Gcn5p-containing complexes and Sas3p had been implicated in *FLO1* activation, the hypothesis was that H3K14ac at the *FLO1* promoter would precede Pol II occupancy at *FLO1.* Anchor away would also determine any differences in H3 loss at the *FLO1* promoter between cells containing and lacking Ada2p and Sas3p, and give insight into the relationship between histone occupancy and *FLO1* transcription upon loss of Ssn6p.

6.2. Results

6.2.1. Ssn6-FRB is detectable in an Ssn6p anchor away strain

To show that Ssn6p was tagged with an FRB epitope and that this protein was expressed, an Ssn6-FRB strain and the HHY221 parent were analysed by Western blot (Figure 6.2A). The data showed FRB-tagged Ssn6p was detectable in the Ssn6-FRB strain, with the expected molecular weight of ~130kDa (Fig. 6.2A). This was in contrast to the un-tagged parent strain where no protein was detected. This suggests that the Ssn6-FRB strain was successfully constructed and does indeed express an FRB-tagged Ssn6 protein.

Additionally, it was essential to show that the integrity of the Tup1-Ssn6 complex was unaffected in the Ssn6p anchor away (Ssn6-AA) strain, and that Ssn6-AA could be depleted of Tup1-Ssn6 at target gene promoters. To investigate this, and to show that the addition of rapamycin did not affect Tup1-Ssn6 occupancy, Tup1p occupancy was analysed by ChIP in un-tagged (wt) and FRB-tagged (Ssn6-AA) anchor away strains in the presence and absence of rapamycin (Fig. 6.2B). Tup1p was monitored instead of Ssn6-FRB as I was unable to detect the

FRB epitope by ChIP, and because Tup1p occupancy is representative of the Tup1-Ssn6 complex (Fig. 4.9).

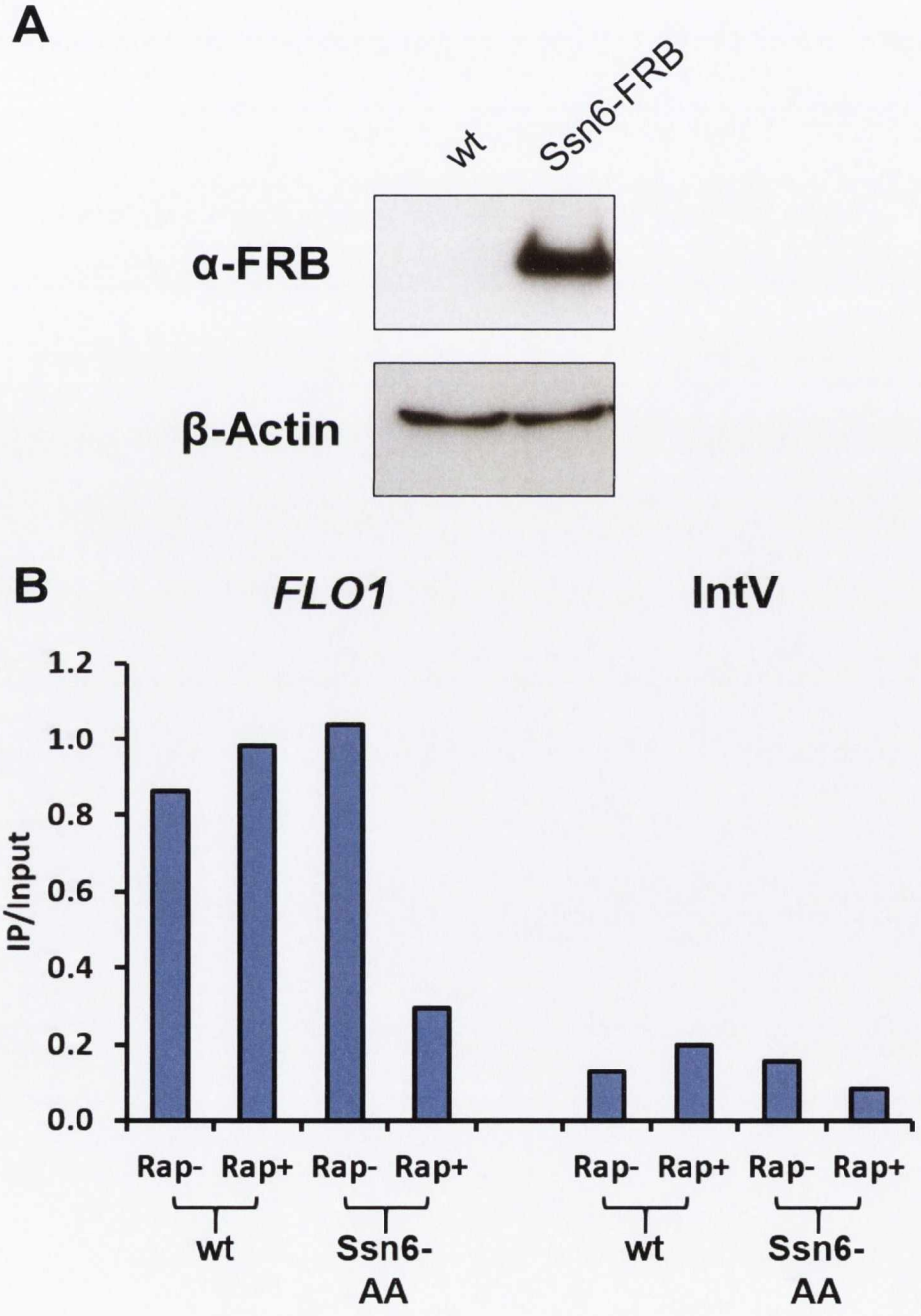
A
wt
Ssn6-FRB
α-FRB
β-Actin
B
FLO1
IntV
IP/Input
1.2
1.0
0.8
0.6
0.4
0.2
0.0
Rap- Rap+ Rap- Rap+ Rap- Rap+ Rap- Rap+
wt
Ssn6-AA
wt
Ssn6-AA

Figure 6.2. Ssn6-FRB in anchor away strains. (A) Western blot of Ssn6-FRB in un-tagged (wt) and FRB-tagged Ssn6-anchor-away strains (Ssn6-FRB). β-actin was used as a loading control. (B) ChIP analysis of Tup1p occupancy at the *FLO1* promoter in both the untagged (wt) and FRB-tagged (Ssn6-AA) strains both in the absence (Rap-) and after growth for 2 hours in (Rap+) YEPD containing 1μg/ml rapamycin. Data is shown as IP/input at 585 bp upstream of the *FLO1* transcription start site (*FLO1*) and at an intergenic region of chromosome V (IntV) as a negative control.

Tup1p occupancy was first confirmed at *FLO1* in the Ssn6-AA strain in the absence of rapamycin, where it was shown to be present at the same level as that seen in the wt (untagged) strain (Fig. 6.2B, compare Ssn6-AA Rap- and wt Rap-). However, after incubation with rapamycin, Ssn6-AA strains exhibited Tup1p levels at the *FLO1* promoter comparable to the intergenic negative control region, suggesting complete loss of Ssn6-FRB from the *FLO1* promoter.

As a further control, Tup1p occupancy was also monitored at the *FLO1* promoter and at an intergenic control region (IntV) in the untagged anchor away parent strain (wt). The data showed that Tup1p occupancy at *FLO1* was not affected by rapamycin (Fig. 6.2B, compare wt Rap- and Rap+).

Together, these data suggest that Ssn6p was successfully tagged with an FRB epitope in the Ssn6-AA strain, and that the presence of the tag did not affect the integrity and occupancy of the Tup1-Ssn6 complex. Furthermore, these data confirm that Tup1-Ssn6 levels can be fully depleted from the *FLO1* promoter upon addition of rapamycin.

6.2.2. FRB-tagged Ssn6p is exported from the cell nucleus upon the addition of rapamycin

The binding of FRB-tagged Ssn6p (Ssn6-FRB) to an FKBP12-tagged ribosomal protein in the presence of rapamycin promotes export of Ssn6-FRB from the cell nucleus and determines a successful anchor away experiment. If this was occurring in the strains studied, it was predicted that Ssn6-FRB, when stained with a fluorescent dye, would be visible leaving cell nuclei after incubation with rapamycin. Sphaeroplasts were therefore incubated with a primary antibody directed against the FRB epitope and a fluorescently-labelled (AlexaFluor 488)

secondary antibody. Sphaeroplasts were also stained with 4', 6-diamidino-2-phenylindole (DAPI) to visualise DNA. This allowed visualisation of Ssn6-FRB (green) and cell nuclei (blue) in cells incubated for three hours with or without rapamycin. As a control, cells that were not incubated with the primary (anti-FRB) antibody were also analysed. All cells were visualised using a Nikon Ti Eclipse fluorescence microscope and Volocity software at 40 X magnification (Figure 6.3).

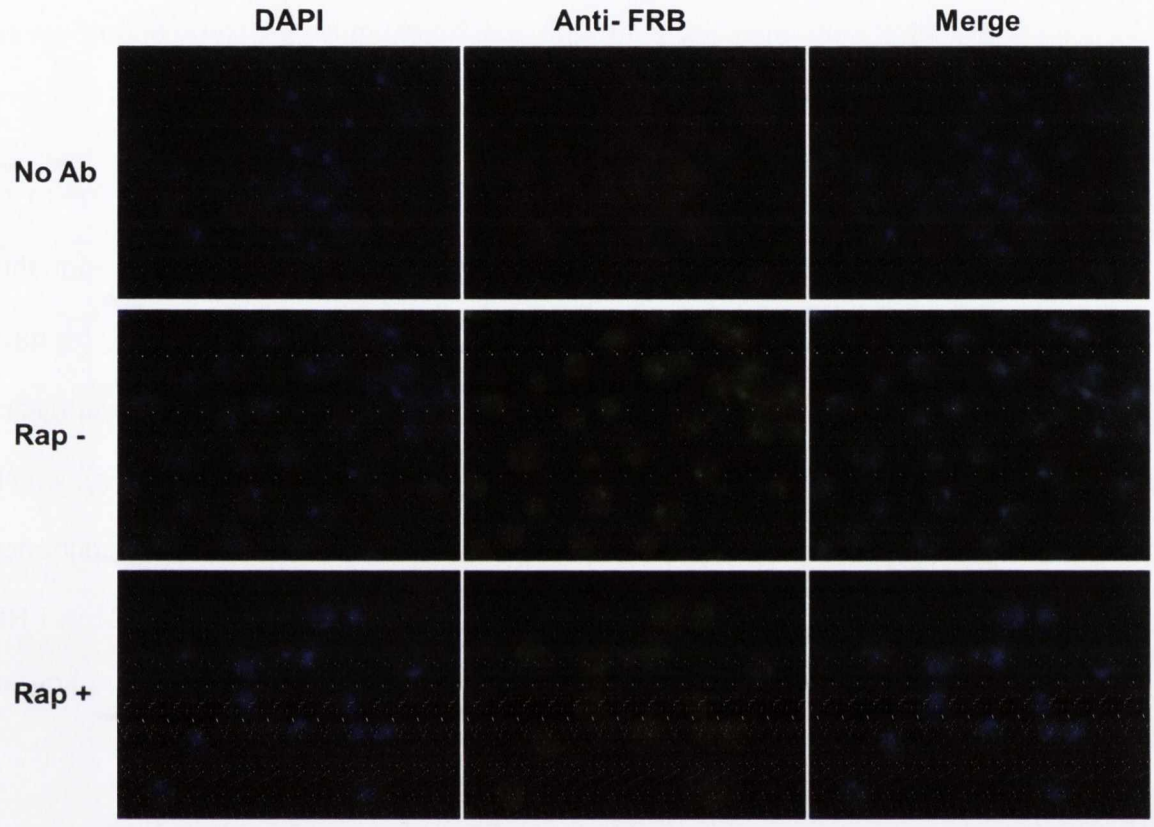

Figure 6.3. Microscopic analysis of FRB-tagged Ssn6p. Fluorescent microscopy analysis of FRB-tagged Ssn6p before (Rap-) and after (Rap+) the growth in rapamycin-containing medium. Column 1 shows DAPI-stained DNA, column 2 shows green AlexaFluor 488-dyed FRB and column 3 shows a merged image of these two image sets. A control that lacked addition of a primary anti-FRB antibody was included (No Ab).

In the absence of a primary antibody directed against FRB, DAPI-stained nuclei (blue) were clearly visible, but there was no fluorescently-labelled Ssn6-FRB (green) detected (Fig. 6.3, No Ab). This suggests that the fluorescently-labelled secondary antibody does not bind non-specifically, and any detection of green fluorescent dye is specific for Ssn6-FRB.

In the absence of rapamycin, Ssn6-FRB should be found in cell nuclei due to its role as a transcriptional repressor. It was therefore expected that under this condition, Ssn6-FRB detection would overlap with DAPI-stained DNA. The data revealed that in Ssn6-AA strains that had not been incubated with rapamycin, discrete nuclei were visible (blue) along with FRB-tagged Ssn6p (green), which appeared as distinct foci (Fig. 6.3, Rap-). Importantly, Ssn6-FRB occupancy overlapped with the DNA, indicating that in the absence of rapamycin, Ssn6-FRB was found in the cell nucleus. This result is consistent with the role of Ssn6p as a nuclear protein.

The addition of rapamycin to Ssn6-AA strains should result in the export of FRB-tagged Ssn6p from the cell nucleus, resulting in detection of fluorescently-labelled Ssn6-FRB (green) that does not overlap with DAPI-stained DNA (blue) (Haruki et al., 2008).In Ssn6-AA strains that had been treated with rapamycin, Ssn6-FRB formed granules scattered throughout the cell that did not overlap with cell nuclei (Fig. 6.3, Rap+). This suggests that under these conditions, Ssn6-FRB was no longer bound to genomic DNA and had been depleted from the nucleus. Overall, this analysis shows that Ssn6-FRB was exported from the cell nucleus upon addition of rapamycin.

6.2.3. Ssn6-FRB cells exhibit more diffuse DNA after rapamycin treatment

It was interesting to note that when DAPI-stained cells were observed after incubation with rapamycin, the DNA appeared to be more diffuse than in untreated cells. Indeed, in untreated cells, the cell nuclei appeared as very distinct foci. In order to more clearly investigate this result, DAPI-stained cells were viewed without an anti-FRB or a no primary antibody control (Figure 6.4).

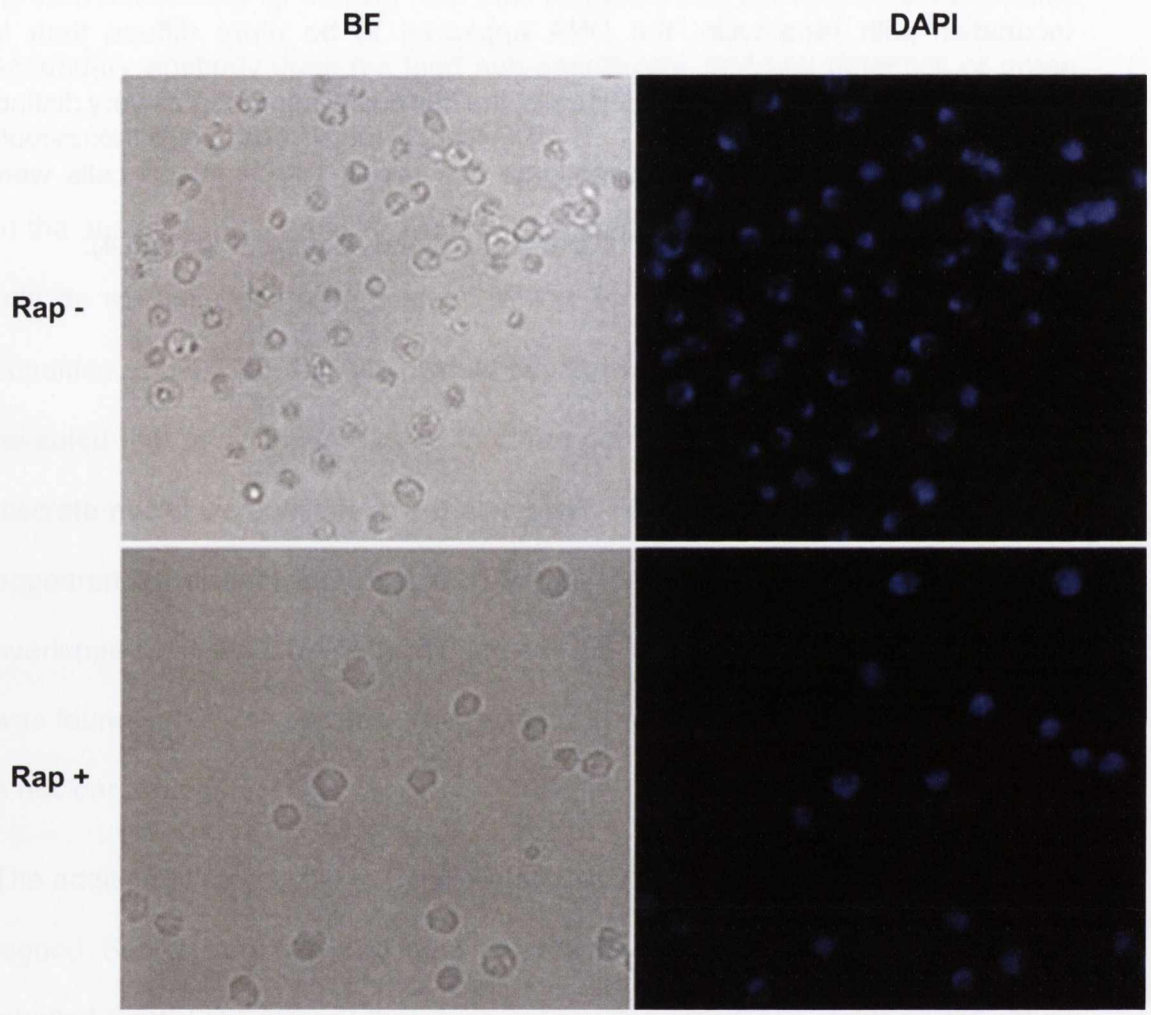

Figure 6.4. Microscopic analysis of DAPI-stained DNA in Ssn6-AA. Fluorescent microscopy analysis of FRB-tagged Ssn6p before (Rap-) and after (Rap+) the growth in rapamycin-containing medium showing BF (bright field) and DAPI-stained cells.

When Ssn6-FRB cells were grown in the absence of rapamycin, DAPI-stained DNA was clearly visible as distinct foci (Fig. 6.4, Rap-). However, after treatment with rapamycin, DAPI-stained DNA was more diffuse (Fig. 6.4, Rap+). This could indicate that when grown in the absence of rapamycin, genomic DNA compaction in part depends on Ssn6p. When cells are grown in the presence of rapamycin, Ssn6-FRB is exported from the nucleus and is unable to influence chromatin. This loss of Ssn6-FRB may lead to less genomic DNA compaction.

6.2.4. *SUC2* is de-repressed following Ssn6-anchor-away.

The next experiment performed on the Ssn6-FRB anchor-away strain was analysis of *SUC2* transcription upon loss of Ssn6p from the cell nucleus. Analysis of the Tup1-Ssn6 repressed *SUC2* gene would serve the dual purpose of establishing a time-course for later analyses at *FLO1* and offer validation of the anchor away method. Using *SUC2* as a control for de-repression in an Ssn6p-depleted strain and using an anchor away time-course similar to that used by Wong and Struhl in their analysis of Tup1-Ssn6 function (Wong and Struhl, 2011), rapamycin was added to FRB-tagged Ssn6p cultures and samples were removed over a 120 minute time course. *SUC2* mRNA abundance was monitored by qPCR at the time-points indicated (Figure 6.5A) in wild type (untagged) and Ssn6-anchor-away (Ssn6-AA) strains. In addition, Pol II occupancy at the *SUC2* 5' ORF was also measured by ChIP analysis in order to monitor active transcription over a similar time course (Figure 6.5B).

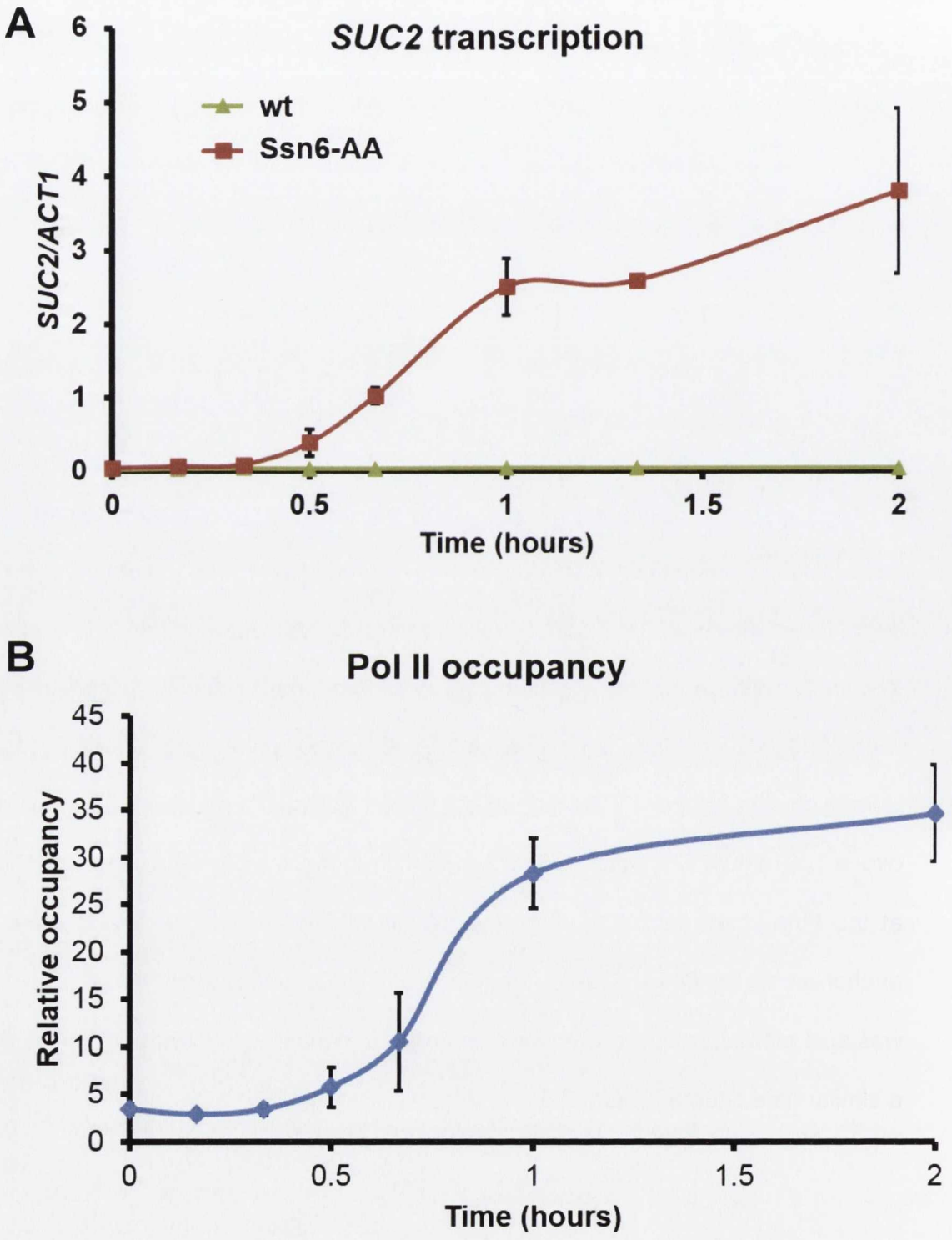
A
SUC2 transcription
wt
Ssn6-AA
SUC2/ACT1
0
1
2
3
4
5
6
0
0.5
1
1.5
2
Time (hours)
B
Pol II occupancy
Relative occupancy
0
5
10
15
20
25
30
35
40
45
0
0.5
1
1.5
2
Time (hours)

Figure 6.5. *SUC2* de-repression coincides with Ssn6-FRB loss during Anchor Away. (A) Wild type (wt) and Ssn6-AA strains were treated with rapamycin and *SUC2* transcription was analysed by qPCR. *SUC2* 5' ORF transcript levels were normalised to *ACT1* 5' ORF transcript levels. (B) ChIP analysis of RNA Polymerase II (Pol II) occupancy at the *SUC2* 5' ORF in an Ssn6-AA strain following addition of 1µg/ml rapamycin. Pol II levels at the *SUC2* 5' ORF were normalised to a telomeric control region. Error bars represent standard error of the mean (SEM) from two independent experiments.

The results suggested that over a period of 120 minutes following rapamycin addition, the *SUC2* gene was de-repressed in the strain containing FRB-tagged Ssn6 (Fig. 6.5A, Ssn6-AA). However, *SUC2* transcription was not induced in the untagged strain following similar treatment (Fig. 6.5A, wt). The levels of *SUC2* transcripts observed at 60 minutes in Ssn6-AA strains were almost identical to those seen in a steady state *ssn6* mutant, indicating that *SUC2* was fully de-repressed by this time (Compare Fig. 6.5 and Fig. 3.6). This suggests that the nuclear loss of Ssn6-FRB was successful in the presence of rapamycin, and that *SUC2* de-repression observed upon addition of rapamycin to an Ssn6-AA strain was comparable to *SUC2* de-repression during growth in low glucose in conventional null *ssn6* mutant strains. These data were consistent with previous data (Wong and Struhl, 2011), and suggest that *SUC2* is rapidly de-repressed upon loss of Ssn6p from the gene promoter.

To determine more clearly whether *SUC2* mRNA levels were indicative of active transcription upon addition of rapamycin to Ssn6-AA strains, Pol II levels at the *SUC2* 5' ORF were monitored during *SUC2* de-repression (Fig. 6.5B). This analysis showed a Pol II occupancy time-course at the *SUC2* promoter following rapamycin addition which closely resembled the *SUC2* mRNA accumulation data. Indeed, Pol II accumulated to maximum levels at the *SUC2* promoter by 60 minutes post rapamycin addition. Together, these data confirmed that *SUC2* was rapidly de-repressed upon treatment of Ssn6-AA cells with rapamycin, indicating that Ssn6-FRB was rapidly lost from the *SUC2* promoter.

6.2.5. Histone H3 is rapidly lost from the *SUC2* gene promoter

The previous data revealed that upon the addition of rapamycin and following the loss of Ssn6-FRB from the *SUC2* gene promoter, *SUC2* was rapidly de-repressed

(Fig. 6.5). Conventional mutants lacking Ssn6p have been shown to exhibit dramatic histone loss at gene promoters (Fig. 5.3) (Gavin and Simpson, 1997; Fleming and Pennings, 2001, 2007). Previous studies have also shown that a rapid and dramatic loss of histone H3 at the *SUC2* promoter occurs upon the addition of rapamycin in Tup1-AA strains (Wong and Struhl, 2011). To verify if this also occurred following Ssn6p anchor away, H3 loss at the *SUC2* promoter was monitored by ChIP over the 2 hour time-course (Fig. 6.6).

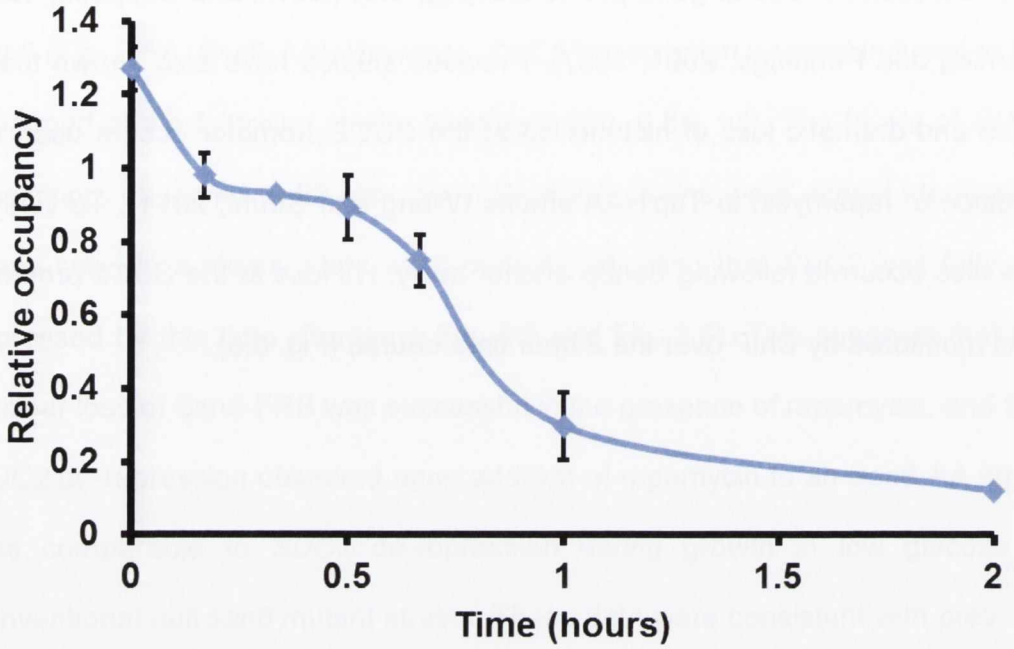

Figure 6.6 H3 loss at the *SUC2* promoter upon addition of rapamycin. ChIP analysis of H3 occupancy after the addition of rapamycin in an Ssn6-AA anchor away strain at the *SUC2* promoter. H3 levels were normalised to an intergenic region of chromosome V. Error bars represent standard error of the mean (SEM) from two independent experiments.

After the addition of rapamycin to Ssn6-AA cells, H3 loss from the *SUC2* promoter began almost immediately (Fig. 6.6). By 30 minutes post-rapamycin treatment, H3 occupancy at the *SUC2* promoter had declined by approximately 50% compared to the level of H3 occupancy at time 0. By 1 hour after the addition of rapamycin, H3 levels at *SUC2* had reached a plateau, indicating a minimal nucleosome occupancy at the *SUC2* promoter had been reached. This H3 loss correlated with the rapid *SUC2* induction observed after the addition of rapamycin (Fig. 6.5). However, the sequence of events indicates that although H3 depletion starts almost immediately, Pol II only arrives 20-30 minutes following addition of rapamycin (compare Fig. 6.6 and Fig. 6.5B). This suggests that following loss of Tup1-Ssn6 from the *SUC2* promoter, H3 promoter loss precedes *SUC2* transcription (Wong and Struhl, 2011).

6.2.6. H3K14ac at the *SUC2* promoter increases upon addition of rapamycin

Taking into account the rapid *SUC2* de-repression of transcription and concomitant H3 loss at the *SUC2* promoter following Ssn6 anchor away, it was hypothesised that this would coincide with anincrease in histone acetylation at the *SUC2* promoter. Since it had been established in Chapter 3 that H3K14ac was required for *FLO1* de-repression in the absence of Tup1-Ssn6 (Fig. 5.1), this mark was monitored over time at the *SUC2* promoter after the addition of rapamycin (Fig. 6.7).

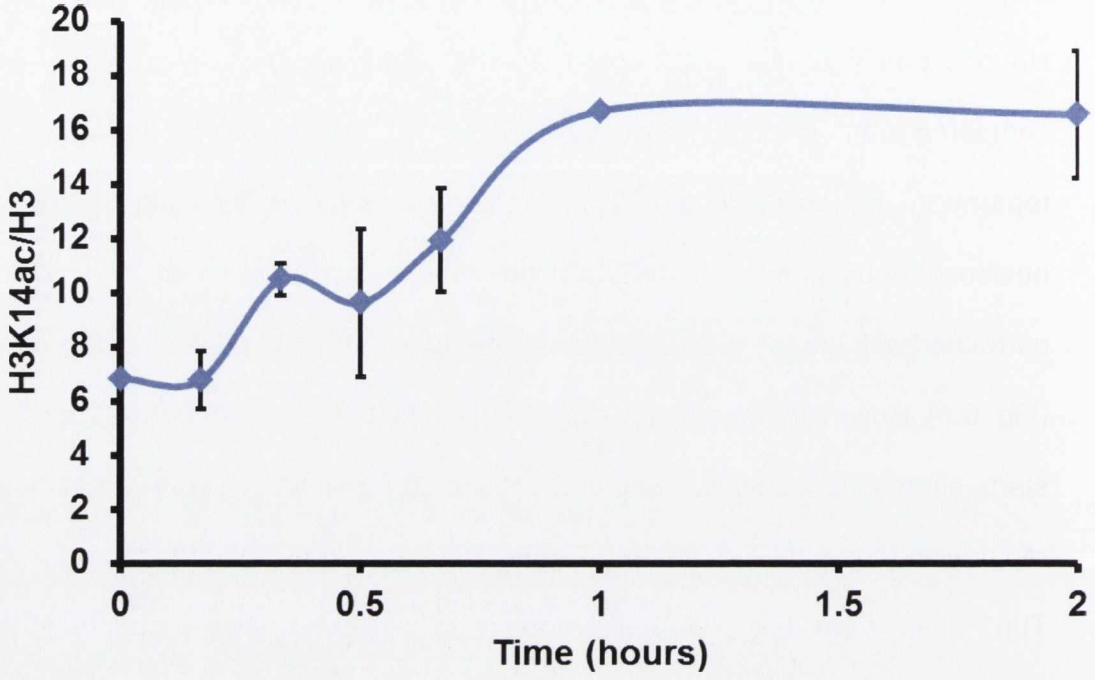

Figure 6.7. H3K14ac levels at the *SUC2* promoter increase rapidly upon addition of rapamycin. ChIP analysis of H3K14ac occupancy after the addition of rapamycin in an Ssn6-AA anchor away strain at the *SUC2* promoter. H3K14ac levels were normalised to an internal telomeric control and then to H3 occupancy at *SUC2*. Error bars represent standard error of the mean (SEM) from two independent experiments.

The data showed that H3K14ac levels at the *SUC2* promoter increased upon the addition of rapamycin to the Ssn6-AA anchor away strain (Fig. 6.7). The rate of increase was similar to that seen with H3 loss at the *SUC2* promoter, though H3K14ac levels did not increase until 10 minutes following rapamycin treatment, whereas H3 loss from the *SUC2* promoter occurred immediately (compare Fig. 6.6 and Fig. 6.6). However, the increase in H3K14ac levels preceded recruitment of Pol II to the *SUC2* ORF (Fig. 6.5B). This suggests that H3 was acetylated at the *SUC2* promoter after the promoter had been depleted of nucleosomes, but before transcription commenced (Fig. 6.8). Thus, the data suggests that loss of histones is not sufficient for initiation of transcription, but rather the acetylation of the depleted nucleosome template at the gene promoter may be a critical determinant for the de-repression of transcription.

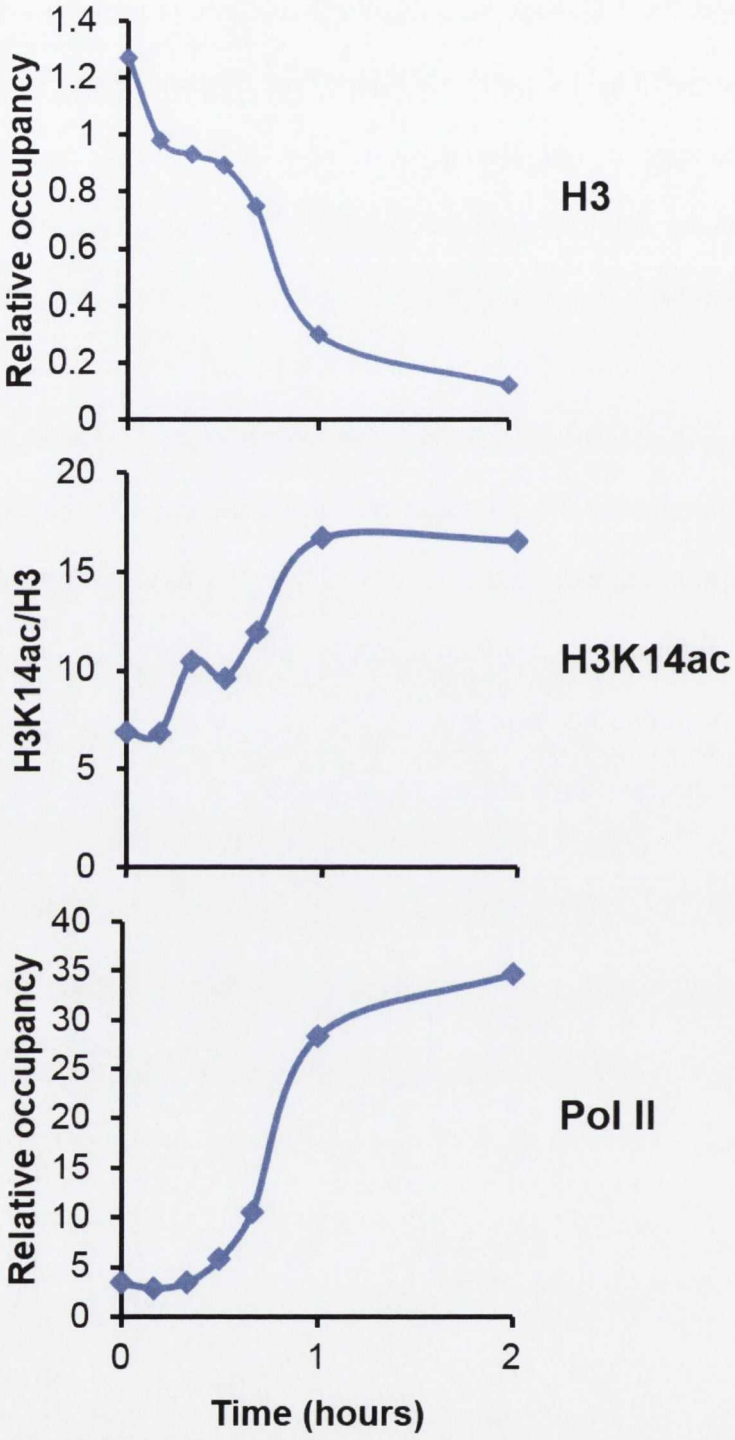

Figure 6.8. Summary of events occurring during anchor-away dependent *SUC2* de-repression. ChIP data for H3, H3K14ac and Pol II occupancy at the *SUC2* promoter following rapamycin treatment in Ssn6-AA. Data taken from Fig. 6.5, Fig. 6.6 and Fig. 6.7.

6.2.7. Analysis of *FLO1* regulation using the anchor away technique.

The data showing the Tup1-Ssn6 regulated *SUC2* gene was de-repressed in an Ssn6-AA strain upon the addition of rapamycin demonstrated that the anchor away technique was successfully functioning. I therefore next wanted to examine events at *FLO1* using the anchor away technique. This analysis also included an Ssn6 anchor away strain additionally deleted for the Ada2p and Sas3p HATs, since the aim was to analyse the impact of acetylation upon *FLO1* transcription.

6.2.7.1. *FLO1* is slowly de-repressed upon loss of Ssn6-FRB

Having established an anchor away time-course for de-repression of a Tup1-Ssn6-regulated gene using *SUC2* (Fig. 6.5-Fig. 6.7), it was decided to monitor de-repression of *FLO1* using the same conditions. Untagged (wild type) strains, and Ssn6-AA strains both with (Ssn6-AA) and without Ada2p and Sas3p (*ada2 sas3* Ssn6-AA) were first analysed for *FLO1* transcription by qPCR (Figure 6.9). It was predicted that the loss of Ada2p and Sas3p at *FLO1* would impair gene transcription. However, when *FLO1* transcription was monitored up to 2 hours, it was found that there was very little de-repression in any of the strains tested (Figure 6.9). The time-course was therefore extended to 12 hours, after which an *ssn6* mutant-level of *FLO1* de-repression was observed, indicating full *FLO1* transcription was reached by this time (compare Fig. 3.5, *ssn6* and Fig. 6.8, Ssn6-AA).

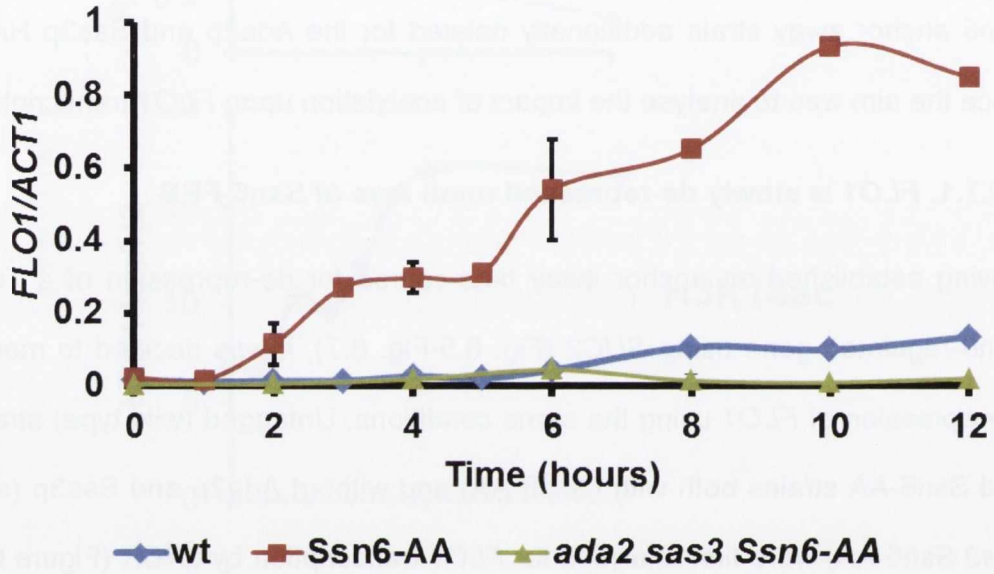

6.9. *FLO1* de-repression during Ssn6p Anchor-Away. Wild type (wt) and Ssn6-AA strains with (Ssn6-AA) and without Ada2p and Sas3p (*ada2 sas3* Ssn6-AA) were treated with rapamycin and *FLO1* transcription was analysed by qPCR. *FLO1* 5' ORF transcript levels were normalised to *ACT1* 5' ORF transcript levels. Error bars represent standard error of the mean (SEM) from up to three independent experiments.

In contrast to *SUC2, FLO1* transcript levels had barely risen by 2 hours post-rapamycin treatment (Fig. 6.9). At this time, *SUC2* transcript levels were at equivalent levels to those observed in an *ssn6* mutant (Fig. 6.5). Subsequent experiments confirmed that *FLO1* transcription did not approach levels observed in an *ssn6* mutant until 10 hours post-rapamycin treatment. This indicated either a much slower induction of *FLO1* transcription compared to *SUC2*, or a delay in the loss of Ssn6-FRB from the *FLO1* promoter.

Another striking result was observed in Ssn6 anchor away strain additionally deleted for *ada2 sas3.* In this strain, even by the time the 12 hour time point, *FLO1* transcription was completely absent,. This suggests a reliance on Ada2p and Sas3p at *FLO1* for de-repression upon loss of Ssn6p, and supports previous data that showed Gcn5p-containing complexes and Sas3p were redundantly required for *FLO1* de-repression in a conventional *ssn6* deletion mutant (Fig. 5.1).

6.2.7.2. Rapamycin levels are sufficient to induce flocculation over long periods.

The unexpectedly-long *FLO1* transcription time-course was an interesting result. However, it raised questions about the ability of rapamycin to remain active in the growth medium over such a long time. In order to test this, the supernatant from culture medium from a completed anchor away experiment that rapamycin had been added to 12 hours previously was used to re-treat fresh cells.

Growth medium was harvested after a completed 12 h anchor away time-course and supplemented with glucose to a final concentration of 2 %. If the rapamycin that remained in this 'spent' medium was still sufficient to anchor away Ssn6-FRB, then we expected fresh untreated Ssn6-AA cells to be flocculent after

growth in this 'spent' medium overnight. As a control, medium not containing rapamycin was also used (Figure 6.10)

When grown in medium that was used for a previous anchor away experiment that contained rapamycin, the Ssn6-AA strain was highly flocculent (Fig. 6.10, Ssn6-AA Rap+). However, when grown in medium without rapamycin, an Ssn6-AA strain does not flocculate (Fig. 6.10, Ssn6-AA Rap-). . As a control, a non FRB-tagged control strain (wt) does not display a flocculent phenotype (Fig. 6.10, wt) when grown in medium with or without rapamycin,.

These data suggest that even after medium containing rapamycin has been used in a 12 hour anchor away experiment, this same medium can be used to induce flocculation in an Ssn6-AA strain. This means that the rapamycin introduced to media in anchor away experiments is stable and remains active throughout a 12 hour-long time course.

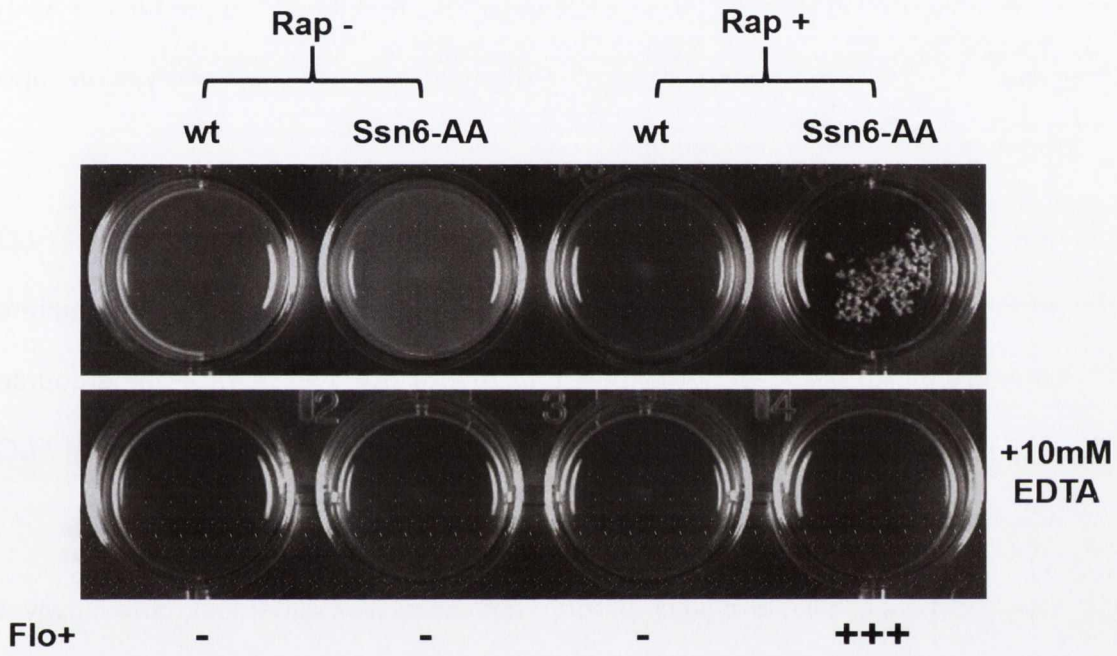

Figure 6.10. Rapamycin-treated cells exhibit a flocculent phenotype. Flocculation assay performed on strains without (wt) and with an FRB-tagged Ssn6p (Ssn6-AA). Cells previously grown to log phase in the absence of rapamycin were washed, and resuspended in medium with rapamycin (Rap+) and without (Rap-) that had been previously used to perform an anchor away experiment, and grown for a further 12 hours (overnight). Cells were treated with EDTA to disperse flocs. Strains were also scored for flocculation (Flo+), with non-flocculent strains being denoted by a "-"and flocculent strains being denoted by a "+++".

6.2.7.3. Tup1p is rapidly lost from the *FLO1* promoter upon addition of rapamycin

The previous experiments confirmed that the anchor away technique was successful. However, the time-course required for full *FLO1* de-repression was much longer than the time course required for full *SUC2* de-repression (Fig. 6.9). I therefore next monitored the kinetics of various events during the anchor away-induced *FLO1* de-repression and examined the role of acetylation upon regulation of *FLO1* transcription.

The data in figure 6.2 confirmed that Ssn6-FRB was present at the *FLO1* promoter in the absence of rapamycin. Addition of rapamycin to Ssn6-AA cultures caused de-repression of both *FLO1* and *SUC2*, but over different time-courses (Fig. 6.5 and Fig. 6.9). However, the reason for the slow de-repression of *FLO1* was unknown, and was therefore investigated.

The first possibility examined was that Tup1-Ssn6 was either lost more slowly, or was only partially lost from the *FLO1* promoter upon addition of rapamycin to Ssn6-AA strains. To test this, Tup1p loss from the *FLO1* promoter was monitored over time by ChIP in wild type Ssn6-anchor-away strains (Figure 6.11). If slow loss or partial retention of Tup1-Ssn6 at the *FLO1* promoter was responsible for the delayed de-repression of *FLO1,* it was expected that Tup1p levels would either fall more slowly over time, or would not fall completely. The loss of Tup1p from the *FLO1* promoter in the *ada2 sas3* Ssn6-AA strain, which does not show *FLO1* de-repression upon addition of rapamycin, (Fig. 6.9), was also investigated

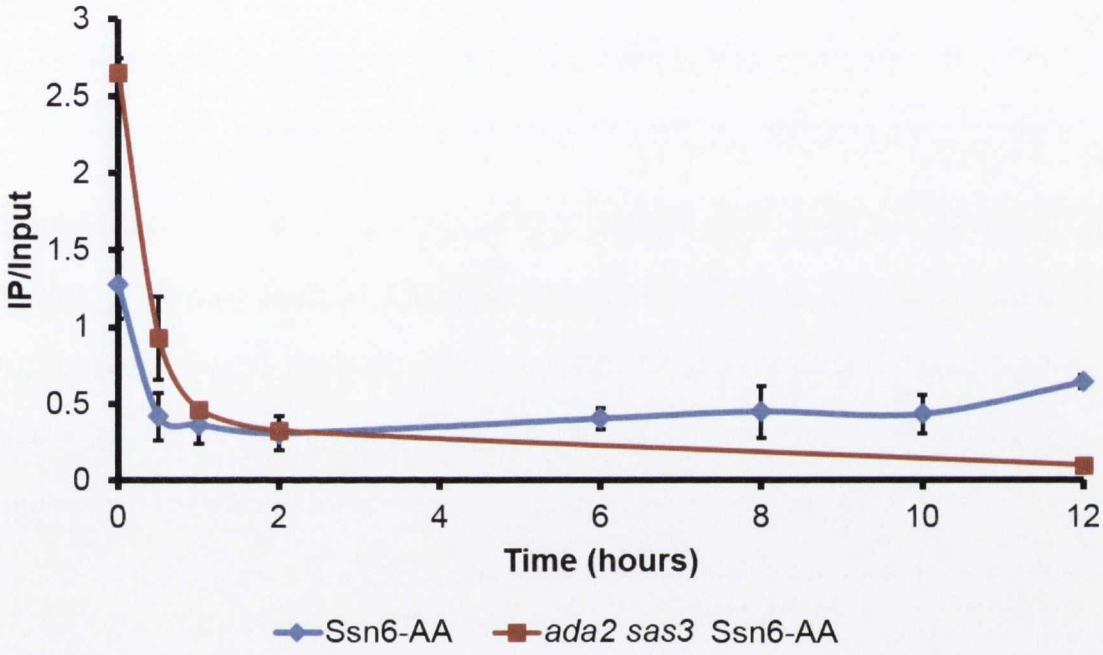

Figure 6.11. Tup1p loss from the *FLO1* promoter during Ssn6p anchor away. ChIP analysis of Tup1p occupancy in the Ssn6-anchor-away strain (Ssn6-AA) and in the *ada2 sas3* double mutant in an Ssn6-AA background (*ada2 sas3* Ssn6-AA). Tup1p occupancy at the Tup1-Ssn6 binding site (-585bp) of *FLO1* was measured using IP/Input. Error bars represent standard error of the mean (SEM) from 2-3 independent experiments.

Upon the addition of rapamycin to Ssn6-AA strains, Tup1p was lost rapidly from the *FLO1* promoter (Fig. 6.11). Maximum depletion occurred by 60 minutes post-rapamycin treatment and was to the same extent as Tup1p occupancy at the IntV negative control region suggesting Tup1 depletion at this time point was complete (Fig. 6.2A). Tup1p remained absent from the *FLO1* promoter until 10 hours post-rapamycin treatment, although by 12 hours low levels of Tup1p could be detected at *FLO1.* This suggests that the slow *FLO1* de-repression is not due to the slow loss or partial retention of Tup1-Ssn6 at the gene promoter.

Although *SUC2* was used previously as a control for the anchor away technique, loss of Tup1p (or Ssn6-Flag, AF personal communication) from *SUC2* could not be assayed since no Tup1p ChIP signal can be detected at the repressed *SUC2* promoter The hypothesis is that epitope masking may be the cause of the lack of a Tup1p ChIP signal at the repressed *SUC2* gene due to chromatin structure or the presence of additional factors at this site.

In the *ada2 sas3* mutants, Tup1p levels were initially higher than in the Ssn6-AA strain, but Tup1p was also lost as rapidly as in the Ssn6-AA wt strain (Fig. 6.11). In this strain, Tup1p levels at the *FLO1* promoter remained depleted at 12 hours following rapamycin treatment. This suggests that in this mutant, there is a lack of *FLO1* de-repression despite the absence of the co-repressor.

These data suggest that the loss of Tup1-Ssn6 from the *FLO1* promoter is not sufficient for *FLO1* de-repression, as mutants lacking Ada2p and Sas3p which do not transcribe *FLO1* also show rapid Tup1p loss from the *FLO1* promoter. I therefore decided to monitor other factors that may be required for *FLO1* de-repression in the absence of Tup1-Ssn6.

6.2.7.4. H3 is lost rapidly at the *FLO1* promoter following Tup1-Ssn6 depletion.

Previous analyses indicated that while *SUC2* was rapidly de-repressed in Ssn6-AA strains upon the addition of rapamycin (Fig. 6.5), *FLO1* was de-repressed much more slowly (Fig. 6.9). This slow *FLO1* de-repression was not due to retention of Tup1-Ssn6 at the *FLO1* promoter, as in both wild type and *ada2 sas3* mutant Ssn6-AA strains Tup1p was lost rapidly and fully from the *FLO1* promoter upon addition of rapamycin (Fig. 6.11).

Swi-Snf has been shown to be required for de-repression of Tup1-Ssn6 regulated genes, where it remodels the nucleosomal array upstream of *FLO1* that is considered a barrier to gene transcription (Fleming and Pennings, 2001). If nucleosomes were lost more slowly at *FLO1* than at *SUC2*, then this could explain the slow *FLO1* de-repression observed upon addition of rapamycin to Ssn6-AA strains. To determine whether a slower loss of histones from the *FLO1* promoter caused the delayed *FLO1* derepression, an H3 ChIP was carried out in wild type strains following rapamycin addition. This experiment was also repeated in *ada2 sas3* Ssn6-AA strains to determine the impact of histone H3 acetylation on this process (Figure 6.12)

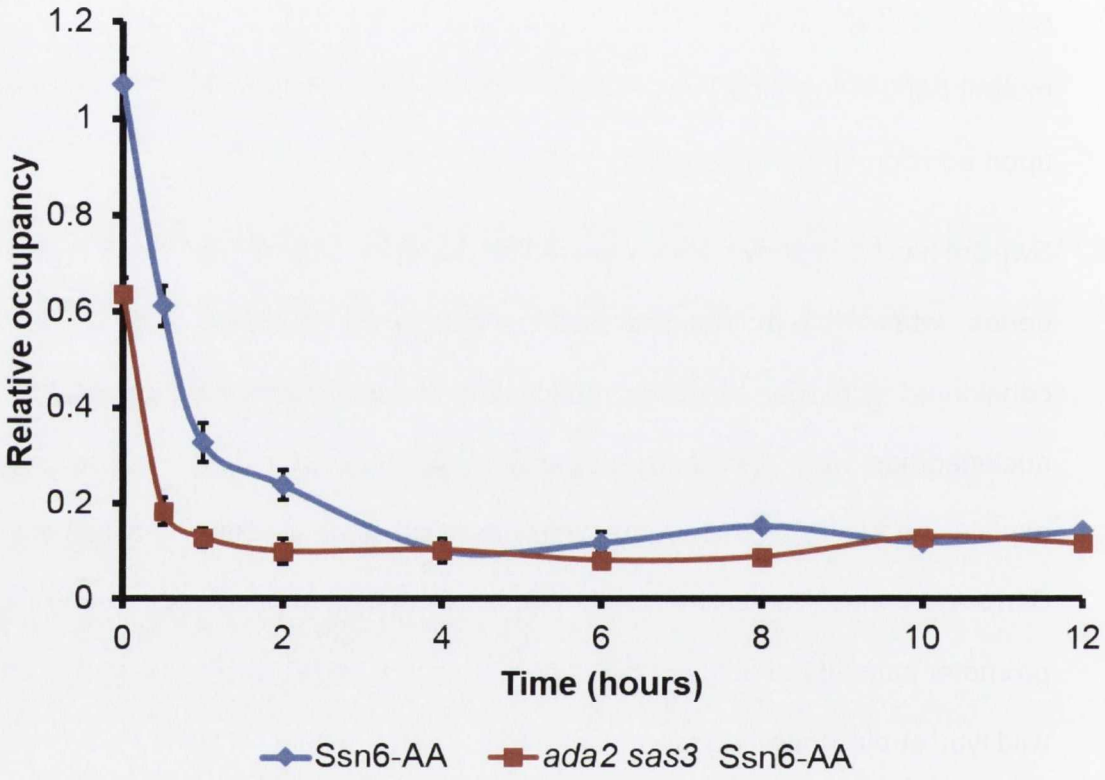

Figure 6.12. H3 loss at the *FLO1* promoter during Ssn6p anchor away. H3 ChIP in in the Ssn6-anchor-away strain (Ssn6-AA) and in the *ada2 sas3* double mutant in an Ssn6-AA background (*ada2 sas3* Ssn6-AA). H3 levels were measured over time at the *FLO1* promoter (-585bp) and were normalised to H3 levels at an intergenic region of chromosome V. Error bars represent standard error of the mean (SEM) from two independent experiments.

In wild type Ssn6-AA strains, where *FLO1* was slowly transcribed upon loss of Ssn6p, there was a rapid loss of H3 at the *FLO1* promoter (Fig. 6.12) This loss of H3 began immediately after the addition of rapamycin to this strain. By 1 hour, H3 levels were almost equivalent to levels in an *ssn6* mutant, although by this time point, *FLO1* transcription was not detectable (compare Fig. 6.12, wt and Fig. 6.9, Ssn6-AA). This H3 loss indicates that the slow *FLO1* de-repression observed previously was not due to the slow or partial loss of nucleosomes from the *FLO1* promoter.

Previous data from Chapter 3 indicated that loss of H3 was not sufficient for *FLO1* transcription, as *ada2 sas3 ssn6* mutants showed dramatic H3 loss at the *FLO1* promoter, despite very low *FLO1* transcription (Fig. 5.1 and 5.2). The kinetic analysis data shown here confirmed that although *FLO1* was not transcribed in an *ada2 sas3* double mutant lacking Ssn6p (either *ada2 sas3 ssn6 or ada2 sas3* in Ssn6-AA with rapamycin), there was still a rapid and dramatic loss of H3 at the *FLO1* promoter (Fig 6.12 *ada2 sas3* Ssn6-AA). This indicates that the presence of Ada2p and Sas3p, while essential for *FLO1* de-repression in the absence of Ssn6p, have no impact on the eviction of nucleosomes from the *FLO1* promoter. Taken together, these data show that H3 loss at the *FLO1* promoter occurrs before the initiation of *FLO1* transcription, but is not a pre-requisite for *FLO1* de-repression.

6.2.7.5. Snf2p recruitment to the *FLO1* promoter occurs in the absence of *FLO1* transcription.

The previous data had shown that H3 occupancy at the *FLO1* promoter was rapidly and dramatically reduced in both wild type and *ada2 sas3* anchor away strains following incubation with rapamycin. This histone loss was hypothesised

to be the result of remodelling activity by Swi-Snf, as this ATP-dependent remodelling complex is known to be involved in nucleosome remodelling at the *FLO1* promoter (Fleming and Pennings, 2001). To investigate this, Snf2p occupancy of the *FLO1* promoter was analysed by ChIP in wild type and *ada2 sas3* anchor away strains (Figure 6.13). It was expected that Snf2p levels would rise quickly post-rapamycin treatment in these strains.

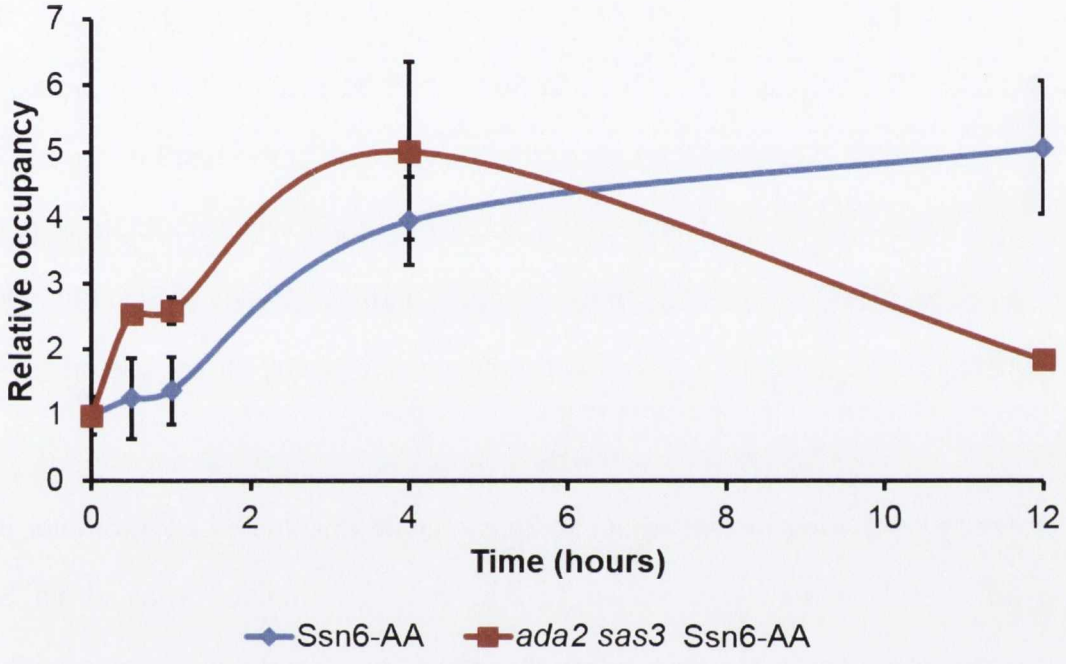

Figure 6.13. Snf2p occupancy of the *FLO1* promoter. Snf2p ChIP in the Ssn6-anchor-away strain (Ssn6-AA) and in the *ada2 sas3* double mutant in an Ssn6-AA background (*ada2 sas3* Ssn6-AA). Snf2p levels were measured over time at the *FLO1* promoter (-585bp) and were normalised to Snf2p levels at an intergenic region of chromosome V and further normalised to Snf2p levels at time 0 for each strain. Error bars represent standard error of the mean (SEM) from 2-3 independent experiments.

Following rapamycin treatment, Snf2p occupancy at the *FLO1* promoter was detected at low levels within 30 minutes in wt Ssn6-AA strains (Fig. 6.13, Ssn6-AA). Snf2p levels peaked at 4 hours following rapamycin treatment, and a similar level of Snf2p was detected at the *FLO1* promoter at 12 hours post-rapamycin treatment.

In an Ssn6-AA strain lacking Ada2p and Sas3p (*ada2 sas3* Ssn6 AA), Snf2p levels followed a similar pattern to that in the wt strain containing Ada2p and Sas3p at the *FLO1* promoter rose more rapidly than in the Ssn6-AA strain, while also reaching maximum levels by 4 hours post-rapamycin treatment (Fig. 6.13, *ada2 sas3* Ssn6-AA). However the level of Snf2p occupancy at *FLO1* then fell by 12 hours post-rapamycin treatment in the anchor away strain deleted for *ada2* and *sas3*.

These data suggest that while Snf2p recruitment to the *FLO1* promoter in the *ada2 sas3* mutant was similar to that in the wt anchor away strain Snf2p occupancy was less stable in the absence of ada2 and sas3. . Importantly this timeline of Snf2p recruitment in both strains correlated with H3 loss at the *FLO1* promoter, with maximum Snf2p levels and minimum H3 levels observed in both strains by 4 hours post-rapamycin treatment (compare Fig. 6.12 and Fig. 6.13).

6.2.7.6. H3K14ac levels increase rapidly at the *FLO1* promoter upon addition of rapamycin to Ssn6-AA strains.

Despite the rapid loss of Tup1p and H3 following the addition of rapamycin in Ssn6-AA strains, a slow *FLO1* de-repression was observed in wild type strains (Fig. 6.9). In Ssn6-AA strains lacking Ada2p and Sas3p (*ada2 sas3*), no *FLO1* transcription was detected, despite the rapid loss of H3 and Tup1p upon addition

of rapamycin (Fig. 6.12, Ssn6-AA and *ada2 sas3* Ssn6-AA). This suggests the loss of H3 is not sufficient for *FLO1* transcription (Fig. 5.1 and 6.9).

Ada2p and Sas3p acetylate H3K14, and in the absence of these HATs this mark is abolished at the *FLO1* promoter and *FLO1* transcription is absent (Fig. 5.1). With this in mind, it was decided to monitor H3K14ac occupancy at the *FLO1* promoter. We hypothesised that firstly, H3K14ac levels would correlate to *FLO1* transcription in the Ssn6-AA strain and secondly, H3K14ac would be absent in the *ada2 sas3* Ssn6-AA strain due to the lack of HATs that acetylate H3K14. To test this, ChIP was carried out on both Ssn6-AA and *ada2 sas3* Ssn6-FRB (*ada2 sas3* Ssn6-AA) strains that were treated with rapamycin to induce loss of Ssn6-FRB from the cell nucleus (Fig. 6.14).

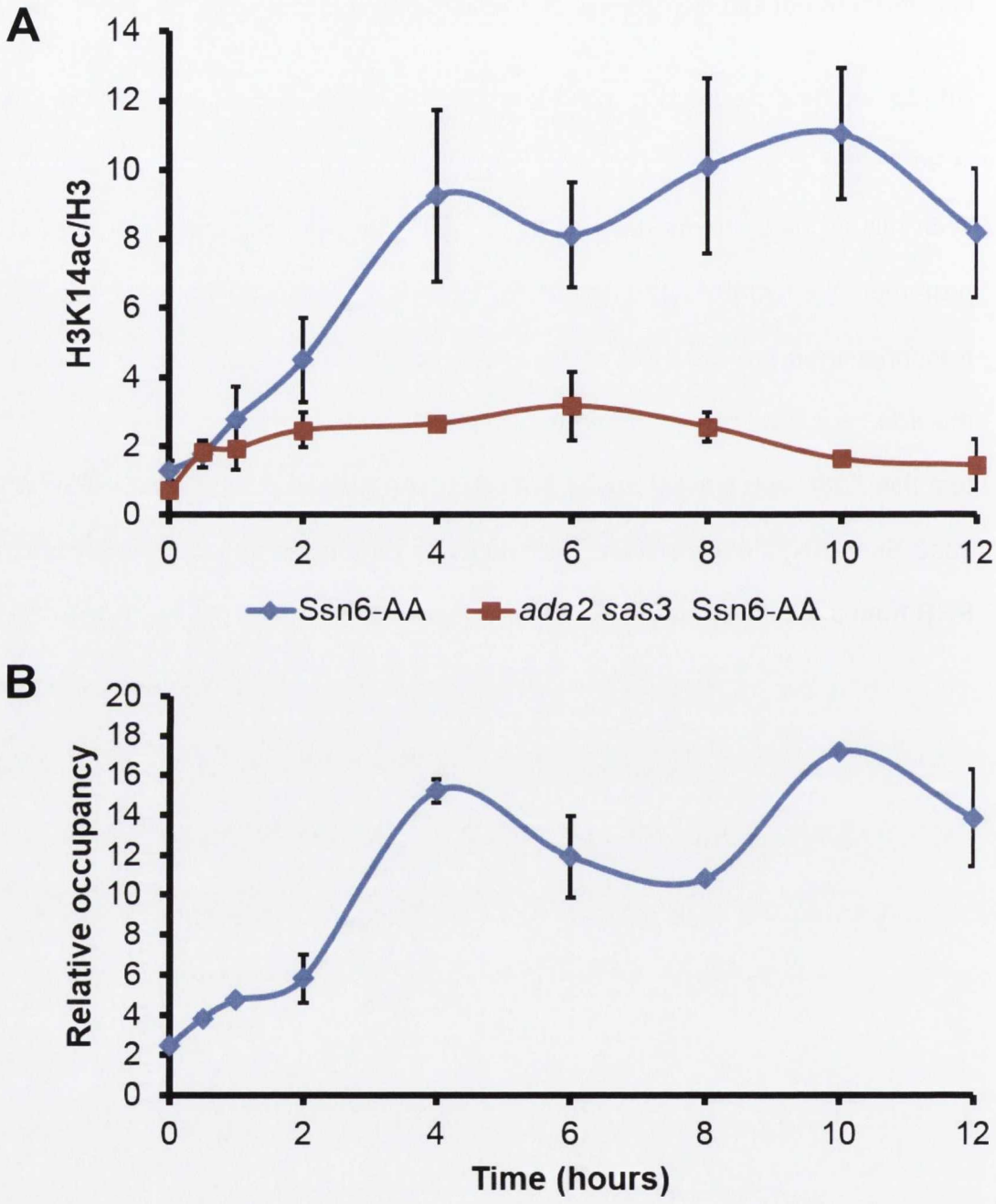
A
H3K14ac/H3
0
2
4
6
8
10
12
14
0
2
4
6
8
10
12
Ssn6-AA
ada2 sas3 Ssn6-AA
B
Relative occupancy
0
2
4
6
8
10
12
14
16
18
20
0
2
4
6
8
10
12
Time (hours)

Figure 6.14. H3K14ac at the *FLO1* promoter. (A) H3K14ac ChIP in the Ssn6-anchor-away strain (Ssn6-AA) and in the *ada2 sas3* double mutant in an Ssn6-AA background (*ada2 sas3* Ssn6-AA). H3K14ac levels were measured over time at the *FLO1* promoter (-585bp) and were normalised to H3 levels at *FLO1*. (B) H3K14ac ChIP in FRB-tagged Ssn6p strain. H3K14ac levels were measured over time at the *FLO1* promoter (-585bp) and were normalised to a telomeric control region and also to H3 levels at *FLO1*. Error bars represent standard error of the mean (SEM) from 2-3 independent experiments.

In Ssn6-AA strains where *FLO1* is slowly de-repressed upon loss of Ssn6-FRB from the cell nucleus, H3K14ac levels rise almost immediately following rapamycin treatment (Fig. 6.14A). H3K14ac levels peak at the 4 hour time-point, but show a reproducible drop at 6 hours, only to rise again at 8 hours. H3K14ac levels drop once again after 8 hours and remain low at the 12 hour time-point.

In *ada2 sas3* strains, where *FLO1* is not transcribed upon loss of Ssn6-FRB, there was no significant H3K14ac occupancy detected at the *FLO1* promoter, in line with previous data that showed this mark is abolished globally in the absence of Ada2p and Sas3p (Fig. 5.6).

Because an *ada2 sas3* mutant abolishes global H3K14ac levels, when performing H3K14ac ChIP experiments involving this strain, the H3K14ac levels are not internally normalised . This is to avoid introducing large errors into the data that normalising to very low levels of acetylation at an internal site would cause. However, when the H3K14ac occupancy data set solely from the Ssn6-AA strain (Fig. 6.14A, Ssn6-AA) at the *FLO1* promoter are internally normalised , the loss of H3K14ac after 4 hours post-rapamycin treatment (Fig. 6.14B) appears much more robust. This suggests that the twin peaks pattern of H3K14ac observed at the *FLO1* promoter over time following depletion of ssn6 is significant. .

In summary, these data suggest that H3K14ac occupancy at the *FLO1* promoter is required before *FLO1* transcription can take place and also reveals H3K14ac levels fluctuate over the time period leading to *FLO1* de-repression.

6.2.7.7. RNA Polymerase II (RNAP II) occupancy at the *FLO1* 5' ORF is dependent on the presence of H3K14ac

H3K14ac at the *FLO1* promoter has been shown to correlate with *FLO1* transcription, and loss of Ada2p and Sas3p was shown to severely inhibit *FLO1* de-repression in an *ssn6* mutant (Fig. 5.4, *ada2 sas3 ssn6* and Fig. 5.1, *ada2 sas3 ssn6*). In addition, H3K14ac at the *FLO1* promoter also increased rapidly following addition of rapamycin to an Ssn6-AA strain (Fig. 6.14). We therefore hypothesised that H3K14ac may be required for recruitment of RNA Pol II to the *FLO1* ORF in the absence of Tup1-Ssn6. To test this, RNA Pol II occupancy at the *FLO1* 5' ORF was monitored by ChIP analysis before and during growth in rapamycin in strains both containing (Ssn6-AA) and lacking Ada2p and Sas3p (*ada2 sas3* Ssn6-AA) (Fig. 6.15). The hypothesis would predict Pol II occupancy would correlate with H3K14ac occupancy following rapamycin addition, whereas Pol II would be absent in the similarly-treated *ada2 sas3* anchor away strains.

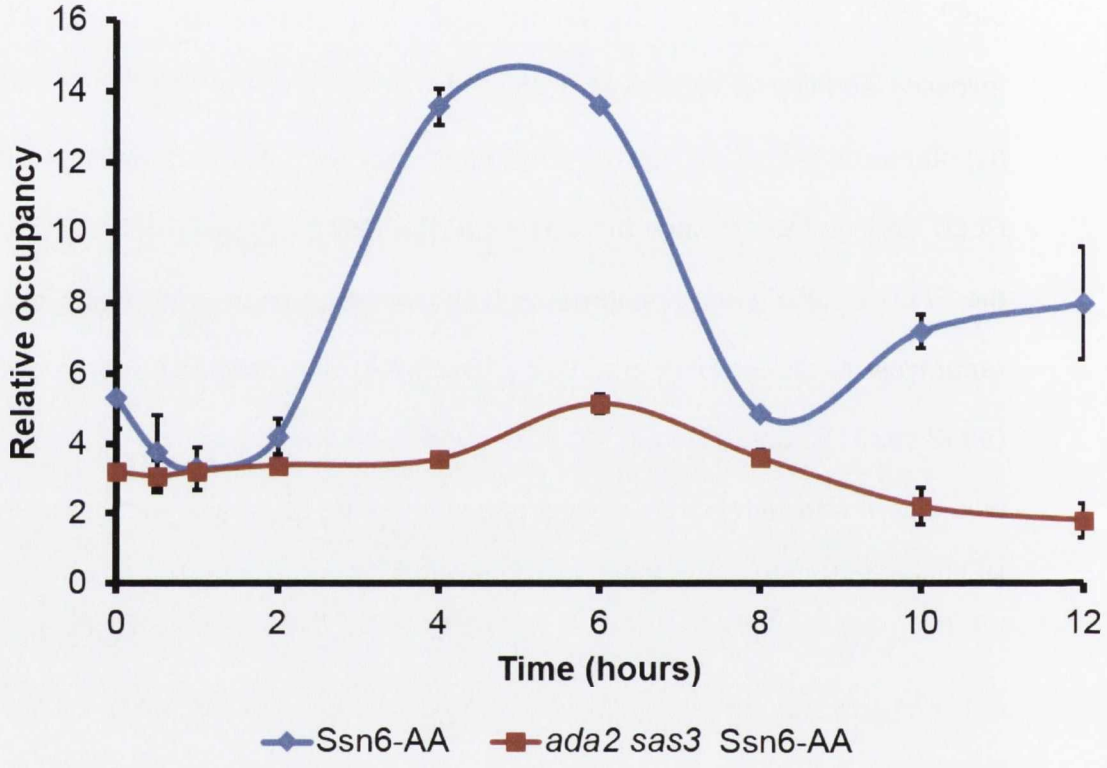

Figure 6.15. RNA Polymerase II occupancy at the *FLO1* 5' ORF. RNA Polymerase II (Pol II) ChIP in the Ssn6-anchor-away strain (Ssn6-AA) and in the *ada2 sas3* double mutant in an Ssn6-AA background (*ada2 sas3* Ssn6-AA). Pol II levels were measured over time at the *FLO1* 5' ORF and normalised to Pol II levels at a telomeric control region. Error bars represent standard error of the mean (SEM) from 2-3 independent experiments.

In Ssn6-AA strains that contain both Ada2p and Sas3p (Ssn6 AA), Pol II levels at the *FLO1* ORF were low before the addition of rapamycin, consistent with *FLO1* transcription being off (Fig. 6.15, Ssn6-AA). However, following addition of rapamycin, Pol II levels fall slightly before increasing to a level at 4 hours which is similar to that in a conventional *ssn6* deletion mutant (compare Fig. 6.15, Ssn6-AA and Fig. S1, *ssn6*). Interestingly however, this level of Pol II occupancy is only maintained until 6 hours post-rapamycin treatment, after which RNAP II levels fall dramatically by 8 hours. However, after this time point, Pol II levels at the *FLO1* 5' ORF again begin to rise.

In Ssn6-AA strains lacking Ada2p and Sas3p (*ada2 sas3*), there was no significant increase in Pol II occupancy across the entire time course (Fig. 6.15A, *ada2 sas3*). This suggests that in strains lacking Ada2p and Sas3p, Pol II is not recruited to the *FLO1* ORF and transcription cannot take place.

6.2.7.8. RNA Polymerase II levels oscillate most dramatically at *FLO1*.

The fluctuation in Pol II occupancy at *FLO1* observed in the Ssn6-AA strain following rapamycin treatment was interesting, but it was unknown whether this loss of Pol II after 6 hours was unique to *FLO1* or was a more general phenomenon. To investigate this, Pol II occupancy was also analysed by ChIP at the 5' ORFs of (i) *SUC2*, which is another Tup1-Ssn6 regulated gene; (ii) *PMA1*, which is a highly transcribed gene during exponential growth (Rao et al., 1993) and (iii) *BAP2*, which is a constitutively transcribed gene in rich medium (Didion et al., 1996)(Fig. 6.15B).

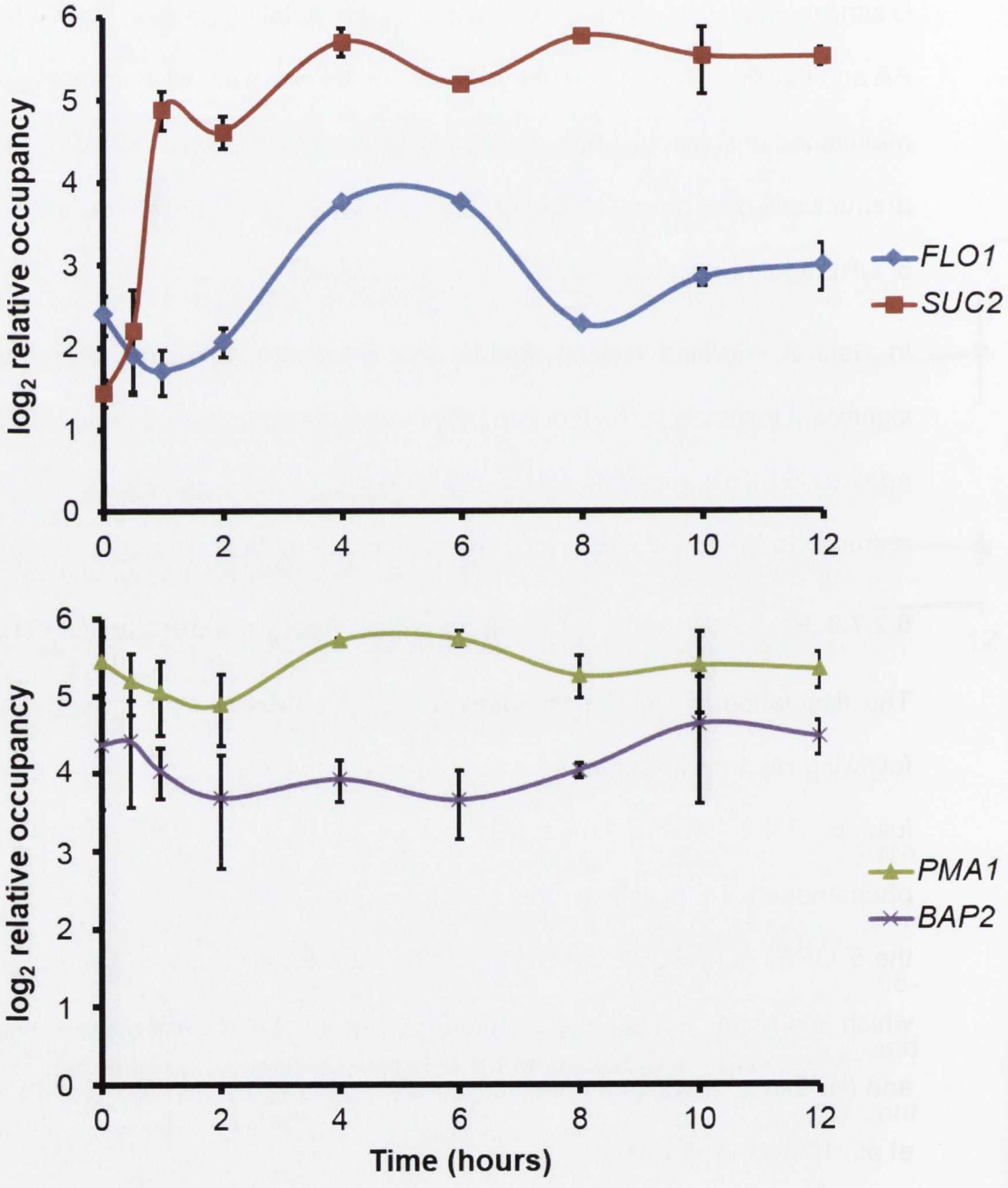
log2 relative occupancy
0
1
2
3
4
5
6
0
2
4
6
8
10
12
FLO1
SUC2
log2 relative occupancy
PMA1
BAP2
Time (hours)

Fig 6.16. RNA Polymerase II occupancy at the *SUC2*, *FLO1, PMA1* and *BAP2* 5' ORFs. Pol II occupancy was analysed at the *SUC2* vs *FLO1* 5' ORFs, and *PMA1* vs *BAP2* 5' ORFs using a $\log_2$ scale. *FLO1* data is from Fig. 6.15 (Ssn6-AA). Pol II levels at the ORFs of interest were normalised to Pol II levels at a telomeric control region. Error bars represent standard error of the mean (SEM) from 2-3 independent experiments.

The data showed that Pol II levels at the *SUC2* ORF were low in the absence of rapamycin but had risen 5-fold by 60 min post-rapamycin addition (Fig. 6.16, *SUC2*). High Pol II occupancy was then detected throughout the remaining time-course but did show some fluctuation in levels However, the fluctuation in SUC2 Pol II occupancy levels was not as dramatic as that seen at *FLO1* (Fig 6.16, compare *FLO1* and *SUC2* levels).

PMA1 transcription was not affected by Tup1-Ssn6, and Pol II occupancy at this constitutively active gene was high throughout the time-course (Fig. 6.16, *PMA1*). There was a slight increase in Pol II occupancy at *PMA1* between 4 and 6 hours following rapamycin treatment, though this was also relatively minor. The actively transcribed *BAP2* gene also displayed relatively consistently high Pol II occupancy throughout the time-course (Fig. 6.16, *BAP2*). These data suggest that the pattern of Pol II occupancy at *FLO1* following Ssn6 depletion is not observed at all genes or even at all Tup1-Ssn6 regulated genes.

Together, these data indicate that Pol II occupancy at the *FLO1* ORF is dependent on Ada2p and Sas3p, as Pol II is absent from the *FLO1* ORF in a strain lacking these HATs and subsequently no de-repression of *FLO1* transcription occurs. In strains that contain these factors (Ssn6-AA), Pol II levels oscillate whereby Pol II reaches maximum levels by 4 hours, which is also the time that H3K14ac levels at the *FLO1* promoter are at their highest (Compare Fig. 6.14, Ssn6-AA and Fig 6.15,Ssn6-AA). H3K14ac levels at *FLO1* fall at 6 hours, which corresponds to a drop in Pol II occupancy at *FLO1* after this time. This indicates that Pol II may be dependent on H3K14ac at the *FLO1* promoter for recruitment to the *FLO1* ORF, and loss of this modification abolishes the ability of Pol II to transcribe *FLO1* in the absence of Ssn6-FRB.

Based on this analysis, the sequence of events leading up to *FLO1* de-repression can be described. Upon addition of rapamycin to Ssn6-AA strains, Tup1p loss begins immediately and is at minimal levels by 1 hour post rapamycin treatment (Fig. 6.17, Tup1p). This loss is accompanied by rapid loss of H3 from the *FLO1* gene promoter, which begins almost immediately, and reaches its lowest extent by 4 hours post-rapamycin treatment (Fig. 6.17, H3). Snf2p is recruited to the *FLO1* promoter rapidly, but does not reach its greatest occupancy level upon 4 hours post rapamycin addition (Fig. 6.17, Snf2p). H3K14ac levels at *FLO1* rise rapidly following loss of Tup1-Ssn6 from the promoter, and these peak at 4 hours post rapamycin treatment, only to fall slightly at 6 hours, before peaking again at 8 hours and finally falling again at 10 and 12 hours post rapamycin. Pol II is not recruited to *FLO1* until 4 hours post-rapamycin treatment, and is the last factor in this analysis to occupy *FLO1* (Fig. 6.17, Pol II). Pol II levels remainstable until 6 hours after which they drop to time 0 levels at 8 hours. Pol II levels then begin to rise again slightly at 10 hours and 12 hours post-rapamycin addition. After H3 loss reaches its greatest extent at 4 hours, H3 levels do not recover in the absence of Tup1-Ssn6. Tup1p loss follows a similar pattern. Snf2p occupancy of the *FLO1* promoter is also constant after it reaches its greatest extent at 4 hours, indicating that Swi-Snf continually remodels the *FLO1* promoter in the absence of Tup1-Ssn6.

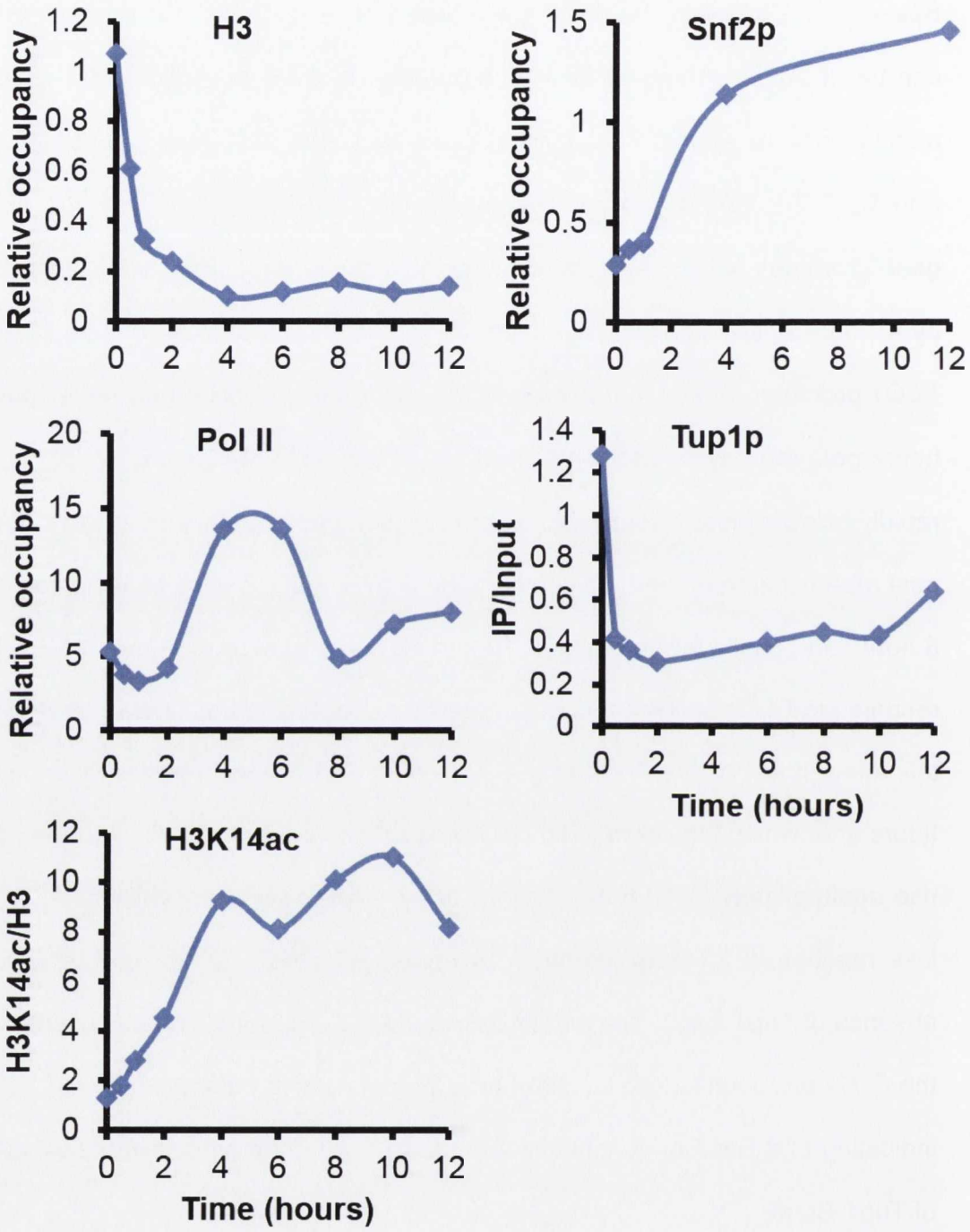

Figure 6.17. Schematic of *FLO1* de-repression in wild type Ssn6-AA cells. ChIP data for H3, H3K14ac, Tup1p, Snf2p and Pol II occupancy at the *FLO1* promoter in the wild type anchor away strain taken from Fig. 6.11, Fig. 6.12, Fig. 6.13, Fig. 6.14 and Fig. 6.15.

6.2.7.10. *FLO1* transcription may be related to cell metabolism

The data in this chapter suggest that upon loss of Ssn6p from the *FLO1* promoter, *FLO1* mRNA accumulates slowly, only reaching *ssn6* mutant levels at 10 hours post-rapamycin treatment (Fig. 6.8). This is in contrast to the relatively rapid *SUC2* induction observed in the same strain (Fig. 6.2). Pol II recruitment to the *FLO1* ORF appears to be dependent on H3K14ac levels at the *FLO1* promoter (Fig. 6.14 and Fig. 6.15). Considering it had been previously shown that global acetylation levels in yeast were linked to cellular metabolism and glucose availability (Friis et al., 2009), and due to the extended time period over which *FLO1* is de-repressed in the anchor-away experiment it was decided to monitor growth and glucose utilisation of Ssn6-AA cells during the anchor-away time course. The aim was to determine how the H3K14ac and Pol II levels at *FLO1* correlated with cell growth over our anchor away time course.

Figure 6.18. Cell growth upon loss of Ssn6-FRB. Optical density (OD_{600}) and glucose readings from cultures grown as part of an anchor away experiment. Error bars represent standard error of the mean (SEM) from three independent experiments.

Ssn6-AA strains are in log phase when rapamycin is added to the growth medium, and continue to grow exponentially until 6 hours post-rapamycin treatment (Fig. 6.18, OD_{600}). After this time point, growth slows down. This slower growth correlates to a drop in H3K14ac at the *FLO1* promoter, and occurs before Pol II levels at the *FLO1* ORF drop dramatically (Fig. 6.16, compare H3K14ac and Pol II).

Glucose levels in Ssn6-AA cultures decrease steadily from approximately 1.6% upon addition of rapamycin to about 0.2% at the 6 hour time-point (Fig. 6.18, Glucose). Glucose is completely expended by 8 hours post-rapamycin treatment, which correlates to the slow increase in optical density after this time.

Together, the data in this chapter show a correlation between cellular growth and *FLO1* ORF Pol II and H3K14ac occupancy, in which levels of Pol II and H3K14ac oscillate at the *FLO1* ORF in response to changes in cell growth. . These changing H3K14ac levels may be linked to glucose availability or cell density and may signal cells to transcribe *FLO1* in response to stress.

6.3. Discussion

In previous chapters the importance of Gcn5p-containing complexes and Sas3p in *FLO1* de-repression in the absence of Ssn6p were identified (Fig. 5.1). The impact of an *ssn6* mutant on histone occupancy and acetylation upstream of the *FLO1* promoter was also investigated, with the conclusion that nucleosome eviction may be necessary for *FLO1* de-repression but was not sufficient (Fig. 5.2, *ada2 sas3 ssn6*). To monitor the events that lead to *FLO1* de-repression in an *ssn6* mutant, a kinetic analysis was required. This analysis had the added advantage of allowing observation of cells that had lost Ssn6p from the cell nucleus, rather than of multiple generations of *ssn6* mutants which may have developed compensatory mechanisms.

The first experiments to be performed on the newly-constructed Ssn6-AA strains were to verify that Ssn6-FRBwas expressed and that Tup1-Ssn6 could be detected at the Flo1 promoter in the anchor-away strain. Western blot analysis confirmed that Ssn6-FRB was expressed, and ChIP analysis of Tup1p confirmed occupancy of the Tup1-Ssn6 complex at the *FLO1* promoter in an Ssn6-AA strain (Fig. 6.2).

Next, it was decided to monitor loss of fluorescently-labelled Ssn6-FRB from cell nuclei by microscopy. It was found that in the absence of rapamycin, Ssn6-FRB overlapped with DAPI-stained DNA in the cell nucleus (Fig. 6.3, Rap-). However, in the presence of rapamycin, Ssn6-FRB moved toward the cell periphery and aggregated in granules (Fig. 6.3, Rap+). Another interesting result was that when grown in the absence of rapamycin, well-defined nuclei could be observed in cells (Fig. 6.4, Rap-). However, when cells were grown in the presence of rapamycin, DAPI-stained DNA became more diffuse (Fig. 6.4, Rap+). This may indicate that

in the absence of Ssn6-FRB, genomic DNA is less well condensed, pointing to a role for Ssn6p in influencing higher-order chromatin architecture.

Having established that the anchor away technique was successful in depleting Ssn6-FRB from cell nuclei, a time-course had to be established in which to monitor gene de-repression upon loss of Ssn6 from gene promoters. As a guide, we used a time-course modelled on that used by Wong and Struhl, where Tup1p was the target and *SUC2* was the gene used to monitor de-repression over time. Using qPCR, it was found that *SUC2* was fully de-repressed to *ssn6* mutant levels by 60 minutes after the addition of rapamycin in an Ssn6-AA strain (compare Fig. 6.4A, Ssn6-AA and Fig. 3.6, *ssn6*). This de-repression was not observed in cells lacking an FRB-tagged Ssn6p. RNA Polymerase II occupancy at the *SUC2* 5' ORF was also monitored in Ssn6-AA strains following the addition of rapamycin, and Pol II occupancy reached maximum levels by 60 minutes, which correlated with *SUC2* transcription (Fig. 6.5B). H3 occupancy at the *SUC2* promoter was also monitored by ChIP, and it was found that H3 depletion started almost immediately following addition of rapamycin, and occurred before the arrival of Pol II (Fig. 6.6). H3K14ac at the *SUC2* promoter was similarly monitored and it was found that H3K14 was acetylated at the *SUC2* promoter rapidly following rapamycin addition (Fig. 6.7). This acetylation occurred in tandem with H3 loss from the *SUC2* promoter, but before the arrival of Pol II to the *SUC2* 5' ORF (Compare Fig. 6.5, 6.6 and 6.7).

Because Ada2p and Sas3p had been shown to be important factors in *FLO1* regulation, the relationship between these HATs and *FLO1* de-repression was to be further investigated by kinetic analysis. After a time course for gene de-repression had been empirically tested, *FLO1* transcription was monitored in

Ssn6-AA strains in which Ada2p and Sas3p were both present (Ssn6-AA) and absent (*ada2 sas3* Ssn6-AA), and also in a strain that did not contain FRB-tagged Ssn6p (wt).

Interestingly, in the Ssn6-AA strain, *FLO1* transcription did not reach maximum levels until 10 hours post-rapamycin treatment (Fig. 6.9, Ssn6-AA). In strains lacking an FRB-tagged Ssn6p and in the *ada2 sas3* mutant anchor away strains, no *FLO1* transcription was detected in the 12 hours post-rapamycin treatment (Fig. 6.9, wt and *ada2 sas3* Ssn6-AA). The very slow accumulation of *FLO1* transcripts following addition of rapamycin in an Ssn6p anchor away strain was unexpected. However, the absence of *FLO1* transcription in the *ada2 sas3* strain confirmed the requirement for Gcn5p-containing complexes and Sas3p in *FLO1* de-repression following loss of Tup1-Ssn6. Importantly, it was also confirmed that rapamycin in the growth medium retained the ability to induce the anchor away mechanism over the full 12 hour experiment (Fig. 6.10).

As stated, *FLO1* showed an unexpectedly long de-repression following addition of rapamycin to Ssn6-AA strains. To investigate if this was due to a slow loss of Tup1-Ssn6 from the *FLO1* promoter, ChIP analysis was carried out on Tup1p at the *FLO1* promoter following addition of rapamycin. It was found that Tup1p was rapidly lost from the *FLO1* promoter in Ssn6-AA strains, and the time-course for Tup1p loss from *FLO1* was in line with the *SUC2* transcription time course, with Tup1p being fully depleted by 60 minutes (Fig. 6.11, wt). However, Tup1p levels did appear to rise slightly in the Ssn6-AA strain at 12 hours post-rapamycin treatment, which may indicate that the anchor away technique has a time limit of efficiency. This is likely not due to a defect with the rapamycin in the growth medium, as even spent medium containing rapamycin was shown to induce

flocculation in fresh cultures (Fig. 6.10). Rather, the failure to export all FRB-tagged Ssn6p from cell nuclei at 12 hours may instead be due to the slow cell growth at this time point, resulting in fewer ribosomal proteins being transported from the nucleus (Kohler and Hurt, 2007). Interestingly, Tup1p was lost as rapidly in an *ada2 sas3* mutant, which does not transcribe *FLO1* (Fig. 6.11, *ada2 sas3* Ssn6-AA). This suggests that *FLO1* transcription does not occur for several hours after the *FLO1* promoter is depleted of Tup1p, and in the case of *ada2 sas3* mutants, transcription does not take place despite the absence of Tup1p at *FLO1*.

In an effort to account for the slow *FLO1* de-repression observed, the next factor investigated was H3 occupancy at the *FLO1* promoter. Nucleosomes present a barrier to gene transcription, and their eviction is one method by which Tup1-Ssn6-mediated repression of a gene can be relieved (Gavin and Simpson, 1997). If H3 was being evicted slowly from the *FLO1* promoter, it could inhibit recruitment of Pol II and cause delayed *FLO1* transcription. H3 occupancy of the *FLO1* promoter was therefore analysed by ChIP following the addition of rapamycin. In Ssn6-AA strains that contained Ada2p and Sas3p, H3 was evicted rapidly from the *FLO1* promoter (Fig. 6.12, Ssn6-AA). In this strain, the majority of H3 was lost from the *FLO1* promoter by 1 hour, with the lowest level of H3 occupancy being reached by 4 hours. Interestingly, an *ada2 sas3* mutant had a similarly rapid and potentially more dramatic loss of H3 from the *FLO1* promoter upon addition of rapamycin (Fig. 6.12, *ada2 sas3* Ssn6-AA). In this strain, that lacked any detectable *FLO1* transcription over 12 hours, H3 loss reached maximum levels by 2 hours. This indicates that H3 occupancy at *FLO1* does not impede gene transcription upon loss of Tup1-Ssn6 and further separates transcription from H3 eviction, as a strain unable to transcribe *FLO1* shows no deficiency in loss of histones from the *FLO1* promoter.

Ada2p and Sas3p in combination are required for the deposition of the H3K14ac post-translational modification at the *FLO1* promoter (Fig. 5.4). *ssn6* mutant strains lacking these HATs have also been shown not to transcribe *FLO1* (Fig. 5.1 and Fig. 6.9). Therefore we decided to monitor H3K14ac levels at the *FLO1* promoter in order to elucidate any function this mark had in activating *FLO1* transcription in the absence of Tup1-Ssn6.

In strains containing Ada2p and Sas3p, H3K14ac levels at the *FLO1* promoter began to rise soon after the addition of rapamycin, reaching peak levels by 4 hours (Fig. 6.14, Ssn6-AA). Interestingly, a reproducible drop in H3K14ac at the *FLO1* promoter is seen at 6 hours post-rapamycin treatment, followed by another rise in H3K14ac levels. After this second peak, H3K14ac levels at *FLO1* drop once again. This pattern of H3K14ac was surprising, even though peak H3K14ac levels are reached long before *FLO1* transcripts reach maximum levels (Compare Fig. 6.14 and Fig. 6.9). In *ada2 sas3* mutants, no H3K14ac was detected at *FLO1* over the time course (Fig. 6.14, *ada2 sas3* Ssn6-AA). This result was consistent with loss of global H3K14ac in the *ada2 sas3* mutant.

The next factor to be investigated was Pol II occupancy at the *FLO1* ORF, the presence of which is considered indicative of active transcription. In an Ssn6-AA strain containing Ada2p and Sas3p, there was no Pol II occupancy detected for 2 hours post-rapamycin treatment, with peak Pol II levels being reached by 4 hours (Fig. 6.15, Ssn6-AA). This Pol II occupancy level is sustained at 6 hours post-rapamycin, but falls dramatically by 8 hours. However, at 10 and 12 hours post-rapamycin treatment, Pol II levels begin to rise again. Interestingly, the drop in Pol II occupancy between 6 and 8 hours post-rapamycin treatment follows the drop in H3K14ac at the *FLO1* promoter between 4 and 6 hours (Compare Fig.

6.14 and Fig. 6.15). Intriguingly, the later recovery of Pol II levels also coincides with a second H3K14ac peak. It is possible that H3K14ac occupancy of the *FLO1* promoter is essential for recruitment of Pol II to the *FLO1* ORF. This is further supported by the absence of Pol II at *FLO1* in the *ada2 sas3* anchor away strain. This oscillation of Pol II occupancy at *FLO1* could also account for the slow rise in *FLO1* mRNA observed previously (Fig. 6.9). If only a small amount of stable *FLO1* transcripts are produced following each wave of Pol II occupancy, these transcripts would slowly accumulate, rather than being rapidly produced as in the case of genes such as *SUC2* (Fig. 6.5).

Another factor that had to be accounted for over such a long time-course was the growth of cells during the experiment. Over the course of a *SUC2* anchor away experiment, cells would have only undergone ~1 doubling. One question raised by monitoring *FLO1* over 12 hours was whether metabolic factors would come into play, and in what way would they influence gene transcription. To answer this question, we monitored cell density and glucose concentration in Ssn6-AA strains over the 12 hour time-course (Fig. 6.18). This analysis showed that cells grew exponentially for the first 6 hours of the experiment, but began to slow at the 6-8h time point, which is also the point at which H3K14ac occupancy and Pol II occupancy fall at *FLO1* (Fig. 6.14 and Fig. 6.15). This slowing of growth corresponded to the diauxic shift as glucose was shown to be exhausted from the growth medium between 6-8 hours post-rapamycin treatment, potentially leading to a drop in *FLO1* promoter acetylation and subsequently to a drop in Pol II at *FLO1*.

In summary these data establish a timeline of events that lead to de-repression of *FLO1* following loss of Tup1-Ssn6 from the gene promoter. Following loss of

Tup1-Ssn6, nucleosomes are rapidly evicted from the *FLO1* promoter region (Fig. 6.19A, compare Rap- and +1h). This eviction is not in itself sufficient to activate *FLO1* transcription; rather the depleted nucleosomal template is required to be acetylated. H3K14ac in particular is important for *FLO1* activation, and this mark reaches peak occupancy at the *FLO1* promoter approximately 4 hours after loss of Tup1-Ssn6 (Fig. 6.19A, +4h). This increase in H3K14ac correlates with recruitment of Pol II to the *FLO1* 5' ORF. Indeed, Pol II is not recruited to *FLO1* in the absence of H3K14ac, indicating that this mark is essential for Pol II recruitment. Furthermore a critical threshold of H3K14ac occupancy at *FLO1* may have to be reached and maintained to enable transcription, as a drop in H3K14ac at 6 hours post-rapamycin treatment correlates with a dramatic drop in Pol II occupancy (Fig. 6.19B, compare H3K14ac and Pol II). This drop in H3K14ac may be metabolically-linked, as it corresponds to a slowing of cellular growth and depletion of glucose from the growth medium after this time. Interestingly though, H3K14ac levels recover after this initial drop and this corresponds to a recovery in Pol II occupancy of *FLO1.* This pattern of transcription may serve to conserve energy by preventing costly constitutive *FLO1* transcription, while allowing for expression of some Flo1p on the cell wall in each generation, which would lead to protection from cellular stress within a population.

A

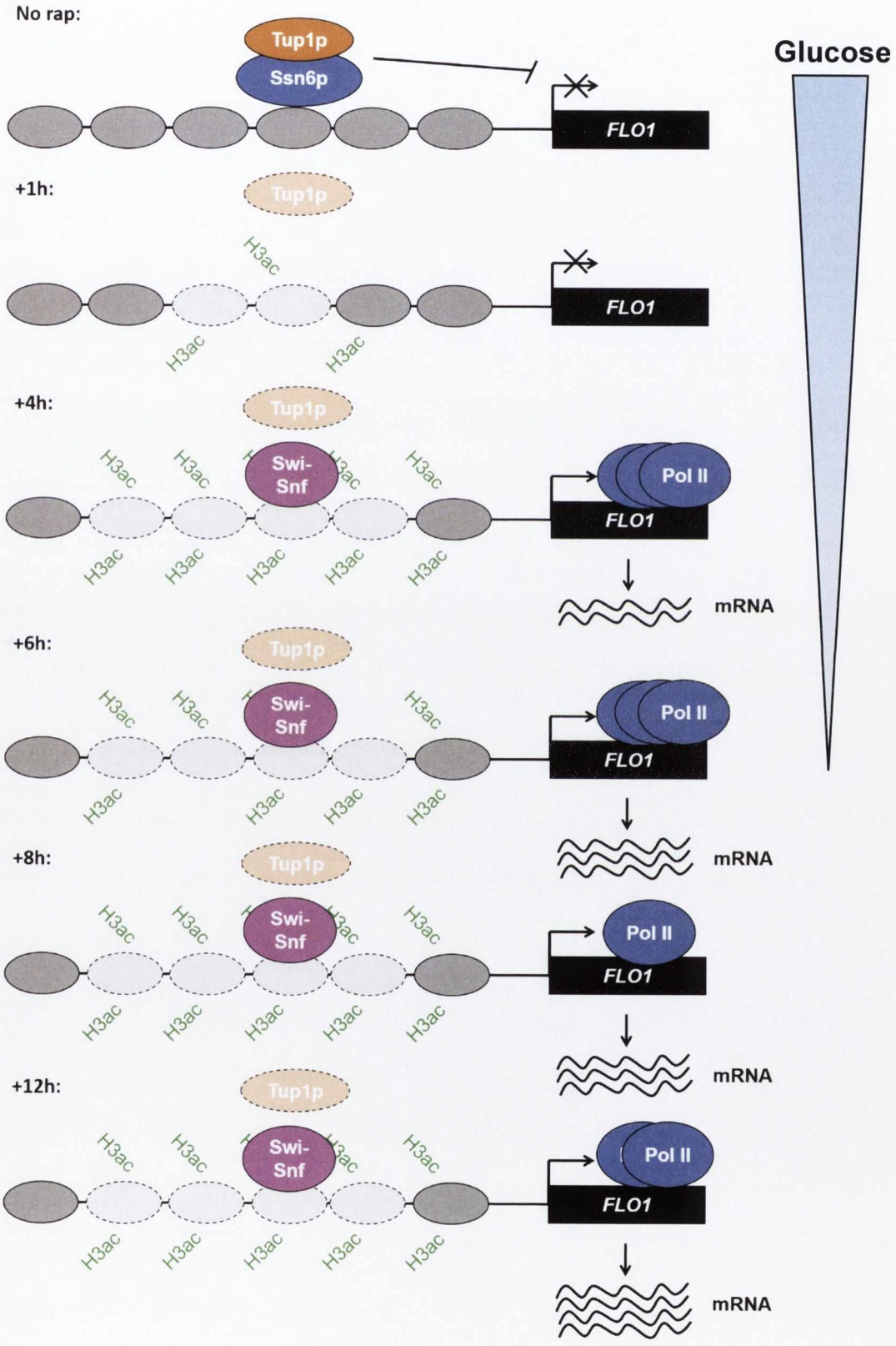
No rap:
Tup1p
Ssn6p
FLO1
Glucose
+1h:
Tup1p
H3ac
FLO1
+4h:
Tup1p
Swi-Snf
Pol II
FLO1
mRNA
+6h:
Tup1p
Swi-Snf
Pol II
FLO1
mRNA
+8h:
Tup1p
Swi-Snf
Pol II
FLO1
mRNA
+12h:
Tup1p
Swi-Snf
Pol II
FLO1
mRNA

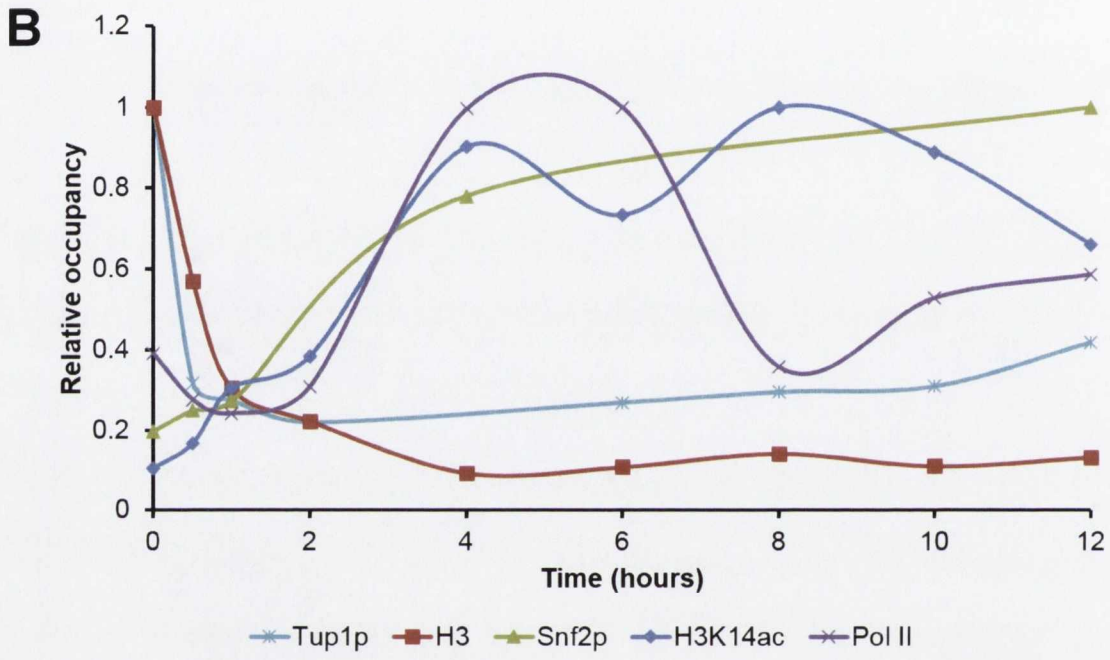
B
1.2
1
0.8
0.6
0.4
0.2
0
Relative occupancy
0
2
4
6
8
10
12
Time (hours)
Tup1p
H3
Snf2p
H3K14ac
Pol II

Figure 6.19. Timeline of events leading to *FLO1* de-repression. (A) Schematic of timeline of events leading up to and during *FLO1* de-repression. Before addition of rapamycin to Ssn6-AA strains (Rap-), Tup1-Ssn6 is present at the repressed *FLO1* promoter. 1 hour after the addition of rapamycin (+1h), there is a dramatic histone loss, no detectable Tup1p and some H3 acetylation. 4 hours post-rapamycin nucleosome loss is at its greatest extent, H3K14 is highly acetylated, Swi-Snf is present at the *FLO1* promoter and a high level of Pol II is present at the *FLO1* ORF. 6 hours post-rapamycin, there is also a high level of Pol II occupancy at *FLO1*, though H3K14ac levels have dropped at *FLO1* at this time-point and glucose in the growth medium is almost depleted. At 8 hours post-rapamycin, H3 occupancy is also low at the *FLO1* promoter, and H3 is highly acetylated. Snf2p is present and there is more *FLO1* mRNA detected, though low levels Pol II are detectable at the *FLO1* ORF. There is no glucose in the growth medium by this time point. By 12 hours post rapamycin (+12h), *FLO1* transcription is at its maximum level, though there is little Pol II at the *FLO1* ORF. Snf2p is still present and H3 is highly depleted at the *FLO1* promoter, though H3K14ac levels have fallen since +8h. At the 12h time-point there is also a low level of Tup1p detected at the *FLO1* promoter. (B) ChIP data for H3, H3K14ac, Tup1p, Snf2p and Pol II occupancy at the *FLO1* promoter in the wild type anchor away strain taken from Fig. 6.11, Fig. 6.12, Fig. 6.13, Fig. 6.14 and Fig. 6.15.

Chapter 7.

Restoration of *FLO8* in *Saccharomyces cerevisiae* strain BY4741

7.1. Introduction

Most genetic analyses of *FLO1* transcription have been carried out using *tup1* and *ssn6* mutants, as Tup1-Ssn6 is a well-known regulator of *FLO1* transcription (Fleming et al., 2014). However, though these analyses are useful when investigating the function of Tup1-Ssn6 and the importance of factors associated with *FLO1* de-repression, they do not provide insight into *FLO1* transcription under non-mutant conditions. This is because the protein responsible for activation of *FLO1* transcription, Flo8p is not present in most laboratory yeast strains, due to a nonsense mutation in the *FLO8* gene (H. Liu et al., 1996).

Flo8p is a DNA-binding transcription factor long associated with *FLO1* activation (Kobayashi et al., 1999). In most laboratory strains the *FLO8* gene contains a nonsense mutation at position +425 in the *FLO8* ORF, which results in a premature stop codon (H. Liu et al., 1996). Thus, little is known about the molecular basis of Flo8p activity, though it has been shown to activate flocculin-encoding genes, and genes involved in filamentous growth in other fungal species (Cao et al., 2006). Flo8p has also been shown to bind the ATP-dependent chromatin remodeller Swi-Snf (H. Y. Kim et al., 2014).

Tup1-Ssn6 is recruited to gene promoters by site-specific DNA-binding proteins (Treitel and Carlson, 1995; Hanlon et al., 2011). These Tup1-Ssn6 recruiting proteins have traditionally been thought of as being transcriptional repressors. Recently though, a number of studies have indicated that these factors can have a dual activation/repression role at target genes, and in some cases are required for maximum gene de-repression (Treitel and Carlson, 1995; Wong and Struhl, 2011). However, although Flo8p is a known activator of *FLO1,* its absence from 'wild type' laboratory strains challenges the model that all Tup1-Ssn6-regulated

genes are repressed and activated by the same Tup1-Ssn6 recruiting proteins. Indeed, as this study has shown, Tup1-Ssn6 clearly binds to the FLO1 gene to repress transcription in the absence of *FLO8*. Thus, it appears that in the case of *FLO1*, the mechanism of repression and de-repression is more complicated than the models predict.

The aim of this analysis was to gain a better understanding of Flo8p function at the *FLO1* promoter. Specifically, it was hoped restoration of Flo8p function would allow the monitoring of chromatin organisation at the de-repressed *FLO1* promoter without the need for loss of Tup1p or Ssn6p. The role of Swi-Snf and Tup1-Ssn6 during *FLO1* transcription is currently unclear, and elucidating each complex's role in *FLO1* de-repression in the presence of the Flo8p activator was considered a key step to gaining a better insight into the regulation of this model gene.

7.2. Results.

7.2.1. Strain construction

To study the role of Flo8p in the de-repression of *FLO1*, the genomic *FLO8* gene was restored by removing the premature stop codon at position +425 in the *FLO8* ORF. This was accomplished by PCR mutagenesis (Gietz and Schiestl, 2007). First, primers were designed that were complementary to the *FLO8* 3' ORF and the region immediately downstream of the *FLO8* stop codon. These primers were used in conjunction with a pYM20 plasmid to generate a PCR product containing a hygromycin resistance cassette with flanking sequences that would allow insertion of the marker immediately downstream of *FLO8* (Fig. 7.1A). This integration was selected for by growth on hygromycin-containing media.

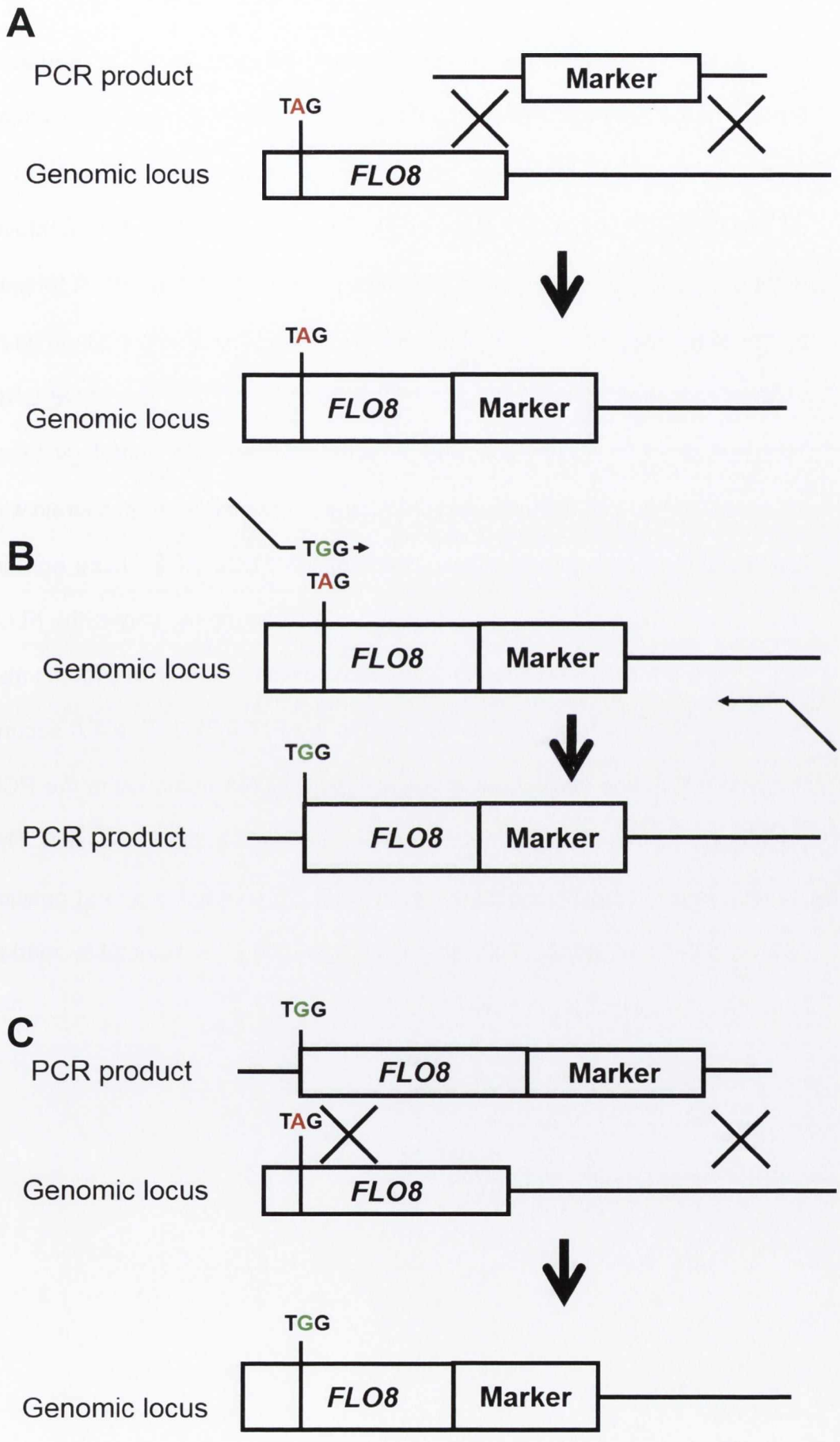
A
PCR product
Marker
TAG
Genomic locus
FLO8
TAG
Genomic locus
FLO8
Marker
B
TGG
TAG
Genomic locus
FLO8
Marker
TGG
PCR product
FLO8
Marker
C
TGG
PCR product
FLO8
Marker
TAG
Genomic locus
FLO8
TGG
Genomic locus
FLO8
Marker

Figure 7.1. Restoration of a functional *FLO8* gene by PCR-mediated mutagenesis. (A) In the first round of mutagenesis, a PCR product containing a selectable marker integrates into the position immediately downstream of the *FLO8* 3' ORF by homologous recombination. The resulting strain contains a genomic copy of *FLO8* immediately followed by this marker. (B) A forward primer was designed with homology to the *FLO8* 5' ORF that contained an A-G base-pair substitution corresponding to position +425 of the *FLO8* ORF. This was used in conjunction with a reverse primer with homology to an intergenic region downstream of *FLO8*. Using genomic DNA from a strain with a selectable marker directly downstream of the *FLO8* ORF, these primers were used to generate a PCR product that contained the majority of the *FLO8* ORF, though with the A-G point mutation at position +425. This product also contained the selectable marker adjacent to the *FLO8* 3' ORF. (C) A second transformation was carried out in a wild type BY4741 strain using the PCR product containing the point mutation at position +425 in the *FLO8* ORF. This resulted in a strain with a genomic copy of *FLO8* containing a G at position +425 in place of an A. This strain also contained a selectable marker immediately downstream of the *FLO8* ORF.

Following confirmation of insertion of a hygromycin resistance cassette downstream of *FLO8* by PCR (See materials and methods), another PCR product containing the resistance cassette and the majority of the *FLO8* ORF was generated using the newly constructed strain as a template. The primers used for this PCR were designed to have a single A-G base pair change corresponding to position +425 in the *FLO8* open reading frame (Fig. 7.1B). When amplified, this product would contain a TGG codon in place of the TAG stop codon present in the BY4741 parent strain. This PCR product was then transformed into a wild type BY4741 to integrate into the genomic *FLO8* gene, inserting a selectable marker downstream of the ORF and changing the single base pair at position +425 (Fig. 7.1C). The resulting strain was sequenced to confirm the point mutation.

7.2.2. Flo8p can be C-terminally tagged and is expressed *in vivo.*

In order to elucidate the role of Flo8p in *FLO1* regulation it was necessary to restore *FLO8* gene function. However, to fully understand how *FLO1* is activated in the context of chromatin, it was also important to show whether Flo8p bound directly to the *FLO1* promoter. In the absence of a suitable antibody against Flo8p, an epitope tag on the Flo8p protein was required to allow detection of Flo8p at *FLO1*. It was decided to use a C-terminal 9-Myc tag in this instance, and this strain was constructed identically to the previous *FLO8+* strain (Fig. 7.1), with the exception that in the initial transformation, an epitope tag-encoding sequence was included in the PCR product along with a selectable marker (Fig. 7.1A) .In order to verify that this tag sequence was present in the genome, PCR was carried out on the final strain, and a Western blot was carried out to show that the new strain (Flo8-Myc) could express Myc-tagged Flo8p (Fig. 7.2).

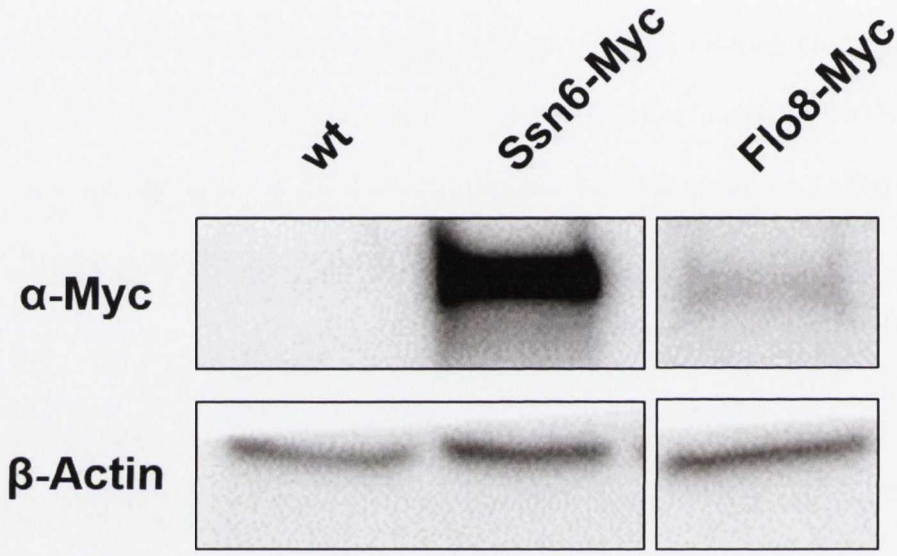

Figure 7.2. Analysis of Flo8-Myc expression. Western blot analysis monitoring the presence of a Myc epitope in un-tagged wild type (wt), a Myc-tagged Ssn6p (Ssn6-Myc) and a Myc-tagged Flo8p (Flo8-Myc) strains. β-Actin was used as a loading control.

In an un-tagged wild type strain (wt), there was no Myc tag detectable by Western blot (Fig. 7.2). In an Ssn6-Myc strain, a strong band was visible when membranes are probed with anti-Myc. In a strain with a restored *FLO8* gene and tagged Flo8p protein, a band of approximately 130kDa was visible, indicating that Flo8p was successfully tagged and was expressed under normal growth conditions.

7.2.3. *FLO1* is transcribed in strains with a restored *FLO8* gene.

Previous data had shown that *FLO1* is de-repressed to a dramatic extent in an *ssn6* mutant (Fig. 3.5). We were interested in whether this level of *FLO1* de-repression represented the level of gene transcription seen in a wild type population containing Flo8p, or was a mutant phenotype and not representative of natural *FLO1* gene activation. In order to test this, *FLO1* transcription was monitored in wild type cells without a functional *FLO8* gene (wt), in an *ssn6* mutant, and in cells with a restored *FLO8* gene (*FLO8+*). Transcription was monitored by RT-qPCR (Fig. 7.3).

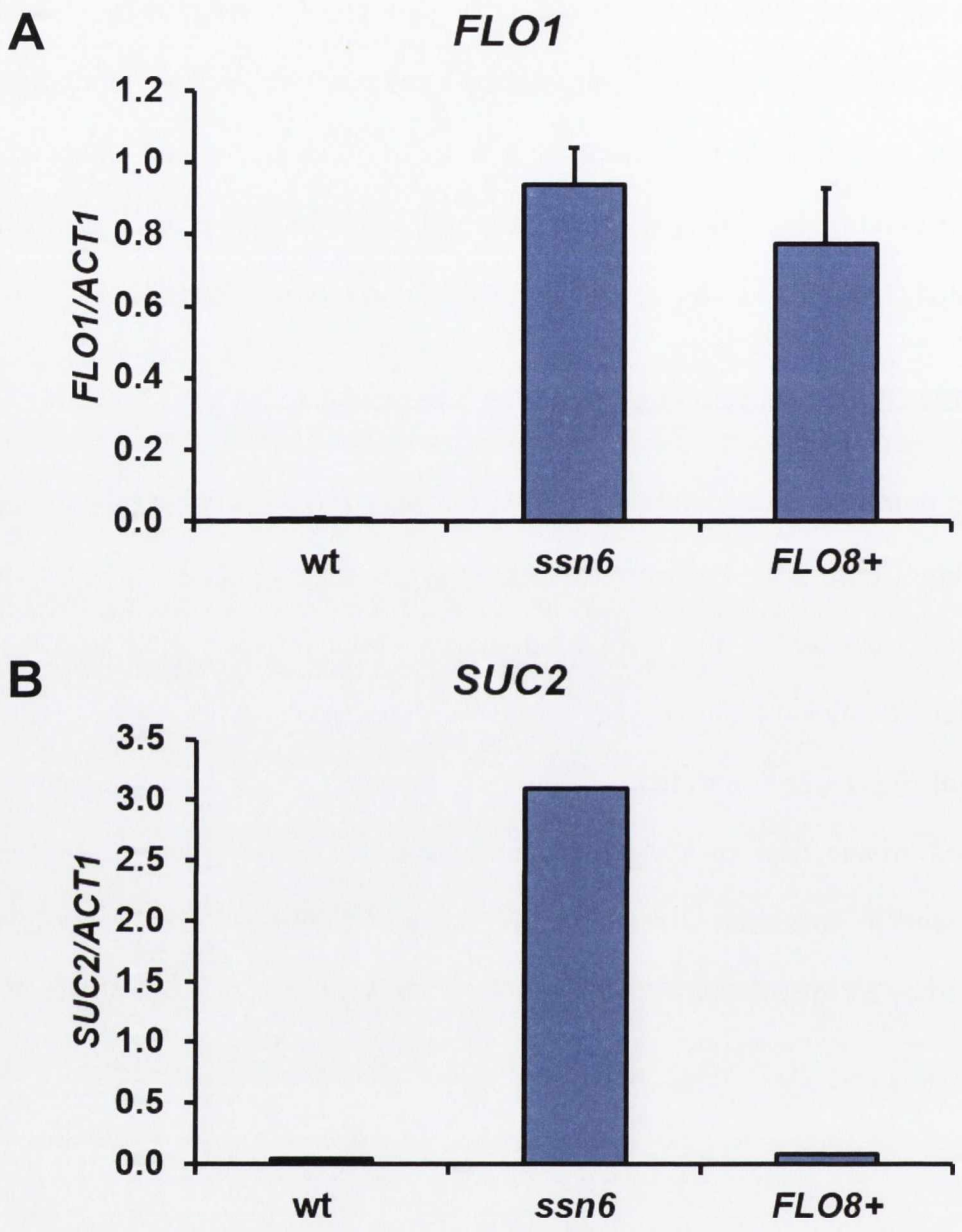

Figure 7.3. *FLO1* and *SUC2* transcription in *FLO8+* strains. RT-qPCR analysis of (A) *FLO1* and (B) *SUC2* transcription in wild type cells lacking a functional *FLO8* gene (wt), *ssn6* mutants and a strain containing a restored *FLO8* gene (*FLO8+*). *FLO1* and *SUC2* transcription were normalised to *ACT1* transcription. Error bars represent standard error of the mean (SEM) from two independent experiments.

In wild type cells without a functional *FLO8* gene, no *FLO1* transcription can be detected (Fig. 7.3A). As seen previously, in an *ssn6* mutant lacking Flo8p, *FLO1* is de-repressed (Fig. 7.3 and Fig. 3.5). However, when *FLO8* is restored (*FLO8+*), *FLO1* is de-repressed to a similar level as in an *ssn6* mutant (Fig. 7.3, compare *ssn6* and *FLO8+*). This indicates that restoration of *FLO8* leads to significant *FLO1* de-repression. This analysis also suggests that the de-repression of *FLO1* observed previously in *ssn6* mutants was representative of levels of *FLO1* transcription in the presence of the Flo8p activator.

As a control, analysis of *SUC2* transcription was carried out during growth under high glucose conditions. In wild type cells, *SUC2* was not de-repressed (Fig. 7.3B). Under these conditions, *ssn6* mutants displayed high levels of *SUC2* de-repression. However, *FLO8+* strains showed a repressed *SUC2* gene. This confirms that the observed *FLO1* de-repression in this strain was specific to genes under the transcriptional control of Flo8p and not due to a general de-repression of Tup1-Ssn6 regulated genes.

7.2.4. A Myc-tagged Flo8p is detectable at the *FLO1* promoter

Following the result that a restored *FLO8* gene had such a dramatic impact on *FLO1* transcription, it was decided to establish whether this was the result of a direct interaction between Flo8p and the *FLO1* promoter. To do this, a strain containing a restored *FLO8* gene encoding a Myc-tagged Flo8p protein (Flo8-Myc), was used for ChIP analysis to investigate whether Flo8-Myc could be detected at the *FLO1* promoter. *SUC2* was also used as a negative control (Fig. 7.4).

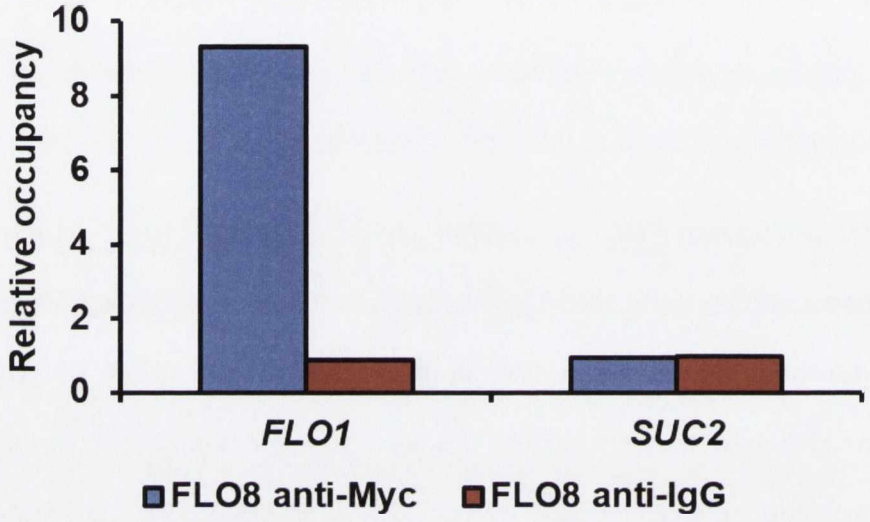

Figure 7.4. Myc ChIP at the *FLO1* and *SUC2* gene promoters. ChIP analysis of Flo8-Myc occupancy of the *FLO1* and *SUC2* gene promoters. A strain in which *FLO8* had been restored with a Myc-tagged Flo8p (Flo8-Myc) strain was analysed using either anti-Myc (FLO8 anti-Myc) or a non-specific IgG control (FLO8 anti-IgG) at *FLO1* and *SUC2*. Flo8-Myc occupancy at *FLO1* and *SUC2* was normalised to occupancy at an intergenic region of chromosome V.

When Flo8-Myc was analysed by ChIP using a non-specific IgG antibody as a negative control, a large enrichment of Flo8-Myc was found at the *FLO1* promoter in the Tup1-Ssn6 binding site (Fig. 7.4, *FLO1*). However, there was no Flo8-Myc enrichment detected at *SUC2* in this analysis (Fig. 7.4, *SUC2*). This suggests that when *FLO8* is restored by point mutation, the Flo8p protein will specifically bind the *FLO1* gene promoter and induce transcription.

7.2.5. Tup1p is present at the de-repressed *FLO1* promoter in the *FLO8+* strain.

The result that *FLO1* was equally highly de-repressed in *ssn6* mutants and wild type strains containing an intact *FLO8* gene was unexpected (Fig. 7.3). The mechanism by which Flo8p de-repressed *FLO1* transcriptionwas therefore investigated. If a *FLO8+* strain and an *ssn6* mutant had a similar level of *FLO1* de-repression, it was hypothesised that Flo8p would cause loss of Tup1-Ssn6 from the *FLO1* promoter. To test this hypothesis, Tup1p occupancy at the *FLO1* promoter was analysed by ChIP in a wild type strain, a *tup1* mutant and a strain with a restored *FLO8* gene (Figure 7.5).

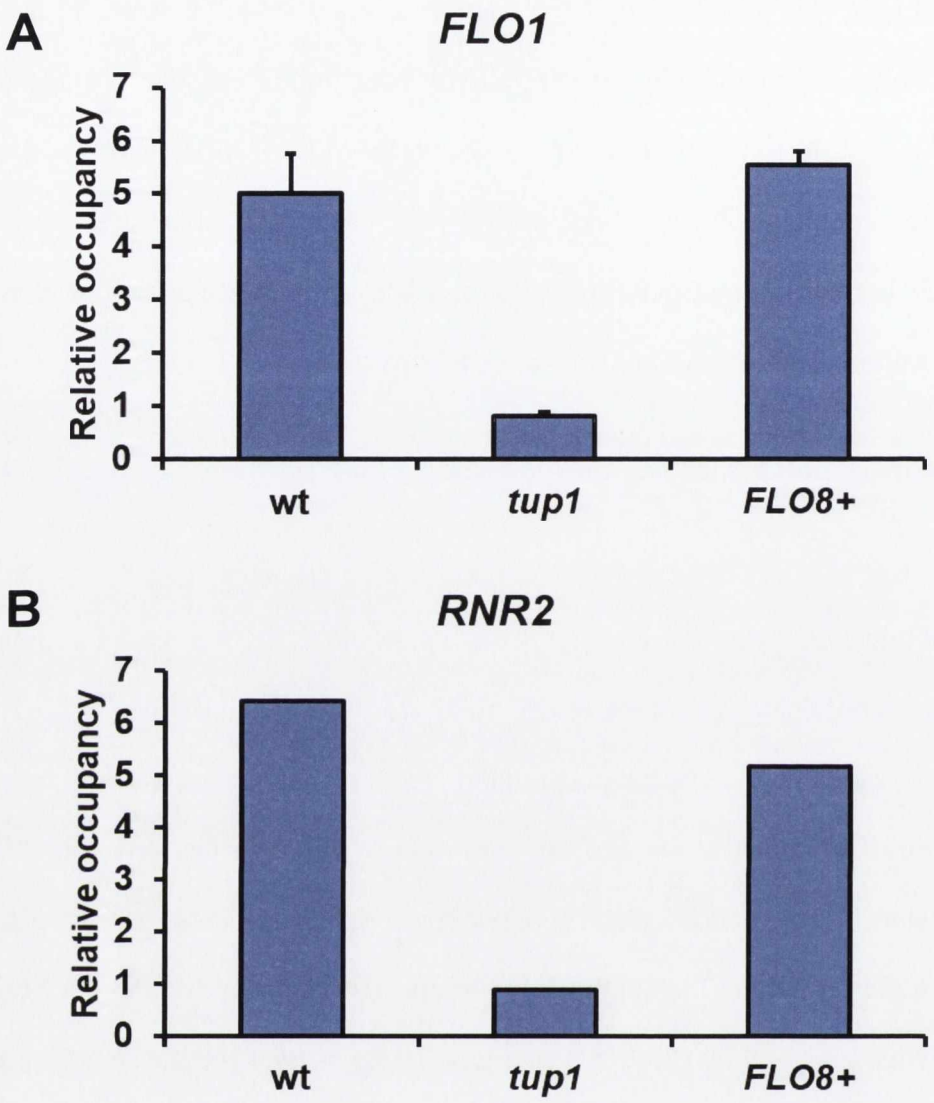

Figure 7.5. Tup1p occupancy at *FLO1* and *RNR2* in a *FLO8+* strain. ChIP analysis of Tup1p occupancy at the *FLO1* and *RNR2* promoters in wild type cells lacking Flo8p (wt), a *tup1* mutant and a strain with a restored *FLO8* gene (*FLO8+*). Tup1p levels at the *FLO1* and *RNR2* promoters were normalised to Tup1p occupancy at the *STE6* promoter region. Error bars represent standard error of the mean (SEM) from two independent experiments.

If the presence of Flo8p at the *FLO1* promoter led to the loss of Tup1-Ssn6 from the *FLO1* promoter, and subsequent *FLO1* de-repression, then it was expected to find a lower level of Tup1p at the *FLO1* promoter in a *FLO8+* strain. In wild type strains at the repressed *FLO1* promoter, Tup1p was detected (Fig. 7.5A). In *tup1* mutants used as a negative control, no Tup1p can be detected at the *FLO1* promoter. Surprisingly, in strains with a restored *FLO8* gene that transcribe *FLO1*, Tup1p was detected at levels comparable to repressed wild type strains (Fig. 7.5, compare wt and *FLO8+*). This unexpected result indicates that Tup1-Ssn6 is present at the de-repressed *FLO1* promoter in the presence of Flo8p.

As a control for Tup1p occupancy, but where Flo8p does not bind, *RNR2* was also analysed. In wild type cells, Tup1p was detected at the gene promoter (Fig. 7.5B). In the *tup1* mutant control, no Tup1p was detected at *RNR2*. In the *FLO8+* strain, Tup1p was detected at the *RNR2* promoter at similar levels to those seen in wild type strains.

Taken together these data suggest that the presence of Flo8p at the *FLO1* promoter allows full *FLO1* de-repression without the need for loss of Tup1-Ssn6 from the *FLO1* promoter (Fig. 7.4 and Fig. 7.5).

7.2.6. Nucleosome loss at the *FLO1* promoter is less severe in a *FLO8+* strain compared to an *ssn6* mutant.

Investigation into the effect a restored *FLO8* gene had on *FLO1* regulation demonstrated that Flo8p could lead to *FLO1* de-repression while retaining Tup1-Ssn6 at the *FLO1* promoter (Fig. 7.4 and Fig. 7.5). This was an interesting result, and we therefore investigated if the persistence of Tup1-Ssn6 played any role at a de-repressed *FLO1* promoter. To investigate this, H3 occupancy at the *FLO1*

promoter was analysed by ChIP in wild type cells, *ssn6* mutants and the *FLO8+* strain (Figure 7.6).

In wild type cells that did not transcribe *FLO1*, there was a high level of H3 across the *FLO1* promoter (Fig. 7.6, wt). In *ssn6* mutants where *FLO1* was fully de-repressed, long-range nucleosome depletion resulted in low levels of H3 being detected across the entire *FLO1* promoter region tested (Fig. 7.6, *ssn6*). However, in the *FLO8+* strain that also displayed full *FLO1* de-repression, there was less H3 depletion observed than that seen in an *ssn6* mutant (Fig. 7.6, *FLO8+*).Specifically, H3 occupancy at the -100 bp and -1200 bp positions was similar to those seen in wild type strains. However, at -585 bp, which is also the Tup1-Ssn6 binding site, there was the most significant H3 depletion compared to the wild type strain, although the depletion at this site was less severe than the H3 loss seen in an *ssn6* mutant. This suggests that the extensive nucleosome depletion detected at the *FLO1* promoter is not essential for *FLO1* transcription to take place. Rather, the targeted nucleosome loss at the Tup1-Ssn6 binding site may be required to allow *FLO1* de-repression in the presence of Flo8p

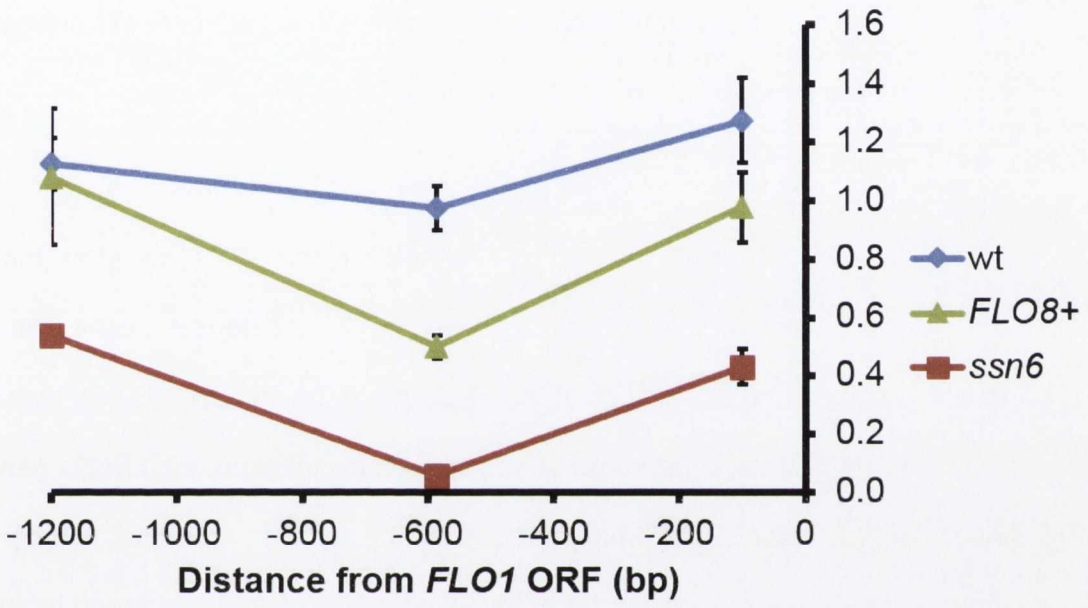

Figure 7.6. H3 occupancy at the *FLO1* promoter. ChIP analysis of H3 occupancy at the *FLO1* promoter in wild type cells lacking Flo8p (wt), an *ssn6* mutant and a strain with a restored *FLO8* gene (*FLO8+*). H3 levels at -1200 bp, -585 bp and -100 bp upstream of the *FLO1* transcription start site (TSS) were normalised to H3 occupancy at an intergenic region of chromosome V. Error bars represent standard error of the mean (SEM) from two independent experiments.

7.2.7. Swi-Snf occupies the *FLO1* promoter in the presence of Flo8p

Previous data indicated that H3 depletion at the *FLO1* promoter in a *FLO8+* strain was more localised and less extensive than in an *ssn6* mutant, despite similar levels of *FLO1* de-repression in these strains (Fig. 7.6). This suggested that in a strain containing functional Flo8p, Swi-Snf would be recruited to the *FLO1* gene promoter. To test this, Snf2p occupancy was monitored at the *FLO1* promoter by ChIP analysis in wt, *ssn6* and *FLO8+* strains (Fig. 7.7).

In wild type cells where *FLO1* is not de-repressed and there is a high level of nucleosome occupancy, no Snf2p was detected at the *FLO1* promoter (Fig. 7.7). In an *ssn6* mutant that displays a high level of *FLO1* de-repression and a low level of nucleosome occupancy at the *FLO1* promoter, Snf2p was detected at the *FLO1* promoter. In a *FLO8+* strain that has a highly de-repressed *FLO1* gene and intermediate nucleosome occupancy at the *FLO1* promoter, Snf2p was detectable at the *FLO1* promoter at levels comparable to those found in an *ssn6* mutant (Fig. 7.7, compare *ssn6* and *FLO8+*). This suggests that Swi-Snf is recruited to the *FLO1* promoter and carries out remodelling in the presence of Flo8p. However, the remodelling activity of Swi-Snf is less dramatic in the presence of Flo8p than it is in an *ssn6* mutant (Fig. 7.5).

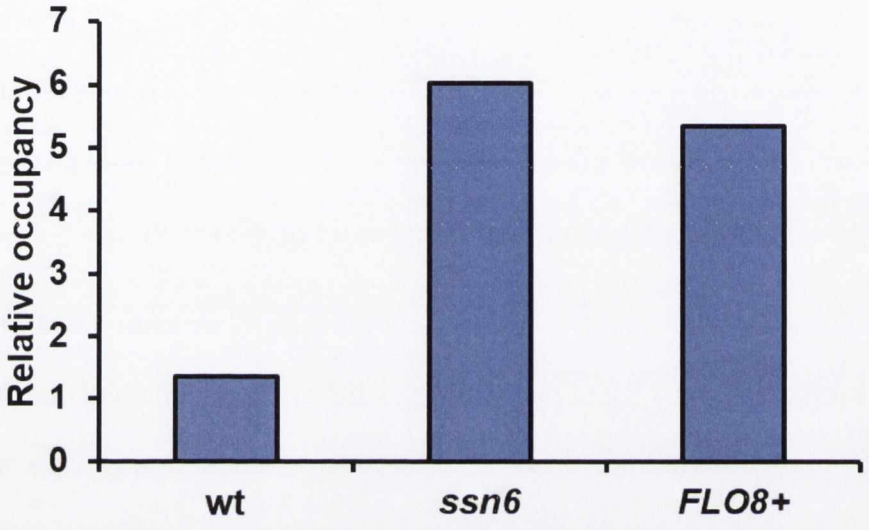

Figure 7.7. Snf2p occupancy at the *FLO1* promoter. ChIP analysis of Snf2p occupancy at the *FLO1* promoter in wild type cells lacking Flo8p (wt), an *ssn6* mutant and a strain with a restored *FLO8* gene (*FLO8+*). Snf2p levels at the *FLO1* promoter were normalised to Snf2p occupancy at an intergenic region of chromosome V.

7.2.8. H3K14ac levels at the *FLO1* promoter are elevated in the presence of Flo8p.

The data from chapters 3 and 4 indicated that histone acetylation, and particularly H3K14ac, was essential for *FLO1* de-repression in the absence of Ssn6p. The fact that strains that contained a functional *FLO8* gene exhibited levels of *FLO1* transcription comparable to an *ssn6* mutant suggested that in these strains, H3K14ac levels would also be high at the *FLO1* promoter. To investigate this, H3K14ac occupancy at two positions in the *FLO1* promoter were analysed by ChIP in the wild type, *ssn6* mutant and *FLO8+* strains (Fig. 7.8).

In wild type strains where *FLO1* is repressed, there is a low level of H3K14ac at the *FLO1* promoter (Fig. 7.8). In *ssn6* mutants that show a high level of *FLO1* de-repression, there was a high level of H3K14ac relative to wild type strains. However, in *FLO8+* strains that also show a high level of *FLO1* de-repression, there was H3K14ac present at the *FLO1* promoter, but at a much lower level than that seen in *ssn6* mutants. This suggests that the very high H3K14ac levels at the *FLO1* promoter seen in *ssn6* mutants may not be necessary for full *FLO1* de-repression when Flo8p is present. Rather, more modest levels of histone acetylation may be sufficient for *FLO1* transcription in the presence of Flo8p.

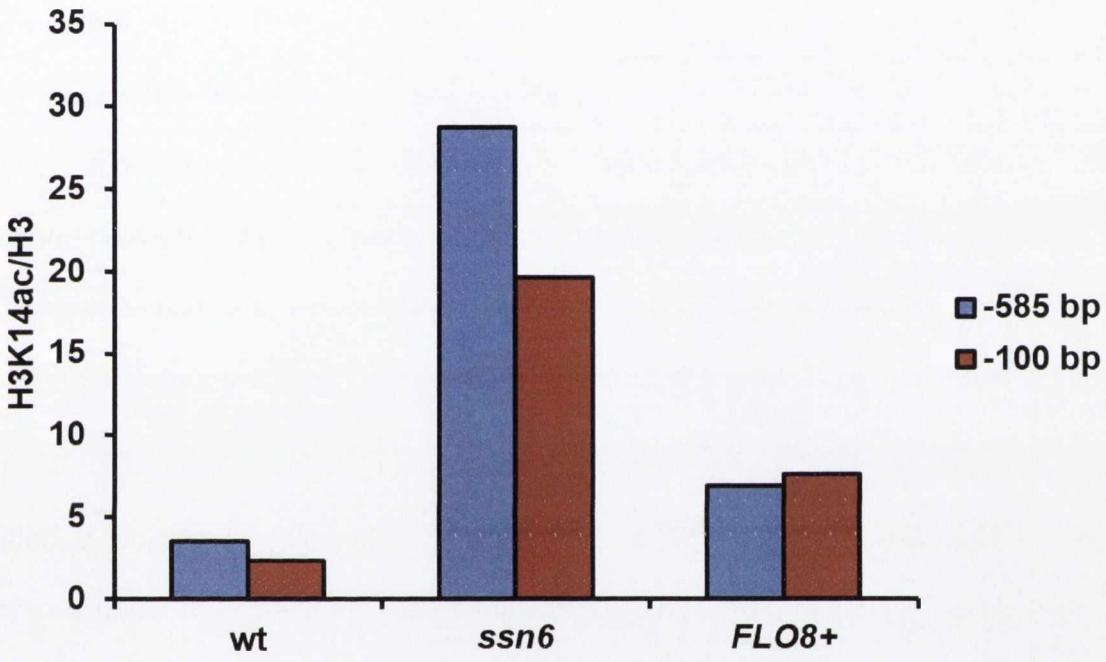

Figure 7.8. H3K14ac occupancy at the *FLO1* promoter. ChIP analysis of H3K14ac occupancy at the *FLO1* promoter in wild type cells lacking Flo8p (wt), an *ssn6* mutant and a strain with a restored *FLO8* gene (*FLO8+*). H3K14ac levels at regions -100 bp and -585 bp upstream of the *FLO1* transcription start site (TSS) were normalised to H3K14ac occupancy at a telomeric control region and also to H3 occupancy at *FLO1.*

7.2.9. Restoration of a galactose-inducible *FLO8* gene.

The previous data in this chapter had shown that *FLO8* could be restored genomically by introducing a point mutation in the 5' *FLO8* ORF, which allows expression of a C-terminally tagged *FLO8* protein (Fig. 7.1 and Fig. 7.2). Restoration of the *FLO8* gene correlated with *FLO1* de-repression at levels comparable to those seen in an *ssn6* mutant (Fig. 7.3). Previous data from our kinetic analysis in chapter 4 had also shown that loss of Ssn6p at *FLO1* resulted in slow *FLO1* de-repression (Fig. 6.9). We therefore hypothesised that it was the absence of Flo8p at *FLO1* that caused the slow *FLO1* de-repression upon loss of Tup1-Ssn6 from the *FLO1* promoter. To address this, a kinetic analysis of *FLO8* induction was required to discover whether *FLO1* was de-repressed more quickly in the presence of Flo8p.

This was accomplished by constructing a plasmid containing a galactose-inducible *FLO8* gene. The host plasmid was obtained from Open Biosystems, and contained the *FLO8* ORF with a premature stop codon at position +425. This plasmid-borne galactose-inducible *FLO8* gene was then restored using inverse PCR (Figure 7.9).

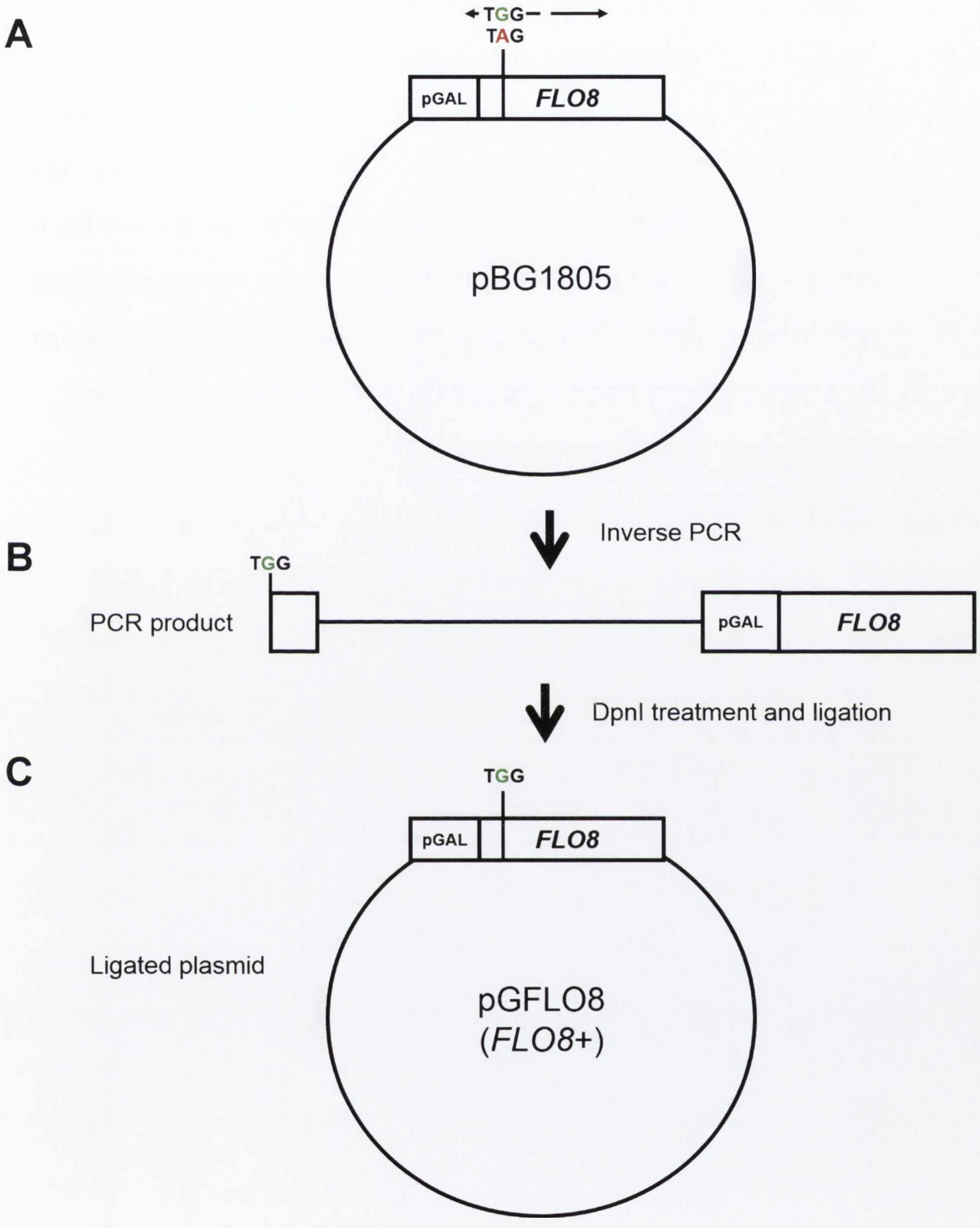
A
TGG
TAG
pGAL
FLO8
pBG1805
Inverse PCR
B
TGG
PCR product
pGAL
FLO8
DpnI treatment and ligation
C
TGG
pGAL
FLO8
Ligated plasmid
pGFLO8
(FLO8+)

Figure 7.9. Restoration of a galactose-inducible *FLO8* gene. (A) Primers were designed to amplify the entire BG1805 plasmid (Open Biosystems), with the left primer containing an A-G nucleotide substitution corresponding to position +425 in the *FLO8* ORF. (B) A PCR product containing the point mutation was generated using Q5 High-Fidelity DNA Polymerase (NEB), and this was DpnI-treated in order to digest any BG1805 template plasmid not containing the desired point mutation. (C) The PCR product was ligated and transformed into an *Escherichia coli* vector before being sequenced to verify the point mutation.

Inverse PCR was successfully carried out on plasmid BG1805 to introduce a point mutation into the *FLO8* ORF to reverse the stop codon at position +425 (Fig. 7.9A). The PCR product containing the point mutation was DpnI-treated to digest any of the remaining BG1805 (Fig. 7.9B). Finally, the DpnI-treated plasmid was ligated to form a circular plasmid containing a restored, galactose-inducible *FLO8* gene (Fig. 7.9C). This point mutation was confirmed by sequencing (GATC Biotech) and then transformed into wild type yeast.

When grown in –Ura dropout medium with 2% glucose, strains containing the galactose-inducible *FLO8* plasmid (pGFLO8) had a wild type phenotype (Flo-). However, when grown in –Ura medium containing 2% galactose, this strain exhibited a flocculent phenotype similar to that seen in the genomic *FLO8+* strain, indicating that induction of *FLO8* under these conditions led to de-repression of *FLO1*. When this phenotype was monitored over time, it was found that strains containing pGFLO8 only displayed a flocculent phenotype after an overnight incubation in galactose-containing medium, following raffinose treatment (data not shown). Subsequent work using this strain established that flocculation was not observed until >13 hours post-galactose addition to culture medium (AF, personal communication). This phenotype also correlated with the accumulation of *FLO1* mRNA in this strain. This suggests that a galactose-inducible *FLO8* gene can activate *FLO1* transcription and flocculation. Importantly, this slow galactose-dependent rate of *FLO1* activation was similar to that seen in an Ssn6p anchor away strain, indicating that the slow *FLO1* de-repression observed in the anchor-away strain was not due to a lack of Flo8p. Instead the data suggests slow *FLO1* mRNA accumulation is a feature inherent to the *FLO1* gene (Fig. 6.9, Ssn6-AA).

7.3. Discussion

Most laboratory strains of *S. cerevisiae* contain a nonsense mutation in the *FLO8* gene which means in these strains *FLO1* is not transcribed (Soares, 2011). Previous studies involving *FLO1* have therefore relied on the use of *tup1* and *ssn6* mutants to de-repress the *FLO1* gene. While this method is informative, it does not represent natural *FLO1* transcription. In order to investigate true wild type regulation of *FLO1* transcription, the Flo8p protein needed to be expressed. To achieve this, the nonsense mutation in the *FLO8* ORF was amended by point mutation using PCR mutagenesis (Fig. 7.1). This experiment was carried out by generating a restored *FLO8* gene both with and without a 9-Myc tag (*FLO8+* and Flo8-Myc, respectively). The base-pair change in the genome was verified by sequencing and expression of tagged Flo8p was verified by Western blot (Fig. 7.2).

Next, the effect that a restored Flo8p had on de-repression of *FLO1* was investigated. Wild type cells lacking a functional *FLO8* gene did not transcribe *FLO1* (Fig. 7.3A, wt), whereas in *ssn6* mutants, *FLO1* was highly de-repressed (Fig. 7.3A, *ssn6*). In strains with a restored *FLO8* gene, *FLO1* de-repression was comparable to that seen in an *ssn6* single mutant, suggesting that Flo8p allows full de-repression of *FLO1*. *SUC2* was used as a control gene in this analysis, and it was found that while *SUC2* was fully de-repressed in *ssn6* mutants, the restored *FLO8* gene had no impact on transcription of this gene. This suggests that Flo8p is capable of activating *FLO1*-specific transcription in the *FLO8+* strain.

Having observed a significant effect on *FLO1* transcription in the *FLO8+* strain, the next issue to be addressed was whether this was the result of direct action of Flo8p at the *FLO1* promoter, or some indirect effect of having a restored *FLO8*

gene. To test this, a strain containing a Myc-tagged Flo8p was analysed for Flo8-Myc binding at the *FLO1* and *SUC2* promoters (Fig. 7.4). A high level of Flo8-Myc was detected at the Tup1-Ssn6 binding site at the *FLO1* promoter using anti-Myc, but no enrichment was detected using a non-specific anti-IgG antibody. No Flo8-Myc was detected at *SUC2* using either antibody. This suggests that Flo8-Myc can specifically be detected at the *FLO1* gene promoter, and indicates that Flo8p occupies the same binding site as Tup1-Ssn6.

Taking into account the result that *FLO1* was fully de-repressed in a *FLO8+* strain, and that Flo8-Myc occupied the *FLO1* promoter at the Tup1-Ssn6 binding site (Fig. 7.3 and Fig. 7.4), it was hypothesised that binding of Flo8p to the *FLO1* promoter would cause loss of Tup1-Ssn6 from this region, leading to *FLO1* de-repression. If this was the case, it was predicted that *FLO8+* strains would show a lower level of Tup1p at the *FLO1* promoter than wild type strains. However, the data showed there was no difference in Tup1p occupancy at *FLO1* between wild type and *FLO8+* strains, both of which contained high Tup1p occupancy levels at *FLO1* compared to the negative *tup1* mutant control (Fig. 7.5A). *RNR2* was also used as a control gene, and similar levels of Tup1p occupancy were observed between wild type and *FLO8+* strains (Fig. 7.5B). This suggests that when Flo8p occupies the *FLO1* promoter, full *FLO1* de-repression occurs in the presence of fully retained Tup1-Ssn6 (Fig. 7.3, Fig. 7.4 and Fig. 7.5).

Having shown Tup1-Ssn6 occupied the de-repressed *FLO1* promoter in the presence of Flo8p, the function of Tup1-Ssn6 under these conditions was addressed. This was investigated by first monitoring H3 occupancy across the *FLO1* promoter. It was found that in wild type cells where *FLO1* is repressed, there was a high level of H3 occupancy (Fig. 7.6, wt). In *ssn6* mutant cells where

FLO1 is highly de-repressed, there was a low level of H3 across the entire *FLO1* promoter region tested (Fig. 7.6, *ssn6*). Interestingly in *FLO8+* strains, where *FLO1* is also highly de-repressed, there was significant H3 loss focused at the Tup1-Ssn6 binding site, but up- and downstream of this site, H3 occupancy was at wild type levels (Fig. 7.6, *FLO8+*). This suggests that activation of *FLO1* by Flo8p does not involve the dramatic and widespread promoter nucleosome loss seen in *ssn6* mutants. It is possible that by retaining Tup1-Ssn6 during *FLO1* de-repression, Flo8p allows a localised nucleosome loss required for *FLO1* transcription, but keeps an otherwise ordered nucleosome structure propagated by Tup1-Ssn6.

The localised nucleosome loss at the de-repressed *FLO1* gene promoter in the presence of Flo8p suggested that Swi-Snf was carrying out nucleosome eviction in the presence of Flo8p. This was addressed by monitoring Snf2p binding to the *FLO1* promoter. In wild type cells that show high levels of H3 at *FLO1*, no Snf2p was detected (Fig. 7.6, wt). In *ssn6* mutants that display low levels of H3 at the *FLO1* promoter, high levels of Snf2p were detected (Fig. 7.7, *ssn6*). In *FLO8+* strains that showed only localised depletion of H3 in the *FLO1* promoter, Snf2p can be detected at levels comparable to those found in an *ssn6* mutant (Fig. 7.7, *FLO8+*). This suggests that the difference in H3 occupancy at the *FLO1* promoter between *ssn6* mutants and *FLO8+* strains is not due to differences in Swi-Snf occupancy. This also indicates that Swi-Snf and Tup1-Ssn6 co-occupy the de-repressed *FLO1* promoter in the presence of Flo8p.

Previous data had shown the importance of Gcn5p-containing complexes and Sas3p for *FLO1* de-repression in an *ssn6* mutant (Fig. 5.1). Strains lacking Ada2p and Sas3p were unable to transcribe *FLO1*, possibly due to the global lack of

H3K14ac in these strains (Fig. 5.6). With this in mind, H3K14ac occupancy was monitored at two positions in the *FLO1* promoter. In wild type cells that do not transcribe *FLO1*, there was a low level of H3K14ac at the *FLO1* promoter (Fig. 7.8, wt). In *ssn6* mutants where *FLO1* was highly de-repressed, there was a high level of H3K14ac detected at the *FLO1* promoter (Fig. 7.8, *ssn6*). In *FLO8+* strains where *FLO1* is also highly de-repressed, there was a H3K14ac which was lower than that seen in an *ssn6* mutant, but higher than that found in wild type strains at *FLO1* (Fig. 7.8, *FLO8+*). This indicates that H3K14 is acetylated when *FLO1* is de-repressed in the presence of Flo8p, but this acetylation is less dramatic than that seen in an *ssn6* mutant.

This analysis also led to the construction of a strain that allowed kinetic analysis of *FLO8* transcription using a galactose-inducible promoter (Fig. 7.9). Preliminary analysis carried out using this strain indicated that *FLO1* was de-repressed slowly following *FLO8* induction, which correlated with previous data carried out in an Ssn6p anchor away strain. Future work will focus on analysis of this strain and the timeline of events that lead up to a more natural *FLO1* de-repression.

Taken together, these data give a more complete view of the molecular basis of *FLO1* activation by Flo8p. In wild type strains that lack a functional *FLO8* gene, Tup1-Ssn6 occupies the *FLO1* promoter where there is a high nucleosome occupancy of the *FLO1* promoter, with very low levels of histone acetylation (Fig. 7.10, wt) and *FLO1* gene transcription is repressed. .

In *ssn6* mutants where Tup1-Ssn6 and Flo8p are absent, Swi-Snf occupies the *FLO1* promoter where there is widespread nucleosome depletion leaving a residual highly acetylated chromatin template which correlates with high levels of *FLO1* transcription (Fig. 7.10, *ssn6*). .

In strains containing a functional *FLO8* gene, Flo8p is present at the Tup1-Ssn6 binding site at the *FLO1* promoter (Fig. 7.10, *FLO8+*). There is a localised nucleosome depletion at this site, and there is a raised level of histone acetylation compared to strains lacking Flo8p. Interestingly, both Swi-Snf and Tup1-Ssn6 occupy the same binding site as Flo8p, and under these conditions, *FLO1* is fully de-repressed.

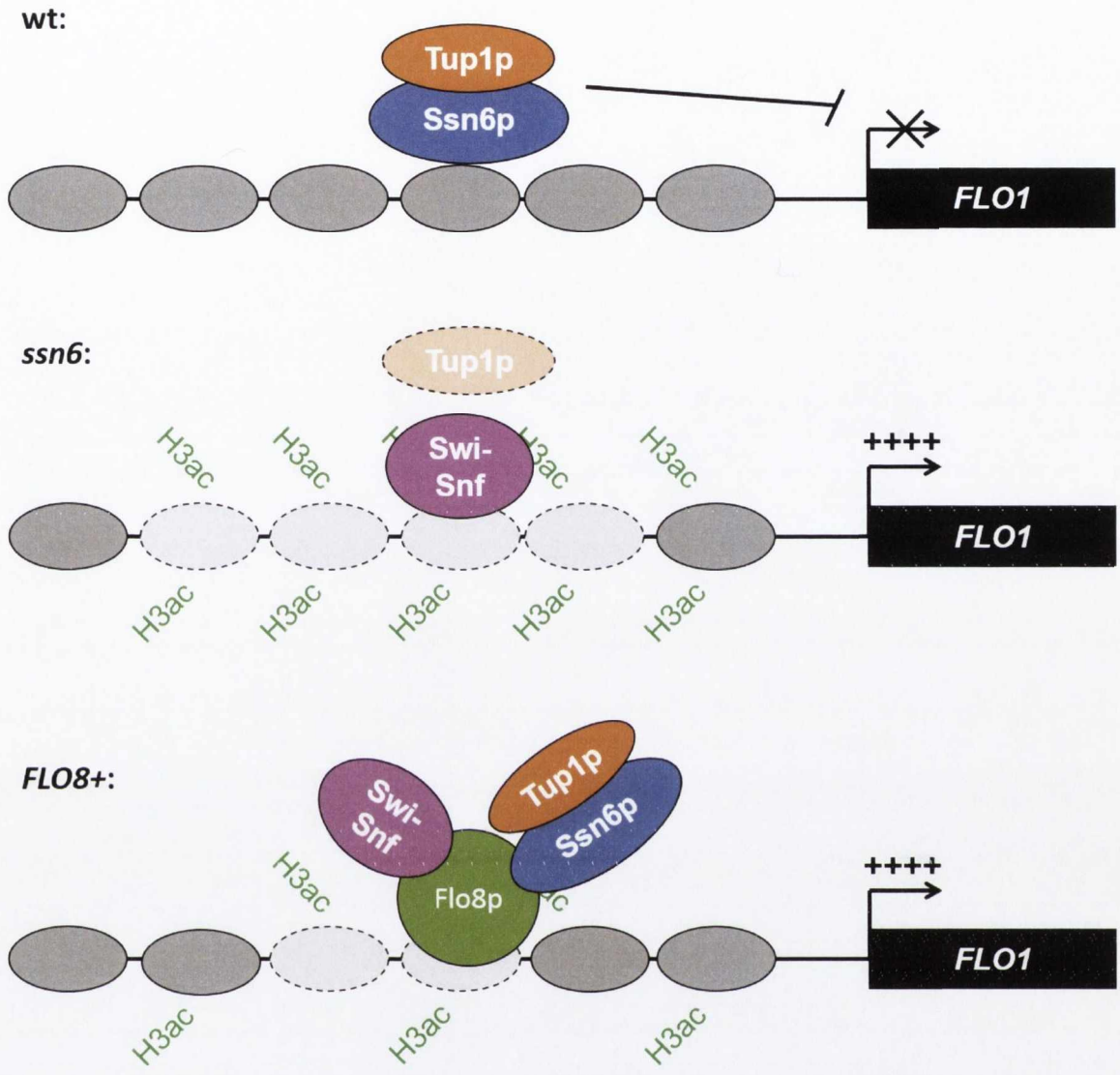

Figure 7.10. Model for Tup1-Ssn6 and Flo8p action at the *FLO1* promoter. Summary of protein occupancy at the *FLO1* promoter and *FLO1* transcription in Wild type strains, *ssn6* mutants and *FLO8+* strains. Dashed lines indicate protein loss. "++++" indicates level of *FLO1* transcription

Chapter 8

Final Discussion

8.1 Discussion

Tup1-Ssn6 has long been studied as a model for co-repressor function and, as the first co-repressor complex characterised, has led the way in research into these important regulators of gene transcription. Human co-repressors function in much the same way as Tup1-Ssn6, and have been shown to be important factors in development, failure of which can result in diseases including cancer (Payankaulam et al., 2010). Tup1-Ssn6 interacts with numerous important regulators of chromatin structure, many of which are highly conserved from yeast to humans, including SAGA, Swi-Snf and components of RNAPII and Mediator (Malave and Dent, 2006). Ssn6p can also co-operate with mammalian TLE1 to silence genes in mammalian cells further demonstrating the relevance of using yeast as a model organism for the study of chromatin-mediated gene repression (Grbavec et al., 1999).

Tup1-Ssn6 is recruited to target genes by DNA-binding transcription factors, where it can repress transcription via a number of mechanisms (Malave and Dent, 2006). First, Tup1-Ssn6 can interact directly with components of the general transcription machinery to prevent transcription initiation (M. Lee et al., 2000). Second, Tup1-Ssn6 can recruit HDACs that de-acetylate nucleosomes at target promoters, and prevent transcription (Fleming et al., 2014). Third, Tup1-Ssn6 can occlude activation domains on DNA-binding transcription factors, and prevent recruitment of transcriptional activators to gene promoters (Wong and Struhl, 2011). Finally, Tup1-Ssn6 can interact with ATP-dependent chromatin remodellers to propagate a repressive chromatin structure at gene promoters, occluding important regulatory sites and preventing transcriptional activation (B. Li and Reese, 2001). Tup1p has been proposed to contain the repressive activity

of the complex, and has the ability to bind hypoacetylated histone tails (Davie et al., 2002). Ssn6p, on the other hand, can contact multiple HDACs and other proteins to influence chromatin at target promoters (Davie et al., 2003).

One well-characterised gene under the transcriptional control of Tup1-Ssn6 in *S. cerevisiae* is *FLO1*. *FLO1* is the major flocculin-encoding gene in yeast, and *FLO1*-expressing strains display a flocculent phenotype (Bidard et al., 1995). Flocculation is the non-sexual, calcium-dependent aggregation of cells that is caused by mannose-binding, lectin-like proteins on the cell wall (Verstrepen and Klis, 2006). The flocculation phenotype imparts cellular protection from stress, but also has industrial uses such as in brewing and in the removal of heavy metal ions (Verstrepen et al., 2003; Machado et al., 2008). The chromatin at the *FLO1* promoter and upstream region is organised into an extensive array of well-positioned nucleosomes, the correct positioning of which depends on Tup1-Ssn6 (Fleming and Pennings, 2001). *FLO1* has proved to be an ideal model gene for the study of chromatin because of the interplay of Tup1-Ssn6 and Swi-Snf at the *FLO1* promoter. It has been shown that long-range remodelling occurs in a Swi-Snf-dependent manner in the absence of Tup1-Ssn6 (Fleming and Pennings, 2001). However, the importance of this remodelling and the mechanisms by which *FLO1* is de-repressed are still unclear.

This project aimed to identify the contribution of Tup1p and Ssn6p to gene repression both globally, and specifically at the *FLO1* gene. The aim was to identify factors that are required for de-repression of *FLO1*, and establish a timeline of events that lead to *FLO1* transcription in the absence of Tup1-Ssn6. Finally, this project aimed to construct a strain expressing the putative activator

of *FLO1,* Flo8p, and monitor transcription, chromatin structure and protein occupancy in the presence of this activator.

8.1.1 *tup1* and *ssn6* mutants have distinct phenotypes.

To establish whether there were phenotypic differences between *tup1* and *ssn6* mutants, a number of phenotypic tests were carried out to monitor the effect of loss of Tup1p and Ssn6p, both separately and in combination. If both subunits operated solely within the Tup1-Ssn6 complex and were required for complex function, it would be expected that the *tup1, ssn6* and *tup1 ssn6* mutants would all have similar phenotypes. The first of these experiments monitored cell growth at 30°C in YEPD broth (Fig. 3.1). Under these conditions, *ssn6* mutants had a slower growth rate than *tup1* mutants (Fig. 3.1, compare *ssn6* and *tup1*) and *tup1 ssn6* double mutants had the slowest growth rate. This indicated that Tup1p and Ssn6p can each contribute separately to gene regulation and cell growth.

Stress tests were next carried out on wild type cells, *ssn6* and *tup1* single mutants and the *tup1 ssn6* double mutant (Fig. 3.2). It was found that *ssn6* and *tup1 ssn6* mutants were extremely sensitive to heat shock and replication stress, whereas *tup1* mutants were unaffected by these stresses. This interesting result suggests that loss of Ssn6p has a greater impact on the cells' ability to respond to stress than loss of Tup1p. This also suggests that *ssn6* mutants have a replication defect which is not present in *tup1* mutants. Observation of *tup1* and *ssn6* mutants by microscopy led to the discovery that *ssn6* and *tup1 ssn6* mutants appeared larger than wild type cells and *tup1* single mutants (Fig. 3.3). Subsequent analysis using a cytometer revealed that this size difference was due to a broader range of cell sizes in *ssn6* mutants compared to wild type cells and *tup1* mutants. *ssn6* single and *tup1 ssn6* double mutants were also found to have

a different flocculation phenotype than *tup1* single mutants, with *tup1* mutants appearing to form tighter flocs than *ssn6* mutants (Fig. 3.4). The reason for this difference in flocculation is unknown, but may be the result of the smaller *tup1* mutant cells having the ability to pack more tightly than the larger *ssn6* mutants.

To investigate flocculation differences between *tup1* and *ssn6* mutants, and also to determine whether other *FLO* genes were de-repressed in the absence of Tup1-Ssn6, *FLO1, FLO5* and *FLO9* gene transcription were monitored (Fig. 3.5). It was found that all *FLO* genes were repressed in wild type strains, and all genes were de-repressed in *tup1* and *ssn6* mutants, albeit to different extents. *FLO1* was found to be the most highly-transcribed gene, in line with its role as the major flocculin-encoding gene in *S. cerevisiae* (Govender et al., 2008). This suggests that Tup1-Ssn6 represses *FLO5* and *FLO9* transcription in addition to its role in *FLO1* regulation. This analysis also revealed that the *ssn6* and *tup1 ssn6* double mutant displayed similar levels of *FLO1* de-repression which was significantly higher than the de-repression in the *tup1* mutant. This indicates that Ssn6p may play a repressive role at *FLO1* in the absence of Tup1p.

A similar pattern was observed at *SUC2* gene (Fig. 3.6), consistent with previous studies (Treitel and Carlson, 1995). Interestingly, in *tup1* and *ssn6* mutants the levels of *SUC2* transcription under *SUC2* inducing conditions (low glucose) were even higher than that seen under repressing conditions (high glucose). This suggests that in wt cells under *SUC2* de-repressing conditions the Tup1-Ssn6 complex, which has been shown to be present at the *SUC2* promoter, still provides some level of repression. Furthermore, these data also indicate that under *SUC2* repressing conditions and in the absence of Tup1-Ssn6, *SUC2* cannot be fully de-repressed. This suggests that other proteins are required for

full *SUC2* de-repression in response to low glucose, such as the repressing/activating protein Mig1p (Treitel and Carlson, 1995).

Having observed differences in levels of de-repression between *tup1* and *ssn6* mutants at *FLO1* and *SUC2,* we next investigated gene repression on a global scale by analysing previously published data by DeRisi et al (1997) and unpublished work by A. B. Fleming (personal communication). Comparing global gene transcription in *tup1* and *ssn6* mutants, it was found that while there was an overlap in genes de-repressed >2-fold in these strains, but there were also many genes uniquely de-repressed in *tup1* and *ssn6* mutants (Fig. 3.7). This result also showed that an *ssn6* mutant has a greater number of genes de-repressed than a *tup1* mutant, and in the group of genes that were de-repressed commonly in both mutants, *ssn6* mutants showed a higher level of de-repression compared to *tup1* mutants. This suggests that Ssn6p repressed more genes than Tup1p, and loss of Ssn6p had a greater impact on global transcription than loss of Tup1p. Although this was in contrast to a recent study that indicated loss of Tup1p had a greater impact on transcription, both studies found that unique subsets of genes were de-repressed in *tup1* and *ssn6* mutants (K. Chen et al., 2013).

The types of genes de-repressed in *tup1* and *ssn6* mutants were also found to be different indicating that Tup1p and Ssn6p specialise at repressing different subsets of genes. This observation was supported by analysis of global Tup1p and Ssn6p ChIP data by Venters et al (2011), which showed that while there is a large overlap in gene promoter binding between Tup1p and Ssn6p, Ssn6p was found to bind many more genes independent of Tup1p (Fig. 3.9) (Venters et al., 2011). This was surprising, but is in-line with the role of Ssn6p as a factor that interacts with DNA-binding proteins (Treitel and Carlson, 1995; Tzamarias and

Struhl, 1995). We hypothesise that due to the role of Ssn6p as an adaptor between Tup1p and various DNA-binding transcription factors, Ssn6p would be found at many more sites throughout the genome. However, this analysis was based on ChIP-chip data investigating binding to UAS regions only. To gain a better understanding of the global binding sites of Tup1p and Ssn6p, an experiment using ChIP-seq or similar technology would be useful, as this would potentially identify Tup1p and Ssn6p binding sites that may not be in canonical regulatory regions tested by ChIP-chip arrays.

The final analysis detected differences in small RNAs extracted from glucose-starved *tup1* and *ssn6* mutants (Fig. 3.10). When grown in medium containing low glucose, *ssn6* mutants displayed an increase in small RNA, and this increase was not seen in *tup1* mutants. We hypothesise that this small RNA includes tRNAs and 5S RNA, an hypothesis supported by the fact that Tup1-Ssn6 was found to occupy the promoters of genes encoding tRNAs (Hanlon et al., 2011). If this is the case, this result implicates Tup1-Ssn6 in the regulation of RNA Polymerase III-transcribed genes and protein synthesis. To investigate this, it would be useful to perform Northern blot analysis on several tRNAs in *tup1* and *ssn6* mutants and perform gene-specific ChIP to determine if Tup1-Ssn6 was present at these gene promoters in wild type cells.

8.1.2 Tup1p and Ssn6p contribute differently to *FLO1* regulation.

Tup1p and Ssn6p were shown to contribute differently to flocculation and *FLO1* gene repression (Fig. 3.6). We therefore focussed on *FLO1* regulation, and attempted to uncover the reason for the differences in *FLO1* de-repression between *tup1* and *ssn6* mutants. Since Swi-Snf had previously been shown to be required for *FLO1* de-repression, the first question we asked was whether

differences in *FLO1* de-repression between *tup1* and *ssn6* mutants were due to differences in Swi-Snf occupancy or activity at the *FLO1* promoter (Fig. 4.1 and 4.2). We first confirmed Swi-Snf was present at the de-repressed *FLO1* promoter and then showed that there were no differences in Snf5-Myc occupancy in the *tup1* or *ssn6* mutants. We also showed that all mutants exhibited H3 loss at the *FLO1* promoter to the same extent. Together these data indicated that differences in Swi-Snf occupancy or activity were not responsible for the differences in *FLO1* de-repression observed between *tup1* and *ssn6* mutants.

Having identified that differences in nucleosome occupancy at the *FLO1* promoter were not responsible for the differences in *FLO1* de-repression observed in the *tup1* and *ssn6* mutants, we next investigated whether transcriptional differences could be attributed to differences in post-translational modification (PTM) of *FLO1* promoter nucleosomes. It was found that differences in H3K4me3, H4ac4 and H3K9ac all correlated with the *FLO1* transcription result, with *tup1* mutants showing a lower enrichment of these modifications at the *FLO1* promoter than *ssn6* mutants (Fig. 4.4-4.6). Based on these results, we hypothesised that in the *tup1* mutant, Ssn6p was present and exerting a repressive effect by preventing histone modification(s) required for *FLO1* de-repression. To test this, a strain containing a Myc-tagged Ssn6p was constructed (Fig. 4.8). Using this strain, Tup1p and Ssn6-Myc occupancy at the *FLO1* promoter was measured by ChIP (Fig. 4.9). In wild type strains, both Tup1p and Ssn6-Myc were detectable at *FLO1,* and in a *tup1* mutant Ssn6-Myc was present at the *FLO1* promoter. However, in an *ssn6* mutant, Tup1p could not be detected at *FLO1*, indicating that Ssn6p is required for Tup1p occupancy at the *FLO1* promoter. The fact that Ssn6-Myc was present at *FLO1* in a *tup1* mutant also

suggested that in this strain, Ssn6p could be carrying out repression in the absence of Tup1p.

This analysis indicated that *FLO1* de-repression in a *tup1* mutant was not total because of the presence of Ssn6p at the *FLO1* promoter in this strain. It also suggested that Ssn6p does not mediate repression by excluding Swi-Snf from the *FLO1* promoter, but rather by preventing post-translational modification of *FLO1* promoter histones.

8.1.3 Acetylation by Gcn5p and Sas3p are required for *FLO1* de-repression.

Having established that histone PTMs were likely required for full *FLO1* de-repression in the absence of Tup1-Ssn6, the next step was to identify the essential modifications and also the factors that conferred them at *FLO1*. Since there was a long-established link between histone acetylation and active transcription, it was decided to focus on HATs for this analysis. To discover the HAT(s) responsible for *FLO1* activation, a mutational analysis was carried out on *GCN5* and *SAS3*, which encode proteins that acetylate lysine residues of H3 (Howe et al., 2001). An *ada2 sas3* mutant was included to analyse loss of both Gcn5p and Sas3p HAT activity, as *gcn5 sas3* mutants are inviable, and Ada2p is required for Gcn5p acetyltransferase function (Howe et al., 2001). This analysis showed that when combined with *ssn6* mutations, loss of Gcn5p and Sas3p individually had only modest impacts on *FLO1* de-repression. However, an *ada2 sas3 ssn6* mutant was dramatically impaired for *FLO1* transcription compared to an *ssn6* single mutant (Fig. 5.1). This indicated that it was the redundant HAT activity of Gcn5p and Sas3p that was required for *FLO1* activation.

Having established that Ada2p and Sas3p were both required for *FLO1* transcription, we therefore decided to investigate the impact of loss of these factors on chromatin at the *FLO1* promoter. First, H3 occupancy at the *FLO1* promoter was analysed from -100 bp to – 1200 bp upstream of the *FLO1* transcription start site (TSS) (Fig. 5.2). This analysis showed that an *ssn6* mutant displayed a dramatic loss of histones across the *FLO1* promoter, in line with previously published data (Fleming and Pennings, 2001). Interestingly, all HAT mutants showed this histone loss including the transcriptionally-impaired *ada2 sas3 ssn6* mutant. In this strain, H3 levels were close to wild-type levels near the *FLO1* TSS and downstream from the Tup1-Ssn6 binding site, although showed *ssn6* single mutant levels of H3 loss at the Tup1-Ssn6 binding site. This suggests that loss of Ada2p and Sas3p affected *FLO1* transcription independent of *FLO1* promoter nucleosome eviction and that *FLO1* transcription was not inhibited due to elevated H3 levels at the *FLO1* promoter.

Since it had been established that loss of HATs affected *FLO1* de-repression, histone PTMs upstream of the *FLO1* TSS were investigated by ChIP. If a particular acetyl mark was required for *FLO1* de-repression, then the histone modification profile of mutant strains should match the *FLO1* transcription profile in these strains. With this in mind, H3K9ac, H3K14ac and H4ac4 were monitored. It was found that the pattern of H3K14ac most closely matched *FLO1* transcription, as individual HAT mutations did not affect H3K14ac levels compared to an *ssn6* mutant at *FLO1,* but loss of both Ada2p and Sas3p abolished H3K14ac and also significantly reduced *FLO1* transcription (Fig. 5.4). Loss of these HATs had no effect on H4ac4 levels at *FLO1* (Fig. 5.5). In line with previous studies, H3K14ac was found to be globally abolished in *ada2 sas3*

mutants, though loss of this mark did not affect transcription of other genes studied (Fig. 5.6 and 5.7).

To show that Gcn5p and Sas3p acted directly at the *FLO1* promoter, Myc-tagged Gcn5p and Sas3p strains were constructed and their occupancy was analysed by ChIP. Gcn5-Myc was detected at *FLO1* in an *ssn6* mutant, occupying the same site as Tup1-Ssn6 (Fig. 5.9). However, Sas3-Myc could not be detected under any conditions. This may be due to sub-optimal ChIP conditions, or interference of the Myc-tag with the ability of Sas3p to occupy the *FLO1* promoter, or Sas3p is simply undetectable by ChIP analysis. Future work would focus on finding a definitive answer to the question of Sas3p occupancy at *FLO1*.

Snf2p was also detected at the *FLO1* promoter in an *ssn6* single mutant and *ada2 sas3 ssn6* triple mutant, indicating that loss of Ada2p and Sas3p does not impair Swi-Snf occupancy at *FLO1*. This result also showed that Swi-Snf and Gcn5p are recruited to the Tup1-Ssn6 binding site upon loss of Tup1-Ssn6, and that they potentially co-occupy this site to de-repress *FLO1*. This also shows that loss of Ada2p, Sas3p and H3K14ac does not affect Swi-Snf recruitment to *FLO1*.

This analysis has identified factors important for the de-repression of *FLO1*, and investigated the contribution of these factors to the chromatin at the *FLO1* promoter. It has established the importance of the HATs Gcn5p and Sas3p and the H3K14ac modification for *FLO1* activation, but shown that these factors are not required for nucleosome eviction from the *FLO1* promoter. Gcn5p has also been shown to directly interact with the *FLO1* promoter, indicating that it is responsible for acetylating *FLO1* promoter histones in the absence of Ssn6p. Finally, in strains that lack Ada2p and Sas3p where H3K14ac is not present at the *FLO1* promoter, Swi-Snf is still recruited to *FLO1* in the absence of Ssn6p

and remodels nucleosomes to the same level as in an *ssn6* single mutant. Thus, repression of FLO1 transcription is not dependent on histone occupancy, but transcription is dependent on histone acetylation. This suggests a low level of nucleosomes remain at the de-repressed *FLO1* after remodelling which must be acetylated in order to enable *FLO1* transcription. Future work will focus on monitoring *FLO1* de-repression in site-specific histone tail mutants, to further implicate histone acetylation in *FLO1* de-repression and definitively show which histone residue is required for transcription to take place.

8.1.4 Kinetic analysis of *FLO1* de-repression.

My data has shown that Ada2p and Sas3p are important factors for *FLO1* activation. However, to fully explore the mechanism of *FLO1* de-repression, a kinetic analysis of events during de-repression was deemed necessary. To achieve this, the anchor away method was used. Anchor away creates a conditional mutant of a nuclear protein by tagging the target protein and a ribosomal protein with epitopes that will bind to each other in the presence of rapamycin. As the ribosomal proteins constantly shuttle out of the nucleus, the target protein is rapidly transported into the cytoplasm in the presence of rapamycin (Haruki et al., 2008). Using this method, a strain with an FRB-tagged Ssn6p (Ssn6-AA) was analysed for de-repression of *FLO1*. The strains were first confirmed and the technique validated using the control gene, *SUC2*. (Wong and Struhl, 2011). Fluorescently-labelled Ssn6-FRB was also visualised by microscopy both before and after treatment with rapamycin, showing that this protein was exported from the nucleus upon incubation with rapamycin (Fig. 6. 3).

Interestingly, when *FLO1* transcription was monitored during an anchor away experiment, it was found that *FLO1* was not fully de-repressed until 10 hours after the addition of rapamycin. In an Ssn6-AA strain lacking Ada2p and Sas3p (*ada2 sas3* Ssn6-AA), no *FLO1* transcription was detected over this time course (Fig. 6. 9). The slow *FLO1* de-repression was not due to retention of Tup1p at the *FLO1* promoter, as Tup1p was lost in both Ssn6-AA and *ada2 sas3* Ssn6-AA strains by 2 hours post-rapamycin treatment (Fig. 6.11). H3 was also lost from the *FLO1* promoter rapidly in both strains, showing that loss of Ada2p and Sas3p did not impair histone eviction, despite the absence of transcription over this time-course (Fig. 6.12). Snf2p recruitment to *FLO1* was also not delayed in this strain, although Snf2p levels were less stable in the Ssn6-AA strain at later time points (Fig. 6.13). This suggested that Gcn5p and Sas3p HAT activity are essential for *FLO1* transcription, but have no effect on Swi-Snf-dependent nucleosome remodelling upon loss of Tup1-Ssn6.

Further analysis showed that H3K14ac levels in the Ssn6-AA strains were dynamic. H3K14ac levels increased to a peak by 4 hours post-rapamycin treatment, before dropping at 6 hours, only for levels to recover by 8-10 hours post-rapamycin treatment (Fig. 6.14). H3K14ac was not detected in the *ada2 sas3* Ssn6-AA strain. RNA Polymerase II (Pol II) levels were also dynamic over the anchor-away time-course in the Ssn6-AA strain, and were undetectable in the *ada2 sas3* Ssn6-AA strain. Following the addition of rapamycin, Pol II levels rose between 2-4 hours in the Ssn6-AA strain, before dropping by 8 hours, after which levels then rose again (Fig. 6.15). This Pol II "wobble" was investigated at other genes, and was found to be present only at *FLO1* (Fig. 6.16). Since Pol II occupancy at *FLO1* followed the H3K14ac pattern, and together with the reliance

on Ada2p and Sas3p for *FLO1* transcription, we hypothesise that Gcn5p and Sas3p HAT activity is required for Pol II to initiate *FLO1* transcription.

Interestingly it was also found that the drop in Pol II occupancy occurs following the diauxic shift (Fig. 6.18). Considering that there is a link between histone acetylation and nutrient availability and that Pol II recruitment to *FLO1* may rely on H3K14ac, this could indicate that *FLO1* transcription is directly linked to cellular metabolism, and will only occur in response to certain stimuli such as glucose availability or cell density, even in the absence of Tup1-Ssn6 (Friis et al., 2009). To better establish a link between the acetyl state of the *FLO1* promoter and Pol II occupancy, more acetyl marks should be studied at *FLO1,* and a finer Tup1-Ssn6 anchor-away time-course should be established between 2 and 8 hours to track changes in H3 acetylation and Pol II occupancy in more detail. This would provide a greater understanding of how these factors are coordinated at *FLO1*.

8.1.5 *FLO1* and the green beard gene hypothesis.

FLO1 has been characterised as a "green beard" gene, which means that within a yeast cell population, individuals expressing Flo1p are recognised by other individuals expressing Flo1p and these individuals gain a benefit. Conversely "cheaters" that do not express Flo1p do not gain the same benefit (Smukalla et al., 2008). In the case of *FLO1*, it was found that when cells form flocs, individuals expressing *FLO1* were found at the centre of the floc, and receive greater protection from external stress than those not expressing *FLO1* which were exiled on the outside of the floc. This means that despite the metabolic cost to the cell of *FLO1* expression, it is still advantageous to that cell within a mixed population to transcribe the gene.

The slow pattern of *FLO1* transcription described here would allow cells within a population to express some Flo1p, thereby allowing that flocculent population of cells to benefit from having a Flo+ phenotype, but without the heavier cost associated with rapid, high-level *FLO1* expression. This is in contrast to a gene such as *SUC2*, which benefits individual cells by enabling alternative carbon source utilisation. Cells have an incentive to rapidly transcribe many copies of *SUC2* because each individual cell is in competition for resources. However, because flocculation is a community trait, there is incentive to find a balance between transcribing *FLO1* at a metabolic cost to the cell, and not receiving the herd protection that flocculation offers. It is tempting to speculate that H3K14ac offers a "switch" at *FLO1* that is not found at *SUC2* that may be linked to glucose availability and/or cell density. This would allow a short burst of *FLO1* transcription when resources are available, followed by a shutdown when resources become more scarce and growth slows.

8.1.6 Flo8p and Tup1-Ssn6 co-occupy the *FLO1* promoter.

Although *FLO1* has been studied as a model for chromatin-mediated gene regulation, laboratory yeast strains do not normally transcribe *FLO1* due to the absence of the Flo8p activator, which is required for *FLO1* transcription (H. Liu et al., 1996). This ensures most lab strains do not display a flocculation phenotype and are easier to work with. To monitor the *FLO1* promoter in the presence of Flo8p, the functional genomic *FLO8* gene was first restored and the Flo8 protein expressed with and without a Myc-tag (Fig. 7.1 and 7.2). *FLO1* transcription was monitored and it was found that both *FLO8*+ strains constitutively transcribed *FLO1* at a level similar to the de-repression in an *ssn6* mutant (Fig. 7.3). ChIP

analysis of Flo8-Myc also showed that Flo8p was present at the *FLO1* promoter at the Tup1-Ssn6 binding site (Fig. 7.4). These data suggest that when Flo8p is expressed, it is present at the *FLO1* promoter and activates *FLO1* transcription directly.

The next aim of this analysis was to monitor chromatin-associated factors at the *FLO1* promoter in the presence of Flo8p. First, Tup1p occupancy at *FLO1* was monitored in strains with and without a functional *FLO8* gene. It was found that in *FLO8*+ strains, where *FLO1* was transcribed, Tup1p occupied the *FLO1* promoter to the same level as in strains without an intact *FLO8* gene where *FLO1* was repressed (Fig. 7.5, compare wt to *FLO8*+). This suggests that Flo8p does not function by competing with Tup1-Ssn6 for binding to the *FLO1* promoter during *FLO1* activation, and shows Tup1-Ssn6 and Flo8p occupy the same position upstream of *FLO1* when *FLO1* is transcribed.

H3 occupancy at the *FLO1* promoter was also analysed in the *FLO8*+ strains, and it was found that while *ssn6* mutant strains show extensive and dramatic nucleosome loss at *FLO1*, *FLO8*+ strains show only localised nucleosome loss at the Tup1-Ssn6 binding site (Fig. 7.6). Snf2p was also detected at the *FLO1* promoter in *FLO8*+ strains at a level comparable to that seen in an *ssn6* mutant (Fig. 7.7). H3K14ac at *FLO1* was also found to be elevated in *FLO8*+ strains, but levels in this strain were much lower than those seen in an *ssn6* mutant (Fig. 7.8). This indicates that when Flo8p is expressed, *FLO1* transcription and Swi-Snf occupancy were at high, *ssn6* mutant levels even though Tup1-Ssn6 persists at the *FLO1* promoter, and nucleosome remodelling occurred to a lower extent than in *ssn6* mutants. This persistence of Swi-Snf at *FLO1* in the presence of Flo8p

and Tup1-Ssn6 can be explained by the fact that Flo8p and Swi-Snf have been shown to physically interact (H. Y. Kim et al., 2014).

Overall, these results show that the presence of Flo8p at the *FLO1* promoter allows Swi-Snf and Tup1-Ssn6 to occupy the same position at the *FLO1* promoter, activating *FLO1* transcription but without the dramatic histone acetylation and loss observed in an *ssn6* mutant. We hypothesise that although Tup1-Ssn6 repression is overcome by Flo8p, Tup1-Ssn6 can still influence chromatin structure and histone acetylation during *FLO1* transcription, and that the nucleosome loss in an *ssn6* mutant is not representative of events that occur at a "naturally" de-repressed *FLO1* promoter.

The slow de-repression of *FLO1* transcription observed in the anchor-away experiment could potentially be explained by the absence of Flo8p in that strain background. A strain was therefore constructed to analyse *FLO1* de-repression using a galactose-inducible *FLO8* gene. This would allow a kinetic analysis of *FLO1* de-repression in the presence of Flo8p. Preliminary analysis suggested that de-repression of *FLO1* in this background also occurred over a 13 hour time-course (A. B. Fleming, personal communication). This suggests that the slow *FLO1* de-repression observed using the anchor away technique was not due to a lack of Flo8p, but rather because this is an inherent feature of *FLO1* gene expression. Together, this analysis offers an insight into *FLO1* de-repression in the presence of its natural activator, Flo8p. The results described here not only elucidate the role of Flo8p in *FLO1* activation, but when compared to results obtained in strains lacking Flo8p, this analysis gives a better insight into Tup1-Ssn6 function and the role of chromatin in *FLO1* regulation.

One aspect of *FLO1* regulation that would be important for future study is the identification of the Tup1-Ssn6 recruiting factor(s) at *FLO1*. Current models propose that the DNA-binding proteins that recruit Tup1-Ssn6 also play the role of transcriptional activators (Treitel and Carlson, 1995; Wong and Struhl, 2011). However, this model does not seem to apply at FLO1 since we have shown Flo8p can activate *FLO1,* and yet Tup1-Ssn6 occupies the *FLO1* promoter in laboratory strains where this protein is absent. Identifying the transcription factor (or factors) that recruits Tup1-Ssn6 in these strains would give a better insight into Tup1-Ssn6 activity, either challenging this model or providing evidence for redundancy of Tup1-Ssn6 recruiters at *FLO1* thereby demonstrating the versatility of this complex in gene repression.

8.2. Concluding remarks.

Tup1-Ssn6 is an important transcriptional co-repressor in *S. cerevisiae*. Though it has long been studied, its role in chromatin-mediated gene repression and the mechanisms by which Tup1-Ssn6 functions have been difficult to determine. Tup1-Ssn6 has been shown to interact with many factors such as HATs, HDACs, ATP-dependent nucleosome remodelling complexes and components of the general transcription machinery, but no one mechanism appears to apply to all genes under the transcriptional control of Tup1-Ssn6 (Tzamarias and Struhl, 1995; M. Lee et al., 2000; Davie et al., 2003). Recent studies using high-throughput techniques place importance on the role of Tup1-Ssn6 in masking the activation domain of the Tup1-Ssn6 recruiting protein, and positioning promoter nucleosomes over important regulatory elements (Wong and Struhl, 2011; K. Chen et al., 2013).

As a regulator of many gene subsets, any gene-specific Tup1-Ssn6 analysis will have difficulty in addressing the full range of activities of the complex. However, by studying multiple genes and different mechanisms of repression by Tup1-Ssn6, we can gain a better understanding of gene regulation by the complex. Although less well-studied than some other Tup1-Ssn6-repressed genes, *FLO1* is a good model for study of Tup1-Ssn6 function due to its promoter architecture, the factors that regulate it and its similarity to genes important for adhesion and biofilm formation in pathogenic fungi. Co-repressors and co-activators are also important factors in human development and disease, and learning more about how they function is important for understanding these processes.

The work presented in this thesis provides an insight into regulation of *FLO1* by Tup1-Ssn6. It provides a model whereby histone acetylation is required for gene transcription independent of promoter nucleosome loss, and has established a timeline of events leading up to de-repression of the *FLO1* gene. This work has also investigated the role of Flo8p, and offered empirical evidence of Flo8p binding to the *FLO1* promoter which it may co-occupy with Swi-Snf and Tup1-Ssn6. It is hoped that this work will be useful in enhancing the understanding of Tup1-Ssn6 function, and also potentially provide an insight into regulation of filamentation and adhesion in other fungal species.

Supplemental data

Name	Sequence (5'-3')	Description
ACT1-F	CTGAATTAACAATGGATTCTGG	PCR control
ACT1-R	AGATACCTCTCTTGGATTGAGC	PCR control
KANB	CTGCAGCGAGGAGCCGTAAT	Confirmation
KANC	TGATTTTGATGACGAGCGTAAT	Confirmation
HIS3con-F	GACGACCATCACACCACTGA	Confirmation
HIS3con-R	GATCATTCTTGCCTCGCAGA	Confirmation
LEU2Chk-B	ACCGGTACCCCATTTAGGAC	Confirmation
LEU2Chk-A	CACGGTTCTGCTCCAGATTT	Confirmation
URA3con-F	GCAAGGGCTCCCTAGCTACT	Confirmation
URA3con-R	AATGCGTCTCCCTTGTCATC	Confirmation
FLO8ver-F	GTCGACGGACCCAAATCTAA	Confirmation
FLO8ver-R	TTCGTTCTGCATCGTGTTGT	Confirmation
FLO8-A	CAACGAGTGTATAGTGCATGAAATC	Confirmation
FLO8-D	ATTATTGTATGGTGGAATGGAAAAA	Confirmation
SSN6DFcon-F	CCCCTATCCAACTCGAACAA	Confirmation
SSN6DFcon-R	CACCGTAGAACCCAAAGCAT	Confirmation
TUP1DFcon-F	TGCGCTGACGTTTTTGATAG	Confirmation
TUP1DFcon-R	GTG GCC CCT GTA AGA TGA TG	Confirmation
GCN5con2-F	CGAACTCATATAGTGCCAGT	Confirmation
GCN5con2-R	AATTGGTATTGCCACGAAAG	Confirmation
SSN6-S3	AAGAGAAAATGTAGTAAGGCAAGTGGAAGAAGAT GAAAACTACGACGACCGTACGCTGCAGGTCGAC	Tagging
SSN6-S2	CATTTCTCGTTGATTATAAATTAGTAGATTAATTTT TTGAATGCAAACTTTTTAATCGATGAATTCGAGTC G	Tagging
SSN6AA-F	TGTAGTAAGGCAAGTGGAAGAAGATGAAAACTAC GACGACCGGATCCCCGGGTTAATTAA	Tagging
SSN6AA-R	GATTATAAATTAGTAGATTAATTTTTTGAATGCAAA CTTTGAATTCGAGCTCGTTTAAAC	Tagging
GCN5-S3	TAAAGTAAAAGAAATACCTGAATATTCTCACCTTAT TGATCGTACGCTGCAGGTCGAC	Tagging
GCN5-S2	CATTTATTTCTTCTTCGAAAGGAATAGTAGCGGAA AAGCTTCTTCTACGCATTAATCGATGAATTCGAGT CG	Tagging
SAS3tag-F	AGAAAAAGAAGAAAAATAACTCTAATAGAGGATGA CGAAGAACGTACGCTGCAGGTCGAC	Tagging
SAS3tag-R	CATGTATATGCTTATATCCAATATATACCCATCGC CGCTTAATCGATGAATTCGAGCTCG	Tagging
Flo8pFA6-F	AAATGAAAATGATTTCAATTTTATTAATTGGGAAGG CTGACGTACGCTGCAGGTCGAC	Tagging
FLO8tag-F	TACAAATGAAAATGATTTCAATTTTATTAATTGGGA AGGCCGTACGCTGCAGGTCGAC	Tagging
Flo8pFA6-R	AAGAGTTTTTATTTTTTATTATAATACTCAACACGT GACTATCGATGAATTCGAGCTCG	Tagging
FLO8mut-F	GGCTTTTTGTATGAATGGTGGCAAAT	*FLO8* restoration
Ssn6DF-F	CCCTTCCGAT TATCAAAGCA	Gene deletion
Ssn6DF-R	TCGGGAAAACCTTTTAAGCA	Gene deletion
Snf2DF-F2	CCTGAGGCGGTAGGACAATA	Gene deletion
Snf2DF-R2	CATCCCAACTCGGTTAATGG	Gene deletion
Ssn6PRS-F	GCAGCAGTTCCTCAGCAGCCACTCGACCCATTAA CACAATAGATTGTACTGAGAGTGCAC	Gene deletion
Ssn6PRS-R	AACAGAAGCTGCTTTGGTAGCTTCTTCAGCAGGA CTAGCTGCTGTGCGGTATTTCACACCG	Gene deletion

Tup1DF-F	CTCTCCCGTCAAAGCAACA	Gene deletion
Tup1DF-R	TGCTTTAGAGAAGGGAATCAAA	Gene deletion
Tup1PRS-F	AGCAGGGGAAGAAAGAAATCAGCTTTCCATCCAA ACCAATAGATTGTACTGAGAGTGCAC	Gene deletion
Tup1PRS-R	GCCGGATTTCTTATCCCAAAACAGGACACCACGA TCTTTGGCTGTGCGGTATTTCACACCG	Gene deletion
FLO8DF-F	TGTGTTTGCCAACGAGTGTA	Gene deletion
FLO8DF-R	GGTTCAGTTCACAGGGCTTA	Gene deletion
FLO8pRS-F	TTATAGACATAAATAAAGAGGAAACGCATTCCGTG GTAGAAGATTGTACTGAGAGTGCAC	Gene deletion
FLO8pRS-R3	AAGAGTTTTTATTTATTATAATACTCAACACGTGAC TCTGTGCGGTATTTCACA	Gene deletion
ADA2DF-F	AATTCTTCGGAATGCCCATA	Gene deletion
ADA2DF-R	TTGAAAAAGATGAATGCAGAAGA	Gene deletion
ADA2pRS-F	TATCAGCGTAGTCTGAAAATATATACATTAAGCAA AAAGAAGATTGTACTGAGAGTGCAC	Gene deletion
ADA2pRS-R	AACTAGTGACAATTGTAGTTACTTTTCAATTTTTTT TTTGCTGTGCGGTATTTCACACCG	Gene deletion
SAS3DF-F	GGGGCTTCATTGTTTGAAAT	Gene deletion
SAS3DF-R	AAATTAATCGCACCCACACA	Gene deletion

Table S1. Oligonucleotides used in strain construction and genetic manipulation. Oligonucleotides were used to produce disruption fragments (DF) by amplifying selectable markers for gene deletions either using genomic DNA from existing mutants or from the pRS series of vectors. Also listed here are oligonucleotides used to tag genes of interest and oligonucleotides to confirm strains.

Name:	Sequence:	Description:	Distance from ATG:
TEL VI-R 121 F	CGTGTGTAGTGATCCGAACTCAGT	Control region	N/A
TEL VI-R 121 R	GACCCAGTCCTCATTTCCATCAATAG		
Int-V-F	TAAGAGGTGATGGTGATAGGCGT	Control region	N/A
Int-V-R	CCCTCGGGTCAAACACTACAC		
IPSTE6-F	GATATGGCTGAACTATCTCCCG	Control region	-60
IPSTE6-R	GCTTGTTCTTTGTTTCCTAGTGG		
PMA1 ORF-F	GAAAAAGAATCTTTAGTCGTTAAGTTCGTT	Control region	+322
PMA1 ORF-R	AATTGGACCGACGAAAAACATAA		
ACT1 ORF-F	GAGGTTGCTGCTTTGGTTATTGA	Control region	+318
ACT1 ORF-R	ACCGGCTTTACACATACCAGAAC		
FLO1RT-F	TACCACCACAGACGGGTTCT	*FLO1* transcription	+481
FLO1RT-R	CAACAGTTGAACGCGGTTGC		
FLO5RT5'-F2	GGATGGAAGTCTCCCTGACA	*FLO5* transcription	+635
FLO5RT5'-R2	GGAAACGGCATTGGAGTAAA		
FLO9RT5'-F	TCGTCACATTGCTGGGATTA	*FLO9* transcription	+105
FLO9RT5'-R	TGCTGCATTCGAATATGTGG		
SUC2RT486-F	AGCTGCCAACTCCACTCAAT	*SUC2* transcription	+486
SUC2RT486-R	ATTTGGCAGCCGTCATAATC		
IPFLO1-F	AAAGGAACATATTTCACTCTTGCTC	*FLO1* ChIP	-52
IPFLO1-R	TCTGTTTACTGGTGACAAGAATTAAAA		
IPFLO2-F	TGTGGAACCTTCTACAGTACTTCGG	*FLO1* ChIP	-370
IPFLO2-R	TTTGAGTGCCTTTCAACAATTTCAGACTT		
IPFLO3-F	GCTTCCAGTATGCTTTCACG	*FLO1* ChIP	-585
IPFLO3-R	GCCTACGTATTCTCCGTCAC		
IPFLO4-F	AGTCTCATTACCTAAACGCCAG	*FLO1* ChIP	-920
IPFLO4-R	CTGAAACTGGCTAGCATAACAC		
NUC4-F (TATA)	TGGAAGAAAGATTTGACGACTTT	*SUC2* ChIP	-168
NUC4-R (TATA)	TGTTTCTTTTCAGGAGGAAGGA		
BAP2 5' F	ATCCGGGAGTGACAAACTTATAC	"Constitutive" gene	+132
BAP2 5' R	ACTCAACGCCATCCTCTAAATC		

Table S2. Oligonucleotides used in qPCR.

Plasmid	Selectable marker	Source
pRS403	*HIS3*	(Christianson et al., 1992)
pRS405	*LEU2*	(Christianson et al., 1992)
pRS406	*URA3*	(Christianson et al., 1992)
pFA6a-hphNT1	*hphNT1*	(Janke et al., 2004)
pYM18	*KanMX4*	(Janke et al., 2004)
pYM20	*hph1NT1*	(Janke et al., 2004)
pFA6a-FRB-His3MX6	*HIS3*	(Haruki et al., 2008)

Table S3. Plasmids used in this study.

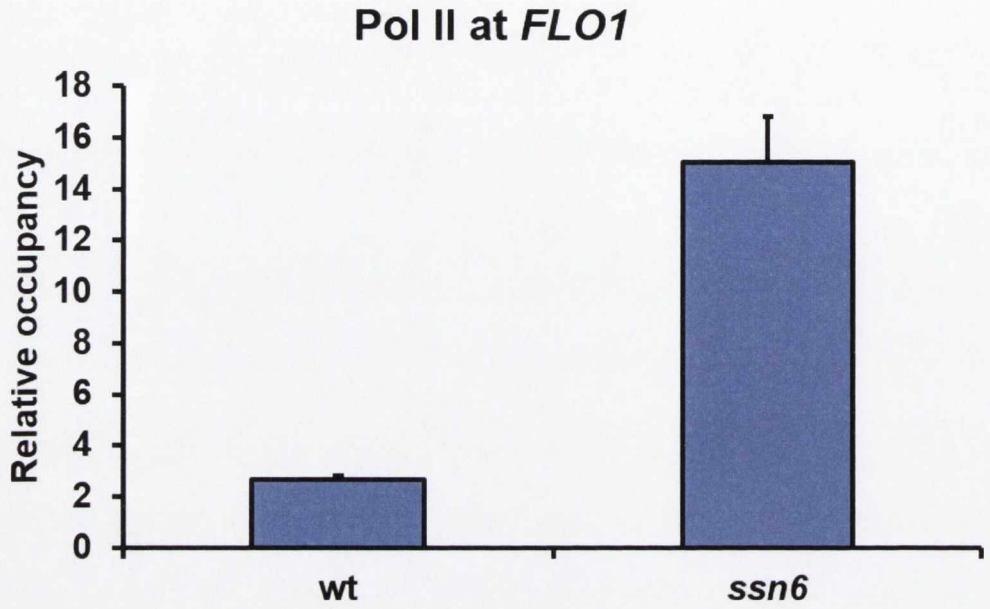

Figure S1. RNA polymerase II occupancy at *FLO1*. ChIP analysis of RNA Polymerase II (Pol II) occupancy at the *FLO1* 5' ORF in wild type (wt) and an *ssn6* mutant. Pol II levels at the *FLO1* 5' ORF were normalised to a telomeric control region. Error bars represent standard error of the mean (SEM) from 2 independent experiments.

References

Agalioti, T., Chen, G., and Thanos, D. (2002). Deciphering the transcriptional histone acetylation code for a human gene. Cell *111*, 381-392.

Akoulitchev, S., Makela, T.P., Weinberg, R.A., et al. (1995). Requirement for TFIIH kinase activity in transcription by RNA polymerase II. Nature *377*, 557-560.

Allard, S., Utley, R.T., Savard, J., et al. (1999). NuA4, an essential transcription adaptor/histone H4 acetyltransferase complex containing Esa1p and the ATM-related cofactor Tra1p. EMBO J *18*, 5108-5119.

Allfrey, V.G., and Mirsky, A.E. (1964). Structural Modifications of Histones and their Possible Role in the Regulation of RNA Synthesis. Science *144*, 559.

Altschul, S.F., Madden, T.L., Schaffer, A.A., et al. (1997). Gapped BLAST and PSI-BLAST: a new generation of protein database search programs. Nucleic Acids Res *25*, 3389-3402.

Aparicio, O., Geisberg, J.V., Sekinger, E., et al. (2005). Chromatin immunoprecipitation for determining the association of proteins with specific genomic sequences in vivo. Curr Protoc Mol Biol *Chapter 21*, Unit 21 23.

Aparicio, O., Geisberg, J.V., and Struhl, K. (2004). Chromatin immunoprecipitation for determining the association of proteins with specific genomic sequences in vivo. Curr Protoc Cell Biol *Chapter 17*, Unit 17 17.

Aparicio, O.M., Billington, B.L., and Gottschling, D.E. (1991). Modifiers of position effect are shared between telomeric and silent mating-type loci in S. cerevisiae. Cell *66*, 1279-1287.

Awad, S., and Hassan, A.H. (2008). The Swi2/Snf2 bromodomain is important for the full binding and remodeling activity of the SWI/SNF complex on H3- and H4-acetylated nucleosomes. Ann N Y Acad Sci *1138*, 366-375.

Basehoar, A.D., Zanton, S.J., and Pugh, B.F. (2004). Identification and distinct regulation of yeast TATA box-containing genes. Cell *116*, 699-709.

Bazett-Jones, D.P., Cote, J., Landel, C.C., et al. (1999). The SWI/SNF complex creates loop domains in DNA and polynucleosome arrays and can disrupt DNA-histone contacts within these domains. Mol Cell Biol *19*, 1470-1478.

Belotserkovskaya, R., Sterner, D.E., Deng, M., et al. (2000). Inhibition of TATA-binding protein function by SAGA subunits Spt3 and Spt8 at Gcn4-activated promoters. Mol Cell Biol *20*, 634-647.

Bester, M.C., Jacobson, D., and Bauer, F.F. (2012). Many Saccharomyces cerevisiae Cell Wall Protein Encoding Genes Are Coregulated by Mss11, but Cellular Adhesion Phenotypes Appear Only Flo Protein Dependent. G3 (Bethesda) *2*, 131-141.

Bhaumik, S.R., and Green, M.R. (2001). SAGA is an essential in vivo target of the yeast acidic activator Gal4p. Genes & development *15*, 1935-1945.

Bhaumik, S.R., and Green, M.R. (2002). Differential requirement of SAGA components for recruitment of TATA-box-binding protein to promoters in vivo. Mol Cell Biol *22*, 7365-7371.

Bhaumik, S.R., Raha, T., Aiello, D.P., et al. (2004). In vivo target of a transcriptional activator revealed by fluorescence resonance energy transfer. Genes & development *18*, 333-343.

Bidard, F., Bony, M., Blondin, B., et al. (1995). The Saccharomyces cerevisiae FLO1 flocculation gene encodes for a cell surface protein. Yeast *11*, 809-822.

Blander, G., and Guarente, L. (2004). The Sir2 family of protein deacetylases. Annual review of biochemistry *73*, 417-435.

Bony, M., Thines-Sempoux, D., Barre, P., et al. (1997). Localization and cell surface anchoring of the Saccharomyces cerevisiae flocculation protein Flo1p. J Bacteriol *179*, 4929-4936.

Brachmann, C.B., Davies, A., Cost, G.J., et al. (1998). Designer deletion strains derived from Saccharomyces cerevisiae S288C: a useful set of strains and plasmids for PCR-mediated gene disruption and other applications. Yeast *14*, 115-132.

Braun, B.R., and Johnson, A.D. (1997). Control of filament formation in Candida albicans by the transcriptional repressor TUP1. Science *277*, 105-109.

Brownell, J.E., and Allis, C.D. (1996). Special HATs for special occasions: linking histone acetylation to chromatin assembly and gene activation. Curr Opin Genet Dev *6*, 176-184.

Burke, T.W., and Kadonaga, J.T. (1996). Drosophila TFIID binds to a conserved downstream basal promoter element that is present in many TATA-box-deficient promoters. Genes & development *10*, 711-724.

Burke, T.W., and Kadonaga, J.T. (1997). The downstream core promoter element, DPE, is conserved from Drosophila to humans and is recognized by TAFII60 of Drosophila. Genes & development *11*, 3020-3031.

Bustin, S.A., Benes, V., Garson, J.A., et al. (2009). The MIQE guidelines: minimum information for publication of quantitative real-time PCR experiments. Clin Chem *55*, 611-622.

Butler, J.E., and Kadonaga, J.T. (2002). The RNA polymerase II core promoter: a key component in the regulation of gene expression. Genes & development *16*, 2583-2592.

Cao, F., Lane, S., Raniga, P.P., et al. (2006). The Flo8 transcription factor is essential for hyphal development and virulence in Candida albicans. Molecular biology of the cell *17*, 295-307.

Carlson, M., and Laurent, B.C. (1994). The SNF/SWI family of global transcriptional activators. Curr Opin Cell Biol *6*, 396-402.

Carrozza, M.J., John, S., Sil, A.K., et al. (2002). Gal80 confers specificity on HAT complex interactions with activators. J Biol Chem *277*, 24648-24652.

Chatterjee, N., Sinha, D., Lemma-Dechassa, M., et al. (2011). Histone H3 tail acetylation modulates ATP-dependent remodeling through multiple mechanisms. Nucleic Acids Res *39*, 8378-8391.

Chen, E.H., Grote, E., Mohler, W., et al. (2007). Cell-cell fusion. FEBS letters *581*, 2181-2193.

Chen, K., Wilson, M.A., Hirsch, C., et al. (2013). Stabilization of the promoter nucleosomes in nucleosome-free regions by the yeast Cyc8-Tup1 corepressor. Genome research *23*, 312-322.

Christianson, T.W., Sikorski, R.S., Dante, M., et al. (1992). Multifunctional yeast high-copy-number shuttle vectors. Gene *110*, 119-122.

Clapier, C.R., and Cairns, B.R. (2009). The biology of chromatin remodeling complexes. Annual review of biochemistry *78*, 273-304.

Clarke, A.S., Lowell, J.E., Jacobson, S.J., et al. (1999). Esa1p is an essential histone acetyltransferase required for cell cycle progression. Mol Cell Biol *19*, 2515-2526.

Clos, J., Buttgereit, D., and Grummt, I. (1986). A purified transcription factor (TIF-IB) binds to essential sequences of the mouse rDNA promoter. Proceedings of the National Academy of Sciences of the United States of America *83*, 604-608.

Collart, M.A., and Oliviero, S. (2001). Preparation of yeast RNA. Curr Protoc Mol Biol *Chapter 13*, Unit13 12.

Connelly, S., and Manley, J.L. (1988). A functional mRNA polyadenylation signal is required for transcription termination by RNA polymerase II. Genes & development *2*, 440-452.

Cote, J., Quinn, J., Workman, J.L., et al. (1994). Stimulation of GAL4 derivative binding to nucleosomal DNA by the yeast SWI/SNF complex. Science *265*, 53-60.

Courey, A.J., and Jia, S. (2001). Transcriptional repression: the long and the short of it. Genes & development *15*, 2786-2796.

Davie, J.K., Edmondson, D.G., Coco, C.B., et al. (2003). Tup1-Ssn6 interacts with multiple class I histone deacetylases in vivo. J Biol Chem *278*, 50158-50162.

Davie, J.K., and Kane, C.M. (2000). Genetic interactions between TFIIS and the Swi-Snf chromatin-remodeling complex. Mol Cell Biol *20*, 5960-5973.

Davie, J.K., Trumbly, R.J., and Dent, S.Y. (2002). Histone-dependent association of Tup1-Ssn6 with repressed genes in vivo. Mol Cell Biol *22*, 693-703.

Dechassa, M.L., Sabri, A., Pondugula, S., et al. (2010). SWI/SNF has intrinsic nucleosome disassembly activity that is dependent on adjacent nucleosomes. Molecular cell *38*, 590-602.

Dengis, P.B., Nelissen, L.R., and Rouxhet, P.G. (1995). Mechanisms of yeast flocculation: comparison of top- and bottom-fermenting strains. Appl Environ Microbiol *61*, 718-728.

DeRisi, J.L., Iyer, V.R., and Brown, P.O. (1997). Exploring the metabolic and genetic control of gene expression on a genomic scale. Science *278*, 680-686.

Desimone, A.M., and Laney, J.D. (2010). Corepressor-directed preacetylation of histone H3 in promoter chromatin primes rapid transcriptional switching of cell-type-specific genes in yeast. Mol Cell Biol *30*, 3342-3356.

Didion, T., Grauslund, M., Kielland-Brandt, M.C., et al. (1996). Amino acids induce expression of BAP2, a branched-chain amino acid permease gene in Saccharomyces cerevisiae. J Bacteriol *178*, 2025-2029.

Duan, M.R., and Smerdon, M.J. (2014). Histone H3 lysine 14 (H3K14) acetylation facilitates DNA repair in a positioned nucleosome by stabilizing the binding of the chromatin Remodeler RSC (Remodels Structure of Chromatin). J Biol Chem *289*, 8353-8363.

Duttke, S.H., Lacadie, S.A., Ibrahim, M.M., et al. (2015). Human promoters are intrinsically directional. Molecular cell *57*, 674-684.

Edmondson, D.G., Smith, M.M., and Roth, S.Y. (1996). Repression domain of the yeast global repressor Tup1 interacts directly with histones H3 and H4. Genes & development *10*, 1247-1259.

Elford, H.L. (1968). Effect of hydroxyurea on ribonucleotide reductase. Biochem Biophys Res Commun *33*, 129-135.

Elgin, S.C. (1996). Heterochromatin and gene regulation in Drosophila. Curr Opin Genet Dev *6*, 193-202.

Fagerstrom-Billai, F., Durand-Dubief, M., Ekwall, K., et al. (2007). Individual subunits of the Ssn6-Tup11/12 corepressor are selectively required for repression of different target genes. Mol Cell Biol *27*, 1069-1082.

Fleming, A.B., Beggs, S., Church, M., et al. (2014). The yeast Cyc8-Tup1 complex cooperates with Hda1p and Rpd3p histone deacetylases to robustly repress transcription of the subtelomeric FLO1 gene. Biochimica et biophysica acta *1839*, 1242-1255.

Fleming, A.B., Kao, C.F., Hillyer, C., et al. (2008). H2B ubiquitylation plays a role in nucleosome dynamics during transcription elongation. Molecular cell *31*, 57-66.

Fleming, A.B., and Pennings, S. (2001). Antagonistic remodelling by Swi-Snf and Tup1-Ssn6 of an extensive chromatin region forms the background for FLO1 gene regulation. EMBO J *20*, 5219-5231.

Fleming, A.B., and Pennings, S. (2007). Tup1-Ssn6 and Swi-Snf remodelling activities influence long-range chromatin organization upstream of the yeast SUC2 gene. Nucleic Acids Res *35*, 5520-5531.

Formosa, T. (2013). The role of FACT in making and breaking nucleosomes. Biochimica et biophysica acta *1819*, 247-255.

Friis, R.M., Wu, B.P., Reinke, S.N., et al. (2009). A glycolytic burst drives glucose induction of global histone acetylation by picNuA4 and SAGA. Nucleic Acids Res *37*, 3969-3980.

Fyodorov, D.V., Blower, M.D., Karpen, G.H., et al. (2004). Acf1 confers unique activities to ACF/CHRAC and promotes the formation rather than disruption of chromatin in vivo. Genes & development *18*, 170-183.

Garcia, I., Mathieu, M., Nikolaev, I., et al. (2008). Roles of the Aspergillus nidulans homologues of Tup1 and Ssn6 in chromatin structure and cell viability. FEMS microbiology letters *289*, 146-154.

Gaupel, A.C., Begley, T., and Tenniswood, M. (2014). High throughput screening identifies modulators of histone deacetylase inhibitors. BMC Genomics *15*, 528.

Gavin, I.M., and Simpson, R.T. (1997). Interplay of yeast global transcriptional regulators Ssn6p-Tup1p and Swi-Snf and their effect on chromatin structure. EMBO J *16*, 6263-6271.

Geng, F., Cao, Y., and Laurent, B.C. (2001). Essential roles of Snf5p in Snf-Swi chromatin remodeling in vivo. Mol Cell Biol *21*, 4311-4320.

Gietz, R.D., and Schiestl, R.H. (2007). High-efficiency yeast transformation using the LiAc/SS carrier DNA/PEG method. Nat Protoc *2*, 31-34.

Goldman, S.R., Ebright, R.H., and Nickels, B.E. (2009). Direct detection of abortive RNA transcripts in vivo. Science *324*, 927-928.

Gounalaki, N., Tzamarias, D., and Vlassi, M. (2000). Identification of residues in the TPR domain of Ssn6 responsible for interaction with the Tup1 protein. FEBS letters *473*, 37-41.

Govender, P., Domingo, J.L., Bester, M.C., et al. (2008). Controlled expression of the dominant flocculation genes FLO1, FLO5, and FLO11 in Saccharomyces cerevisiae. Appl Environ Microbiol *74*, 6041-6052.

Govind, C.K., Yoon, S., Qiu, H., et al. (2005). Simultaneous recruitment of coactivators by Gcn4p stimulates multiple steps of transcription in vivo. Mol Cell Biol *25*, 5626-5638.

Grant, P.A., Duggan, L., Cote, J., et al. (1997). Yeast Gcn5 functions in two multisubunit complexes to acetylate nucleosomal histones: characterization of an Ada complex and the SAGA (Spt/Ada) complex. Genes & development *11*, 1640-1650.

Grbavec, D., Lo, R., Liu, Y., et al. (1999). Groucho/transducin-like enhancer of split (TLE) family members interact with the yeast transcriptional co-repressor SSN6 and mammalian SSN6-related proteins: implications for evolutionary conservation of transcription repression mechanisms. The Biochemical journal *337 (Pt 1)*, 13-17.

Green, M.R. (2000). TBP-associated factors (TAFIIs): multiple, selective transcriptional mediators in common complexes. Trends in biochemical sciences *25*, 59-63.

Green, S.R., and Johnson, A.D. (2005). Genome-wide analysis of the functions of a conserved surface on the corepressor Tup1. Molecular biology of the cell *16*, 2605-2613.

Greenfield, A., Carrel, L., Pennisi, D., et al. (1998). The UTX gene escapes X inactivation in mice and humans. Human molecular genetics *7*, 737-742.

Gromoller, A., and Lehming, N. (2000). Srb7p is a physical and physiological target of Tup1p. EMBO J *19*, 6845-6852.

Guillemette, B., Drogaris, P., Lin, H.H., et al. (2011). H3 lysine 4 is acetylated at active gene promoters and is regulated by H3 lysine 4 methylation. PLoS Genet *7*, e1001354.

Han, M., Kim, U.J., Kayne, P., et al. (1988). Depletion of histone H4 and nucleosomes activates the PHO5 gene in Saccharomyces cerevisiae. EMBO J *7*, 2221-2228.

Hanlon, S.E., Rizzo, J.M., Tatomer, D.C., et al. (2011). The stress response factors Yap6, Cin5, Phd1, and Skn7 direct targeting of the conserved co-repressor Tup1-Ssn6 in S. cerevisiae. PloS one *6*, e19060.

Haruki, H., Nishikawa, J., and Laemmli, U.K. (2008). The anchor-away technique: rapid, conditional establishment of yeast mutant phenotypes. Molecular cell *31*, 925-932.

Hassan, A.H., Neely, K.E., and Workman, J.L. (2001). Histone acetyltransferase complexes stabilize swi/snf binding to promoter nucleosomes. Cell *104*, 817-827.

Hassan, A.H., Prochasson, P., Neely, K.E., et al. (2002). Function and selectivity of bromodomains in anchoring chromatin-modifying complexes to promoter nucleosomes. Cell *111*, 369-379.

Hirschhorn, J.N., Brown, S.A., Clark, C.D., et al. (1992). Evidence that SNF2/SWI2 and SNF5 activate transcription in yeast by altering chromatin structure. Genes & development *6*, 2288-2298.

Holstege, F.C., Jennings, E.G., Wyrick, J.J., et al. (1998). Dissecting the regulatory circuitry of a eukaryotic genome. Cell *95*, 717-728.

Holstege, F.C., van der Vliet, P.C., and Timmers, H.T. (1996). Opening of an RNA polymerase II promoter occurs in two distinct steps and requires the basal transcription factors IIE and IIH. EMBO J *15*, 1666-1677.

Hong, L., Schroth, G.P., Matthews, H.R., et al. (1993). Studies of the DNA binding properties of histone H4 amino terminus. Thermal denaturation studies reveal that acetylation markedly reduces the binding constant of the H4 "tail" to DNA. J Biol Chem *268*, 305-314.

Howe, L., Auston, D., Grant, P., et al. (2001). Histone H3 specific acetyltransferases are essential for cell cycle progression. Genes & development *15*, 3144-3154.

Hughes, T.R., Marton, M.J., Jones, A.R., et al. (2000). Functional discovery via a compendium of expression profiles. Cell *102*, 109-126.

International Human Genome Sequencing, C. (2004). Finishing the euchromatic sequence of the human genome. Nature *431*, 931-945.

Izban, M.G., and Luse, D.S. (1991). Transcription on nucleosomal templates by RNA polymerase II in vitro: inhibition of elongation with enhancement of sequence-specific pausing. Genes & development *5*, 683-696.

Jabet, C., Sprague, E.R., VanDemark, A.P., et al. (2000). Characterization of the N-terminal domain of the yeast transcriptional repressor Tup1. Proposal for an association model of the repressor complex Tup1 x Ssn6. J Biol Chem *275*, 9011-9018.

Jamai, A., Puglisi, A., and Strubin, M. (2009). Histone chaperone spt16 promotes redeposition of the original h3-h4 histones evicted by elongating RNA polymerase. Molecular cell *35*, 377-383.

Janke, C., Magiera, M.M., Rathfelder, N., et al. (2004). A versatile toolbox for PCR-based tagging of yeast genes: new fluorescent proteins, more markers and promoter substitution cassettes. Yeast *21*, 947-962.

Jedidi, I., Zhang, F., Qiu, H., et al. (2010). Activator Gcn4 employs multiple segments of Med15/Gal11, including the KIX domain, to recruit mediator to target genes in vivo. J Biol Chem *285*, 2438-2455.

Keleher, C.A., Redd, M.J., Schultz, J., et al. (1992). Ssn6-Tup1 is a general repressor of transcription in yeast. Cell *68*, 709-719.

Kent, N.A., Karabetsou, N., Politis, P.K., et al. (2001). In vivo chromatin remodeling by yeast ISWI homologs Isw1p and Isw2p. Genes & development *15*, 619-626.

Kim, H.Y., Lee, S.B., Kang, H.S., et al. (2014). Two distinct domains of Flo8 activator mediates its role in transcriptional activation and the physical interaction with Mss11. Biochem Biophys Res Commun *449*, 202-207.

Kim, J.H., Saraf, A., Florens, L., et al. (2010). Gcn5 regulates the dissociation of SWI/SNF from chromatin by acetylation of Swi2/Snf2. Genes & development *24*, 2766-2771.

Knezetic, J.A., and Luse, D.S. (1986). The presence of nucleosomes on a DNA template prevents initiation by RNA polymerase II in vitro. Cell *45*, 95-104.

Kobayashi, O., Suda, H., Ohtani, T., et al. (1996). Molecular cloning and analysis of the dominant flocculation gene FLO8 from Saccharomyces cerevisiae. Mol Gen Genet *251*, 707-715.

Kobayashi, O., Yoshimoto, H., and Sone, H. (1999). Analysis of the genes activated by the FLO8 gene in Saccharomyces cerevisiae. Current genetics *36*, 256-261.

Kohler, A., and Hurt, E. (2007). Exporting RNA from the nucleus to the cytoplasm. Nat Rev Mol Cell Biol *8*, 761-773.

Komachi, K., Redd, M.J., and Johnson, A.D. (1994). The WD repeats of Tup1 interact with the homeo domain protein alpha 2. Genes & development *8*, 2857-2867.

Komissarova, N., Becker, J., Solter, S., et al. (2002). Shortening of RNA:DNA hybrid in the elongation complex of RNA polymerase is a prerequisite for transcription termination. Molecular cell *10*, 1151-1162.

Kornberg, R.D., and Stryer, L. (1988). Statistical distributions of nucleosomes: nonrandom locations by a stochastic mechanism. Nucleic Acids Res *16*, 6677-6690.

Krebs, J.E. (2007). Moving marks: dynamic histone modifications in yeast. Mol Biosyst *3*, 590-597.

Kuchin, S., and Carlson, M. (1998). Functional relationships of Srb10-Srb11 kinase, carboxy-terminal domain kinase CTDK-I, and transcriptional corepressor Ssn6-Tup1. Mol Cell Biol *18*, 1163-1171.

Kurdistani, S.K., Robyr, D., Tavazoie, S., et al. (2002). Genome-wide binding map of the histone deacetylase Rpd3 in yeast. Nat Genet *31*, 248-254.

Lafon, A., Chang, C.S., Scott, E.M., et al. (2007). MYST opportunities for growth control: yeast genes illuminate human cancer gene functions. Oncogene *26*, 5373-5384.

Lam, F.H., Steger, D.J., and O'Shea, E.K. (2008). Chromatin decouples promoter threshold from dynamic range. Nature *453*, 246-250.

Laurent, B.C., Treich, I., and Carlson, M. (1993). The yeast SNF2/SWI2 protein has DNA-stimulated ATPase activity required for transcriptional activation. Genes & development *7*, 583-591.

Lee, J.E., Oh, J.H., Ku, M., et al. (2015). Ssn6 has dual roles in Candida albicans filament development through the interaction with Rpd31. FEBS letters *589*, 513-520.

Lee, J.S., and Shilatifard, A. (2007). A site to remember: H3K36 methylation a mark for histone deacetylation. Mutation research *618*, 130-134.

Lee, K.K., Prochasson, P., Florens, L., et al. (2004). Proteomic analysis of chromatin-modifying complexes in Saccharomyces cerevisiae identifies novel subunits. Biochem Soc Trans *32*, 899-903.

Lee, M., Chatterjee, S., and Struhl, K. (2000). Genetic analysis of the role of Pol II holoenzyme components in repression by the Cyc8-Tup1 corepressor in yeast. Genetics *155*, 1535-1542.

Lemon, B., and Tjian, R. (2000). Orchestrated response: a symphony of transcription factors for gene control. Genes & development *14*, 2551-2569.

Li, B., Carey, M., and Workman, J.L. (2007). The role of chromatin during transcription. Cell *128*, 707-719.

Li, B., and Reese, J.C. (2001). Ssn6-Tup1 regulates RNR3 by positioning nucleosomes and affecting the chromatin structure at the upstream repression sequence. J Biol Chem *276*, 33788-33797.

Li, E., Yue, F., Chang, Q., et al. (2013). Deletion of intragenic tandem repeats in unit C of FLO1 of Saccharomyces cerevisiae increases the conformational stability of flocculin under acidic and alkaline conditions. PloS one *8*, e53428.

Li, X.Y., Bhaumik, S.R., and Green, M.R. (2000). Distinct classes of yeast promoters revealed by differential TAF recruitment. Science *288*, 1242-1244.

Lipke, P.N., and Hull-Pillsbury, C. (1984). Flocculation of Saccharomyces cerevisiae tup1 mutants. J Bacteriol *159*, 797-799.

Liu, C.L., Kaplan, T., Kim, M., et al. (2005). Single-nucleosome mapping of histone modifications in S. cerevisiae. PLoS Biol *3*, e328.

Liu, H., Styles, C.A., and Fink, G.R. (1996). Saccharomyces cerevisiae S288C has a mutation in FLO8, a gene required for filamentous growth. Genetics *144*, 967-978.

Liu, N., and Hayes, J.J. (2010). When push comes to shove: SWI/SNF uses a nucleosome to get rid of a nucleosome. Molecular cell *38*, 484-486.

Logan, J., Falck-Pedersen, E., Darnell, J.E., Jr., et al. (1987). A poly(A) addition site and a downstream termination region are required for efficient cessation of transcription by RNA polymerase II in the mouse beta maj-globin gene. Proceedings of the National Academy of Sciences of the United States of America *84*, 8306-8310.

Lohr, D. (1997). Nucleosome transactions on the promoters of the yeast GAL and PHO genes. J Biol Chem *272*, 26795-26798.

Longtine, M.S., McKenzie, A., 3rd, Demarini, D.J., et al. (1998). Additional modules for versatile and economical PCR-based gene deletion and modification in Saccharomyces cerevisiae. Yeast *14*, 953-961.

Luger, K., Rechsteiner, T.J., Flaus, A.J., et al. (1997). Characterization of nucleosome core particles containing histone proteins made in bacteria. Journal of molecular biology *272*, 301-311.

Machado, M.D., Santos, M.S., Gouveia, C., et al. (2008). Removal of heavy metals using a brewer's yeast strain of Saccharomyces cerevisiae: the flocculation as a separation process. Bioresour Technol *99*, 2107-2115.

Magraner-Pardo, L., Pelechano, V., Coloma, M.D., et al. (2014). Dynamic remodeling of histone modifications in response to osmotic stress in Saccharomyces cerevisiae. BMC Genomics *15*, 247.

Malave, T.M., and Dent, S.Y. (2006). Transcriptional repression by Tup1-Ssn6. Biochem Cell Biol *84*, 437-443.

Maltby, V.E., Martin, B.J., Brind'Amour, J., et al. (2012). Histone H3K4 demethylation is negatively regulated by histone H3 acetylation in Saccharomyces cerevisiae. Proceedings of the National Academy of Sciences of the United States of America *109*, 18505-18510.

Mazeyrat, S., Saut, N., Sargent, C.A., et al. (1998). The mouse Y chromosome interval necessary for spermatogonial proliferation is gene dense with syntenic homology to the human AZFa region. Human molecular genetics *7*, 1713-1724.

Micelli, C., and Rastelli, G. (2015). Histone deacetylases: structural determinants of inhibitor selectivity. Drug Discov Today.

Miki, B.L., Poon, N.H., James, A.P., et al. (1982). Possible mechanism for flocculation interactions governed by gene FLO1 in Saccharomyces cerevisiae. J Bacteriol *150*, 878-889.

Nakanishi, S., Lee, J.S., Gardner, K.E., et al. (2009). Histone H2BK123 monoubiquitination is the critical determinant for H3K4 and H3K79 trimethylation by COMPASS and Dot1. J Cell Biol *186*, 371-377.

Neigeborn, L., and Carlson, M. (1984). Genes affecting the regulation of SUC2 gene expression by glucose repression in Saccharomyces cerevisiae. Genetics *108*, 845-858.

Nogi, Y., and Fukasawa, T. (1980). A novel mutation that affects utilization of galactose in Saccharomyces cerevisiae. Current genetics *2*, 115-120.

Ozcan, S., Vallier, L.G., Flick, J.S., et al. (1997). Expression of the SUC2 gene of Saccharomyces cerevisiae is induced by low levels of glucose. Yeast *13*, 127-137.

Papamichos-Chronakis, M., Conlan, R.S., Gounalaki, N., et al. (2000). Hrs1/Med3 is a Cyc8-Tup1 corepressor target in the RNA polymerase II holoenzyme. J Biol Chem *275*, 8397-8403.

Papamichos-Chronakis, M., Petrakis, T., Ktistaki, E., et al. (2002). Cti6, a PHD domain protein, bridges the Cyc8-Tup1 corepressor and the SAGA coactivator to overcome repression at GAL1. Molecular cell *9*, 1297-1305.

Patel, B.K., Gavin-Smyth, J., and Liebman, S.W. (2009). The yeast global transcriptional co-repressor protein Cyc8 can propagate as a prion. Nature cell biology *11*, 344-349.

Payankaulam, S., Li, L.M., and Arnosti, D.N. (2010). Transcriptional repression: conserved and evolved features. Current biology : CB *20*, R764-771.

Peterson, C.L., Dingwall, A., and Scott, M.P. (1994). Five SWI/SNF gene products are components of a large multisubunit complex required for transcriptional enhancement. Proceedings of the National Academy of Sciences of the United States of America *91*, 2905-2908.

Phatnani, H.P., and Greenleaf, A.L. (2006). Phosphorylation and functions of the RNA polymerase II CTD. Genes & development *20*, 2922-2936.

Pickles, L.M., Roe, S.M., Hemingway, E.J., et al. (2002). Crystal structure of the C-terminal WD40 repeat domain of the human Groucho/TLE1 transcriptional corepressor. Structure *10*, 751-761.

Pollard, K.J., and Peterson, C.L. (1997). Role for ADA/GCN5 products in antagonizing chromatin-mediated transcriptional repression. Mol Cell Biol *17*, 6212-6222.

Pray-Grant, M.G., Schieltz, D., McMahon, S.J., et al. (2002). The novel SLIK histone acetyltransferase complex functions in the yeast retrograde response pathway. Mol Cell Biol *22*, 8774-8786.

Proft, M., and Struhl, K. (2002). Hog1 kinase converts the Sko1-Cyc8-Tup1 repressor complex into an activator that recruits SAGA and SWI/SNF in response to osmotic stress. Molecular cell *9*, 1307-1317.

Proudfoot, N.J. (1989). How RNA polymerase II terminates transcription in higher eukaryotes. Trends in biochemical sciences *14*, 105-110.

Proudfoot, N.J., Furger, A., and Dye, M.J. (2002). Integrating mRNA processing with transcription. Cell *108*, 501-512.

Qiu, H., Hu, C., Yoon, S., et al. (2004). An array of coactivators is required for optimal recruitment of TATA binding protein and RNA polymerase II by promoter-bound Gcn4p. Mol Cell Biol *24*, 4104-4117.

Rando, O.J., and Winston, F. (2012). Chromatin and transcription in yeast. Genetics *190*, 351-387.

Rao, R., Drummond-Barbosa, D., and Slayman, C.W. (1993). Transcriptional regulation by glucose of the yeast PMA1 gene encoding the plasma membrane H(+)-ATPase. Yeast *9*, 1075-1084.

Richmond, T.J., and Davey, C.A. (2003). The structure of DNA in the nucleosome core. Nature *423*, 145-150.

Rine, J., and Herskowitz, I. (1987). Four genes responsible for a position effect on expression from HML and HMR in Saccharomyces cerevisiae. Genetics *116*, 9-22.

Rine, J., Strathern, J.N., Hicks, J.B., et al. (1979). A suppressor of mating-type locus mutations in Saccharomyces cerevisiae: evidence for and identification of cryptic mating-type loci. Genetics *93*, 877-901.

Roberts, S.M., and Winston, F. (1997). Essential functional interactions of SAGA, a Saccharomyces cerevisiae complex of Spt, Ada, and Gcn5 proteins, with the Snf/Swi and Srb/mediator complexes. Genetics *147*, 451-465.

Rosaleny, L.E., Ruiz-Garcia, A.B., Garcia-Martinez, J., et al. (2007). The Sas3p and Gcn5p histone acetyltransferases are recruited to similar genes. Genome biology *8*, R119.

Rundlett, S.E., Carmen, A.A., Kobayashi, R., et al. (1996). HDA1 and RPD3 are members of distinct yeast histone deacetylase complexes that regulate silencing and transcription. Proceedings of the National Academy of Sciences of the United States of America *93*, 14503-14508.

Rusche, L.N., Kirchmaier, A.L., and Rine, J. (2003). The establishment, inheritance, and function of silenced chromatin in Saccharomyces cerevisiae. Annual review of biochemistry *72*, 481-516.

Sanada, M., Kuroda, K., and Ueda, M. (2011). GTS1 induction causes derepression of Tup1-Cyc8-repressing genes and chromatin remodeling through the interaction of Gts1p with Cyc8p. Biosci Biotechnol Biochem *75*, 740-747.

Schultz, J., Marshall-Carlson, L., and Carlson, M. (1990). The N-terminal TPR region is the functional domain of SSN6, a nuclear phosphoprotein of Saccharomyces cerevisiae. Mol Cell Biol *10*, 4744-4756.

Schwabish, M.A., and Struhl, K. (2007). The Swi/Snf complex is important for histone eviction during transcriptional activation and RNA polymerase II elongation in vivo. Mol Cell Biol *27*, 6987-6995.

Sekinger, E.A., Moqtaderi, Z., and Struhl, K. (2005). Intrinsic histone-DNA interactions and low nucleosome density are important for preferential accessibility of promoter regions in yeast. Molecular cell *18*, 735-748.

Shatkin, A.J., and Manley, J.L. (2000). The ends of the affair: capping and polyadenylation. Nat Struct Biol *7*, 838-842.

Shukla, A., Bajwa, P., and Bhaumik, S.R. (2006). SAGA-associated Sgf73p facilitates formation of the preinitiation complex assembly at the promoters either in a HAT-dependent or independent manner in vivo. Nucleic Acids Res *34*, 6225-6232.

Sims, R.J., 3rd, Belotserkovskaya, R., and Reinberg, D. (2004). Elongation by RNA polymerase II: the short and long of it. Genes & development *18*, 2437-2468.

Smale, S.T., and Kadonaga, J.T. (2003). The RNA polymerase II core promoter. Annual review of biochemistry *72*, 449-479.

Smit, G., Straver, M.H., Lugtenberg, B.J., et al. (1992). Flocculence of Saccharomyces cerevisiae cells is induced by nutrient limitation, with cell surface hydrophobicity as a major determinant. Appl Environ Microbiol *58*, 3709-3714.

Smukalla, S., Caldara, M., Pochet, N., et al. (2008). FLO1 is a variable green beard gene that drives biofilm-like cooperation in budding yeast. Cell *135*, 726-737.

Soares, E.V. (2011). Flocculation in Saccharomyces cerevisiae: a review. Journal of applied microbiology *110*, 1-18.

Stern, M., Jensen, R., and Herskowitz, I. (1984). Five SWI genes are required for expression of the HO gene in yeast. Journal of molecular biology *178*, 853-868.

Sterner, D.E., Grant, P.A., Roberts, S.M., et al. (1999). Functional organization of the yeast SAGA complex: distinct components involved in structural integrity, nucleosome acetylation, and TATA-binding protein interaction. Mol Cell Biol *19*, 86-98.

Sudarsanam, P., and Winston, F. (2000). The Swi/Snf family nucleosome-remodeling complexes and transcriptional control. Trends in genetics : TIG *16*, 345-351.

Svejstrup, J.Q., Vichi, P., and Egly, J.M. (1996). The multiple roles of transcription/repair factor TFIIH. Trends in biochemical sciences *21*, 346-350.

Swigut, T., and Wysocka, J. (2007). H3K27 demethylases, at long last. Cell *131*, 29-32.

Syntichaki, P., and Thireos, G. (1998). The Gcn5.Ada complex potentiates the histone acetyltransferase activity of Gcn5. J Biol Chem *273*, 24414-24419.

Teunissen, A.W., and Steensma, H.Y. (1995). Review: the dominant flocculation genes of Saccharomyces cerevisiae constitute a new subtelomeric gene family. Yeast *11*, 1001-1013.

Thoma, F., Koller, T., and Klug, A. (1979). Involvement of histone H1 in the organization of the nucleosome and of the salt-dependent superstructures of chromatin. J Cell Biol *83*, 403-427.

Thomas, J.O., and Kornberg, R.D. (1975). An octamer of histones in chromatin and free in solution. Proceedings of the National Academy of Sciences of the United States of America *72*, 2626-2630.

Tora, L. (2002). A unified nomenclature for TATA box binding protein (TBP)-associated factors (TAFs) involved in RNA polymerase II transcription. Genes & development *16*, 673-675.

Treitel, M.A., and Carlson, M. (1995). Repression by SSN6-TUP1 is directed by MIG1, a repressor/activator protein. Proceedings of the National Academy of Sciences of the United States of America *92*, 3132-3136.

Tsukuda, T., Fleming, A.B., Nickoloff, J.A., et al. (2005). Chromatin remodelling at a DNA double-strand break site in Saccharomyces cerevisiae. Nature *438*, 379-383.

Tzamarias, D., and Struhl, K. (1994). Functional dissection of the yeast Cyc8-Tup1 transcriptional co-repressor complex. Nature *369*, 758-761.

Tzamarias, D., and Struhl, K. (1995). Distinct TPR motifs of Cyc8 are involved in recruiting the Cyc8-Tup1 corepressor complex to differentially regulated promoters. Genes & development *9*, 821-831.

Untergasser, A., Nijveen, H., Rao, X., et al. (2007). Primer3Plus, an enhanced web interface to Primer3. Nucleic Acids Res *35*, W71-74.

van Bakel, H., Tsui, K., Gebbia, M., et al. (2013). A compendium of nucleosome and transcript profiles reveals determinants of chromatin architecture and transcription. PLoS Genet *9*, e1003479.

Van Mulders, S.E., Christianen, E., Saerens, S.M., et al. (2009). Phenotypic diversity of Flo protein family-mediated adhesion in Saccharomyces cerevisiae. FEMS Yeast Res *9*, 178-190.

Varanasi, U.S., Klis, M., Mikesell, P.B., et al. (1996). The Cyc8 (Ssn6)-Tup1 corepressor complex is composed of one Cyc8 and four Tup1 subunits. Mol Cell Biol *16*, 6707-6714.

Varv, S., Kristjuhan, K., Peil, K., et al. (2010). Acetylation of H3 K56 is required for RNA polymerase II transcript elongation through heterochromatin in yeast. Mol Cell Biol *30*, 1467-1477.

Venter, U., Svaren, J., Schmitz, J., et al. (1994). A nucleosome precludes binding of the transcription factor Pho4 in vivo to a critical target site in the PHO5 promoter. EMBO J *13*, 4848-4855.

Venters, B.J., Wachi, S., Mavrich, T.N., et al. (2011). A comprehensive genomic binding map of gene and chromatin regulatory proteins in Saccharomyces. Molecular cell *41*, 480-492.

Verstrepen, K.J., Derdelinckx, G., Verachtert, H., et al. (2003). Yeast flocculation: what brewers should know. Appl Microbiol Biotechnol *61*, 197-205.

Verstrepen, K.J., and Klis, F.M. (2006). Flocculation, adhesion and biofilm formation in yeasts. Mol Microbiol *60*, 5-15.

Wach, A. (1996). PCR-synthesis of marker cassettes with long flanking homology regions for gene disruptions in S. cerevisiae. Yeast *12*, 259-265.

Wang, L., and Dent, S.Y. (2014). Functions of SAGA in development and disease. Epigenomics *6*, 329-339.

Watari, J., Takata, Y., Ogawa, M., et al. (1994). Molecular cloning and analysis of the yeast flocculation gene FLO1. Yeast *10*, 211-225.

Watson, A.D., Edmondson, D.G., Bone, J.R., et al. (2000). Ssn6-Tup1 interacts with class I histone deacetylases required for repression. Genes & development *14*, 2737-2744.

Weinmann, R., and Roeder, R.G. (1974). Role of DNA-dependent RNA polymerase 3 in the transcription of the tRNA and 5S RNA genes. Proceedings of the National Academy of Sciences of the United States of America *71*, 1790-1794.

Whitehouse, I., Flaus, A., Cairns, B.R., et al. (1999). Nucleosome mobilization catalysed by the yeast SWI/SNF complex. Nature *400*, 784-787.

Winston, F., and Carlson, M. (1992). Yeast SNF/SWI transcriptional activators and the SPT/SIN chromatin connection. Trends in genetics : TIG *8*, 387-391.

Wong, K.H., and Struhl, K. (2011). The Cyc8-Tup1 complex inhibits transcription primarily by masking the activation domain of the recruiting protein. Genes & development *25*, 2525-2539.

Workman, J.L., and Kingston, R.E. (1998). Alteration of nucleosome structure as a mechanism of transcriptional regulation. Annual review of biochemistry *67*, 545-579.

Wu, L., and Winston, F. (1997). Evidence that Snf-Swi controls chromatin structure over both the TATA and UAS regions of the SUC2 promoter in Saccharomyces cerevisiae. Nucleic Acids Res *25*, 4230-4234.

Wu, Y., Reece, R.J., and Ptashne, M. (1996). Quantitation of putative activator-target affinities predicts transcriptional activating potentials. EMBO J *15*, 3951-3963.

Xu, J., and Andreassi, M. (2011). Reversible histone methylation regulates brain gene expression and behavior. Hormones and behavior *59*, 383-392.

Yan, Q., Moreland, R.J., Conaway, J.W., et al. (1999). Dual roles for transcription factor IIF in promoter escape by RNA polymerase II. J Biol Chem *274*, 35668-35675.

Yang, C., Bolotin, E., Jiang, T., et al. (2007). Prevalence of the initiator over the TATA box in human and yeast genes and identification of DNA motifs enriched in human TATA-less core promoters. Gene *389*, 52-65.

Yang, X.J., and Gregoire, S. (2005). Class II histone deacetylases: from sequence to function, regulation, and clinical implication. Mol Cell Biol *25*, 2873-2884.

Yu, F., Imamura, Y., Ueno, M., et al. (2015). The yeast chromatin remodeler Rsc1-RSC complex is required for transcriptional activation of autophagy-related genes and inhibition of the TORC1 pathway in response to nitrogen starvation. Biochem Biophys Res Commun *464*, 1248-1253.

Zhang, Z., and Reese, J.C. (2004). Ssn6-Tup1 requires the ISW2 complex to position nucleosomes in Saccharomyces cerevisiae. EMBO J *23*, 2246-2257.

Zlatanova, J., and Thakar, A. (2008). H2A.Z: view from the top. Structure *16*, 166-179.